

Issue 2
Volume 2
September, 2025

ISSN 2818-0313
DOI Prefix : 10.62252

Naturalis



Scientias

www.naturalisscientias.com



TABLE OF CONTENTS

Original Articles

1. Comparative assessment of aquifers in a typical karst sedimentary system, South-West Nigeria.....	494
2. Some questions about the book titled <i>A History of Development of Geological Sciences in China</i>	517
3. Assessment of aquifer vulnerability status and groundwater management studies using integrated geophysical techniques in Ewekoro South-West Nigeria.....	549
4. Proof of the true motion of the North Celestial Pole	574
5. Estimation of hydraulic diffusivity and associated hydraulic parameters using pumping test and lithological data in Wasinmi residential community, south-west Nigeria	586
6. Preliminary investigation and extent of hydrogeochemical concentration for groundwater exploration using electromagnetic method of terrain conductivity variation and analytical technique in Papalanto, South-West Nigeria.....	623



Original Article

Comparative assessment of aquifers in a typical karst sedimentary system, South-West NigeriaS. A. Ishola¹ **Abstract**

The necessity of hydraulic assessment of groundwater system for practical application in any lithospheric environment cannot be overemphasized. The subject matter includes formulae to quantitatively appraise the hydraulic parameters influencing the water-yielding capacity of boreholes which tap a typical sedimentary karst rock mass. Pumping test was carried in a total of 25 boreholes each from different autonomous residential communities around 4 towns within Ewekoro Local Government Area to quantitatively appraise the hydraulic parameters influencing the water-yielding capacity of boreholes abstracting water from a typical sedimentary karst rock mass. The measurements were carried out at a controlled rate and water-level response was measured separately from Wasinmi, Itori, Ewekoro and Papalanto. The rise in water levels was recorded as residual drawdowns', and the water level measured at a residual time t' after the pump has been turned off. Hydraulic properties were estimated with discharge, drawdown and specific capacity data. The values of the hydraulic parameters are consistent with what obtains in the sedimentary aquifer. The average measured values of the basic and estimated hydraulic parameters are: borehole depth, 51, 50.36, 60.32, 95.36 m; specific discharge, 4.0×10^{-2} , 5.0×10^{-2} , 4.0×10^{-2} , 5.0×10^{-2} l/s; specific capacity, 6.3×10^{-3} , 7.0×10^{-2} , 6.0×10^{-3} , 5.0×10^{-2} m²/s; well loss constant, 5.98×10^4 , 4.30×10^5 , 6.16×10^2 , 5.19×10^3 s²/m⁵; transmissibility, 94.8 m²/s respectively recorded for Wasinmi, Itori, Ewekoro and Papalanto. Further research should employ precise, quantitative data concerning requisite geologic information about sedimentary rock aquifer system.

Key words: Pumping; karst; drawdown; transmissibility; residual; permeability soil geochemistry

Affiliation Info: ¹ Department of Earth Sciences, Olabisi Onabanjo University Ago-Iwoye, P.M.B 2002, Ago-Iwoye, Ogun State, Nigeria.

Corresponding Author : Ishola, S. A. PhD, Exploration Geophysics and Geomathematics; Email: ishola.sakirudeen@oouagoiwoye.edu.ng.

Citation: Ishola, S.A. 2025. Comparative assessment of aquifers in a typical karst sedimentary system, South-West Nigeria. *Naturalis Scientias*, 2 (2): 494-516. DOI: <https://doi.org/10.62252/NSS.2025.1031>. www.naturalisscientias.com.

Copyright © 2025 by the author. Published by *Naturalis Scientias*. This is an open access article under the Creative Commons Attribution-NonCommercial 4.0 International (CC BY-NC 4.0) License. (<https://creativecommons.org/licenses/by-nc/4.0/>).



1. Introduction

Water bearing rocks in large quantity are found in the sedimentary rocks, the basement rocks which underlies the area though hydrogeologically problematic appears to present relatively good ground water potential thought to be the reliable aquifers for small scale village, institution, industries and other water supply schemes. Comparative assessment of aquifers in a typical sedimentary system is crucial for understanding groundwater resources, vulnerability to contamination and optimizing water management strategies. This analysis helps to identify variations in aquifer properties like storage, permeability, and recharge rates allowing for tailored resource extraction and protection measures¹. By comparing the hydrogeological characteristics of different aquifers, scientists can assess their susceptibility to contamination. Factors like the presence of confining layers, the depth of the water table and the type of geological formations all influence how easily pollutants can reach groundwater. Comparative analysis provides the data needed to make informed decisions about groundwater extraction, recharge and protection. Understanding the storage capacity, recharge potential and potential for contamination in different aquifers allows for better planning and management of resources. Comparative assessments help to delineate different aquifer types within a sedimentary system. For example, some sedimentary units may be more permeable and thus better suited for groundwater extraction while others might be prone to contamination. Comparative assessments can highlight the geological controls on aquifer behavior. For instance, certain rock types or formations may naturally act as barriers to pollutant migration while others might be more susceptible¹⁻². It explained that the crystalline rocks are poor ground water regions with recorded average yield of 3960 liters /hrs (880gph) at average depth of 37.3m (123ft) and over 30% failure rate in water borehole drilling³. Previous work shows that sedimentary aquifers give higher groundwater yield than the basement complex aquifer. The evaluation of depth, yield and specific capacity of tube wells which tap the Abeokuta and Ewekoro formations (Dahomey Basin) and coastal plain sands with recent alluvium, in the Niger delta get complex⁴. These are important aquifer units in the Dahomey basin and Niger delta complex respectively. It is revealed that yields in excess of 10,000 l/hrs are common as a result of lateral changes in lithology of the Abeokuta formation and coastal Plain sands. The evaluations of the various aquifer units in the Anambra basin, and on the basis of grain-size distribution were carried out in 1983 by Egboka⁵. The Ajali sandstone is identified to have great potentials for groundwater with a total discharge of $9.6 \times 10^5 \text{ m}^3 \text{ yr}^{-1}$. Although the water bearing rocks in large quantity are the sedimentary rocks, the basement rocks though may be hydrogeologically problematic appears to present relatively good ground water potential thought to be the reliable aquifers for small scale village, institution, industries and other water supply schemes. By understanding the strengths and weaknesses of different aquifers, managers can develop strategies for sustainable groundwater use. This could involve prioritizing extraction from more robust aquifers implementing measures to protect vulnerable aquifers and promoting sustainable recharge practices considers accurate estimation of aquifer properties from grain-size distribution data crucial for successful groundwater development and management practices²⁻⁷. However, this method is inadequate as its ability to define precisely, aquifer geometry and hydraulic boundaries is limited to sedimentary basins. Offodile is of that the idea that more productive aquifers occur in sedimentary geologic formations than in weathered and fractured crystalline



rocks⁸. Some researchers employed textural characteristics to define the hydraulic conductivity of the Ajali sandstone in the Anambra basin⁹. Classical analytical method of pumping test is expensive and depends on aquifer's hydraulic boundaries and geometry, but remains the only reasonable procedure for obtaining accurate transmitting properties in the basement aquifer. In hydrogeological literature, the petrology of the basement complex has a considerable influence on flow direction and potential zones of groundwater. Offodile shows that over 50 % failure rates have been recorded from the boreholes drilled so far in the basement complex area¹⁰. The Abeokuta group, coastal plain sand, Ewekoro formation and recent sediment constitute aquifers in the Dahomey basin in which the study area is found. Sand and Gravel constitute materials in the aquifer of recent sediment, coastal plain sand and Abeokuta formation while limestone forms the aquifer material in Ewekoro formation. Most wells in the area for domestic water supply are shallow hand-dug wells. These wells make use of generally small, discrete bodies of groundwater in the weathered zone; their yield varies enormously and many fail completely towards the end of the dry season. Also, Limestone is a sedimentary rock composed largely of the minerals calcite and aragonite, which are different crystal forms of calcium carbonate (CaCO_3). Many limestones are composed of skeletal fragments of marine organisms such as coral or foraminifera. Limestone makes up about 10 % of the total volume of all sedimentary rocks. The solubility of limestone in water and weak acid solutions leads to karst landscapes, in which water erodes the limestone over thousands to millions of years. Most cave systems are through limestone bedrock. Limestone is a very common sedimentary rock consisting of more than 50 % calcium carbonate. Although it occurs in many different forms, its origins can be traced back to either chemical or biochemical processes that occurred in the geological past, often tens to hundreds of millions of years ago. Many different types of marine organisms have developed the ability to precipitate calcium carbonate from seawater to serve as a protective shell or exoskeleton. For example, scallops have a two-piece outer shell that can be opened to allow the scallop to feed and closed to give protection, whereas bryozoans produce an outer casing within which they live. When these organisms die, their shells accumulate on the seafloor. The soft parts decay, leaving only the hard shells (exoskeletons or tests), which typically become broken down by current action and biological predators. Over long periods of time, the loose skeletal sediments are transformed into bioclastic limestone by the addition of chemically precipitated carbonate cement between the shell fragments. In the warm low-latitude waters of the tropics, these are called tropical bioclastic limestones, while in the cooler waters, at mid to high latitudes, they are known as temperate bioclastic limestones. In the case of large congregations of tropical marine organisms, like reef-building corals, the normally very large structure remains intact as it is transformed into tropical limestone reef rock. Limestone is the primary constituent raw material for cement manufacturing. Physical observation of Ewekoro limestone deposit reveals the rock to be highly fossiliferous with the identified fossils indicating deposition in an open shelf environment. Moreover, the limestone deposit was equally observed to be principally mud supported which is indicative of rocks deposited in quiet water and a low energy environment¹¹. Groundwater in the study area is recharged from, and eventually flows to, the surface naturally. Water flows directly between the surface and the saturated zone of an overburden aquifer, which is unconfined. The deeper parts of unconfined aquifers are usually more saturated since gravity causes water to flow downward. Aquifer characteristics vary with the mode of geological formation, mineralogical composition and structure of the substrate as well as the



topography in which they occur. Generally, fractured crystalline rocks yield smaller quantities of groundwater in many environments in comparison with sedimentary aquifer. This makes it an important resource which can act as a natural storage that can buffer against shortages of surface water, as in during times of drought. Groundwater is naturally replenished by surface water from rivers when this recharge reaches the water table.

However, favourable geophysical and geological evidences improved the chances of locating joints and fracture zones in order to obtain a considerable amount of water from this source. This is evident as most crystalline rocks in Nigeria are located in high relief areas where runoff is high and infiltration rate is low. These are complemented by tropical climatic condition, as the crystalline rocks weather more easily and deeply only under humid condition. High cost of drilling tube wells hindered intensive research on hydrogeology of crystalline rocks in Nigeria. However serious research began in recently times, due to rapidity in urban development and improved economy. In this research work emphasis is placed on the quantitative evaluation of the practical yields of wells and aquifer by field and analytical methods¹². The hydraulic properties of the aquifer and appropriate groundwater formulae are used to construct a mathematical model which provides a means of evaluating the performance of the sedimentary aquifer system. This will enable a workable data can be obtained from a considerable number of tube wells, which are widely distributed in the southwestern Nigeria. It is expected that this simple approach to organizing, conducting, and interpreting complex aquifer test data will turn into information that is understandable and useful to better explain the varying values of yield often reported for sedimentary aquifers in the literature. Nevertheless, recent experiences have shown that with appropriate knowledge of the geology and adequate hydro-geophysical surveys with improved drilling techniques much better results can be achieved. When compared with other areas in southern Nigeria with similar rainfall but different hydrogeological environments, the pattern of perennial streams is close. The greater part of the Ewekoro depression is a potential artesian basin but this swampy belt is only sparsely settled and the source of groundwater has been little developed. However, with the growing demands of industry and the need for uncontaminated domestic supplies, an increasing number of water wells are being drilled in the sedimentary rocks. Therefore, in this work comparative analyses were carried out for the Hydraulic evaluations of Sedimentary Karst auriferous System of Ewekoro communities namely Wasinmi, Itori, Ewekoro and Papalanto, South-West Nigeria in order to provide a foundation for making informed decisions about groundwater resources particularly in the context of the complex and varied geological environments of sedimentary system.

2. Theoretical background

The determination of specific yield of a given aquifer is the primary objective of pumping tests aquifer which are often undertaking by field hydrogeologists for the purpose of evaluating the hydraulic attributes of auriferous zones¹³⁻¹⁴. It encompasses pumping water from a given well and consequent measure of the rate of pumping and the corresponding drawdown level of the pumped well, where the output of measurement can be integrated with the appropriate empirical formula for the establishment of the hydraulic parameters of the aquifer¹⁵⁻¹⁷. During the pumping process, the volume of dewatered material found in the

cone of depression can be obtained. The specific yield can then be established by comparing the volume of dewatered material with the total volume of discharged water. The solution of an exponential series that converges very slowly serves as the requirement for the computations of the volume of dewatered material which can be challenging in terms of time consumption and the tasks involved¹²⁻¹⁸.

Earlier research reported that it may be quite easy to directly apply the standard formulae to pumping test field data obtained in a water–table aquifer that are shallow as a result of slow state of the drainage system and (or) variable state of discharge¹³⁻¹⁵. Nevertheless, we can apply the general equilibrium formula if a constant pumping rate Q is experienced for a sufficient period of Time T such that so that the cone of depression reaches approximate equilibrium form is attained by the cone of depression and the decline encountered in the process is also in a slow state. As pumping process progresses, the establishment of a hydraulic gradient which essentially serves as an equilibrium gradient would be found closer to the pumped well, and water would then be transmitted to the well via the auriferous zone in an approximate amount closer to the amount that is being pumped if not in exact proportion. The declined level of the water table as well as the resulting unwatered material in this area would consequently be much slower¹⁴. The basic assumptions adopted in configuration of the general equilibrium formula and reported by authors from published literature of other works are applied here¹²⁻²¹. Although, the decline in water table decline progresses slowly, the assumption that the attainment of steady-state conditions involves only, little error not greater than that observed as fluctuation encountered in pump discharge. An isotropic cum homogeneous water-bearing bed of infinite areal extent is assumed to lie on a relatively impervious formation¹⁴⁻¹⁵. The discharging well, equipped with a pump, is fully screened to the bottom of the water-bearing material. Furthermore, it is assumed that the mobility of water from the outer radius of the screen to the pump intake occurs without loss of head or with a head loss that is insignificant compared with the drawdown in the well. Also, the potentiometric surface of the aquifer is horizontal or nearly horizontal prior to the start of the pumping. The potentiometric surface of the aquifer is horizontal prior to the start of the pumping. The potentiometric surface is not changing with time prior to the start of the pumping rather all changes in the position of the potentiometric surface are the resultant effects of the pumping well alone. Darcy's law is valid and groundwater flow is horizontal¹⁵. The water table before pumping, and the underlying impervious bed, are assumed to be horizontal and infinite horizontal extent. Groundwater has a constant viscosity and density. It is assumed also that there is no recharge to the aquifer during the test and that all the water pumped is removed from storage.

The following terms and representations are utilized in the mathematical derivations for this study where K represents the hydraulic conductivity (LT^{-1}), $\frac{\rho}{\gamma}$ represents the hydrostatic pressure potential (L) and Z represents the gravitational potential (L). The negative sign observed in the equation is an indication that the flow mobility follow the direction of decreasing head, v_s defines the rate of flow which can follow any direction via a porous medium and is proportional to the negative rate of change of head in that direction. Q represents the discharge rate of the pumped well in gallons per day, P represents the field coefficient of permeability of the aquifer in gallons per day per square foot under a unit hydraulic gradient occurring at the prevailing water temperature, r is the horizontal distance from the axis of the pumped well to a point on the cone of depression, in feet, s is the



drawdown at distance r , in feet, s_w is the drawdown just outside the screen of the pumped well, in feet while m represents the thickness of the zone of saturation before pumping or the height of the static water table above the aquifer bottom, in feet

T is the coefficient of transmissibility of the aquifer in gallons per day per foot. It is the measured flow through a vertical strip of the aquifer 1 foot wide and extending via the saturated height of the aquifer, at unit hydraulic gradient. T is technically equal to Pm . Darcy's law can be expressed in a differential form where the velocity of the flow in this direction is given as v_s .

$$v_s = \frac{K\partial(\frac{\rho}{\gamma}+Z)}{\partial s} \quad 1.0$$

If the head; $h(x,y,t) = \frac{\rho}{\gamma} + Z$ is differentiated with respect to s , we obtain equation (2.0)

$$\frac{\partial h}{\partial s} = \frac{\partial(\frac{\rho}{\gamma}+Z)}{\partial s} \quad 2.0$$

If equation (2.0) is substituted into equation (1.0), we obtain equation (3.0)

$$v_s = \frac{K\partial h}{\partial s} \quad 3.0$$

From Darcy's law, groundwater discharge is expressed in equation (4.0) as:

$$Q = 2\pi P(-\frac{\partial s}{\partial r})(m - s) \quad 4.0$$

$$\frac{\partial r}{r} = -\frac{2\pi P}{Q}(m - s) \partial s = -a(m - s)\partial s \quad 5.0$$

$$\text{Where } a = \frac{2\pi P}{Q}$$

$$\text{Integrating, } \ln r = -ams + \frac{as^2}{2} + \ln\beta \quad 6.0$$

Where β is the constant of integration.

$$\text{Then } r = \beta e^{-ams + \frac{as^2}{2}} \quad 7.0$$

The description of the cone of depression when it has virtually attained an equilibrium shape or position is expressed in Equation (7.0) while the volume of dewatered material in cubic feet, V within the cone of depression is expressed in equation (8.0)

$$V = \int_0^{s_w} r^2 \partial s \quad 8.0$$

The limits of integration are being chosen at zero drawdown (for example, the extent of the cone at equilibrium) and at the drawdown outside the screen of the pumped well. The value of r in equation (8.0) may therefore be substituted in equation (5.0) thereby resulting to equation (9.0).

$$V = \pi\beta^2 \int_0^{s_w} e^{-2ams + \frac{as^2}{2}} \partial s \quad 9.0$$

the exponent in equation (9.0) may be written in the equivalent form $[-2ams + (1 - \frac{s}{2m})]$, $\frac{s}{2m}$ may be ignored because it is generally small compared to unity; therefore, equation (9) becomes

$$V = \pi\beta^2 \int_0^{s_w} e^{-2ams} \partial s \quad 10.0$$

$$V = \frac{\pi\beta^2}{-2ams} [e^{-2ams}]_0^{s_w} \quad 11.0$$

$$V = \frac{\pi\beta^2}{2am} \left[1 - \frac{1}{e^{2ams_w}} \right] \quad 12.0$$

For values found during field pumping tests, $2ams_w > 1$

Hence, $\frac{1}{e^{2ams_w}}$ is very small and can be ignored¹⁴. Therefore, equation 9.0 results to

$$V = \frac{\pi\beta^2}{2am} \quad 13.0$$

β can be obtained from from equation (7.0) as $\beta = re^{ams - \frac{as^2}{2}}$

Which when the value of β is substituted in equation (13.0), equation (14.0) is derived as

$$V = \frac{\pi r^2 e^{2ams - as^2}}{2am} \quad 14.0$$

If the exponent of e is re-modified, in the manner shown in equation (10.0), equation (15.0) can be expressed in a simplified form

$$V = \frac{\pi r^2 e^{2ams}}{2am} \quad 15.0$$

Equation (15.0) fully represents the volume of dewatered material as expressed in terms of permeability, drawdown, horizontal distance, aquifer thickness, and pumping rate.

It is often necessary to accomplish pumping tests in hydro-geological site investigations by harnessing wells that only penetrate the aquifer completely or for which insufficient data are available. Therefore, it may be not be possible to determine the coefficient of permeability, P or the full aquifer thickness, m under such circumstances; equation 7.0 cannot be used to determine the volume of dewatered material in the cone of depression¹²⁻²². However, if the drawdown, s at the point of observation is small compared to suspected thickness of the zone of saturation, the thickness may be assumed to remain uniform and Transmissibility, T may be used in lieu of the unknown permeability and aquifer thickness ($T = Pm$).

Several standard groundwater formulae are permitted the direct computations and consequent determination of the coefficient of transmissibility. Therefore, equation (15.0) may re-modified further by substituting therein the equivalents $\frac{2\pi P}{Q}$ for a and T for the product Pm , which yields

$$V = \frac{\pi r^2 e^{4\pi \frac{T_s}{Q}}}{\frac{4\pi T}{Q}}$$

$$V = \frac{Qr^2 e^{4\pi \frac{T_s}{Q}}}{4T} \quad 16.0$$

Taking the logarithm of both sides of equation (16.0) produces

$$\text{Log } V = \text{Log } \frac{Qr^2}{4T} + \frac{4\pi T_s}{Q} \text{Log } e$$

$$\text{Log } V = \text{Log } \frac{Qr^2}{4T} + \frac{5.45 T_s}{Q} \quad 17.0$$

The specific yield can therefore be obtained as the volume of water pumped during the test divided by the gross volume of dewatered material within the cone of depression¹²⁻²².

$$S_Y = \frac{Qt}{7.48V} \quad 18.0$$

Where S_Y = specific yield

Q = average discharge rate of the pumped well in gallons per day

T = time in days, since pumping began

V = volume of dewatered material in cubic feet delivered from either equation 15.0 or 17.0

It is worthy of note that observed formulae derived in this work may be applied only on the condition that the data from an equilibrium pumping test and the test itself should be granted sufficient time long enough for the allowance of the greatest possible dewatering status in the cone of depression without it being affected by prospective recharge¹²⁻¹⁴.

3. Materials and methods

3.1 Location and accessibility of the study area

Ewekoro community in Ogun State is one of the mills of West African Portland Cement Company (WAPCO) and Dangote group Cement Company. It is a sleepy neighbouring town to Papanalato, a name known for sugarcane plantation. It lies between latitude $6^{\circ}53'1''\text{N}$ and longitude $3^{\circ}14'1''\text{E}$. The sedimentary rocks of Ogun State consist of Ewekoro formation and Abeokuta formation. The Ewekoro formation is fossiliferous and consists of economic deposits of limestones that is quarried by WAPCO²³. WAPCO being a public limited liability company registered in Nigeria with its corporate headquarter originally located in Ikeja in Lagos State but later relocated to Ewekoro and Shagamu in Ogun State. The factory occupies approximately 0.4 hectares of land and it was incorporated by the West African Portland Cement Company in March 1959. Production started in 1960 with only one kiln. The initial production was 200,000 tons per annum. The second kiln was constructed in 1967 and this has increased the total annual production 450,000 tons.

3.2 Weather, climate and vegetation



The study areas is generally a low lying to gentle undulating terrain that falls within the humid tropical climate characterized by two distinct seasons predominant in the tropics in the southern part of Nigeria namely, the wet and dry seasons. The wet season usually occur from March to October, the climate is dominated by the tropical maritime air mass or moisture laden Southwest winds from the Atlantic Ocean that produces heavy rainfall; most of the rainfall comes in torrential showers resulting in high run-off while the dry season occurs from November to late February or early March under the influence of the dry continental air mass or North-Easterly winds from Sahara desert. The little dry season in the mid-west season of July/August months is dominant in the area²⁴⁻²⁵. The haematin season, a season of dusty high winds, unusual cold and extremely dry conditions, lasts from November to February. It is caused by the tropical continental air from the Sahara Desert which displaces the tropical Maritime air from the Gulf Guinea²⁶. Ewekoro has no distinct temperature seasons; the temperature is relatively constant during the year. The wet season ensures adequate supply of water and continuous presence of moisture in the air. Hence, the study area experiences high diurnal and annual temperature, lack of cold season, high precipitation, low pressure, high evapotranspiration and high relative humidity²⁵⁻²⁷. The temperatures at night are cooler than during the daytime. November is an average, the month with most sunshine. February is the warmest with an average monthly temperature of 33.5⁰C at noon. August is coldest with an average temperature of 21.9 ⁰C. Rainfall and other precipitation peaks around June. The time around January is the driest.

The study area has a mean annual temperature of 27 ⁰C in July and 32 ⁰C in February, and the average monthly temperature of 25.7 ⁰C. It has relative high humidity of 71.09 % and long wet season that ensures adequate supply of water and continuous presence of moisture in the air. The annual rainfall is estimated to be 1194.33 mm²⁴⁻²⁹. Cold and hazy conditions are usually prevailing especially towards the end of the year while hot and dusty conditions are experienced during dry season. Hence, the study area is characterized by high diurnal and annual temperature, high precipitation, low pressure, high evapo-transpiration and high relative humidity. The major water bodies in the region are Yewa and Ogun rivers which flow into Lagos lagoon while their tributaries are found in Ewekoro Local Government Area as Alaguntan River, Akinbo River and Eshe River. There are however streams running parallel in the area. Also ponds are not left out. Due to the alternation of wet and dry seasons, the water table fluctuates in response to the seasonality of rainfall. During the wet season, groundwater level rises towards the surface and drops as the dry season sets in. The natural vegetation of Ogun State which the study areas belong consists of the forest and the savanna which affect the floristic composition of the plant communities. The forest vegetation is of two types, namely, the fresh water swamp forest and the lowland rain forest. The savanna found in the State is mainly of the derived savanna type. The rainforest vegetation is typified by perennial trees which may vary in height forming storey with characteristics thick vegetation due to high rainfall. The vegetation changes with seasons with the incoming of the rains, the green grasses are back to life and the foliage of the trees becomes green and thick. Where the soil is wet due to river drainage denser fringing forest are found. During dry season some of the trees, which develop umbrella shaped canopies shed their leaves in order to minimize loss of water by transpiration³⁰. The river and the river-fed wetlands support a large number of plants. The wetlands are main sources of freshwater for drinking, domestic and agricultural uses. In the recent years it cannot be considered for drinking and domestic purposes due to variety of pollutants and contaminants from multiple sources such as industrial outputs, irrigation return flow,



domestic discharges and hospital disposals, aggregating the situation water pollution and contamination. Most of these wetlands get dried in dry season and serves as a dumping yard for garbage and industrial wastes. Water-borne diseases have reported in many places of the area where proper sanitation facilities are lacking.

Human activities on the natural vegetation have reduced the original forest to secondary forest bush, regrowth and thickets. One very important impact of the quarry is deforestation. This simply means the loss of vegetation cover that is necessitated by the need to move equipment to the site, removal of the topsoil or (overburden) stemming of explosives and removal of blasted limestones. These effects are normally reduced by appropriate mitigating actions such as massive reclamation of the mined areas using new overburden materials and a forestation programme that involve planting of varieties of trees that have ornamental values, that can hold the soil structure well and could cover the exposed land well. Limestone mining in Ewekoro had resulted into the conversion of many farmlands and settlements into quarry sites. The house types on the site are mainly the makeshift type built for use on no permanent basis. The few landowners on the factory site are resident on site to participate in cement business and no longer to farm as it was before now. The West Africa Portland cement according to the management made frantic effort at re-settling the landowners in the estate built very close to the factory. But since this was rejected, a programme of gradual takeover of the old farm site had started. In the course of using the quarry, farmers had been stopped from the site and the cutting/felling of the trees continued, resulting into a large Expanse of land exposed to rain water and wind. The lake created as a result of blasting of limestone and release of water from within the Limestone deposit ordinarily should serve as habitat to fresh water fish, this has however not been developed. The ammonium compound washed into the lake from its primary source (explosive materials) may serve as manure and may encourage the growth of plankton, algae and aid the liming of the lake and encourage fish production. However, the possibility of having an excess quantity of the ammonium compound washed into the lake may pose a serious hazard on the lives of the aquatic animals¹⁹. The entire study area is generally accessible by major roads and several footpaths, although the road from Abeokuta town to the investigated area is tarred. In addition to Ewekoro-Papalanto road, the survey locations can equally be accessed through a major road from Lagos State through Sango-Ifo express road³¹.

3.3 Deposit geology and hydrogeological setting

Ewekoro formation which is the geology of the study area is an integral part of the sedimentary rocks of Ogun State typically comprising of Ewekoro formation and Abeokuta formation. The Ewekoro formation serves as economic deposits of limestones quarried by WAPCO and it is highly fossiliferous¹⁴. It is generally consistent in line with the regional geology of Eastern Dahomey Basin where non-crystalline and highly non-fossiliferous limestone and thinly laminated fissile and little non-fossiliferous shale were dominant³². The composition of the limestone at the type locality is about 11m to 12m with varying thickness and resistivity; sandy at the base with downward grading towards Abeokuta formation, overlain by phosphoric glauconitic grey shale with some of the well information revealing a thick overburden of between 3m and 16m consisting of silt, clay, sand shale with some alluvium and lateritic deposits in some places¹⁹⁻²⁹. The limestone thickness

ranged between 3m and 40m; the thickest section was found at Fashola community (38.3m) while the thinnest section was identified at Jaguna (1.6m). The overburden thickness varied between 2m to 16m. The reserve estimation the limestone deposit was estimated to be 7.75×10^8 cubic meters and adjudged to be of economic value if exploited especially around Fashola autonomous community in Papalanto. The limestone classifications based on microfacies revealed biomicroparite, shelly biomicrites, algal biosparite and phosphoric biomicrites in stratigraphic sequence³¹. The rock is relatively soft and friable but in some places cemented by ferruginous and siliceous materials. The lithological units in Ewekoro formation are clayey sand, clay, shale, marl, limestone and sandstone³³. On the lithostratigraphic setting, the lithology of Ise and Afowo formations were identified by³⁴ revealing a reasonable level of similarity essentially in sands and sandstones, but with thick shaly interbeddings. It was later observed that the Ise, Afowo and Abeokuta formations share similar lithology and electric log signatures. The uppermost sections of Abeokuta formation cropping out in Ijebu Ode and in shallow boreholes at Itori, Wasimi and Ishaga onshore were found to primarily consist of fine to coarse grained sand and shale, mudstone, limestone and silt as interbeds; there were good correlations of these lithofacies with the upper section of the neostrato type in Ojo-1 borehole³⁵. Jones and Hockey (1964) revealed that Ewekoro limestone and the overlying Akinbo shale to be of lateral equivalents to the Imo formation of eastern Nigeria. The stratigraphy, depositional characteristics of limestone lithofacies and their corresponding hydrogeological characteristics in South-Western Nigeria were equally investigated by other researchers³³⁻³⁷. Although, the more prolific water bearing rocks are the sedimentary rocks but the basement rocks though hydrogeologically challenging appears also serves as potential groundwater sources meeting the domestic needs of small scale village, institution, industries and other water supply schemes.

Furthermore, Some study reported that the crystalline rocks display poor groundwater yield with recorded with recorded mean yield of 880gph (3960 liters /hrs) at mean depth of 123ft (37.3m) and well over 30% failure rate were recorded for borehole drilling³. Sedimentary aquifers have been reported to possess higher rate of groundwater production than the basement complex aquifer¹⁴. Figure 1 shows the Geological Map of the investigated Location within the Nigerian Part of Dahomey Embayment, the map of Ogun State displaying the geology of the study areas is presented in Figure 2, the inset map showing political divisions of the study area within Nigerian continental environment is shown in Figure 3 while Figure 4 is the data acquisition map showing the investigated locations in Ewekoro LGA, Southwest Nigeria¹⁹.

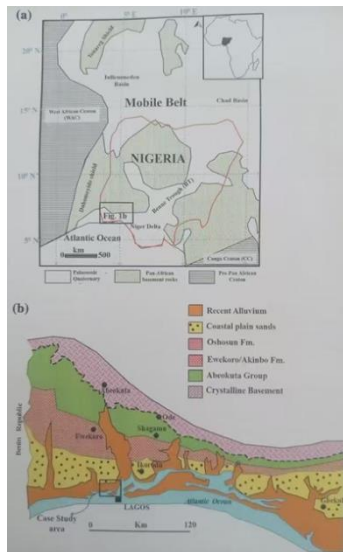


Figure 1. Geological map showing the selected locations of the study area within the Nigerian, part of Dahomey Embayment^{19 & 38}

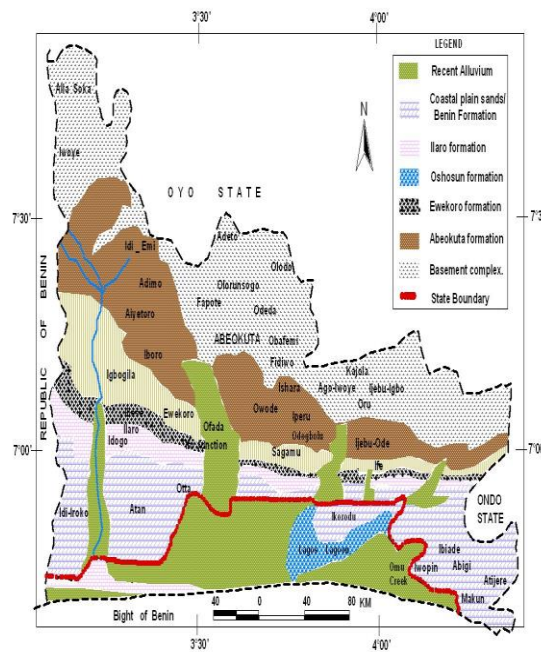


Figure 2. A map of Ogun State showing the geology of the study areas (after Kehinde-Phillips and Obiora & Onwunka)³⁹⁻⁴⁰

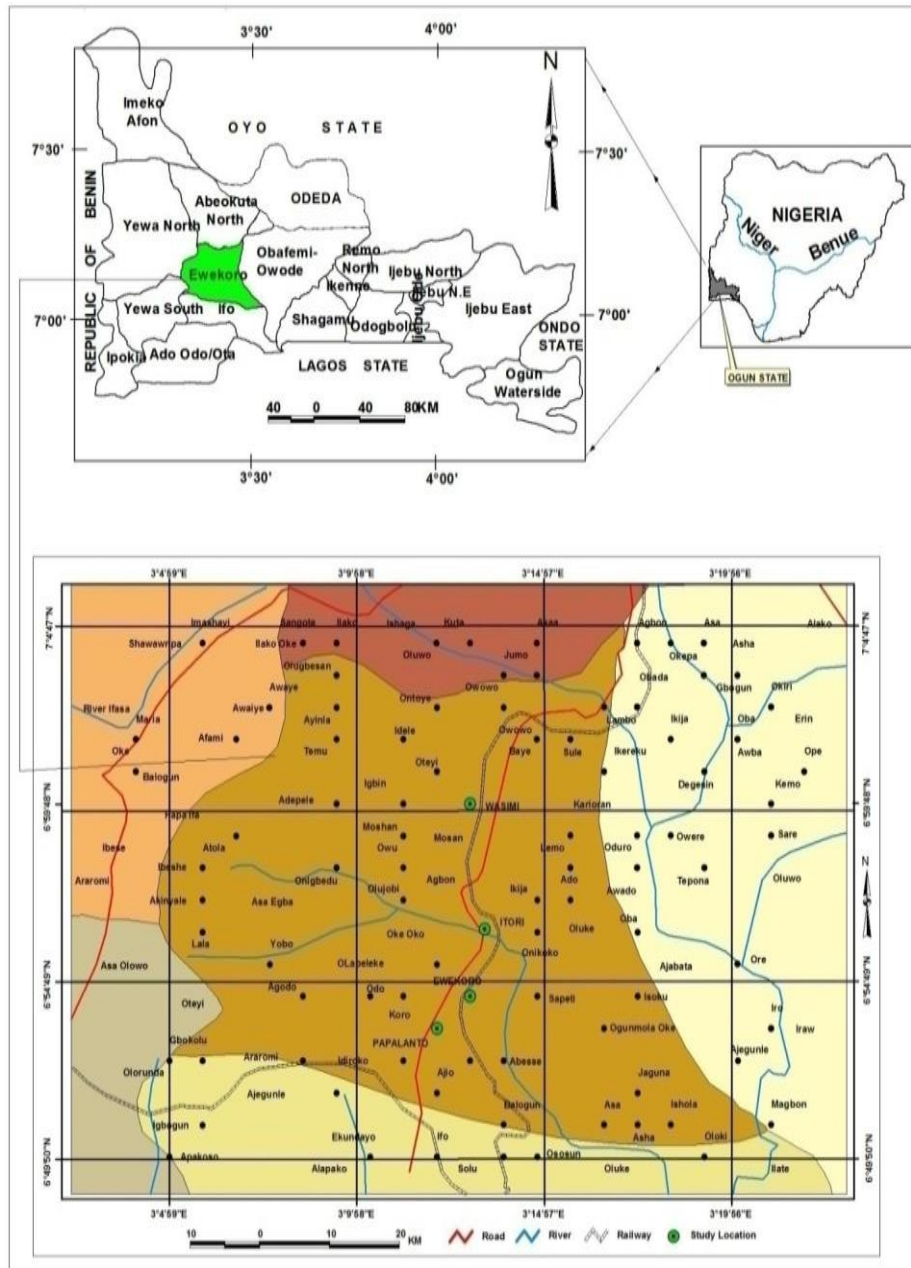


Figure 3. Inset map showing the study areas in Ogun State within Nigeria continental domain using Esri - data/nigeria political information in Arcview GIS 3.2A environment¹⁹

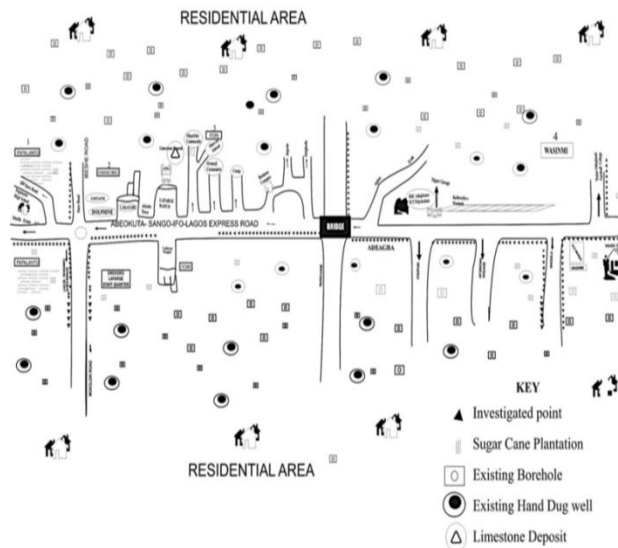


Figure 4. Base map showing the existence, location and accessibility of the investigated points in Ewekoro LGA, Southwest Nigeria¹⁹

4. Field data acquisition

Two major sources of data were used in this study. These are primary and secondary data. The primary data consisted of reconnaissance survey and personal visits to locations of existing boreholes and hand-dug wells in the study area, identifying sampling points and collecting well inventory. Practicing consultants on borehole drilling in Ewekoro Local Government Area were also contacted for information on the boreholes drilled in the study area. The secondary data consisted of published and unpublished documents for relevant information, such information were extracted from journals, conference papers and available textbooks. Existing drilled boreholes were identified across the study areas and where there were no boreholes and well inventories of hand-dug wells were collected. The depth of the boreholes and the overburden thickness were measured using dip metre⁴¹.

5. Constant rate pumping test

Constant rate pumping tests were conducted on the selected boreholes. The materials used for these tests included; 60-litre gallons as a standard measure, generating set to power the pump, stop watch to record time intervals and rubber hose connected to the pipe from the borehole to discharge the water into the gallons. In conducting this test, the initial or static level of the water in the boreholes was measured using a dip metre. The generating set was thereafter switched on to start the pumping. The pumping was allowed to run continuously for a long period of two hours before the rate of pumping was adjusted for the boreholes to maintain constant discharge. At this point, the water level was measured to know the drawdown and a calibrated 60-litre gallon was then filled from the constant discharge from the boreholes while a stopwatch was simultaneously set to record the time taken, in seconds, to fill the bucket. This process was repeated for four hours for each of the selected

boreholes. It was therefore observed that the water level and the drawdown in the boreholes were constant throughout the four hours pumping. With the constant discharge from the boreholes, a state of equilibrium was maintained between the rate of discharge and the rate of recharge from the aquifer. In this condition of equilibrium, the rate of pumping or discharge is directly proportional to the yield of the borehole or well at the constant drawdown. In other words, the discharge per unit time in litres per second gives the yield of each of the selected boreholes at the constant drawdown¹⁹.

6. Results

The classification standards of transmissibility Potentials of Aquifer System and the outputs of the basic well inventories and hydraulic properties of the aquifers via boreholes in the study area are presented as summary in Table 1 and Table 2 respectively. In the evaluation of the aquifer characteristics in the study area, groundwater supply to boreholes were abstracted from fractured sandstone/limestone whose depth ranged from 35 to 75m with mean value of 51m; 35 to 85m with mean value of 50.36 in; 35 to 100m with mean value of 60.32m; 38m to 108m with a mean depth of 75.36m respectively recorded for Wasinmi, Itori, Ewekoro and Papalanto. The static water level ranged from 8.45 to 37.4m with mean value of 17.7m to 27.1m with a mean value of 15.1m; 4.41 to 48.1m with a mean value of 22.1m and 3.43 to 54.3m with a mean value of 33.8m respectively recorded for Wasinmi, Itori, Ewekoro and Papalanto. The well-heads varied from 0.04 to 0.61m with a mean of 0.33m; 0.33 to 0.52m with a mean of 0.13m; 0.58m to 1.38m with a mean of 0.15m and 0.33 to 0.46m with a mean of 0.30m respectively recorded for Wasinmi, Itori, Ewekoro and Papalanto. The observed residual drawdown varied between 3.67 to 11.4m with a mean value of 8.17m; 3.28 to 11.3m with a mean value of 8.41m; 3.53 to 11.6m with a mean value of 7.48m and 2.84m to 12.0m with mean value of 8.10m respectively recorded for Wasinmi, Itori, Ewekoro and Papalanto while the recovery time varied from 850 to 3431s with a mean value of 2254s; 1015 to 8352s with a mean value of 2391; 1566 to 3150s with a mean value of 2483 and 1030 to 3110s with a mean value of 2218s respectively recorded for Wasinmi, Itori, Ewekoro and Papalanto.

Table 1. Transmissibility potentials of the aquifer system^{19, 49 & 56-57}

Transmissibility (T) Range (m ² /day)	Aquifer Potentiality Classification
> 500	High Potentials
100–500	Good Potentials
50–100	Moderately Potentials
5–50	Low Potentials
0.5–5	Very Low Potentials
<0.5	Negligible Potentials



Table 2. Summary of basic and estimated hydraulic parameters of studied aquifer systems of boreholes in selected locations in Ewekoro communities

BASIC HYDRAULIC PARAMETERS							ESTIMATED HYDRAULIC PARAMETERS				
Locations	Well Head (m)	Borehole Depth (m)	Borehole diameter (mm)	Static Water Level (m)	Residual Drawdown (m)	Recovery Time (s)	Specific Discharge Q (l/s)	Specific Capacity Cs (m ² /s)	Well Loss WLC (s ² /m ⁵)	Transmissibility T (m ² /s)	Optimum Operating Capacity OOC
Wasimmi Boreholes											
MEAN	0.33	51	84.80	17.8	8.17	2254	4.0×10 ⁻²	6.3×10 ⁻³	5.98×10 ⁴	4.5×10 ⁻¹	0.252×10 ⁻⁴
MAX	0.61	75.00	125.00	37.4	11.4	3431	11.0×10 ⁻²	2.0×10 ⁻²	2.73×10 ⁶	9.2×10 ⁻¹	2.20×10 ⁻³
MIN	0.04	35.00	25.00	8.45	3.67	850	1.0×10 ⁻²	1.0×10 ⁻⁴	4.77×10 ⁴	1.00×10 ⁻²	1.00×10 ⁻⁶
S.D	0.11	11.58	46.18	8.47	2.49	838	2.0×10 ⁻²	5.0×10 ⁻²	5.60×10 ⁴	2.6×10 ⁻¹	1.00×10 ⁻⁴
CV (%)	33	23	55	48	31	37	50	79	94	58	40
Itori Boreholes											
MEAN	0.33	50.36	87.60	15.1	8.41	2391	5.0×10 ⁻²	7.0×10 ⁻²	4.30×10 ⁵	1.00×10 ⁻²	3.50×10 ⁻³
MAX	0.52	85.00	140.00	27.1	11.3	8352	11×10 ⁻²	48.0×10 ⁻²	1.28×10 ⁴	7.00×10 ⁻²	5.28×10 ⁻²
MIN	0.13	35.00	25.00	3.25	3.28	1015	3.0×10 ⁻²	1.0×10 ⁻²	8.57×10 ⁴	1.00×10 ⁻⁴	3.00×10 ⁻⁴
S.D	0.11	15.07	44.70	7.53	2.51	1418	2.0×10 ⁻²	9.0×10 ⁻²	3.69×10 ⁵	2.00×10 ⁻²	1.80×10 ⁻³
CV (%)	33	30	51	50	30	59	40	12	86	200	51
Ewekoro Boreholes											
MEAN	0.58	60.32	109.40	22.1	7.48	2483	4.0×10 ⁻²	6.0×10 ⁻³	0.616×10 ⁴	9.00×10 ⁻³	2.40×10 ⁻⁴
MAX	1.38	100.0	140.00	48.1	11.6	3150	6.0×10 ⁻²	1.0×10 ⁻²	1.189×10 ⁴	8.00×10 ⁻²	6.00×10 ⁻⁴
MIN	0.15	35.00	25.00	4.41	3.53	1566	3.0×10 ⁻²	1.0×10 ⁻⁴	0.196×10 ⁴	1.00×10 ⁻⁴	3.00×10 ⁻⁶
S.D	0.41	19.15	34.41	14.3	2.45	555	1.0×10 ⁻²	3.0×10 ⁻²	0.365×10 ⁴	1.5×10 ⁻²	3.00×10 ⁻⁵
CV (%)	71	32	32	65	33	22	25	50	59	166	13
Papalanto Boreholes											
MEAN	0.30	75.36	86.600	33.8	8.10	2218	5.0×10 ⁻²	5.0×10 ⁻³	0.519×10 ⁴	9.00×10 ⁻³	2.50×10 ⁻⁴
MAX	0.46	108.0	140.00	54.3	12.0	3110	9.0×10 ⁻²	1.0×10 ⁻²	1.137×10 ⁴	4.00×10 ⁻²	9.00×10 ⁻⁴
MIN	0.33	38.00	25.00	3.43	2.84	1030	3.0×10 ⁻²	1.0×10 ⁻⁴	0.085×10 ⁴	1.0×10 ⁻⁴	3.00×10 ⁻⁶
S.D	0.084	20.73	48.62	16.9	2.65	673	2.0×10 ⁻²	3.0×10 ⁻³	0.307×10 ⁴	7.00×10 ⁻³	6.00×10 ⁻⁵
CV (%)	28	28	56	50	33	30	40	60	59	78	24

7. Discussion

In Wasinmi Boreholes, the studied rock mass aquifer system yields (Q) up to 11.0×10^{-2} l/s with Residual Drawdown (S') ranging between 3.67m and 11.4m. Average Static Water Level (SWL) is 17.8m within a range of 8.45m – 37.4m, while its Depth ranges between 35m and 75m. Mean specific capacity (Cs) and well loss constant (WLC) are 6.30×10^{-3} m²/s and 5.98×10^4 s²/m⁵ respectively, with maximum Transmissibility (T) of 9.2×10^{-1} m²/s (79,488m²/day). Among the tested aquifer properties, Borehole depth (BHD) is the least variable parameter, having coefficient of variation (CV) of 23% followed by Residual Drawdown (S') with CV of 31%. In general, all other parameters have coefficient of variation above 10 %. This implies that the variation caused by the aquifer system on DD, SWL, BHD, Q, Cs, WLC, OOC and T is high enough to be significant in hydrogeological system of Wasinmi Boreholes⁴⁹⁻⁵⁹.

In Itori Boreholes, the studied rock mass aquifer system yields (Q) up to 11.0×10^{-2} l/s with Residual Drawdown (S') ranging between 3.28m and 11.3m. Average Static Water Level (SWL) is 15.1m within a range of 3.25m – 27.1m, while its Depth ranges between 35m and 85m. Mean Specific Capacity (Cs) and Well Loss Constant (WLC) were 7.02×10^{-2} m²/s and 4.30×10^5 s²/m⁵ respectively, with maximum Transmissibility (T) of 7.0×10^{-2} m²/s (6048m²/day). Among the tested aquifer properties, Borehole Specific Capacity (Cs) is the least variable parameter, having coefficient of variation (CV) of 12%; this is in agreement with findings of Knopman and Holliday⁶⁰ followed by Residual Drawdown (S') with CV of 30%. In general, all other parameters have coefficient of variation above 10 %. This implies that the variation caused by the aquifer system on DD, SWL, BHD, Q, Cs, WLC, OOC and T is high enough to be significant in hydrogeological system of Itori Boreholes⁴⁹⁻⁵⁹.

In Ewekoro Boreholes, the studied rock mass aquifer system yields (Q) up to 6.0×10^{-2} l/s with Residual Drawdown (S') ranging between 3.53m and 11.6m. Average Static Water Level (SWL) is 22.1m within a range of 4.41m – 48.1m, while its Depth ranges between 35m and 100m. Mean Specific Capacity (Cs) and Well Loss Constant (WLC) were 6.00×10^{-3} m²/s and 6.16×10^5 s²/m⁵ respectively, with maximum Transmissibility (T) of 8.0×10^{-2} m²/s (6912m²/day). Among the tested aquifer properties, Optimum Operating Capacity (OOC) is the least variable parameter, having coefficient of variation (CV) of 13% followed by Period of Recovery (t) in seconds with CV of 22%. In general, all other parameters have coefficient of variation above 10 %. This implies that the variation caused by the aquifer system on DD, SWL, BHD, Q, Cs, WLC, OOC and T is high enough to be significant in hydrogeological system of Ewekoro Boreholes⁴⁹⁻⁵⁹.

In Papalanto Boreholes, the studied rock mass aquifer system yields (Q) up to 9.0×10^{-2} l/s with Residual Drawdown (S') ranging between 2.84m and 12.0m. Average Static Water Level (SWL) is 33.8m within a range of 3.43m - 54.3m, while its Depth ranges between 38m and 108m. Mean Specific Capacity (Cs) and Well Loss Constant (WLC) are 5.0×10^{-3} m²/s and 0.52×10^4 s²/m⁵ respectively, with maximum Transmissibility (T) of 4.00×10^{-2} m²/s (3456m²/day). Among the tested aquifer properties, Optimum Operating Capacity (OOC) is the least variable parameter, having coefficient of variation (CV) of 22% jointly followed by Well Head (WH) and Borehole Depth (BHD) with CV of 28%. In general, all other parameters have coefficient of variation above 10 %. This implies that the variation caused

by the aquifer system on DD, SWL, BHD, Q, Cs, WLC and T is high enough to be significant in hydrogeological system of Papalanto Boreholes⁴⁹⁻⁵⁹ (Table 2).

The coefficient of variation provides some measure of departure from normality. It is a standardized measure of dispersion of a probability distribution or frequency distribution. A coefficient of variation greater than 100% indicates that the variable in question is not normally distributed. In contrary, a coefficient of variation less than 100% indicates that the data is normally distributed. The coefficient of variation is calculated as follows:

$$CV (\%) = \frac{\sigma}{\mu} \times 100\% \quad 1.4$$

Where CV is the coefficient of variation, σ is the standard deviation, and μ is the arithmetic mean of the distribution.

The data for each tested hydraulic parameter in selected parts of Ewekoro Local Government Area were statistically analyzed by applying the homogeneity test and the results presented in Table 2 alongside with the arithmetic mean and Standard deviation for each hydraulic property.

By applying the normality test and calculation of coefficient of variation for every Hydraulic parameter, it was observed that all the hydraulic units (Basic and Estimated) had normal distribution in all the investigated study area except Transmissibility that exhibited abnormal distribution with Coefficient of Variation of 200% in Itori Boreholes and 166% in Ewekoro Boreholes. When the depths of penetration obtained from the field data were compared to the total depths of the shallow wells dug close to the measurement locations, the results revealed with clear distinction that all the wells at this section were not drilled to the aquifer level; the wells were terminated just slightly above the overburden and some within the overburden. Also, due to the unavoidable irregularities in the size of the borehole and water losses into the fractured rock that occurred in many wells because each construction method adopted has advantages related to the ease of construction, cost factors, character of the formations to be penetrated, well diameter and depth, sanitary protection and intended use of the well itself. Therefore, a careful study of the operating history of the deteriorated and abandoned boreholes and wells in the region should be made in order to reveal some logical steps in devising the maintenance and rehabilitation procedures to be adopted.

8. Conclusions

Evaluation of aquifer properties is often possible with methods of measurement by devising approximate methods of analysis based on idealized models of an aquifer system. Diverse results and variations arise in the attempt to force the application of ideal conditions formulae to sedimentary aquifer situations. Variations of estimated aquifer parameters indicate that the sedimentary nature of the aquifer actually does coincide rather closely with what may be predicted theoretically with model aquifers and mathematical models. It is apparent that quantitative answers to explain the behaviour of the sedimentary rock mass aquifer system depend primarily upon the geologic and hydrologic controls. As the general technique of groundwater resource evaluation is inadequate, a need for more precise,

quantitative data concerning requisite geologic information about typical sedimentary aquifer is strongly recommended.

The varying residual drawdown, high recovery transmissivity, and high specific capacity represent locations that were considered to delineate the potential groundwater zones for development. The aquifer hydraulic characteristics play a major role in the identification of groundwater potential zones, because they reflect the rock structures through which the water flows. In general, transmissivity values greater than 100 m²/day are considered good in hard rock terrains. Basic and estimated aquifer parameters were hydraulically determined based on the existing boreholes in the study areas. Aquifer parameters, such as transmissivity, Specific Discharge and Time required for full recovery, have been analyzed to evaluate the groundwater potential of the study area. Itori borehole has the highest Optimum Operating Capacity with the mean value of 3.50×10^{-2} m²/s. The recovery transmissivity and specific yield are also very high in the study area notably Ewekoro boreholes and Papalanto boreholes with the mean values of 5.02×10^{-2} l/s and 4.02×10^{-2} l/s and 9.00×10^{-2} m²/s. The varying residual drawdown and recovery time observed are due to the structural displacements in the hydrogeological formation of the study area. Low recovery and optimum operating capacity may reflect a lack of secondary porosity, compaction of lithologic units and a shallower weathered layer. The results of the test of normality using the coefficient of variation showed that the field acquired data comprise a highly representative and statistically comparable dataset. The results of the Well loss coefficient reveal most of the studied Boreholes to be either mildly deteriorated or severely deteriorated while few studied wells were unaffected. However, there is availability of groundwater all over the investigation locations in Ewekoro Local Government area that can support domestic and industrial uses. Aside from the expected yield of the studied aquifer system, during the percolation processes potential contaminants from the surface water are removed by filtration, adsorption, reduction and biodegradation while the capacity of self-purification depends mainly on flow velocity, hydraulic residence time and the covered distance determined by the permeability and the hydraulic potential in the aquifer. This hydraulic attempt at assessing the aquifer parameters of this typical sedimentary terrain has revealed the groundwater resource potentials of the study area. The evaluation of the aquifer performance assessment through the constant discharge of the recovery method has provided information regarding the construction and design of discharge wells and development of groundwater in the study area.

9. References

1. Adiat, KAN; Adegoroye, AA; Adebisi, AD; Akeredolu, BE & Akinlalu, AA. 2019. Comparative assessment of aquifer susceptibilities in different geological locations. *Heliyon*, 5 (5): 61-65. <https://doi.org/10.1360/j.helium.2019.e01499>.
2. Akintorinwa, OJ; Atitebi, MO & Akinlalu, AA. 2020. Hydrogeophysical and Aquifer Vulnerability Zonation of a Typical Basement Complex Formation. A Case study of Ododo-Idanre, South-West Nigeria. *Heliyon*, 6 (8): 11-20. <https://doi.org/10.1016/j.heliyon.2020e04541>.
3. Offodile, ME. 1983. The occurrence and exploitation of groundwater: in Nigerian Basement rocks. *Nigeria Journal of Mining and Geology*, 20 (1): 131-146.

4. Jones, HA, & Hockey, RD. 1964. The Geology of parts of Southwestern Nigeria. *Geological Survey of Nigeria Bulletin*, 31 (1): 22-24.
5. Egboka, BCE. 1983. Analysis of the groundwater resources of Nsukka area and environs Anambra State Nigeria. *Journal of Mining and Geology*, 20 (1-2): 1-13.
6. Olanrewaju, I; Rasaan, AI; Ibrahim, KO & Ibrahim, A. 2024. Comparative analysis of aquifer properties in selected geologic terrain. *The Progress Journal of Multidisciplinary Studies*, 5 (2): 12-23. <https://doi.org/10.71016/tp/efnbyt.89.2024>.
7. Uma, KO, Egboka, BCE & Onuoha, KM. 1989. New statistical grain-size method for evaluating the hydraulic conductivity of sandy aquifers. *Journal of Hydrogeology*, 108 (1): 343-366.
8. Offodile, ME. 1992. The occurrence and Exploitation of Groundwater in Nigeria Basement Complex Rocks. *Journal of Mining and Geology*. 28 (2): 5-7.
9. Tijani, MN & Nton, ME. 2009. Hydraulic, textural and geochemical characteristics of the Ajali Formation, Anambra Basin: implication for groundwater quality. *Journal of Environmental Geology*, 56 (2): 935-951.
10. Offodile, ME. 2002. Groundwater study and development in Nigeria. Mecon Geology and Engineering Services Ltd, Jos. *Mecon Geology Bulletin*, 1 (1): 1-453.
11. Akinyemi, LP; Odunaike, RK & Adeyeloja, A. (2015). Physicochemical characterization of limestone deposits at Ewekoro, Ogun State, South-West of Nigeria and the environment impact. *Journal of JEES*, 5 (18): 36. www.iiste.org.
12. Ramsahoye, LE & Lang, SM. 1993. A Simple Method for Determining Specific Yield from Pumping Tests Ground-Water Hydraulics. *Geological Survey Water-Supply Paper*. 136 (3): 41-46.
13. Meizhao, L; Zhonggfeng, X; Zong-Liang, YZ; Hui, L & Meixia, L. 2021. A comprehensive review of specific yield in land surface and groundwater Studies. *Journal of Advances in Modelling Earth Systems*, 13 (1): 13-24.
14. Ishola, SA 2024. Groundwater resource potentials using frequency domain electromagnetic method and associated water quality techniques in Ewekoro communities South-West Nigeria. *Federal University Wukari (FUW) Trends in Science and Technology Journal*, 9 (1): 193-200. www.ftstjournal.com.
15. Balasubramanian, A. 2017. Procedure for conducting pumping tests. *Centre for Advanced Studies in Earth Sciences*, University of Mysore, Mysore. 10-24. <https://doi.org/10.1016/10.13140/RG.2.2.18948.32641>.
16. Gong, C; Zhang, Z; Wang, W; Duan, L & Wang, ZF. 2021. An assessment of different methods to determine the specific yield for estimating groundwater recharges using lysimeters. *The Science of the Total Environment*. 788 (8): 147-799. <https://doi.org/10.1016/j.scitotenv.2021.147799>.
17. Ishola, SA & Gbadebo, AM 2024. Evaluations of the phreatic shallow aquifers using hydraulic and hydraulic and hydrogeochemical techniques in a typical sedimentary part of Ogun State South-West Nigeria. *Journal of Earth Science and Atmospheric Research/JEAR*, 7 (1): 54-71.
18. Pollacco, JA; Galves, JF; Web, T.; Vickers, S; Robertson., R; Mcneill SJE., Liburne, L; Rajannayaka, C & Chau, H. 2024. Derivation of physically based soil hydraulic properties in new Zealand by combining soil physics and hydrogeology. *European Journal of Soil Science*. CCBY-NC-ND. 75 (3): 2-4. <https://doi.org/10.1111/Ejss.13502>.
19. Ishola, SA. 2019. Characterization of groundwater resource potentials using integrated techniques in selected communities within Ewekoro Local Government Area South-West Nigeria. Department of Physics, FUNAAB Ph.D Thesis.



20. Sule, BF; Balogun, OS & Muraina, LB. 2013. Determination of hydraulic characteristics of groundwater aquifer in Ilorin, North-Central Nigeria *Academic Journals*. 8 (25): 1150-1161. <http://www.academicjournals.org/SRE>.
21. Jika, HT & Tse, AC. 2014. Determination of hydraulic characteristics of an aquifer capacity from pumping test: a case study of Konshisha Area, Central Nigeria. *Scientia Africana*. 13 (2): 136-145.
22. Macleod, RG. 1995. Goundwater modelling calculation for the cone of depression. *Research Paper. Department of Mathematical Sciences of Clemson University*. M.Sc Research Paper, 22-23.
23. Omatsola, ME & Adegoke, OS. 1981. Tectonic evaluation and cretaceous stratigraphy of the Dahomey Basin. *Journal of Mining Geology*. 5 (2): 78-83.
24. Oguntoyinbo, JS; Areola, OO & Filani, M. 1978. A geography of Nigerian development, 2nd Edition, Ibadan. Heinemann Educational Books (Nig) Ltd. 45-70.
25. Gbuyiro SO; Lamin, MT & Ojo, O. 2002. Observed characteristics of rainfall over Nigeria during ENSO Years. *Journal of Nigeria Meteorological Society*, 3 (1): 1-17.
26. Olayinka, AI. 1999. Advantage of Two-Dimensional Geoelectrical Imaging for Groundwater Prospecting: case study from Ira, Southwestern Nigeria. *Water Resources Journal*, 10 (1): 55-61.
27. Omogbai, BE. 2010. Rain days and their predictability in South-Western Region of Nigeria. *Journal of Human Ecology*. 31 (3): 185-195.
28. WAPCO, 2000. Environmental Audit Report of the West African Portland Cement Plc, Ewekoro and Shagamu Quarries Submitted To the Federal Ministry of Environment, Abuja by the West African Portland Cement Plc, Elephant House, Alausa-Ikeja Lagos, Nigeria. 1-155.
29. WAPCO 2001. Environmental Impact Assessment of The Proposed Clinker Line Of The West African Portland Cement Plc, At Ewekoro Submitted To The Federal Ministry Of Environment, Abuja By The West African Portland Cement Plc, Elephant House, Alausa-Ikeja Lagos, Nigeria. 149-150.
30. Ayedun, H; Arowolo, Y.A; Gbadebo, A.M. & Idowu, O.A 2013. Groundwater Contamination by Metals, Trace and Rare Elements in Basement and Sedimentary Areas of Ogun and Lagos State, pp 120-266.
31. Fidelis U; Thomas H, & Uduak, A. 2014. Reserve Estimation from geoelectrical sounding of the ewekoro limestone at Papalanto, Ogun State, Nigeria. *Journal of Energy Technologies and Policy*. 4 (5): 28-33.
32. Ushie, F; Harry, T, & Affiah, U. 2014. Reserve estimation from geoelectrical sounding of the ewekoro limestone at Papalanto, Ogun State, Nigeria. *Journal Of Energy Technologies and Policy*. 4 (5): 28.
33. Ishola SA; Makinde V; Gbadebo AM; Mustapha AO & Orebiyi EA. 2021. Quality assessment of groundwater system in Itori community of Ewekoro Local Government Area, South-West Nigeria. *Science and Technology (SCI & TECH) Multidisciplinary Engineering Science Studies*, 5 (12): 2-7. <http://scitechpub.org/index.php/vol-5-issue-12-December-2021>. Retrieved December 27, 2025.
34. Adegoke, OS & Omatsola ME. 1981. The tectonic evolution and the cretaceous stratigraphy of the Dahomey basin. *Journal of Mining and Geology*. 18 (1): 130-137.
35. Okosun, EA. 1998. Review of the early Tertiary stratigraphy of southwestern Nigeria, *Journal of Mining and Geology*, 34 (1): 27-35.



36. Okiongbo, KS & Odubo, E. 2012. Geoelectric sounding for the determination of aquifer transmissivity in parts of Bayelsa State, South-South Nigeria. *Journal of Water Resources and Protection*, 4 (6): 346-353. <https://doi.org/10.4236/JWARP.2012.46059>.
37. Oladeji, BO. 1992. Environmental analysis of Ewekoro formation at the Shagamu Quarry. *Nigerian Journal of Mining and Geology*, 28 (1): 148-156.
38. Billman, HG. 1992. Offshore stratigraphy and paleontology of the dahomey (benin) embayment. West Africa, *1st. NAPE Bulletin*, 7 (2): 121-130.
39. Kehinde-Phillips, T. Ogun State maps, In: Onakomaya, SO; K. Oyesiku & Jegede, 1992. Ogun State in Maps, *Rex Publisher, Ibadan*. 187.
40. Obiora, DN. & Onwuka, OS 2005. "Groundwater Exploration in Ikorodu, Lagos- Nigeria: A Surface Geophysical Survey Contribution", *Pacific Journal of Science and Technology*, 6(1), 86-93.
41. Ale, PO; Aribisala, JO & Awopetu, MS. 2015. Evaluation of yield of wells in Ado-Ekiti, Nigeria. *Nigeria Civil and Environmental Research*, 7 (11), 15-17. www.iiste.org.
42. Taylor, LE, & Werkheiser, WH. 1984. Groundwater resources of the Lower Susquehanna River Basin, Pennsylvania: Water Resource Report 57, *Pennsylvania Geological Survey*, 4 (1): 130-132.
43. Cederstrom. DJ. 2008. Evaluation of Yields of Wells in Consolidated Rocks, Virginia to Maine <http://pubs.usgs.gov/wsp/2021/report.pdf> 02/07/2015. Retrieved February 5, 2024.
44. USDI, 1981. United States Department of Interior. Confined, Unconfined and Perched Aquifer. *USDI Bulletin*. 32 (1): 12.
45. Kumar, DKM & Alappat, BJ. 2014. "Threat to groundwater from the municipal landfills in Delhi, India", In: *Proceedings of the 28th WEDC Conference on sustainable environmental sanitation and water services*, Kolkata (Calcutta), 377-380.
46. Batu, V. 1998. Aquifer hydraulics: a comprehensive Guide to hydrogeologic data analysis. *John Wiley and sons*, Chapter 6, 113-206.
47. Kruseman, GP & de-Ridder, NA. 1990. Analysis and Evaluation of Pumping Test Data (2nd ed.): The Netherlands. *International Institute for Land Reclamation and Improvement*. 47 (1): 377.
48. Todd, DK. 1980. *Groundwater Hydrology* (2nd edition). John Wiley and son Inc. New York. Cambridge University Press. 535, 1-770.
49. Sen-Zekai, S. 2015. Practical and Applied Hydrogeology, chapter, 11-32. www.sciencedirect.com. Retrieved January 20, 2025.
50. Rasmussen, WC. 1964. Permeability and storage of heterogeneous aquifers in the United States. *International Association of Scientific Hydrology*, 64 (1): 317-325.
51. Driscoll, .G. 1986. *Groundwater and Wells*. Collection and analysis of pumping test data; Inc. St. Paul, Minnesota. 2nd Edition. Chapter 16: 534-579.
52. Razack, M & Huntley, D. 1991. Assessing transmissivity from specific capacity in a large and heterogeneous alluvial aquifer. *Groundwater*. 29(6), 856-861.
53. Cooper, HH., Jr and Jacob, CE. 1946. A Generalized graphic method for evaluating formation constants and summarizing well-field history, Transactions, *American Geophysical Union*, 27 (4): 526-354.
54. Sridharan K, Mohan, M; Kumar M.S, & Sekhar, M. 1995. Groundwater flow and storage in hard rock aquifers. In: Proceedings of workshop on granite terrain, CGWB, 86-107.



55. Gheorghe, A. 1978. *Processing and Synthesis of Hydrological Data*. Tumbridge Wells, Kent. Abacus Press: 82.
56. Stefan, JK & Vitaly, AZ. 2005. Influence of Aquifer Heterogeneity and Return Flow on Pumping Test Data Interpretation. *Journal of Hydrogeology*, 300 (1): 267.
57. Weist, D. 1965. *Transmissivity and Hydraulic Conductivity in Aquifer Potentiality Classification*. Chapter 6, 265-272.
58. Acharyya, SK; Chakraborty, P; Lahiri, S; Raymahashay, BC; Guha, S & Bhowmilk, A. 1999. Arsenic Poisoning in the Ganges delta. *Nature*, 6753 (401): 401-545.
59. Rag, D. 1972. *The Design of Sample Surveys*. Mc-Graw Hill, L.T.D., New Delhi, India. 25.
60. Knopman, DS & Holliday, EF. 1993. Variation in specific capacity in fractured rock, Pennsylvania. *Groundwater*, 31 (1): 856-861.

Data availability

The data that support the findings of this study are available from the author upon reasonable request.

Declaration of competing interest

The author declares that he has no competing financial interests or personal relationships that could have appeared to influence the work reported in this paper.

Use of AI tools declaration

The author declares that he has not used Artificial Intelligence (AI) tools in the creation of this article.





Original Article

Some questions about *the book titled the History of Development of Geological Sciences in China*

Lisheng Zhang ¹

Abstract

The monograph *A History of the Development of Geological Science in China* is more a history of the development of China's geological cause than a history of the development of China's geological sciences. The book's description of the first geological college in New China is false. Furthermore, the author of this article questions the book's description of several historical facts related to China's oil surveys, coalfield geological exploration, and uranium geological exploration in the 1950s, as well as its profiles of key figures. The most important thing for a history book is to provide true and reliable history. However, the book *A History of the Development of Geological Science in China* falls far short of reliable history in the areas I'm familiar with.

Key words: The History of Development of Geological Sciences in China; account; question; petroleum prospecting; coalfield geological exploration; uranium geological exploration; true history

Affiliation Info: ¹ Retired research professor, Chengdu Institute of Geology and Mineral Resources, Chinese Academy of Geological Sciences, the Ministry of Natural Resources, P.R. China.

Corresponding Author : Zhang, LS, MSc, Research Professor; Email: mlr1121@126.com.

Citation: Zhang, LS. 2025. Some questions about the book titled *A History of Development of Geological Sciences in China*. *Naturalis Scientias*, 2 (2): 517-548. DOI: <https://doi.org/10.62252/NSS.2025.1032>. www.naturalisscientias.com.

Copyright © 2025 by the author. Published by *Naturalis Scientias*. This is an open access article under the Creative Commons Attribution-NonCommercial 4.0 International (CC BY-NC 4.0) License. (<https://creativecommons.org/licenses/by-nc/4.0/>).

About the author: In 1966, LS Zhang graduated from the Chinese Academy of Geological Sciences with a master's degree in mineral deposits, and has been engaged in the research of geology of mineral deposits, geochemistry, and history of geological sciences for a long period of time since then.



对《中国地质科学发展史》一书的几点质疑¹

张立生

(成都地质矿产研究所, 成都 610081)

摘要

《中国地质科学发展史》与其说是一部关于中国地质科学的发展史, 毋宁说是关于中国地质事业的发展史。该书所论新中国第一所地质专科学校不实。质疑该书关于 20 世纪 50 年代中国石油普查、煤田地质勘探和铀矿地质勘查中若干史实的叙事和对重要人物的简介。一部史书最重要的是提供真实的历史、信史。《中国地质科学发展史》在我熟悉的一些方面距离信史遥远。

关键词: 《中国地质科学发展史》; 叙事; 质疑; 石油普查; 煤田地质勘探; 铀矿地质勘查; 信史

¹本文为老科学家学术成长资料采集工程谢家荣学术成长资料采集(项目编号 2013-K-Q-XH07)的部分成果。本文在作者于 2024 年 10 月提交给中国地质学会地质学史专业委员会第 32 届年会的同名论文的基础上修改而成。

作者简介: 张立生, 男, 1940 年生。原国土资源部成都地质矿产研究所研究员, 1966 年中国地质科学院矿床学研究生毕业, 长期从事矿床地质-地球化学和地质学史研究。E-mail: mlr1121@126.com

1. 是中国地质科学史还是中国地质事业史？

2022年10月，中国科学技术出版社出版了由原地质矿产部部长宋瑞祥先生策划、由孟琪等主编的上、中、下三卷集共六篇二十九章 132 万字的《中国地质科学发展史》（图 1），以资纪念中国地质学会成立 100 周年。

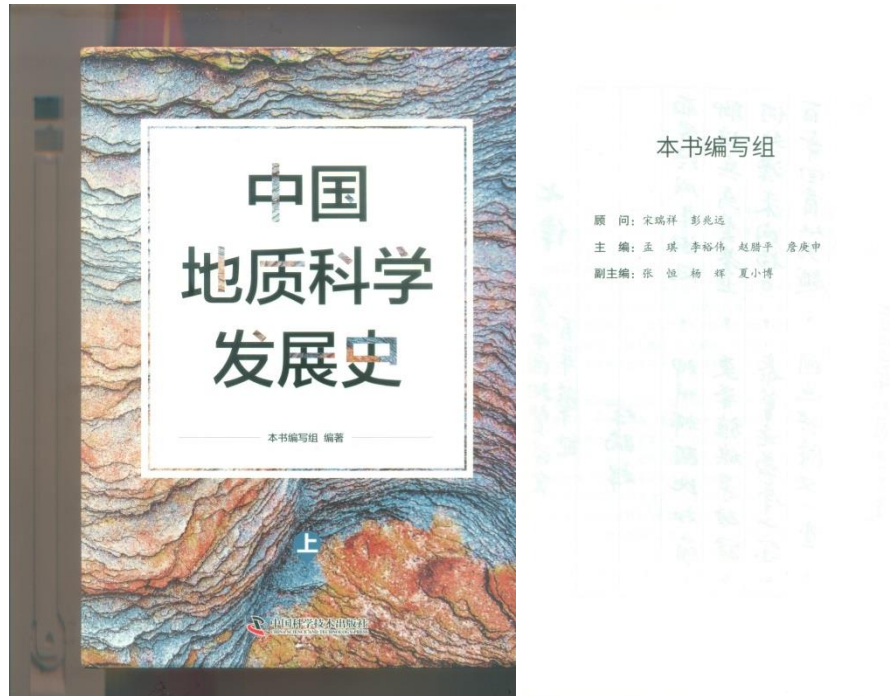


图 1. 《中国地质科学发展史》封面和“本书编写组名单”

Figure 1. Cover (left) and list (right) of Writing Personnel of *The History of Development of Geological Sciences in China*

该书分为第一篇古代和第二篇近代（上卷）、第三篇工业化建设时期和第四篇现代化建设初期（中卷）、第五篇二十一世纪初和第六篇新时代（下卷）。

第一篇含第一章地学思想萌芽、第二章矿业活动。

第二篇含第三章地质科学启蒙、第四章地质事业奠基和第五章矿业经济。

第三篇含第六章地质工作管理机构与地质队伍、第七章政策法规制度、第八章地质科学支撑的地质勘探成就、第九章地质科学支撑的水文地质与工程地质工作成就、第十章地质科学理论、第十一章勘探技术方法和第十二章对外交流合作。

第四篇含第十三章地质工作管理机构与地质队伍、第十四章政策和法规、第十五章地质科学支撑的地质勘探成就、第十六章地质科学支撑的水工环地质工作成就、第



十七章地质科学理论研究成就、第十八章勘探技术方法与创新和第十九章对外交流合作。

第五篇含第二十章行业主体与政策法规、第二十一章基础地质调查工作、第二十二章保障国家矿产资源安全、第二十三章服务防灾减灾事业、第二十四章服务可持续发展和第二十五章地质科技创新。

第六篇含第二十六章自然资源管理体制、第二十七章新一轮地质找矿战略、第二十八章服务生态文明建设和第二十九章地质工作转型升级。

上述章节安排或许就是宋瑞祥先生的总体策划。纵观全书内容，从古代地学思想的萌芽与矿业活动到近代地质科学启蒙，从 20 世纪前半期地质科学的奠基到社会主义建设时期（即所谓现代化建设时期）地质事业各个领域的蓬勃发展，再到“改革开放”以来地质事业的发展，写得颇为全面。但从全书的叙述来看，如果说上卷的叙述还主要是讲地质科学的，那么中、下卷的叙述则主要是讲地质事业的。笔者冒昧地认为，地质科学与地质事业是并不等同的，地质科学是一种事业，它是地质事业的一部分，地质事业是含盖地质科学事业而大于地质科学事业的。这套三卷集的巨著，尤其是中、下卷，与其说是写的中国地质科学的发展史，毋宁说是写的中国地质事业的发展史更为贴切和确当。地质科学含盖许多分支学科，讲地质科学的发展史，理应分门别类，讲述地质科学各个分支学科的发展史，譬如，中国地层学发展史，中国大地构造学发展史，中国矿物学发展史，中国岩石学发展史，中国矿床学发展史，中国煤田地质学发展史，中国石油地质学发展史，中国水文地质学发展史，中国地球物理学发展史，中国地球化学发展史等等……但这部《中国地质科学发展史》不是这样编著的。

2. 对若干史实的讨论与质疑

《中国地质科学发展史》（以下简称《发展史》），长篇巨著，详细研读评述，非我所能为之。本文只就我所读、所知或所经，主要是其中卷所涉及的很小一部分我所熟悉的部分内容说一些意见，不当之处，欢迎批评指正。

2.1 关于“我国第一个地质专业学校”

《发展史》第六章“地质工作管理机构与地质队伍”第一节“地质管理机构”的“地质院校管理机构”中说：“1951 年 8 月，中国地质计划指导委员会建立东北地质专科学校，校长李四光，这是我国第一个地质专业学校（第 243 页）。”

第六章第三节“地质教育”叙述了解放后各高等院校地质专业恢复招生、新增地质系、地质部新建北京、长春、成都地质学院和各其他工业部门相继建立高等、中等地质矿业院校的情况，其中有一句“其中，1949 年 10 月 30 日成立的南京地质探矿专科学校于 1950 年 3 月开学，招收学生 110 人。”没有忘记南京地质探矿专科学校，当然值得肯定。



《发展史》作者在这里所说的“我国第一个地质专业学校”显然指的是新中国第一个地质专业学校，因为我国第一所地质专业学校无疑地应该是 1913 年由章鸿钊、丁文江创办的工（农）商部地质研究所。

读者不明白的是：（1）作者为什么将“1951 年 8 月，中国地质计划指导委员会建立东北地质专科学校，校长李四光，这是我国第一个地质专业学校。”放在“地质院校管理机构”一节中而不是放在本应该放的“地质教育”中？（2）为什么“我国第一个地质专业学校”不是“1949 年 10 月 30 日成立的南京地质探矿专科学校”而是其后几近两年才建立的东北地质专科学校？

因为东北地质专科学校的校长是李四光，而南京地质探矿专科学校的校长（校务委员会主任）是谢家荣，所以东北地质专科学校就应该是第一所？大概没有这个道理。那么，《发展史》的作者究竟依据什么将东北地质专科学校列为第一所呢？

历史的事实是：1949 年 5 月，为协助上海市军管会接收资源委员会在沪各单位，南京的资源委员会办事处特别组织赴沪临时工作队，由各单位推派人员十五人，公推谢家荣为领队，电管处副处长谢佩和及有线电厂协理王能杰为副领队，随进军上海的三野解放大军前往上海，于 5 月 17 日抵达丹阳。在丹阳等待上海解放期间，谢家荣向曾山、孙冶方等华东地区党政军领导建议开办一所地质探矿专科学校，以“保证工业建设原料的供给”，得到领导的大力支持。10 月 24 日，关于筹备建校的讨论会在南京的中央研究院总办事处召开，俞建章等 15 人出席，谢家荣、李春昱、俞建章、徐克勤、李善邦被推为筹备委员。10 月 30 日学校筹备委员会举行第一次筹备会议。12 月初，华东工业部发函指示，学校由矿产测勘处、南京大学地质系、中央研究院地质研究所和中央地质调查所派代表组成校务委员会，指定谢家荣为校务委员会主任委员。12 月 28 日，谢家荣主持召开学校第一次校务会议，规定学生和教师待遇，分配课程，讨论分科，成立招生委员会。1950 年 2 月 23 日，试卷评阅完成。2 月 25 日完成录取工作，录取新生正取生 141 名，备取生 20 名¹。1950 年 3 月 17 日，学校举行开学典礼（图 2），正式开学。除校务委员会成员外，担任过学校教职的还有程裕淇、傅承义、郭文魁、李学清、秦馨菱、王德滋、叶连俊、业治铮、张文佑、张祖还等。学校 1952 年 6 月 6 日举行毕业典礼（图 3），包括刘广润、袁道先、闽豫、张文昭等在内的 111 名学生正式毕业²。毕业人数相当于当时中国所有地质专业人员总数的大约三分之一。



图 2. 华东区工业部南京地质探矿专修学校开学典礼合照

(引自《新中国第一所地质专业高等学校——南京矿专创办 50 周年纪念》)

Figure 2. Celebration of the Nanjing Institute of Geology and Prospecting



图 3. 中国地质工作计划指导委员会地质探矿专科学校毕业典礼留影

(引自《新中国第一所地质专业高等学校——南京矿专创办 50 周年纪念》)

Figure 3. Graduation ceremony of the Nanjing Institute of Geology and Prospecting

因隶属关系变更，学校名称迭次变化：最初称华东区工业部地质探矿专修学校、1950 年夏改名政务院矿产测勘处地质专科学校、1951 年再改名中国地质工作计划指导委员会地质探矿专科学校，同时受南京高等教育处领导²。



从上述可知，新中国第一所地质专科学校应该是南京地质探矿专科学校，说东北地质专科学校是中国第一所地质专科学校没有一点点道理。

2.2 关于“重要人物”

《发展史》第六章专门列出了一节即第四节“重要人物”。依次介绍了 4 位重要人物即李四光、何长工、谢家荣和黄汲清。此外列出了 20 世纪 50-60 年代中国科学院的地学部委员名单。列出这一节，值得称赞。但如果是论中国地质科学发展史，其重要人物中就应该还要特别提到杨钟健、尹赞勋、孙云铸、孟宪民等，而不应该有何长工，因为他并不是一位地质学家，其在地质科学上也没有任何建树。当然，如果是论中国地质事业的发展史，何长工无疑就是一位重要人物了。

《发展史》介绍作为重要人物的李四光、谢家荣、黄汲清，理应叙述他们在地质科学领域的重要贡献，但却只介绍了他们在新中国建立后的成就，这显然就不对了。

例如介绍李四光只提到了三点，即第一，积极寻找铀矿，第二，致力寻找石油，第三钟情地震预报。对李四光对蜓科研究的重大成就、对他创建地质力学理论，对第四纪冰川的研究和他对地热的关注，都只字未提。而所谓李四光认为“松辽平原，包括渤海湾在内的华北平原，江汉平原和北部湾，还有黄海，东海和南海都有（有）经济价值的沉积物”的说法则是完全没有根据的。关于这一点，容后再论。

众所周知，谢家荣是一位“全方位的地质学家”，其涉猎面之广，在中国地质界独一无二，成就卓著，并且在许多领域都居于开拓者和奠基人的地位。但对谢家荣的介绍基本上只限于他在石油地质学方面的贡献与成就，这是远远不够的。当然这方面的介绍是必须的。同时，还应当认为，这部《发展史》对谢家荣的肯定无疑是值得称道的：它不仅承认“谢家荣是中国发现矿床最多的地质学家”，“是中国最早提出陆相生油的学者之一”，而且还指出谢家荣“更是发现松辽盆地大庆油田的主要贡献者。”

对黄汲清的介绍是最失败的。首先，黄汲清是中国大地构造学的奠基人、槽台多旋回学说创立者和二叠系研究的开拓者，却没有被提及。黄汲清也是一位石油地质学家，对中国石油地质学也是有重要贡献的。但对黄汲清对 1950 年代的石油普查中所做的贡献介绍为 1955 年初他“建议在松辽平原、华北平原、鄂尔多斯和四川盆地四大重点地区进行石油和天然气普查勘探”却是完全错误的。这一点，也容后面再论。此外，作者称黄汲清“1982 年，荣获两项国家自然科学一等奖——《大庆油田发现过程中的地球科学工作》（排名第三）”也是完全不对的：排名不是第三，而是第二。虽然这并不合理，但这是当年的真实历史。

2.3 关于谢家荣的《中国的产油区和可能含油区》

谢家荣 1954 年的《中国的产油区和可能含油区》（图 4）是中国石油地质史上一篇非常重要的文章。

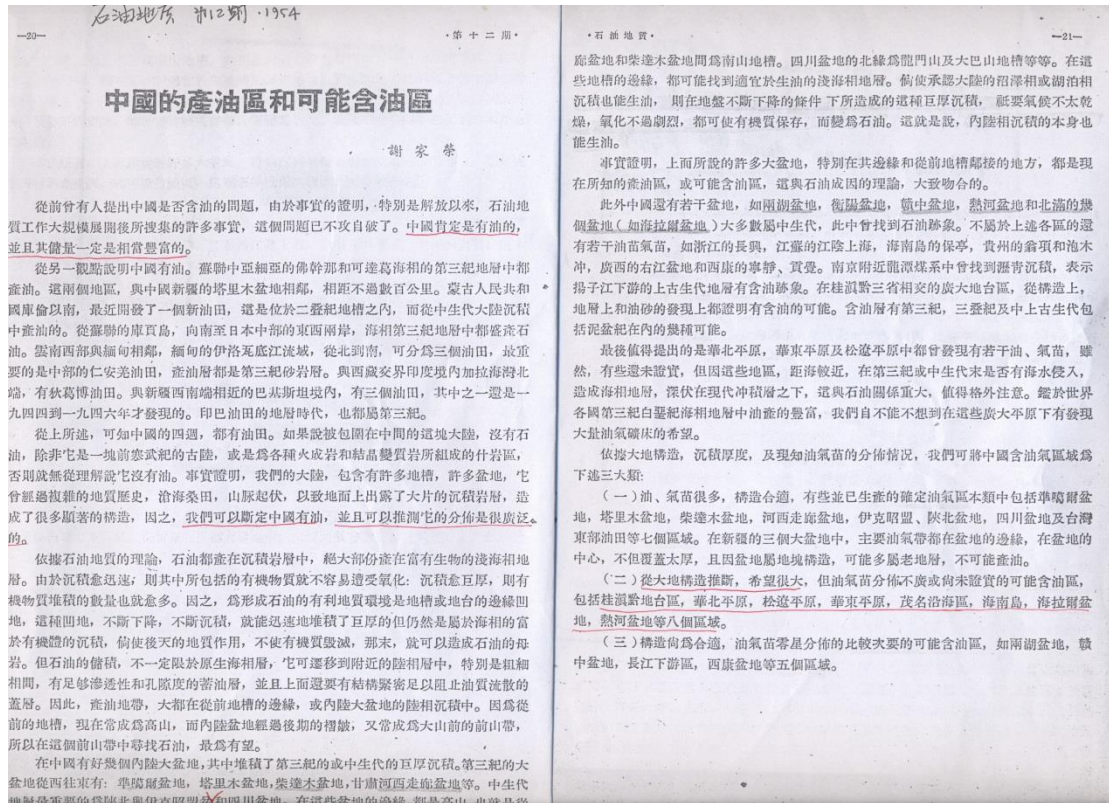


图 4. 谢家荣发表在《石油地质》1954 年第 12 期上的论文“中国的产油区和可能含油区”

Figure 4. Article titled *Oil-producing and potential oil-bearing regions in China* by C.Y. Hsieh

我在《论大庆等油田的发现与李四光的地质力学理论无关》中曾经指出³：

谢家荣在《中国的产油区和可能含油区》中，首先指出“中国肯定是有油的，并且其储量一定是相当丰富的”，然后依据中国周围和我国的地质条件指出“我们可以断定中国有油，并且可以推测它的分布是很广泛的”。该文还在依据石油地质的理论指出“前山带中寻找石油，最为有望”的同时，论述了“内陆相沉积的本身也能生油”。文章在论述了中国各个盆地的可能含油性后，将中国的含油气区域即中国的含油远景区分为三大类总共 20 个区：

“（一）油气苗很多，构造合适，有些并已生产的确定油气区。本类中包括准噶尔盆地，塔里木盆地，柴达木盆地，河西走廊盆地，伊克昭盟-陕北盆地，四川盆地及台湾东部油田等七个区域。

“（二）从大地构造推断，希望很大，但油气苗分布不广或尚未证实的可能含油区，包括桂滇黔台地，华北平原，松辽平原，华东平原，茂名沿海区，海南岛，海拉尔盆地，热河盆地等八个区域。

“（三）构造尚为合适，油气苗零星分布的较次要的可能含油区，如两湖盆地，赣中盆地，长江下游区，西康盆地等五个区域。”

文章在论述华北平原、松辽平原和华东平原的含油远景时指出：“值得提出的是华北平原，华东平原及松辽平原中都曾发现有若干油、气苗，虽然，有些还未证实，但因这些地区，距海较近，在第三纪或中生代是否有海水侵入，造成海相地层，深伏



在现代冲积层之下，这与石油关系重大，值得格外注意。鉴于世界各国第三纪白垩纪海相地层中油产的丰富，我们自不能不想到在这些广大平原下有发现大量油气矿床的希望。”

任何一位不带偏见的读者读了李四光和谢家荣上述两篇几乎同时发表在同一刊物上的重要文献后都会发现，谢家荣的论述远比李四光的论述详尽和透彻，对远景区的预测，谢家荣也比之李四光要全面得多。

但是，《发展史》的作者却声称：“谢家荣、黄汲清、翁文波也共同发表了《中国的产油区和可能含油区》，并编制了《中国含油远景图》。指出‘中国肯定是有油的，并且其储量一定是相当丰富的。’同时分三大类预测了中国含油气区。”（第 283 页）。发表在《石油地质》1954 年第 12 期上的《中国的产油区和可能含油区》的作者是谢家荣（图 4），然而这个最简单明了的事实在《发展史》作者的笔下竟然成了谢家荣、黄汲清、翁文波共同发表的了。历史能这样书写吗？

至于中国的含油远景图，谢家荣早在 1952 年就说过：“依据上述条件，我们编制了一张中国油区和可能油区的分布图。这里指出了两个新的探油方向。”⁴翁文波、邱振馨先生的《中国大陆含油气远景分区图》则是在谢家荣、黄汲清的参与下，于 1954-1955 年编制的，而黄汲清的《中国含油气远景分区图》则是 1957 年编制的。此外，谢家荣 1956 年又编制了一张四百万分之一的中国含油区和可能含油区分布图，这张图经缩绘后分别发表在谢家荣的《中国油气区和可能油气区的划分与评价》⁵和《中国的产油区和可能含油区及对今后勘探工作的意见》⁶中。

还应该指出两点：第一，1955 年 1 月，燃料工业部石油管理总局在北京召开了全国第六次石油勘探会议。翁文波先生在会上作了题为“中国大陆安油气藏希望的区域划分”的报告，并展示了翁文波、邱振馨编制的三百万分之一《中国大陆含油气远景分区图》。同年 2 月 5 日，翁文波在北京举行的中国地质学会第 29 届年会上作“我国含油区域的初步估计”的学术报告。翁文波的报告“把全国大陆按油气希望，区分为第一、第二、第三、第四及第五各级，级数越高，希望越大，根据越充足”⁷。在当天下午的会议上谢家荣主持对翁文波论文的讨论，并在讨论中指出，讨论油气远景要以大地构造为主要依据，主张用分区而不用分级；讨论会结束时，谢家荣对讨论会做了如下的总结⁸：

现在大家的意见较趋一致，大地构造作为研究油田是对的，另一方面说得不清楚还是可以讨论，最明显的是中国地质图也有问题，可是这样的图也起了相当的作用。

其次是分级问题，大家都认为有问题，如唐山与玉门相提并论，现在看起来是不合适的，尚待研究讨论。

至于分层，报告希望明确是根据哪一套。这样就好明确。

第二，中国 1950 年代石油普查的战略选区完成于 1956 年，即当年所有应当进行普查的地区都派出了普查队伍进行工作，以后的工作就是根据这些地区的工作结果，决定下一步的工作任务。所确定的战略选区全部都在谢家荣《中国的产油区和可能含油区》指出的产油区和可能含油区范围内，大多数也在李四光《从大地构造看我国石油勘探远景》指出的范围内。黄汲清《对我国含油气远景分区的初步意见》的



报告是 1957 年作的，是在 1955-1956 年间所做地质工作的基础之上作的，并没有也不可能对石油普查的战略选区产生影响。

2.4 关于李四光《从大地构造看中国石油勘探的远景》报告

“重要人物”一节这样介绍李四光：“第二，致力寻找石油……李四光认为……松辽平原，包括渤海湾在内的华北平原、江汉平原和北部湾，还有黄海、东海和南海，都有（有）经济价值的沉积物。”在第八章“地质科学支撑的地质勘探成就”的第二节“能源矿产地质勘探成就”的“油气地质勘探”中又说：“1954 年 3 月李四光应邀赴燃料工业部石油管理总局作了题为《从大地构造看中国石油勘探的远景》的报告。他指出……‘从东北平原起通过渤海湾到华北平原，再往南到两湖地区，可以做工作。先从新华夏的旁边摸起；同时，在覆盖地区着手摸底，物探、钻探都可以上，看来是有重要意义的（第 282-283 页）。’”

其实，《发展史》作者所说的李四光报告中的那些话并非出自李四光的报告，而是出自国家地质总局“地办 [1978] 426 号文件”“关于黄汲清同志向中央领导同志所反映问题的调查报告”。为了给所谓“地质力学理论指导石油普查”制造“依据”，该文件不惜造假说：“一九五四年三月，他在燃料工业部石油总局的座谈会上所做《从大地构造看我国石油勘探远景》的报告中指出：新华夏的构造带的主要凹陷带，对储存石油具有比较好的条件，并首次明确提出‘在东北平原、通过渤海湾、华北平原，往南两湖地区，可做（石油普查）工作’的意见”（地办 [1978]426 号文件第 3 页）（图 5）。

该调查报告的附件一、关于黄汲清同志给中央领导同志信中所反映问题的调查材料的第二部分“五十年代我国一些地质学家对我国石油远景及普查勘探工作的见解”也造假说：

一九五四年三月，李四光同志在燃料工业部石油总局的座谈会上作了《从大地构造看我国石油勘探远景》的报告指出：“石油勘探远景最大的有：一、青、康、滇、缅大地槽；二、阿拉善—陕北盆地；三、东北平原—华北平原。但并不是说，除了这几个区域外，别处就可以不做工作了。”他还明确指出：“新华夏式的构造带，其主要走向为北 18 度东，包括太平洋一系列弧岛在内。这里所说的是第一级的大地构造，有比较长期的历史发展，其主要凹陷带，对储存石油具有比较好的条件。”“东北平原，通过渤海湾，华北平原，往南两湖地区，可做工作。先从新华夏式的旁边摸起，同时覆盖地区着手摸底。物探、钻探都可以上，看来是有重要意义的（摘自当时的记录：中央档案馆（自然资源部档案室），全宗号 196，目录号 27，案卷号 0014，序号 2，图 5）。”

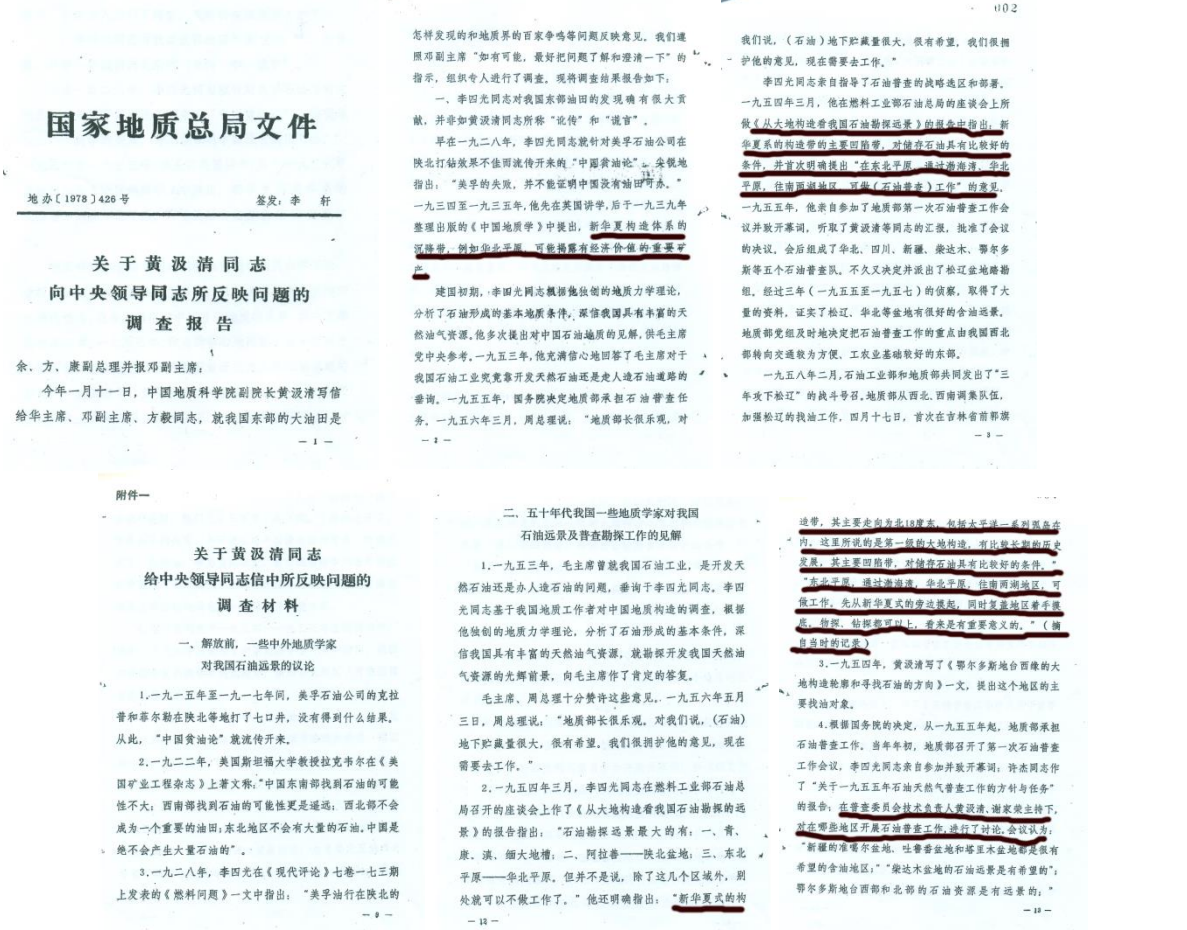


图 5. 地办 [1978]426 号文件“关于黄汲清同志给中央领导同志信中所反映问题的调查报告”及附件一“关于黄汲清同志给中央领导同志所反映问题的调查材料”

注：自左至右、自上至下为文件之第 1、2、3、9、12、13 页（中央档案馆（自然资源部档案室），全宗号 196，目录号 27，案卷号 0014，序号 2）。标下划线部分是调查报告歪曲李四光《中国地质学》原意和造假李四光报告内容的文字。第 13 页下面一段话，则是讲石油普查的地区是在第一次普查会议上集体讨论确定的

Figure 5. Investigation report on the issues T. K. Huang reflected to the Central leaders (the Central Archives, archival code: 196-27-0014-2)

读了《发展史》的上述说法，再看当年国家地质总局的上述调查报告，就很明白，前者引用李四光报告内容的出处就是上述国家地质总局报告中所谓“摘自当时的记录”。

关于国家地质总局这个调查报告如何歪曲李四光《中国地质学》的原意和如何造假李四光《从大地构造看我国石油勘探远景》报告的内容，笔者在《论大庆等油田的发现与李四光的地质力学理论无关》中已有详细的叙述³，本不愿在此耗费笔墨，但为了说明问题起见，还是得简单说上几句。

图 6 是中央档案馆藏李四光《从大地构造看我国石油勘探远景》报告的记录誊清稿原文。李四光报告的记录人、李四光秘书段万侗在记录誊清稿的标题之下、正文之

前加了这样一段注：本篇是李四光部长于 1954 年 3 月 1 日在石油管理总局的报告，因当时记录不全，兹经李部长亲自改正补充如下——记录段万侗注。这无疑是最权威的记录稿。

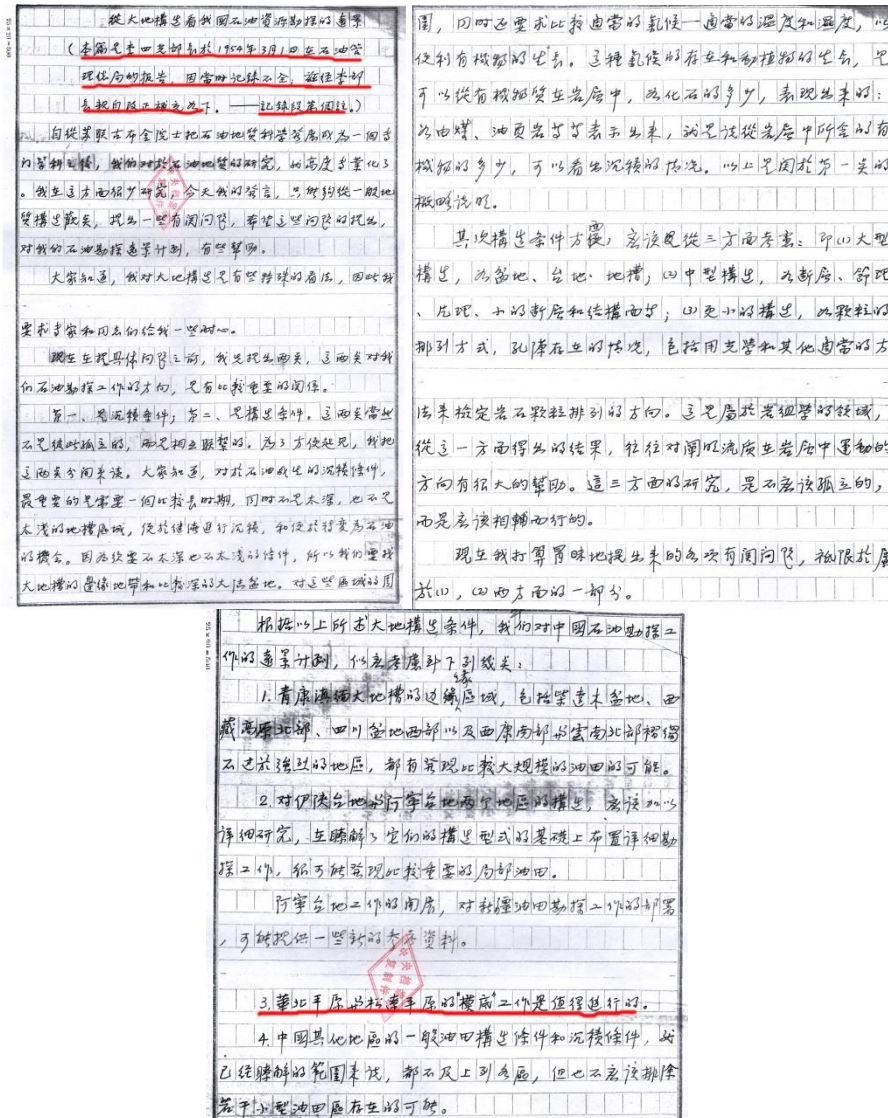


图 6. 中央档案馆藏李四光《从大地构造看我国石油勘探远景》报告原文复印件的扫描件

(中央档案馆，全宗号 196，目录号 4，案卷号 0038，序号 1)

Figure 6. The manuscript of prospect of China's petroleum exploration in terms of geotectonics which J. S. Lee himself dictated (the Central Archives, archival code: 196-4-0038-1)

图 7 是收入《李四光全集》第七卷第 367-269 页的《从大地构造看我国石油勘探远景》的扫描件。读者对照正式发表的文稿和上述誊清稿就知道，除了加了“一、引言”和



“二、从西北大地构造型式的观点推论中国石油勘探远景”两个小标题外，两者一字不差。

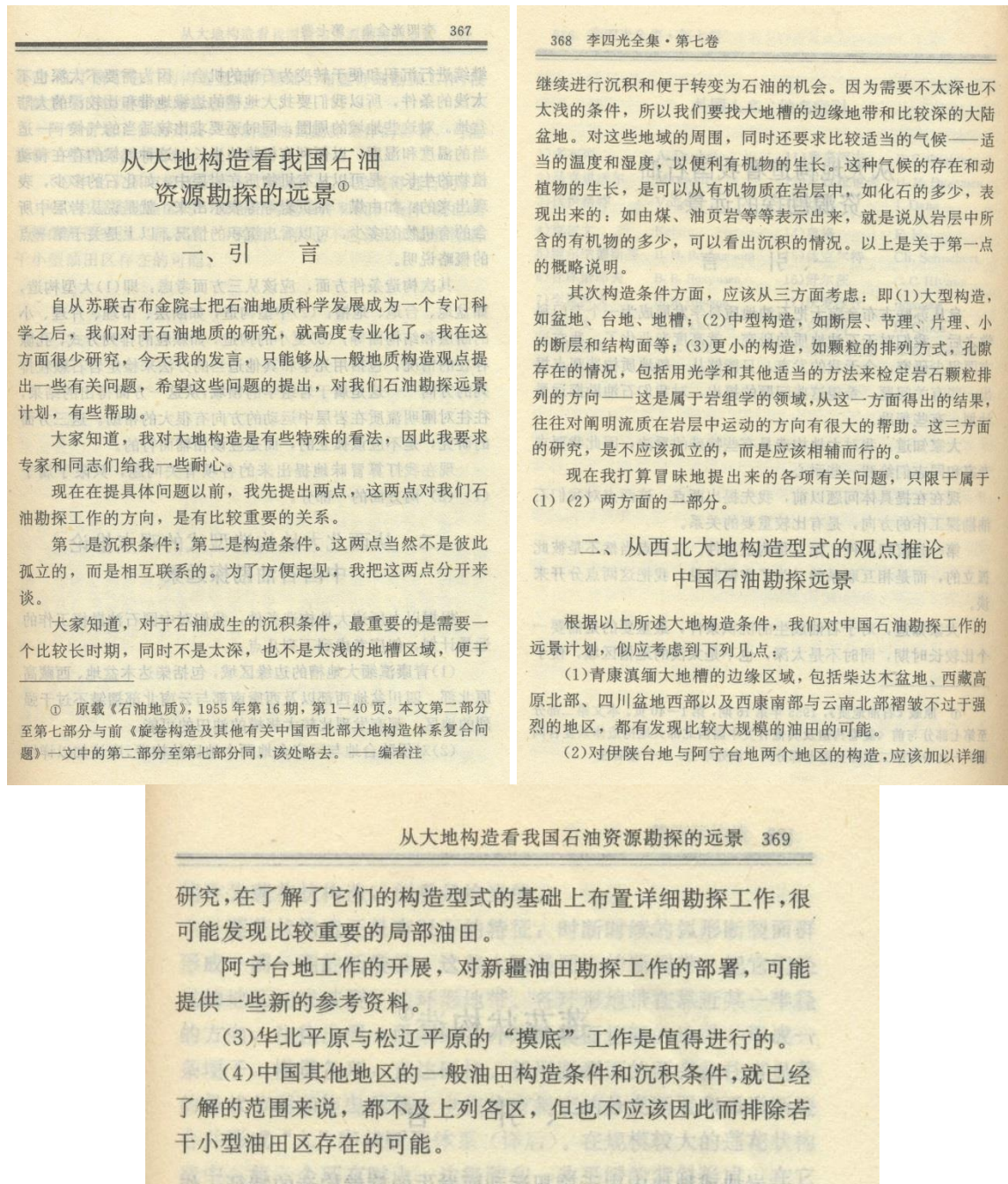


图7. 《李四光全集》第七卷所载“从大地构造看我国石油勘探远景”部分页面影印件

Figure 7. Photocopies of some pages from the article titled *the prospects of petroleum exploration in my country from the perspective of geotectonic structures* in Volume 7 of the monograph *the Complete Works of J. S. Lee*



经过李四光本人“亲自改正和补充”的记录文稿充分证明，那些所谓“摘自当时的记录”的文字是彻头彻尾的造假。

我在“论大庆油田等油田的发现与李四光的地质力学理论无关”一文中曾经指出：

1954年，在全国进行大规模石油普查的前夜，中国地质界有两篇重要文献发表。这两篇重要文献，一篇是谢家荣1954年6月或7月发表在《石油地质》第12期上的《中国的产区区和可能含油区》，另一篇就是前述李四光1954年3月1日在石油管理总局所作的报告，1954年底发表在《石油地质》第16期上的《从大地构造看我国石油资源勘探的远景》。之所以说这两篇文献重要，是因为第一，在1955年之前，对中国石油远景预测最为全面的文献只有这两篇，除此之外，没有其他任何文献对中国石油远景做过如此全面的预测；第二，这两篇文献发表在地质部按照中央的决定负责全国石油普查的前夜，对于指导石油普查的战略选区有着极其重要的意义³。

本来，《发展史》的作者论及李四光的《从大地构造看我国石油勘探远景》时，完全应该也只能引用公开出版的报告原文，但他们却偏偏放着原文不用而要去引用那些造假的文字。究竟是为了什么呢？还必须指出：国家地质总局调查报告造假李四光报告的内容，还打着所谓“摘自当时的记录”的旗号，而《发展史》的作者甚至嫌打这个“旗号”麻烦，干脆明目张胆地直接当作李四光报告的文字引用，连起码的作文常识都不顾了。

2.5 关于黄汲清建议在四大重点地区进行油气普查勘探

《发展史》在“重要人物”一节中说“黄汲清……1955年年初，他与谢家荣一同担任地质部普查委员会技术负责人时，建议在松辽平原、华北平原、鄂尔多斯和四川盆地四大重点地区进行石油和天然气普查勘探（第258页）。”在“第八章 地质科学支撑的地质勘探成就”中的“二、油气地质勘探”中又说：“1955年1-2月……在时任地质部石油局总工程师黄汲清的建议下，决定组成5个石油普查大队……于1955年3-4月分别开赴准噶尔盆地、吐鲁番盆地、柴达木盆地、鄂尔多斯和六盘山地区、四川盆地、华北平原和下辽河盆地展开野外工作（第283页）。”

首先必须指出，《发展史》的普遍存在的问题，即它引用的许多文字都不知道出自何处，不交代它的引文的依据。其次，一会儿说黄汲清1955年初“与谢家荣一同担任地质部普查委员会技术负责人时，建议在松辽平原、华北平原、鄂尔多斯和四川盆地四大重点地区进行石油和天然气普查勘探（第258页）”，一会儿又说“1955年1-2月……在时任地质部石油局总工程师黄汲清的建议下（第283页）”。地质部石油局是1956年才建立的，黄汲清怎么会在1955年1-2月任地质部石油局总工程师呢？作者脑子里怎么会如此混乱？第三，说黄汲清建议在松辽平原、华北平原、鄂尔多斯和四川盆地四大重点地区进行石油和天然气普查勘探，那是根本就没有的事，那是黄汲清为了自己的利益编造的故事，而不是真实的历史。

黄汲清在1978年1月11日上书华国锋、邓小平和方毅的信中说：

我国东部几大油田普查工作是1955年初在当时地质部矿产普查委员会（简称“普委会”）的直接主持下开始进行的，当时我作为“普委会”的主要负责人之一，提出了把华北平原、松辽平原、鄂尔多斯盆地（即陕甘宁盆地）、四川盆地作为“普委会”找油的四大重点地区。“普委会”采纳了我的建议，并很快做了部署，开展了工作。我的建议是根据“陆相生油”理论（这一理论是我国地质学家潘钟祥教授和



我在四十年代初期分别提出和发展起来的) 和我的大地构造观点并结合我国多年来的地质工作实践而提出的。这一历史事实是“普委会”广大干部、技术人员都知道的⁹ (图 8)。

学家”被安排在第六休息室提前就座。党和国家领导人邓小平、乌兰夫、方毅、余秋里、阿沛·阿旺晋美、王震、谷牧、沈雁冰等参加了追悼会。乌兰夫主持大会，方毅致悼词，参加追悼会的还有科学、教育界人士，中共中央、国务院有关部门负责人和吴有训先生的生前友好共数百人。

(中国科学院档案 1977—2—13, 1977 年 12 月 8 日第 2 版)

1978 年 (戊午) 74 岁

要目：第二次上书邓小平。出席全国科学大会。任中国地质科学院学术委员会副主任。

1 月 11 日再次上书邓小平，反映有关大庆油田宣传中的不实之词。全文如下：

邓副主席：

方毅同志：

我在去年 6 月 14 日曾写信给邓副主席反映了地质系统长期以来不能贯彻落实毛主席的“双百”方针的实际情况，党的“十一大”之后不久就听说邓副主席对我的信作了重要批示，强调总而言之一定要执行“双百”方针。尽管邓副主席的批示至今没有向我传达，但是我听到这一消息后心情异常激动和兴奋。因为这不仅仅是对我个人信件批示，而是代表了党对我国地质科学事业的巨大关怀和支持。此后不久，我的生活条件和工作条件有了改善，大地构造研究室正在着手恢复。我衷心感谢党、感谢邓副主席，只有打倒“四人帮”才能出现这种大好局面，我国地质科学事业才大有希望。我决不辜负党中央的殷切期望，我要为繁荣和发展我国地质科学事业，赶超世界先进水平贡献我晚年的全部精力。

但是，在给邓副主席的信中，我当时没有反映存在于地质界的一个重大问题，即我国东部的大油田（包括

· 128 ·

大庆、胜利、大港、长庆等油田）到底是怎么发现的。这主要是考虑到这个问题直接牵涉到我个人的历史作用，而我不想为个人争荣誉，只希望在打倒“四人帮”之后，地质界能够贯彻执行党的“双百”方针，出现一个生气勃勃的局面，各地质学派能在平等的自由讨论中取长补短，共同提高，以利于地质科学的迅速发展。然而现在看来，不把这个问题反映出来，不说清楚，在地质界真正落实党的“双百”方针，充分调动地质战线广大人员的社会主义积极性是有很大困难的。叶副主席、邓副主席在党的“十一大”报告中一再号召我们恢复和发扬党的优良作风，反对弄虚作假、看风使舵、投机取巧；反对华而不实和任何虚夸；提倡实事求是，做老实人，说老实话、办老实事，作为一名科学工作者，我深感有责任响应党中央的号召，有责任把地质界的这个重大问题反映给你们。

我国东部几大油田普查工作是 1955 年初在当时地质部矿产普查委员会（简称“普委会”）的直接主持下开始进行的，当时我作为“普委会”的主要负责人，提出了把华北平原、松辽平原、鄂尔多斯盆地（即陕甘宁盆地）、四川盆地作为“普委会”找油的四大重点地区。“普委会”采纳了我的建议，并很快做了部署，开展了工作。我的建议是围绕“陆相生油”理论（这个理论是我国地质学家潘钟祥教授和我在四十年代初期分别提出和发展起来的）和我的大地构造观点并结合我国多年来的地质工作实践而提出来的。这一历史事实“普委会”广大干部、技术人员都知道的。在此之后，我又编制了《我国含油气远景分区图》，把上述四大地区用橙红色明确圈出，并于 1957 年 3 月 8 日在全国石油普查工作会议上，配合这张大型挂图，作了题为《对我国含油气远景分区的初步意见》的学术报告。“普委会”及下

· 129 ·

图 8. 《黄汲清年谱》所载上述书信中关于他提出四大找油重点地区的段落

Figure 8. The passage in Huang's letter about his proposal of four key oil exploration areas in his Chronicle

黄汲清先生说他“提出了把华北平原、松辽平原、鄂尔多斯盆地（即陕甘宁盆地）、四川盆地作为‘普委会’找油的四大重点地区”的“建议”。证据在哪里？

让我们来看真实的历史是如何记载的：国家地质总局 1978 年 5 月的“调查报告”正确地指出：第一次石油普查工作会议“在普查委员会技术负责人黄汲清、谢家荣主持下，对在哪些地区开展石油普查工作，进行了讨论”（图 5 中末页），讨论的结果认为：“新疆的准噶尔盆地、吐鲁番盆地和塔里木盆地都是很有希望的含油地区”；“柴达木盆地的石油远景是有希望的”；“鄂尔多斯地台西部和西北部的石油资源是有远景的”；“四川盆地的石油和天然气是有远景的”；“华北平原是可能产生石油的”（图 5）¹⁰⁻¹¹。

依据上述讨论所得出的结论，根据当时所能组织起来的力量，1955 年“地质部决定组织地质队 24 个……分赴新疆的准噶尔盆地、吐鲁番盆地、鄂尔多斯、四川盆地、华北平原等五个地区进行工作。”¹²

历史就是这样明明白白地记载着，1955 年的石油普查项目是在第一次石油普查工作会议期间经过专家们集体讨论决定的，所确定的工作地区也是 5 个而不是 4 个，根本就没有什么黄汲清先生提出了所谓“四大重点地区”这回事。



并且，黄汲清先生自己也说，“根据我的回忆和档卷记录，会议闭幕以前是由我代表普委向部务会议汇报最后讨论结果的。令人遗憾的是，我的汇报内容没有记录下来。我自己也没有留下笔记。”¹³

这就是说，连黄汲清先生自己也承认，1955年的石油普查项目是集体讨论决定的。黄汲清先生仅仅因为是他代表普委会向部务会议汇报的，就把集体讨论的意见说成是自己的意见，也是没有一点点道理的。

难道黄汲清先生在讨论会上提出了4大“重点地区”了？非也！

黄汲清先生在写这封上书信17年之后的1994年承认，他自己在1957年之前根本就没有关于中国找油方向的有据可查的意见¹⁴：

全国石油天然气普查的方向问题怎么提出来，这是个重要问题……我自己在这期间发表过什么意见？没有。我记得在1956年阳历过年的时候，清华大学地质系的负责人孟宪民教授，请我到清华大学地质系去作一个学术报告。我记得当时我主要谈的是中国石油远景的问题，其中也谈到在华北平原、松辽平原找油的可能性，可惜我没有把这个学术报告写成文章发表。

最近我又查了一下清华大学的《清华日报》，看有没有记载黄汲清谈过什么问题。结果1956年清华日报还没有恢复印刷，到1957、1958年才恢复了印刷，所以这个问题在现有的文献资料里查不出来，因此这个东西不能算，没有可考的证据。所以上面谈的关于在中国找石油的地区，特别华北平原、松辽平原是不是也可以找油，名见经传的，就只有谢家荣、李四光的文章，其中谢家荣谈得比较明确，且时间在李四光之前。

必须指出，松辽平原是在第一次石油普查工作会议之后才提出并进行踏勘的，而松辽平原石油普查项目则是在1955年秋踏勘所获资料的基础之上才讨论确定的。任何懂得地质勘探程序的人都明白，对一个地质情况知之甚少的地区的矿产勘查，首先是踏勘，然后根据踏勘所获资料判断，是否值得普查，如果不值得普查，就连普查也不会进行，如果值得普查，则先是初查，后是详查，最后才是勘探。黄汲清先生把当时地质情况知之甚少的松辽平原列为“重点地区”，这根本就是天方夜谭。

黄汲清先生说，普委会“采纳”了他“四大重点地区”的“建议”。但是，在第一次石油普查工作会议闭幕之后20天，也就是黄汲清先生所谓普委会“采纳”了他的“建议”之后将近20天，即1955年3月1日，普查委员会总工程师谢家荣在地质部1955年全国地质会议（2月22日至3月17日在北京举行）上所作的题为《1954年普查检查工作中的几个问题》的报告中却是这样说的：

以后数年的石油普查工作应集中力量在准噶尔，柴达木，塔里木及河西走廊的四大盆地之中。华北、松辽及华东平原中亦有产油希望，应予注意。在四川应注意川西川中各区，并应着重天然气的开发和利用，在华北寻找炼油煤，而在华东、中南则注意油页岩¹⁵。

作为普查委员会总工程师的谢家荣说的是“以后数年的石油普查工作应集中力量在准噶尔，柴达木，塔里木及河西走廊的四大盆地之中”，根本不是黄汲清的所谓“四大重点地区”。“普委会采纳了”他的“四大重点地区”的“建议”，但连作为普委总工程师的谢家荣都不知道，遑论“这一历史事实是‘普委会’广大干部、技术人员都知道的”！

黄汲清先生还说：我的建议是根据“陆相生油”理论（这一理论是我国地质学家潘钟祥教授和我在四十年代初期分别提出和发展起来的）和我的大地构造观点并结合我国多年来的地质工作实践而提出的⁹。

让我们来看看所谓“四大重点地区”的有关历史事实。

1) 华北平原 地质部第一次石油普查工作会议决议关于华北平原是这样说的（黑体是本文作者标的）¹²：

华北平原是中生代以来的下沉地带，新生代的泥沙堆积甚厚，其中可能有海相沉积和产生石油的有机质，又由于喜马拉雅运动的发生，较老的平原沉积可能曾遭受到轻微褶皱，因此，华北平原是可能产生石油的。

地质部普查委员会“关于第一次石油普查工作会议的报告”更是这样写道（图 9）：

华北平原冲积层的底部可能有海相沉积和轻微的褶皱以及产生石油的有机物质，近年地质工作及群众报矿都不断发现有油气苗。故华北平原底部很可能储有有工业价值的油气藏，如确属实，则其意义将异常巨大¹⁶。

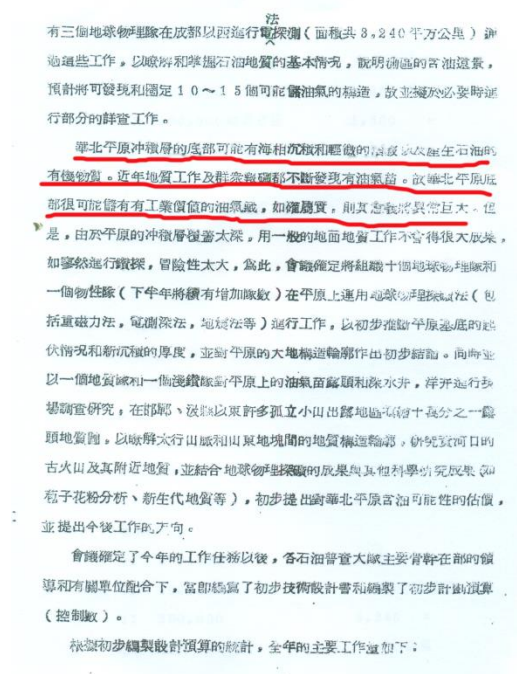


图 9. 地质部普查委员会《关于第一次石油普查工作会议的报告》关于华北平原的论述（中央档案馆（自然资源部档案室），全宗号 196，目录号 4，案卷号 0260，序号 3）

Figure 9. Discussion on the North China Plain in the "Report on the First Petroleum Survey Working Conference" by the Geological Survey Committee of the Ministry of Geology (Central Archives (Ministry of Natural Resources Archives), Archive No. 196, Catalog No. 4, File No. 0260, Serial No. 3)

即使是两年后的 1957 年，黄汲清先生在被他自己广为宣传的《对我国含油气远景分区的初步意见》中关于华北平原和江苏平原的真实版本也还是这样说的（图 10）¹⁷：

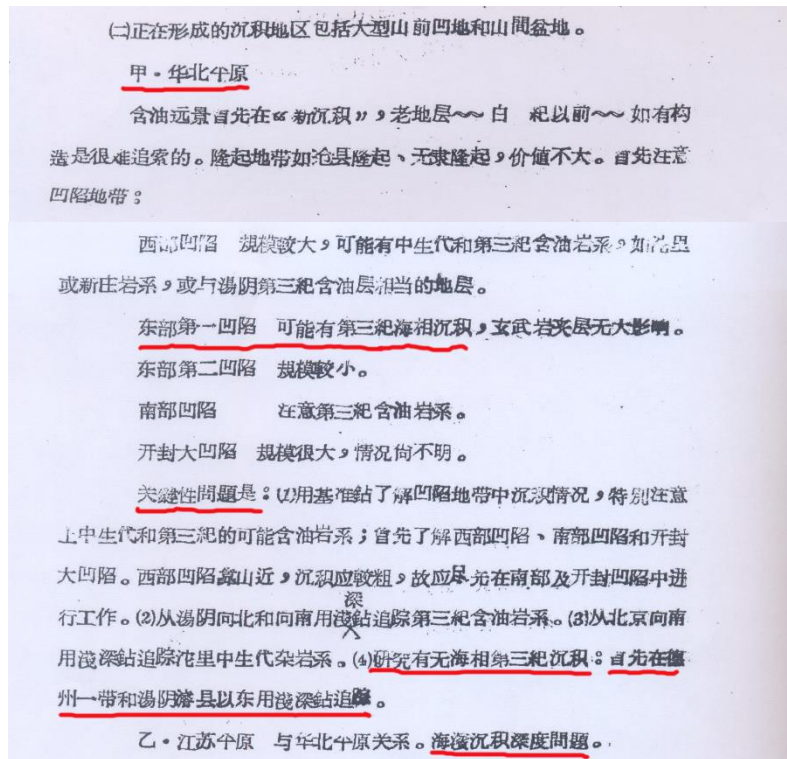


图 10. 黄汲清 1957 年在地质部石油地质专业会议上所作《对我国含油气远景分区的初步意见》的报告中关于华北平原的论述（中央档案馆（自然资源部档案室），全宗号 196，目录号 6，案卷号 050，序号 1）

Figure 10. Huang's discussion of the North China Plain in his report "Preliminary Opinions on the Zoning of Oil and Gas Prospects in my country" delivered at the Ministry of Geology's Petroleum Geology Conference in 1957 (Central Archives (Ministry of Natural Resources Archives), Archive No. 196, Catalog No. 6, File No. 050, Serial No. 1)

(二) 正在形成的沉积地区（包括大型山前凹地和山间盆地）

甲、华北平原：

含油远景首先在“新沉积”，老地层——白垩纪以前——如有构造是很难追索的。隆起地带如沧县隆起、无隶隆起，价值不大。首先注意凹陷地带：

西部凹陷 规模较大，可能有中生代和第三纪含油岩系，如坨里或新庄岩系，或与汤阴第三纪含油层相当的地层。

东部第一凹陷 可能有第三纪海相沉积，玄武岩夹层无大影响。

东部第二凹陷 规模较小。

南部凹陷 注意第三纪含油岩系。

开封大凹陷规模很大，情况尚不明。

关键问题是：（1）用基准站了解凹陷地带中沉积情况，特别注意上中生代和第三纪的可能含油岩系；首先了解西部凹陷、南部凹陷和开封大凹陷。西部凹陷靠山近，沉积应较粗，故应尽早先在南部及开封



凹陷中进行工作。(2)从汤阴向北和向南用浅深钻追踪第三纪含油岩系。(3)从北京向南用浅深钻追踪坨里中生代杂岩系。(4)研究有无海相第三纪沉积:首先在德州一带和汤阴、浚县以东用浅深钻追踪。

乙、江苏平原:

与华北平原关系。海滨沉积深度问题。

历史如此清楚地记载着,无论是 1955 年第一次石油普查工作会议决议还是普查委员会“关于第一次石油普查工作会议的报告”,甚至黄汲清先生自己乃至到了 1957 年的论述,都是将华北平原的含油远景与海相第三系联系在一起的,哪里来的什么以陆相生油理论为指导?

2)四川盆地和鄂尔多斯盆地 地质部第一次石油普查工作会议决议关于这两个地区的石油普查工作,只说了要进行工作的地区的范围和采用的工作方法以及工作量,根本就没有提到生油层,也没有提到海相陆相的问题¹²。

而一年以后的 1956 年 1 月,黄汲清先生在地质部第二次石油普查会议上所作题为“一年来石油地质普查工作中的经验教训及对今后工作的一些建议”的报告中,专门论述了包括四川盆地在内的几个工作地区的生油层,其中所说四川盆地的生油层“主要是三叠纪和二叠纪,在川西北有泥盆纪和石炭纪,可能尚有奥陶志留纪”¹⁸。所有这些地层基本上都是海相的,何来以陆相生油理论为根据?

因此,说四川盆地和鄂尔多斯盆地的石油普查是以陆相生油理论为指导的也完全违背历史事实。

3)松辽平原 黄汲清先生强调他代表普查委员会向部务会议汇报时提出了松辽平原项目,但终归是查无实据。松辽平原的项目是在第一次石油普查工作会议之后由谢家荣和黄汲清共同提出的(关于此一问题的详尽情况请见作者的《论大庆油田发现真相》之《是雪泥鸿爪,还是舞文弄墨》的第一节“关于松辽平原石油普查”,中山大学出版社,2015:129-133)。松辽平原石油普查项目是在地质部第二次石油普查工作会议上确定的,而第二次石油普查工作会议关于松辽平原是这样论述的¹⁹:

七、松辽平原石油普查大队

广阔的松辽平原的大地构造轮廓与华北平原相似,是一个晚近的下沉地带,其中堆积着很厚的新沉积。包括白垩纪地层以及第三纪和第四纪的疏松沉积,其中可能有含油岩系。普查的主要目的是使用大面积的重磁力普查,配合若干电测深剖面 and 地震剖面,初步探测平原基底起伏情况,沉积岩深度和新沉积厚度,结合地面地质观察和地层剖面的研究,以及油苗检查,推断平原的大地构造轮廓和新沉积分布的规律性。选择适当地点准备打基准井,并提出初步钻探设计。

具体任务和要求如下……

读者可以看出,这个决议关于松辽平原的论述,根本就没有提到陆相生油的问题,而是说“广阔的松辽平原的大地构造轮廓与华北平原相似”,而按照第一次石油普查工作会议的决议,华北平原的含油远景则是与海相第三系相联系的。

前述黄汲清 1956 年的报告论及几个地区的生油层时并未提及松辽平原，但他在 1957 年所作《对我国含油气远景分区的初步意见》的报告中关于松辽平原的真实版本是这样说的（图 11）¹⁷：

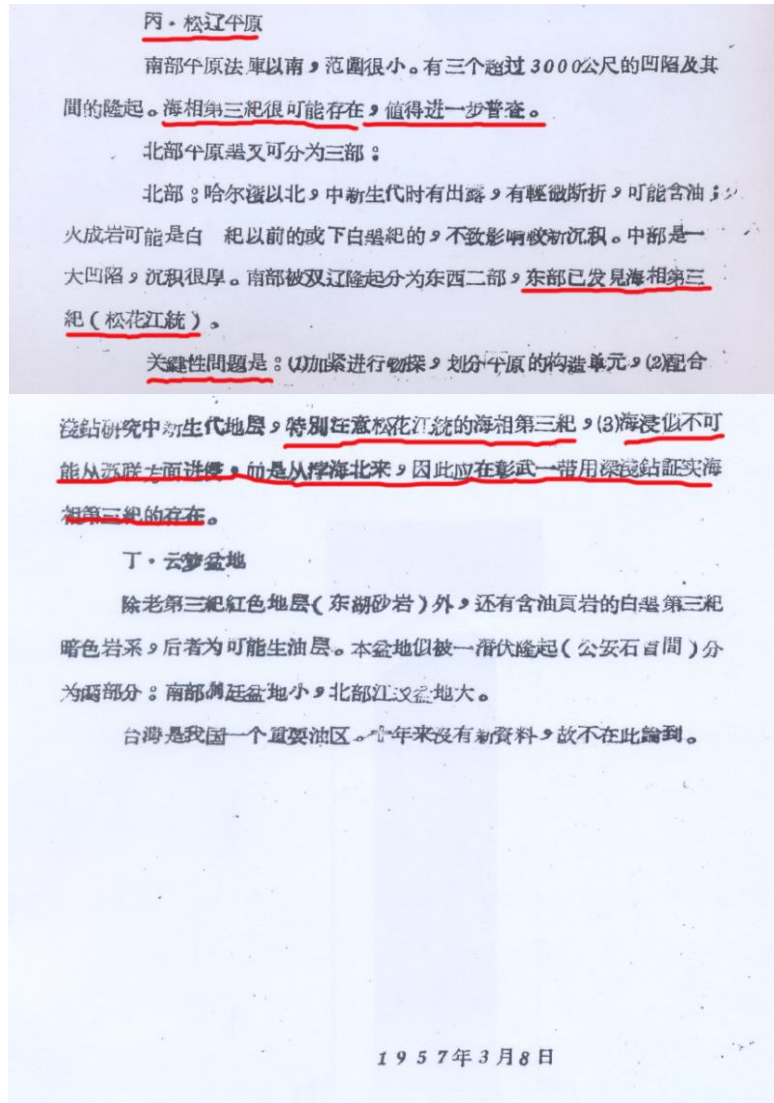


图 11. 黄汲清 1957 年在地质部石油地质专业会议上所作《对我国含油气远景分区的初步意见》的报告中关于松辽平原的论述（中央档案馆（自然资源部档案室），全宗号 196，目录号 6，案卷号 050，序号 1）

Figure 11. Huang's discussion of the Songliao Plain in his report "Preliminary Opinions on the Zoning of Oil and Gas Prospects in my country" delivered at the Ministry of Geology's Petroleum Geology Conference in 1957 (Central Archives (Ministry of Natural Resources Archives), Archive No. 196, Catalog No. 6, File No. 050, Serial No. 1)

丙、松辽平原



南部平原法库以南，范围很小。有三个超过 3 000 公尺的凹陷及其间的隆起。海相第三纪很可能存在，值得进一步普查。

北部平原又可分为三部：

北部：哈尔滨以北，中生代有时出露，有轻微断折，可能含油；火成岩可能是白垩纪以前或下白垩纪的，不致影响较新沉积。中部是一大凹陷，沉积很厚。南部被双辽隆起分为东西二部，东部已发现海相第三纪（松花江统）。

关键性问题是：（1）加紧进行物探，划分平原的构造单元，（2）配合浅钻研究中生代地层，特别注意松花江统的海相第三纪，（3）海侵似不可能从苏联方面进侵，而是从渤海北来，因此应该在彰武一带用深浅钻证实海相第三纪的存在。

看看黄汲清先生 1957 年报告的真实版本对松辽平原的海相第三系是何等的关切：海相第三纪很可能存在，值得进一步普查！哪里来的什么以陆相生油理论为根据？

然而，到 1994 年，黄汲清先生在临终前的口述访谈中，却坚持要把陆相生油理论指导石油普查的故事讲到底，在谈及松辽盆地时，把他 1957 年的论述“忘”了个干干净净，而把所谓陆相生油理论指导松辽平原石油普查及其“根据”搬进 1955 年的黄汲清思想¹⁴：

松辽盆地方面，当时我们知道东西很少，第一，松辽盆地是在大兴安岭隆起带的东面形成的一个凹陷带，布利斯道本一八六几年就提出大兴安岭隆起、松辽盆地中间是个大断层，兴安构造线，松辽盆地是大兴安岭前面一个凹陷带。大兴安岭隆起是侏罗、白垩、第三纪隆。第二，在松辽盆地的东南边，过去日本人有少数报道说那个地方出现松花江群勘探凹陷，以砂页岩为主，分布很广，它们可能是白垩纪的，但是陆相地层，没有看到海相。过去谭锡畴、王鸿桢他们调查嫩江地带的地质，发现在大兴安岭前面，嫩江上游，嫩江西的地层是陆相的砂岩地层，可能白垩纪第三纪的沉积，也是相当普遍，相当厚。这两个地层当时说的都是陆相的，不是海相的。不过不要紧，我们有陆相生油论嘛，陆相也可以有生油层，也可以形成油田。当然有海相就更好了。我当时的这个意见，是从葛利普和我们自己结合中国人、日本人的零星观察得出的一个不同的意见，所以决定要在这一地区进行石油普查，特别是松辽盆地、华北盆地。

“松辽盆地方面，当时我们知道东西很少”。这是真话。人们不禁要问，既然知道的很少，那黄汲清当年凭什么把松辽盆地列为重点地区？可见那是没有的事。黄汲清先生 1957 年的报告明明白白地说“东部已发现海相第三纪（松花江统）”“特别注意松花江统的海相第三纪”，“海侵似不可能从苏联方面进侵，而是从渤海北来，因此应该在彰武一带用深浅钻证实海相第三纪的存在”，这是真话；可到了 1994 年黄汲清却说松花江群（统）“当时说的都是陆相的，不是海相的”。怎么可以这样对待历史？

上述的历史事实充分证明，不仅黄汲清先生所谓提出“四大重点地区”是没有的事，所谓“根据陆相生油理论”提出“四大重点地区”的说法也根本站不住脚。

《发展史》关于 20 世纪 50 年代中国石油普查与大庆油田发现的叙事，没有了所谓“地质力学理论发现大庆油田”和“陆相生油理论指导石油普查发现大庆油田”的套话，本是一大进步，但是它却不愿引用公开发表的文字而原封不动地引用当年那些人编造的所谓“摘自当时的记录”的语句，事实上有意无意地又回到了“地质力学理论发现大庆油田”的悖论上去，同时又引用所谓黄汲清提出了四大重点地区的叙述，事实上又返回到了陆相生油理论指导石油普查发现大庆油田的老路上去。这至少是在糊里糊涂地叙述历史。



2.6 关于 1957 年的石油地质专业会议

《发展史》提到“1957 年 3 月，在地质部石油地质专业会议上，黄汲清作了‘对我国含油气远景分区初步意见’的报告”。

应该指出两点：第一，许杰副部长在此次会议的开幕词中明确指出：“这次会议的目的就是为了讨论我国各含油气区域地质工作的方向，为了总结交流两年来石油地质工作的技术经验，以提高干部的业务水平，确保 1957 年的工作质量，并为今后工作打下基础。”²⁰ 第二，虽然这次会议召开时，普查委员会已经不复存在，谢家荣不在地质部石油局履新，而在地质部地质矿产研究所副所长的岗位上，但却被安排在这个石油局主办的会议上作了题为《对于这个若干油气区的看法》的报告。这个报告是谢家荣在 2 月 16 日至 2 月 27 日的 11 天时间里写成的²¹。报告对当时正在进行工作的主要含油气盆地准噶尔盆地、河西走廊及阿拉善三角地前盆地、柴达木盆地、四川盆地、华北平原、黔桂滇地台区、陕北及鄂尔多斯盆地、华东地区的含油远景和进一步工作的方向，提出了非常具体的意见（由于这时松辽平原的资料还不够多，所以没有提到松辽平原）²²。对照许杰副部长的开幕词和谢家荣的报告，说谢家荣的报告是此次会议的主题报告一点也不夸张。

以陕北-鄂尔多斯盆地为例，报告认为，这里找油的主要方向应该是到古生代地层中去找，即奥陶系顶部的古风化面以及石炭二叠纪地层是可能的油气储层²²。50 多年后，在陕北鄂尔多斯盆地寻找石油天然气的实践证明，这里主要的含油气层系正是谢家荣当年指出的上古生界石炭-二叠系（致密气）和下古生界的奥陶系（碳酸盐岩气藏）。迄至 2017 年，陆续发现了下古生界靖边气田、上古生界榆林气田，亿吨级大型岩性油藏靖安油田，上古生界发现并探明了苏里格、乌审旗、米脂、子洲等气田，累计探明储量达 1.7 万亿立方米；以奥陶系碳酸盐岩风化壳天然气成藏地质理论为指导，扩大了靖边、榆林气田含气范围，累计探明储量 4337 亿立方米²³。相信还会有更多的发现。

请不在石油局履新的谢家荣到石油局主办的石油地质专业会议上作了事实上的主题报告，而作为当时石油局总工程师的黄汲清在 1994 年提及这次会议时大讲特讲他自己所作的报告，竟然完全“忘记”了请谢家荣到会作报告的事，一个字不提¹⁴。

《发展史》也只记得黄汲清的报告，不记得谢家荣的事实上的主题报告。历史不应该是这样书写的。

2.7 关于石油普查向东部转移的意见

《发展史》还说，1955-1957 年间，“李四光、黄汲清、谢家荣等均提出了石油普查向东部转移的意见（第 285 页）。”

据我所知，谢家荣曾在 1956 和 1957 年指出：

为达到第二和第三个五年计划所要求的储量，则必须发现几个大的新油区。而为了要使一部分的新油区能在此时期内投入生产，获得产量，我们不但要在西北广大地区以往曾做过相当工作的如柴达木、



准噶尔等地区内进行勘探，还要在尽管了解还不够但交通较便、开发较易的地区内进行工作，俾可收事半功倍之效²⁴。

为达到第二个五年计划所要求的储量，则必须发现几个大的新油区，而为了要使一部分的新油区，能在此期限内投入生产，获得产量，我们不但要在西北广大地区已证实的油田内进行工作，还要在交通较便，开发较易的地区内，加速勘探，俾可收事半功倍之效（第 123 页）⁶。

这是谢家荣关于石油普查向交通较便、开发较易地区转移即向东转移的具体论述。李四光、黄汲清在 1955—1957 年间在什么时候、什么场合提出过石油普查向东转移的意见呢？《发展史》没有给出（也给不出）任何信息。这样的叙事当然不能认为是在严肃地书写历史。

2.8 关于煤田地质勘探成就

在第八章地质科学支撑的地质勘探成就的标题下的煤田地质勘探成就，《发展史》为读者罗列了 1949-1957 期间一大批煤田地质勘探所获得的储量（第 278-279 页），但却看不到这一时期地质科学是如何支撑煤田地质勘探的，似乎这些煤田的发现与地质科学没有什么关系似的，虽然在最后提了一句“这一时期，王竹泉、岳希新分别对组织部署燃料工业部系统和地质部系统的煤田地质勘探工作发挥了重要的指导作用（第 279 页）。”

实际上，谢家荣对这一时期的煤田地质工作是有过很大贡献的，但《发展史》一字不提。这里略述谢家荣在此时期对中国煤田地质勘探的贡献。

1946 年谢家荣主导发现淮南八公山新煤田，乃中国地质学史上的一段佳话。解放后按照谢家荣的思路进行勘探的结果，到 1952 年底，“已证明它是黄河以南最大的煤田，煤质优良，都是烟煤，其中有一部分还能炼焦。”²⁵

新中国成立后，尤其是在第一个五年计划期间，谢家荣发表了《煤地质的研究》（1952）²⁶、《关于煤地质方面的一些重要知识》（1953）²⁷、《勘探中国煤田的若干地质问题》（1953 年 1 月 22 日在全国地质工作人员会议上的报告，发表于《科学通报》3 月号，并为《地质学报》33 卷第 1 期转载）、《中国的煤田》（1954）²⁸、《煤的成因类型及其意义》（1955）²⁹、关于“煤田类型”（1955）³⁰ 等论文，指导了中国煤田的地质勘探。在《勘探中国煤田的若干地质问题》中更明确指出了中国找煤的方向：

我们要在已知煤田的附近，扩大探勘范围，重新建立起它原来沉积的范围，然后在这个范围内进行测勘和钻探。其次依据地层及构造的推测，可指出若干隐伏的或断陷的新煤田。最后，从海侵和大地构造理论，也可指出若干可能发现煤田的地区……淮南新煤田和大淮南煤田的例子，就是依据沉积范围和地层来决定的。中梁山和雷家沟新煤田的发现，主要是从地层及构造的推测而得到的。而禹密煤田和淮南煤田间的可能新煤田，如果成为事实，那就是大地构造理论之所赐了。

此外可能发现新煤田的地方还很多，太行山东坡若干为冲积层所掩盖的区域、渭北台地、兰州窑街一带、东北完达山脉森林区域、开滦煤田的附近、贾汪、徐州一带等地，都有发现新煤田的希望²⁵。

在学习苏联先进经验的热潮中，中国科学院编译局、科学出版社拟定编译出版一套《科学译丛》，谢家荣应邀主编了其中 4 本地质学译丛，用以作为我国地质工作的借鉴和参考：其中 1 本是关于石油的，1 本是关于金属矿床的，而关于煤的有 2 本即



《煤地质学的理论问题》(1954)和《煤的成因类型与煤岩学研究》(1955)。谢家荣为《煤地质学的理论问题》精选了 8 篇文章并亲译《含煤建造的大地构造类型》和审校了《含煤系中沉积旋回的划分与定型原则》。谢家荣为《煤地质学的理论问题》一书作序,介绍了 8 篇文章的内容,指出阿莫索夫所提出的“造成煤的性质与成分不同的”五个主要原因,综合了现代煤岩学家和煤化学家的最新研究结果,为我们研究煤质变化问题提供了新的方向。指出“在今年春天中央地质部召开的煤田地质会议上,大多数的中国地质工作者都已学习了沉积旋回的原理及其在煤层对比和在阐明整个煤田发展历史上所起的重要作用。”“波特维金娜所著《含煤岩系沉积旋回的划分与定型原则》一文,是关于研究煤系沉积旋回的新著作,它详尽地讨论了划分各型旋回的原理,足为煤田地质会议关于本问题学习资料的补充读物。”“鲁欣所著的《含煤建造的大地构造类型》是从他的巨著《沉积岩原理》中节译出来的。是从沉积型相来研究煤田大地构造的方法,是比较准确而对于中国煤田类型来讲更能给予可靠证据的方法,特别像硅质岩、铝土页岩、菱铁矿层等,都已在中国许多煤田中找到,所以可作为划分煤田类型的标志。”“克拉兴宁尼可夫所著“边缘凹地的含煤沉积”介绍了苏联关于煤田大地构造类型的最新观点,着重指出边缘凹地是造成丰厚煤田的最有利的地质环境,这与中国研究若干重要煤田所得的初步结果是大致相符合的。在这篇文章中详尽地讨论了边缘凹地型煤田的特征,举出了许多实际例子,足为我国研究这个问题的重要参考资料。”“克拉兴宁尼可夫的《苏联的中生代含煤沉积》,讨论了苏联中生代煤田的分布及大地构造类型,着重指出煤系沉积与地盘升降的关系。苏联中生代煤田的地质特性,在许多方面与中国的中生代煤田是很相近似的,因此关于苏联中生代煤田的理论与实践相结合的经验总结,足供我们进一步工作的参考。”

《煤的成因类型与煤岩学研究》精选 7 篇论文,谢家荣亲自翻译了其中的 4 篇,朱夏翻译另外 3 篇。这 7 篇论文集中反映了苏联煤岩学研究的成就和理论发展现状,其中有苏联著名煤岩学家金士蒲格的《陆植煤的煤岩亚种》,基莫菲耶夫的《煤的成因类型与沉积环境的关系》,华西列夫的《探讨煤洗选性的煤岩学研究》,以及克莱洛娃的《陆植煤的光学性质及折光率定煤化程度的方向》等。结合当时我国煤的工业性质,特别是结焦性、炼焦配煤等诸多问题,汲取苏联及其他先进国家的经验,了解他们的理论发展和现状及解决实际问题的经验,尤其是煤的分类体系,高度评价了苏联陆植煤的分类方案,及其对中国煤的分类方案的借鉴意义。

2.9 关于中国铀矿地质与勘查

2017 年 7 月 28 日的《中国矿业报》第 3 版,整版刊登了我的“中国铀(钍)矿地质与勘查的先驱和开拓者——纪念谢家荣教授诞辰 120 周年”。此文经修改和充实后于同年 12 月以“中国铀矿地质与勘查的开拓者和奠基人——纪念谢家荣教授诞辰 120 周年”为题发表于《科学文化评论》第 14 卷第 6 期。《发展史》作者之一的赵腊平当然读过此文。但《发展史》作者讲述中国“放射性矿产地质勘探”时却这样写道:“1954 年 4 月地质部普查委员会设立了第二办公室,负责普查勘探铀矿资源,由副部长刘杰直接领导该办公室,并请高之杖担任技术领导工作。高之杖从仅有的几份 20 世纪 40 年代的铀矿资料中选定了辽宁海城大房身长石矿及广西钟山花山花岗岩体两个矿化异常点进行踏勘检查。同年秋,在花山找到了铀矿化点(第 314 页)。”



历史不应该是这样叙述的。

1943年5月南延宗先生在广西黄羌坪第一次发现铀矿物，同年8月李四光随南延宗和吴磊伯前往黄羌坪考察，再次确认南延宗先生发现的铀矿物。虽然铀矿物的发现对中国的铀矿工业和原子弹无疑非常重要，但是，发现铀矿物与找到铀矿床远不是一回事。从南延宗在黄羌坪发现铀矿物到1954年秋，其间11年的历史，“中国铀（钍）矿地质与勘查的先驱和开拓者——纪念谢家荣教授诞辰120周年”一文中详尽的论述，此不赘述。这11年的中国找铀历史被中国地质界乃至整个中国学术界忘得一干二净，实在不应该。《发展史》提到“高之杖从仅有的几份20世纪40年代的铀矿资料中选定了辽宁海城大房身长石矿及广西钟山花山花岗岩体两个矿化异常点进行踏勘检查。同年秋，在花山找到了铀矿化点”，本文就此说点真正的历史：

1、1946年，为调查黄羌坪铀矿等，谢家荣派出南岭特种矿产队，由张兆瑾、霍学海会同中央地质调查所的徐克勤等前往工作。五月在黄羌坪试探铀矿化约一个月，除地面地质观察外，还动用槽探工程揭露矿化地段，得出了如下的认识：“矿区附近为花岗岩所构成，有长英岩侵入其间，长英岩复被伟晶花岗岩脉侵入。含铀矿物（存）在于长英岩脉中之剪力带内，其旁云英岩化较显。已发现之剪力裂隙，共达十余条，皆互相平行，走向俱为东西，其中四个剪力（裂隙）向南倾斜，倾角八十五度左右，面上产有少量铀矿，其中二个并见黄铁矿矿囊各一，惟延展不广。经掘槽试探，矿脉似有愈下愈薄之势。含铀矿物已知者有 pitchblende, gummite, torbernite, uranophane 和 autunite 五种²，共生矿物则有十余种之多。总观本区矿床，似应属中温热液一类，沿长英岩之扭转面而存在，分布极不均匀，厚自五公厘至六七公厘。各含铀矿物中，pitchblende 似属原生，其他水氧化物类则俱为次生。据目前观察，储量微薄，难言开发，将来应就整个区域内之剪力带继续施探，或有发现堪采矿床之望。”³¹

2、1947年9月，国民政府国防部叶逢耕函告广西省政府建设厅，钟山县黄羌坪发现铀钍矿。接信后，该厅立即派出李祖材前往检查，并拟出进一步探勘铀钍矿的工作计划。次年1月，该厅在贺县、钟山县成立铀钍矿探勘队，由省政府顾问何杰（原两广地质调查所所长、广西大学校长）兼任队长，蔡承云、李祖材参与工作，经工作查明铀矿物有铀钼矿、铀矾石、铀铅矿、铀灰矿、铀灰石等五种。但由于当时政局动荡，经费不足，探矿勘查半途而废³²。

3、1948年2月26日，谢家荣随矿产测勘处派出的广西八步队（成员含南延宗、赵家骧、霍学海、赵宗溥）前往黄羌坪亲自考察铀矿化和八步地区砂锡矿中所含独居石矿等，野外考察持续一个月整，于3月26日结束³³。考察结束后，谢家荣著文《广西钟山县黄羌坪铀矿苗简报》（资源委员会矿产测勘处临时报告第73号）（图12）³⁴。简报叙述了铀矿化的地质产状，详细描述了铀矿化的特征。指出：次生铀矿物成黄色针状、粉状及绿色片状散浸于钟山花岗岩体中细粒花岗岩的东西向和南北向两组节理中。在紫外灯光下，次生铀矿物呈绿色或黄绿色荧光，花岗岩中石英亦发绿色荧光。此外，长石颜色特红，墨水晶众多。在此基础上，谢家荣讨论了黄羌坪铀矿苗的成因及其意义，并指出：

²此五种矿物的中文译名分别为沥青铀矿，脂铅铀矿，铜铀云母，硅钙铀矿，钙铀云母——笔者注

所谓黄羌坪铀矿，不过为铀矿苗之一种指示，而尚未可称为铀矿床也。但此种指示，殊有力量，盖除次生铀矿物外，尚有：（一）细粒花岗岩中长石之特红，（二）墨水晶之存在，（三）绿色荧光之石英，（四）硫化矿脉之存在等等。凡此征象，至少可指示花山花岗岩，尤其细粒花岗岩脉中含有较寻常花岗岩格外丰富之铀量，但是否其下尚有堪采之铀矿床，则殊难断言，盖花岗岩或细粒花岗岩中所含之微量铀质，经过潜水浸溶，经裂隙上升，可复沉淀于节理或岩缝中，造成如今日所见之次生铀矿，但其下未必有堪采之铀矿也。

从另一方面观之，地面发现次生铀矿，其下常有原生铀矿，如沥青铀矿之类。国外实例甚多，我国不能独异。南君最初发现之铀矿苗中有黑色之沥青铀矿，本处张兆瑾、霍学海二君子于去年探勘本矿时亦曾获得厚达数公厘之黑色铀矿脉，其外缘俱已变为黄色及红色之次生铀矿，可见地面所示，原生铀矿之微脉已稍露其端，向下则有扩大为堪采矿脉之希望。

更就地质环境及矿床型式论之，黄羌坪铀矿苗与葡萄牙及英国之康华尔铀矿颇为相似。葡萄牙铀矿于地面上仅见次生铀矿物，但至地面以下 20 余公尺即发现原生铀矿脉，深达百公尺以上。准是以观，则黄羌坪铀矿苗颇有注意之价值。

上述二种相反之推测，俱属可能，究竟如何，只有实施钻探以证实之。

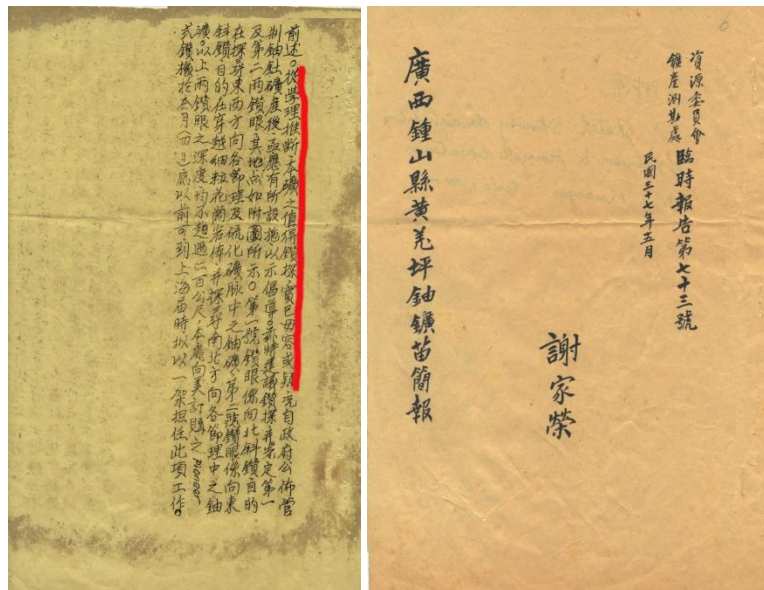


图 12. 谢家荣著《广西钟山县黄羌坪铀矿苗简报》封面及末页（存全国地质资料馆，档号 2618）

Figure 12. Cover and last page of 《Brief Report on the Uranium Mine Seedlings at Huangqiangping, Zhongshan County, Guangxi》 by C.Y. Hsieh (National Geological Information Center, file number 2618) Huang's

为此，谢家荣在简报中提出了钻探计划，并布置了 2 个钻孔：

从学理推断，本矿之值得钻探，实已毋庸置疑……兹特建议钻探，并先订第一及第二两钻眼……第一号钻眼系向北斜钻，目的在探寻东西方向各节理及硫化矿脉中之铀矿。第二号钻眼系向东斜钻，目的在穿越细粒花岗岩体，并探寻南北方向各节理中之铀矿。以上两钻眼之深度，均不超过二百公尺。本处向美订购之 Pioneer 式钻机于本月（四月）底以前可到上海，届时拟以一架担任此项工作。



溥前往辽南地区调查海城的稀有金属矿³⁸。同年9月13日，矿产测勘处举行迁回南京后的第9次学术研讨会，由赵宗溥讲辽宁海城铀矿。赵宗溥指出：矿区附近出露地层为震旦纪的片麻岩、云母片岩及角闪片岩，火成岩大部为花岗片麻岩及花岗伟晶岩脉。铀矿产于黑云母伟晶花岗岩脉中，与围岩界限清晰，带状构造发育，可区分为细粒带、纹象带、粗粒带及分离带，铀矿多产出在分离带至粗粒带部分，几乎全部产于石英脉附近的微斜长石中（黑体是本文作者标的）³⁹。1949年6月，谢家荣在《中国探矿计划》中也安排了海城大房身等地的详测工作，计划派出地质2人，测量2人，工作3个月（图13）。1949年11月，谢家荣在《东北地质矿产概况和若干意见》中也指出，海城铀矿等，“是日本人在抗战末期新发现的矿产，也须继续研究搜探。”⁴⁰。

这里有必要指出，谢家荣1949年《中国探矿计划》中计划进行的铀矿测勘项目共5处，3处为踏勘，工作程度最高的两处进行详测（大房身等地）和钻探（黄羌坪），高之杖选定的两地竟然与《中国探矿计划》中所列工作程度最高的两地一致，难道纯属“巧合”？

6、还必须指出，早在1947年11月谢家荣就指出了在中国寻找铀矿的7个远景区，即 a、辽东湾地区和阴山地区前寒武纪地块中的伟晶岩脉：已经生产了少量黑稀金矿，铀钼矿，褐钨铀矿和铀钍铀矿；b、成矿作用复杂的南岭地区：从东部的赣南，经过湘南、粤北和桂东南，一直延伸到滇南的个旧锡矿区，可望找到康沃尔型的铀产地；c、湘西黔东地区，湘西高地东缘或贵州高原东部与湘西高地之间的过渡带值得仔细研究，可能会有铀矿床产出；d、滇中康南地区，有非常复杂的矿物组合，可以认为是很有希望的铀矿产地；e、玄武岩铜矿区：在云南、贵州、西康、四川四省比邻区，还有滇西和滇西北的部分地区，有许多直接或间接由玄武岩喷发形成的铜矿床，其床中有望找到一些铀或钒的产地；f、沉积建造中的产地：应当注意沉积岩中，特别是四川、西康、云南和新疆中生代盆地沉积中，可能会发现与科罗拉多的钒钾铀矿类似的矿床；g、海滩砂和海岸沉积，整个福建和广东的海岸都有希望找到独居石⁴¹。

迄今中国发现的世界级铀矿大营铀矿产在上述第一个远景区内，而第二个远景区即从东部的赣南，经过湘南、粤北和桂东南，一直延伸到滇南个旧锡矿区的南岭地区——据报道，截至2011年的统计数据，赣、湘、粤、桂四省区的铀矿储量占全国已探明铀工业储量的74%⁴²。

应该说，谢家荣为寻找中国铀矿做出了重大贡献，但是，谢家荣的名字在很长一段时间里成了禁忌，以至而今查遍互联网也找不到谢家荣与中国第一块铀矿石的关系的一点点蛛丝马迹。而在所有中国放射性地质矿产勘查史中也都找不到谢家荣的名字，这部《发展史》也不例外。中国地质界和中国学术界对于谢家荣对中国铀矿地质勘查所做贡献的集体失忆，实在令人唏嘘不已。

3. 呼唤信史

科学发展史也是历史。历史也是科学。科学就应该是严谨的。任何历史，包括科学史，都应该是信史，都应该是记载确切的历史、真实的历史。



宋瑞祥先生在《发展史》的序言中说：“一部好的史书，能够起到‘资政育人’的重要作用。”这话当然是非常正确的。但所谓“好的史书”必须有一个前提，这个前提就是其所提供的历史应该是信史，是真实的历史，如果不是信史，是不真实的历史，那它就不可能是一部“好的史书”，就根本不可能起到“资政育人”的作用，并且恰恰相反，会收到误导读者的效果。

笔者以为，写好一部中国地质科学发展史，或中国地质事业发展史，是一项非常庞大，十分艰巨的工程，必须认真对待，细心查证，反复思考，多方征求意见，才能成为一部为世人尊颂的信史。要完成这么巨大的工程十分不易，绝不是几个人用一年两年时间所能做到的。以作者亲身经历的中国 20 世纪化探史的编著为例，就经历了中国化探界许许多多人长达五年的工作：

2003 年，夏国治等的《二十世纪中国物探》即将出版。受此启发，中国化探界的元老们决定编写 20 世纪的中国化探史，为此向国土资源部申请部科技项目“勘查地球化学在中国的发展与应用”。同年 6 月 30 日项目获批。以谢学锦、李善芳为首的 8 人项目组随即正式成立。11 月，项目组向全国地矿、冶金、有色、石油、核工业、武警黄金部队的主管单位、各省市地勘单位和有关物化探大队发送了开展项目的通报和编写大事记的参考提纲，请各部门、各单位总结自己的工作和成就，并提交给项目组。其后，2004 年 12 月下旬又在北京华北大酒店举行了 20 世纪中国勘查地球化学发展史研讨会，动员中国化探界的同行为编写 20 世纪中国化探史献计献策，全国各省市地勘地球化学界的专家学者近 60 人参加了会议。经过项目组全体同志和有关编写人员及全国各部门、各单位相关同志五年的共同努力，编写出了研究报告，于 2008 年 12 月 11 日通过以孙枢院士为首的评审组的评审验收，最终在 2009 年 12 月由地质出版社出版了 93 万字的《二十世纪中国化探（1950~2000）》。尽管如此，也仍然还存在一些小的错误需要补正。

很遗憾，这样一部凝聚了许多人心血的《二十世纪中国化探》，还有夏国治等人精心编著的《二十世纪中国物探》，甚至都没有能够进入《发展史》编著者的视野，在他们的参考文献中都根本找不到。

虽然，如前文所述这部《发展史》也有不少亮点，但也正如本文所列举的存在编著者不从公开发表的文字、不从反映历史真实的文献中引用文字，而引用歪曲历史真实的资料述说历史的现象，甚至还出现了将谢家荣著《中国的产油区和可能含油区》说成是“谢家荣、黄汲清、翁文波共同发表”这样不可思议的错误。这样对待历史怎么可能写出真正的信史？

长期以来，中国地质界欠着谢家荣一份公道。《发展史》能够将其作为“重要人物”的第三号人物叙事，是一大进步，值得称道。但综观整部书的叙述，在不少具体问题的叙事上（像铀矿勘查史那样完全抹杀谢家荣仅是一例），也仍然还欠着谢家荣一个公道，距离信史十分遥远，限于篇幅，本文不再论及。

上述是笔者阅读《发展史》一书中主要是 1950 年代的很少的一部分文字后所提出的几点质疑，不当之处，欢迎批评指正。



致谢

作者谨向下列各位表示由衷的感谢，他们在阅读本文初稿后提出了不少中肯、宝贵的修改意见；他们是：中国地质科学院地质研究所研究员浦庆余先生，浙江中控研究院高级顾问徐义亨先生，谢渊泓博士，中国第二历史档案馆研究馆员刘鼎铭先生，西南民族大学副教授覃影先生和中国地质图书馆高级工程师张尔平先生。

参考文献

1. 矿产测勘处. 1950. 地质探矿专修学校筹备经过及招生情形. *矿测近讯*. 1950. (107~108) : 7.
2. 《新中国第一所地质专业高等学校》编写组. 1999. *新中国第一所地质专业高等学校——南京矿专创办 50 周年纪念*. 北京：石油工业出版社.
3. 张立生. 2010. 论大庆等油田的发现与李四光的地质力学理论无关. *科学文化评论*, 7 (5) : 5~45.
4. 谢家荣. 1952. 从中国矿床的若干规律提供今后探矿方面的意见. *地质学报*. 32 (3) : 219~231.
5. 谢家荣. 1957. 中国的油气区和可能油气区的划分与评价. *科学*. 33 (1): 13~18.
6. 谢家荣. 1957. 中国的产油区和可能含油区及对今后勘探工作的意见. *谢家荣石油地质论文集*. 北京：地质出版社. 1957.
7. 翁文波. 1955. 中国大陆按油气藏希望的区域划分. *翁文波学术论文选集*. 266~272. 北京：石油工业出版社. 1994.
8. 中国地质学会. 1955. *中国地质学会会讯*. (9) : 10.
9. 中国地质学会. 2004. *黄汲清年谱*. 北京：地质出版社：1~341.
10. *国家地质总局对黄汲清同志反映的问题的调查报告*. 1978. 中央档案馆（或自然资源部档案室），全宗号 196，目录号 27，案卷号 14，序号 2.
11. 赵文津. 2006. 简介“国家地质总局对黄汲清同志反映的问题的调查报告”. *李四光与中国石油大发现*. 北京：地震出版社：66~77.
12. *中华人民共和国地质部第一次石油普查工作会议决议*. 1955. 中央档案馆档案（或自然资源部档案室），全宗号 196，目录号 4，案卷号 0260，序号 2.
13. 黄汲清. 1991. 我与石油、天然气的普查勘探. *黄汲清石油地质著作选集*. 北京：科学出版社. 1993：154~198.
14. 黄汲清. 1994. 黄汲清与石油、天然气的普查、勘探（黄汲清口述，亢宽盈、杨小林整理）. 中国科学院院史文物资料征集委员会办公室，《*院史资料与研究*》. 2008 年第 6 期（总第 108 期）：29~31.
15. *地质部 1955 年地质会议文件汇编*. 1955. 第 520 页，存中国地质图书馆，书号：208/208/55.



16. 地质部普查委员会“关于第一次石油普查工作会议的报告”. 1955. 中央档案馆（自然资源部档案室）. 全宗号 196, 目录号 4, 案卷号 0260, 序号 3.
17. 黄汲清. 1957. *对我国含油气远景分区的初步意见*. 中央档案馆（自然资源部档案室）. 全宗号 196, 目录号 6, 案卷号 050, 序号 1.
18. 黄汲清. 1956. *一年来石油地质普查工作中的经验教训及对今后工作的一些建议*. 中央档案馆（自然资源部档案室）, 全宗号: 196, 目录号: 5, 案卷号: 290, 序号: 5.
19. *中华人民共和国地质部第二次石油普查工作会议决议*. 1956. 中央档案馆（自然资源部档案室）, 全宗号 196, 目录号 5, 案卷号 290, 序号 1.
20. 许杰. 1957. *在石油地质专业会议上的开幕词*. 中央档案馆档案, 全宗号 196, 目录号 6, 案卷号 0050, 序号 1.
21. *谢家荣日记*. 未刊.
22. 谢家荣. 1957. *对于中国若干油气区的看法*. 中央档案馆档案, 全宗号 196, 目录号 6, 案卷号 0050, 序号 1.
23. 谭萍, 闫建文. 2017. 起底鄂尔多斯盆地: 我国最大油气田底气何来? *中国石油报*. 2017-04-26. 第 4 版.
24. 谢家荣. 1956. 石油地质的现状、趋势及今后在中国勘探石油的方向. *科学通报*. 1956. (5): 48~53.
25. 谢家荣. 1953. 勘探中国煤田的若干地质问题. *科学通报*. 1953 年 3 月号. 36~47.
26. 谢家荣. 1952. 煤地质的研究. *地质学报*. 32 (1-2): 61~69.
27. 谢家荣. 1953. 关于煤地质方面的一些重要知识. *煤*. (29): 27~29, 44; (30): 40~48.
28. 谢家荣. 1954. 中国的煤田. *科学大众*. 3 月号.
9. 谢家荣. 1955. 煤的成因类型及其意义. *地质知识*. 新年号: 3~5.
30. 谢家荣. 1955. 关于“煤田类型”. 载: *一九五五年地质会议文献汇编*. 北京: 地质出版社.
31. *资源委员会矿产测勘处三十五年度年报*. 1946. 1~28.
32. 潘其云. 2006. 揭开广西铀矿神秘的“头盖”. *南方国土资源*. 2006. (1): 43~44.
33. 矿产测勘处. 1948. 本处工作近况. *矿测近讯*. 1948 年 3 月号 (第 85 期): 45.
34. 谢家荣. 1948. *广西钟山县黄羌坪铀矿苗简报 (资源委员会矿产测勘处临时报告第 73 号)*. 全国地质资料馆, 档号 2618.
35. 谢家荣. 1949. *中国探矿计划*. 全国地质资料馆. 档号 1322.
36. 搜狐网. 2018-12-15. 寻找原子弹“开业之石”诞生地 (下). https://www.sohu.com/a/282049094_99978166.
37. 谢家荣. 1947. 评述战时中国沦陷区内的矿业经营. *大公报 (上海)*. 1947-01-06: 6.
38. 矿产测勘处. 1947. 本处工作近况. *矿测近讯*. 1947. (73): 14.
39. 矿产测勘处. 1947. 本处工作近况. *矿测近讯*. 1947. (80): 16-18.
40. 谢家荣. 1948. 东北地质矿产概况和若干意见. *科学*. 31 (11): 323-328.
41. C.Y. Hsieh. 1947. *Some promising regions for searching uranium and thorium deposits in China (中国铀钍矿的找矿远景区)*. 北京大学档案馆, 档号: 1RW0172002-0066.
42. 豆丁网. 2011-05-24. 中国铀矿资源的分布情况. <https://www.docin.com/p208621885.html>.



Author contributions

Lisheng Zhang contributed to the data collection, compilation and interpretation and wrote the paper.

Data availability

Data sets generated during the current study and internal reports/files referenced in this paper are available from the corresponding author on reasonable request, but restrictions apply to any data used in these studies.

Declaration of competing interest

The author declares that he has no known competing financial interests or personal relationships that could have appeared to influence the work reported in this paper.

Use of AI tools declaration

The author declares that he has not used Artificial Intelligence (AI) tools in the creation of this article.





Original Article

Assessment of aquifer vulnerability status and groundwater management studies using integrated geophysical techniques in Ewekoro South-West NigeriaS. A. Ishola¹ , V. Makinde², O.O. Alatise², H.O. Edunjobi², and C.O Ogunkoya³**Abstract**

Twenty-five vertical electrical soundings and ten 2D electrical resistivity tomography profiles were undertaken at Ewekoro District in Ogun-State, Nigeria. The work encompassed the utilization of Schlumberger and Wenner Array. Subsurface profiles were obtained using Direct Current Resistivity (DCRE) of Vertical Electrical Sounding using AGI Super-sting Earth Resistivity meter with schlumberger configuration; current electrode spacing (AB/2) ranging from 1.0 to maximum of 200m and the potential electrodes (MN/2) were consequently changed from 0.25 m to 5.0 m respectively which was further complemented by application of 2D electrical resistivity tomography (ERT) adopting Wenner array of electrode spacing of 10 m for the profile length of 200 m was maintained to attain a reading and imaging within the depth range of aquifer in the area for the effective characterization of the subsurface structures and delineation of the underlying aquifer. The interpretations of acquired resistivity data were carried out with manual procedures coupled with Resist, RES2DINV and Surfer software programs for VES, 2D-ERT and contouring respectively. The results of the hydraulic conductivity (K) cum hydraulic resistance (C) for the protective layers were estimated from the geoelectrical parameters estimated have values ranging from 0.00815 cms⁻¹ (VESEWE24) to 5.484 cms⁻¹ (VESEWE1) and 0.0075day⁻¹ (VESEWE21) to 15445.98 day⁻¹ (VESEWE25) respectively. AVI rating implications revealed that the study area is dominantly characterized by Extremely High Vulnerability (EHV); most of the locations were extremely high (88%) while VESEWE23 and VESEWE24 (8%) exhibited high vulnerability status and only VESEWE25 depicted low vulnerability status (4%).

Key words: Vulnerability index; hydraulic resistance; geoelectrical parameters; tomography

Affiliation Info: ¹ Department of Earth Sciences, Olabisi Onabanjo University Ago-Iwoye, P.M.B 2002, Ago-Iwoye, Ogun State, Nigeria; ² Department of Physics, Federal University of Agriculture Abeokuta, P.M.B 2240, Abeokuta, Ogun State, Nigeria; ³ Department of Physics, Ajayi Crowther University, Oyo Oyo, Oyo State, Nigeria.

Corresponding Author : Ishola, S.A. PhD, Exploration Geophysics and Geomathematics; Email: ishola.sakirudeen@oouagoiwoye.edu.ng.

Citation: Ishola, SA; Makinde, V; Alatise, OO; Edunjobi, HO and Ogunkoya, CO. 2025. Assessment of aquifer vulnerability status and groundwater management studies using integrated geophysical techniques in Ewekoro South-West Nigeria. *Naturalis Scientias*, 2 (2): 549-573. DOI: <https://doi.org/10.62252/NSS.2025.1033>. www.naturalisscientias.com.

Copyright © 2025 by the authors. Published by *Naturalis Scientias*. This is an open access article under the Creative Commons Attribution-NonCommercial 4.0 International (CC BY-NC 4.0) License. (<https://creativecommons.org/licenses/by-nc/4.0/>).



1. Introduction

Groundwater found beneath the water table and within the zone of saturation responds to movement and follow the same direction with the sloping of the water table and encompasses the moisture located in the pore spaces in the rock matrix. Obtaining clean and portable water for domestic, industrial and overall usage is a fundamental necessity for household usage and socio-economic development. The basic information obtainable from the controlling force of nature and corresponding geology of subsurface status at any given point in time is very significant in groundwater exploration and development. For efficient maintenance, sustenance and ultimate utilization of groundwater resources for the benefits of all and sundry; adequate protection and effective management of buried aquifers with thick overlying sediments is therefore necessary¹⁻⁴. Seepages of surface pollutants emanating from local environment ranging dumpsites, sewage system and run-off are some of the terrain activities that can the quality of groundwater⁵⁻⁶. Migration of these pollutants into the groundwater table can have unprecedented impacts on the groundwater thereby affecting its potability⁷⁻⁹. The seepages of these pollutants is greatly enhanced as a result of highly permeable overlying layers of the subsurface coupled with the ease at the contaminant fluid flows through the subsurface as the fluid flow is a function of combination of certain hydrogeological features namely intergranular pores, faults, fissures and fractures that are somewhat interconnected. In order to demystify several hydrogeological and hydrological problems, the significance of quantitative description of aquiferous zones cannot be overemphasized¹⁰.

The background knowledge of aquifer characterization and vulnerability studies of the groundwater system is highly expected for effective shielding of the groundwater system from external invasions. Vulnerability of aquifer is a reflection of the strength of the subsurface characteristics; whether they are capable enough to prevent or favour the transportation and consequent migration of the contaminant seepages into the aquifer repositories. Also, the vulnerability of any aquifer system is dependent on groundwater flow whose corresponding velocity (groundwater flow velocity) thereby enhances it; a factor that is very much dependent on both the water table depth as well as the hydraulic conductivity overlying the concerned aquifer. Furthermore, for effective groundwater protection, the overlying cum protective layers must possess a reasonably high thickness with associated low hydraulic conductivity. When the period of percolation exceeded ten years, it is considered necessary as suggested by¹¹ while the presence of abundant intrusions or fissures that are typically of sandy sediments can create pathways for percolation and subsequent migration of contaminant seepages within the protective layers but oftentimes, this inhomogeneous condition of the subsurface are not taken into proper consideration in groundwater studies¹⁻⁴.

Once the sanitary integrity is affected, it can result to various illnesses of water-borne origin which can also affect human health and biological population. This may in one way or the other jeopardize the day to day economic engagement and other associated activities in the area¹².

The vertical electrical sounding (VES) and electrical resistivity tomography (ERT) methods have been profitably applied by numerous researchers and consequently documented and published in literatures in the field of geophysics and groundwater exploration studies in resolving clusters of hydrogeological and hydrogeophysical challenges which includes



delineation of depth to water table, saturated aquifer horizons mapping, aquifer characterization and groundwater development studies, evaluations of rate of vadose zone infiltrations as well as in overall groundwater contamination studies¹³⁻¹⁶. The techniques are highly preferable since the resistivity contrast can be obtained when the aquiferous zones are attained¹⁷⁻²¹. The conductivity/resistivity of the arenaceous or argillaceous geological formations are displayed by the integration of VES and ERT as they are respectively distributed both vertically and laterally thereby serving as a good correlation tool for effective detection and subsequent delineation of aquiferous zone²²⁻²³). The daily increase in human and biological population and general quest water in numerous communities have led to increased agitations for groundwater coupled with unavailability and doubtful quality of available surface water. Most of the boreholes earlier drilled without preliminary professional investigations have failed due borehole collapse and water contamination thereby rendering these boreholes as abandoned wells.

As part of the approach undertaking to salvage these aforementioned problems, the factors contributing to water scarcity and impairment of available water by lithology and local geology have to be evaluated and independently addressed in an area under investigation. The controlling forces governing aquifer condition are reflections of the inherent compositions of the subsurface which play significant roles in assessing groundwater flow from the surface to the subsurface via several networks of recharge processes²³⁻²⁴. The adopted techniques, aside from their relative availability and easy accessibility; their capability in revealing distinctively the subsurface formations that are permeable due to unconsolidated materials and therefore permitting permeability via the infiltrating surface contaminants migrating to the subsurface^{5 & 24}. The VES method is a depth sounding technique which has over the years proven to be effective while possessing a wide range of application in groundwater exploration and development studies, and ERT possesses a wide application for detailed investigative studies encompassing the overlying layers due to its inbuilt sensitivity to contrasts in lithologic unit. These two techniques have proven to be of high reliability measures in aquifer studies and the accompanied software packages that are readily available for post field data processing, analyses and subsequent interpretation of acquired data make them veritable tools in overall groundwater studies. The application of these non-invasive techniques in determining aquifer characteristics encompasses the acquisition, processing, analysis and consequent interpretation of the local hydrogeological conditions for the ease of evaluating aquifer potential evaluations and determination of geohydraulic properties of any given area. Furthermore, the integration of the aquifer vulnerability index (AVI) functions as a complementary evaluation tool whether the overburden layer is shielded from the external contaminant seepages emanating from the surface and estimating the level of protection if it is, if it is will go a long way in demonstrating the effectiveness of these methods. The principal goal of this study was accomplished via the following stated predetermined objectives: determining the depth and corresponding thickness of each geoelectrical layers for the purpose of estimating the geohydraulic parameters of the formation which in turn leads to effective and procedural assessment of the vulnerability index of the protective layers of the aquifer thereby proposing the most effective and economical class of exploration and management techniques for the study area's groundwater system.



2. Study area

2.1 Location and geological setting

Ewekoro community in Ogun State serves as one out of the numerous mills of West African Portland Cement Company (WAPCO) and Dangote group Cement Company. It is a sleepy neighbouring town with close proximity to Papalanto, a town predominantly recognized for sugarcane plantation. It is found between latitude $6^{\circ}53'$ N and longitude $3^{\circ}14'$ E²⁵. Ewekoro formation and Abeokuta formation are geologically part of the sedimentary rocks of Ogun State. Ewekoro subsurface geology is highly fossiliferous and consisting of deposits of limestones being daily quarried by WAPCO for economic purposes²³. The cement manufacturing facility situated in Ewekoro is located 5 kilometres north of Ewekoro town ($6^{\circ}55'$ N and $3^{\circ}12'$ E). Also, this location is calculated to be of 64 kilometers north of Lagos and 42 kilometers south of Abeokuta on the approximate respective distance and is found within the tropical rainforest belt of Nigeria. Olapeleke community is located in the Western side, Itori community located in the Northern side, while Elebute and Alaguntan communities both of which were jointly in the Eastern part predating the factory are located within 10 km radius of the production facility and serve as the notable farming settlements in the investigated area²¹. These aforementioned settlements are perennially drained by Itori, Ewekoro, Eshe, Elebute as well as Alaguntan Rivers where Alaguntan River is the only river directly receiving waste water migrating from the cement plant. Nevertheless, non-point pollutants from run-offs and dust deposits from the atmosphere primarily influenced the sanitary qualities of other catchment rivers. The area is characterized by particulate matters like cement dusts and other material deposits enhanced by an average wind velocity of about 1.0 and 0.72 msG around 10 m higher above the ground level during the dry (January-March) and wet seasons (May-November) respectively²¹. One of the overriding weather situations governing the catchment area of the cement plant is average relative humidity in the recorded range of $65\pm 10\%$ alongside average annual rainfall in the range of 1500 ± 120 mm. Limestone composition of about 11m to 12m is found at the type locality of Ewekoro formation. The base of the formation is typically sandy grading in a downward direction into Abeokuta Formation. The Phosphatic glauconitic grey coloured shale overlain Ewekoro formation^{5 & 25}. Ewekoro formation is consistent generally with the regional geology of eastern section of the Dahomey Basin; it comprises of the limestone that are not only thinly laminated fissile and probably non-fossiliferous shale as predominant rocks but are also non-crystalline and non-fossiliferous²⁶. Furthermore, Ewekoro formation is comprised of intercalations sedimentary deposits of argillaceous origin; though characterized by softness and friability but equally cemented by ferruginous and siliceous materials in some places. The lithological units in Ewekoro formation are clayey sand, clay, shale, marl, limestone and sandstone²⁵.

The investigated area is known to range from a generally low lying to gentle steeping undulating terrain located within the humid tropical climate typified by two notable seasons distinctively predominant in the tropical region of southern Nigeria; the wet and the dry seasons. Usually, the occurrence of wet season varied from March to October where the prevailing climate is predominantly characterized by either the tropical maritime airmass

or the moisture laden Southwest winds migrating the Atlantic Ocean with heavy precipitations; large portion of the precipitations occurs in seemingly torrential downpours displaying high high run-off and sometimes flooding as the resultant effects while the occurrence of the dry season starts in November until late February or beginning of March subjected to the overriding trigger of the dry continental airmass or north-easterly winds migrating from the sahara desert. The major water bodies in the region are Yewa and Ogun rivers which flow into Lagos lagoon while their tributaries are found in Ewekoro Local Government Area as Alaguntan River, Akinbo River and Eshe River. There are however streams running parallel in the area. Also ponds are not left out. The fluctuations of the water table are in response to the seasonality of the observed rainfall resulting from result varying changes in wet and dry season. During the wet season, groundwater level rises towards the surface and drops as the dry season sets in²¹.

Figure 1 shows the Geological Map of the Selected Locations of the Study Area within Dahomey Embayment, the inset map showing political divisions of the study area within Nigerian continental environment is shown in Figure 2, the map of the investigated locations in the study area are shown in Figures 3-4 is a base map displaying the location and accessibility of the study area in Ewekoro LGA.

The entire study area is generally accessible by the main roads alongside numerous footpaths, although the road from Abeokuta town to the investigated area is tarred. In addition to Ewekoro-Papalanto road, the survey locations can equally be accessed through a major road from Lagos State through Sango-Ifo express road.

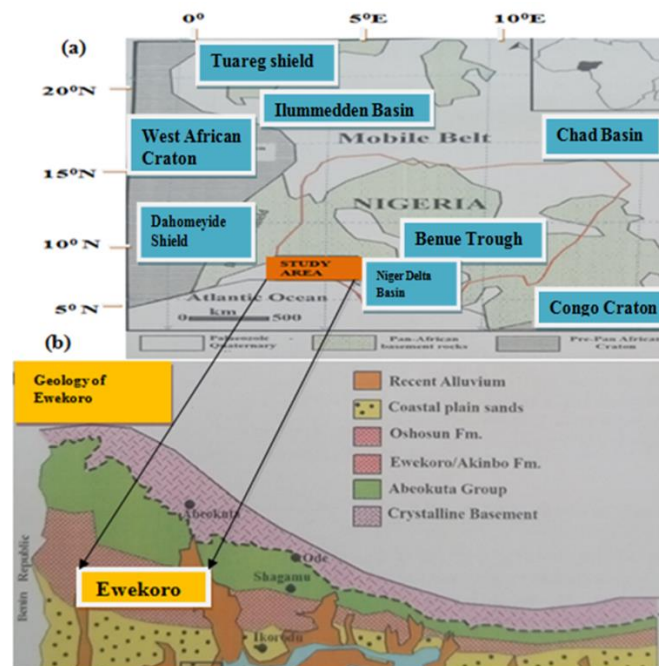


Figure 1. Geological map showing the investigated area within the Nigerian Part of Dahomey Embayment²¹
&27

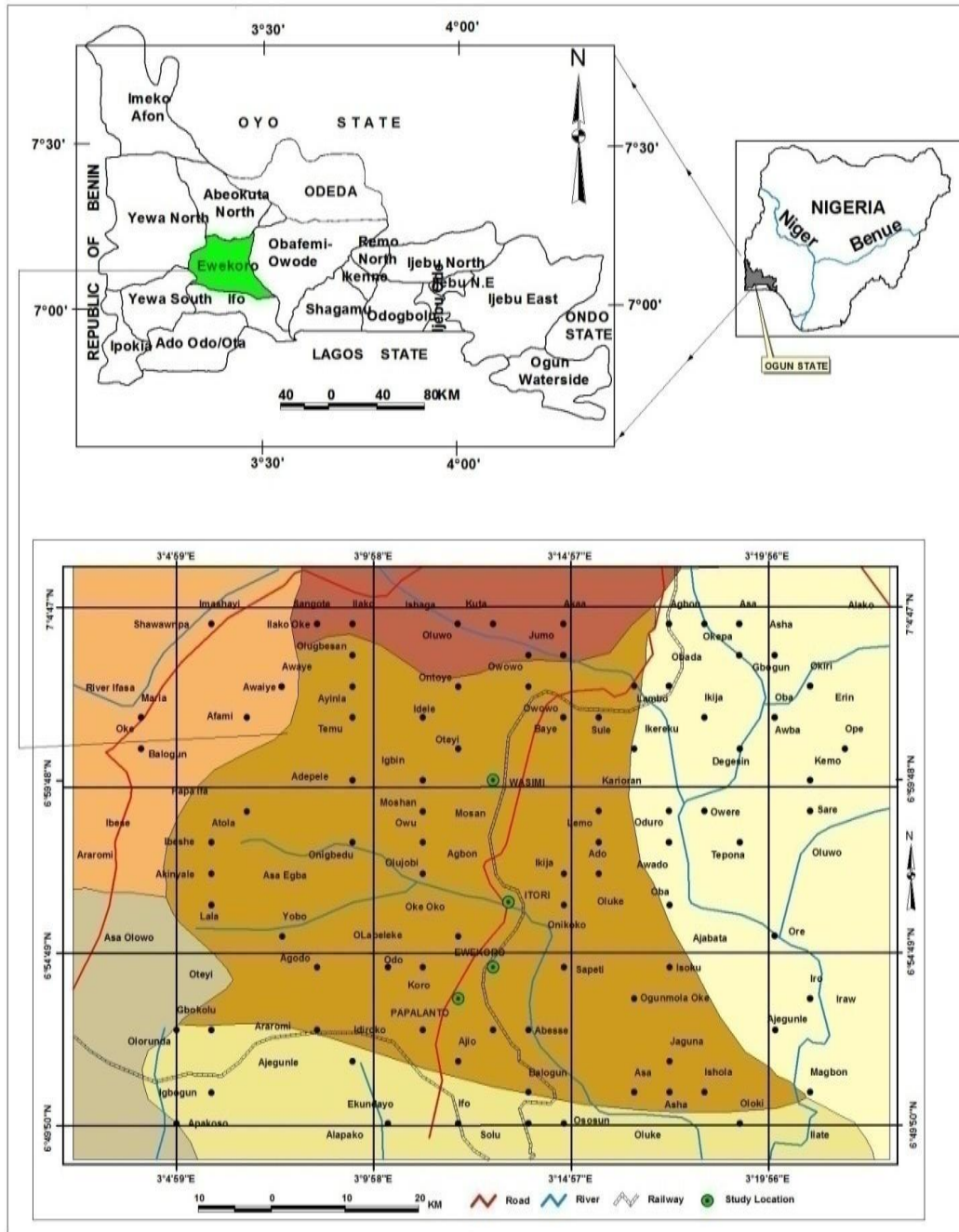


Figure 2. Inset map showing the investigated locations within Nigeria Continental Domain using Esri Data/Nigeria Political Information in Arcview GIS 3.2A Environment²¹

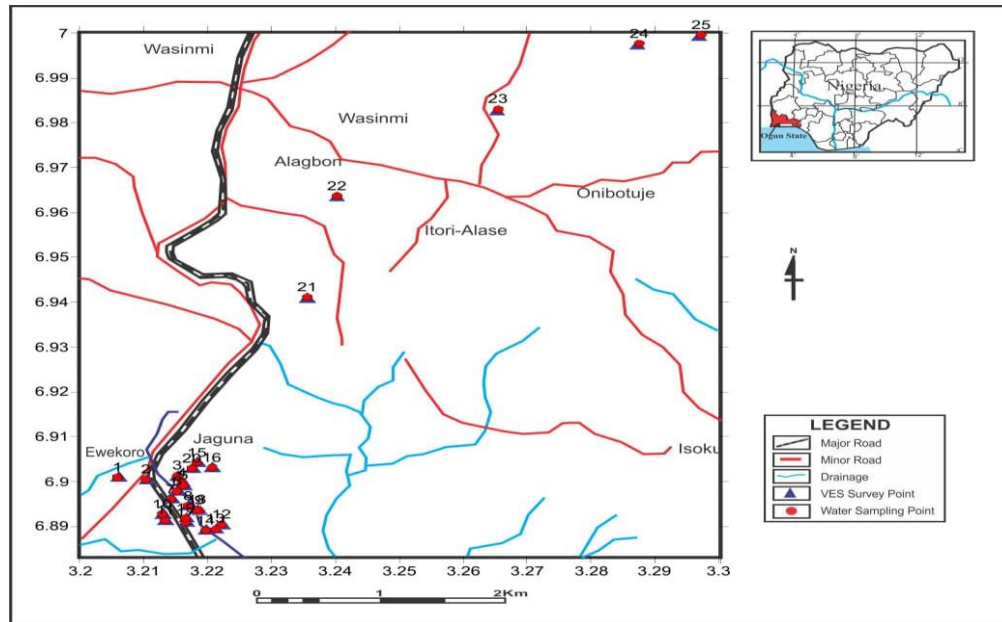


Figure 3. Map showing the data acquisition for the investigated sites in Ewekoro study area, Southwest Nigeria²¹

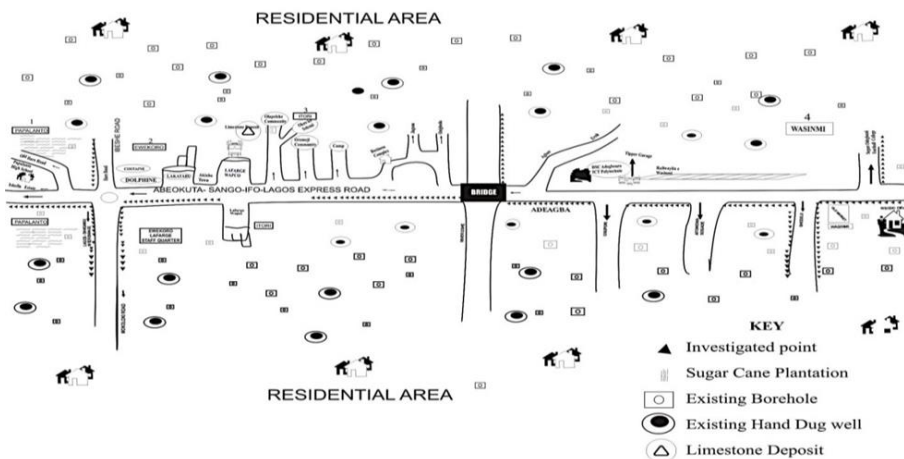


Figure 4. Basemap showing the location and accessibility of the investigated points in Ewekoro LGA, Southwest Nigeria²¹

3. Materials and methods

3.1 Geophysical field data acquisition in Ewekoro

VES and ERT resistivity surveying data were acquired using Integrated Geo and Instrument Services (IGIS), Model: SSR-MP-ATS; Ground Positioning System was used for both coordinate and elevation measurements; Twenty-five vertical electrical soundings and ten 2D electrical resistivity tomography profiles were undertaken respectively for VES and ERT. The work encompassed the utilization of Schlumberger and Wenner electrodes Array. WINRESIST with least square iterative inversion software programs were adopted for 1-D

resistivity inversion; while the RES2DINV.EXE version 3.57.37 iterative software program was adopted for 2-D resistivity inversion; and the contouring of the aquifer parameters was achieved using surfer software program. The vertical electrical sounding investigation adopted Schlumberger electrode array where current was directly sent into the subsurface via a pair of current measuring electrodes denoted as P and Q, and another pair of potential measuring electrodes X and Y responsible for the creation of the resulting potential difference. The apparent resistance R_a of the penetrated subsurface materials was read through the resistivity meter from the crystal displaying the result on the screen. The apparent resistivity was consequently computed by the product of the apparent resistance (R_a) and the geometric factor G, given by the mathematical equations expressed Eq. (1) and Eq. (2):

$$\rho_a = \pi \frac{[(\frac{PQ}{2})^2 - (\frac{XY}{2})^2]}{MN} R_a \quad 1$$

$$G = \pi \frac{[(\frac{PQ}{2})^2 - (\frac{XY}{2})^2]}{XY} \quad 2$$

3.2 Geophysical field data acquisition in Ewekoro

A bilogarithmic graph was used for the plotting of the calculated apparent resistivity, as characterized by a dynamic range for the purpose of smoothening, correcting and overall filtering of outliers that were considered as constituted noise in the field acquired data. This was followed by inverting electronically the already smoothened resistivity curve to true resistivity with the aid of WINRESIST software package. The VES curves were generated by the software program, in turn gave rise to three principal parameters namely true resistivity, thickness and depth. Unit layer resistivities (ρ) as well as the observed depth (h) are the two basic parameters that characterized any given geologic unit and their significance in the background analyses, interpretation and understanding of the given geoelectrical models cannot be overemphasized. These observed parameters served as basic parameters in the derivation of other hydrogeological parameters namely hydraulic conductivity cum hydraulic resistance for the horizontal, homogenous and isotropic layers^{23 & 28-29}. The hydraulic conductivity is presented in accordance to the work of Ishola et al. and Heigold et al.^{4 & 30} as K in Eq. (3). The hydraulic conductivity of the aquifer protective layers served as a principal parameter in evaluating the level of aquifer vulnerability of the area.

$$K = 386.40R_w^{-0.93283} \quad 3$$

where K represents the hydraulic conductivity as earlier stated and R_w represents the aquifer resistivity.

The subsurface rocks are porous and well fractured while the hydraulic conductivity gives the description of the ease at which groundwater propagates through the available porous spaces. Aquifer vulnerability index (AVI) has been defined as a technique that evaluates vulnerability considering the hydraulic resistance to vertical propagation of groundwater flow through the overlying strata. The evaluation of AVI utilizes duo parameters namely the thickness (h) of the protective strata and the hydraulic conductivity (k) estimated for the

strata. The hydraulic resistance (C) was consequently calculated by adopting the aforementioned duo parameters and is therefore presented as k_i

$$C = \sum_{i=1}^n \frac{h_i}{k_i} \tag{4}$$

Table 1. Aquifer Vulnerability Index (AVI) and Hydraulic Resistance²⁸

C	Log C	Vulnerability Status	Vulnerability Code
0 – 10	< 1	Extremely High Vulnerability	EHV
10 – 100	1 – 2	High Vulnerability	HV
100 – 1000	2 – 3	Moderate Vulnerability	MV
1000 – 10000	3 – 4	Low Vulnerability	LV
> 1000	> 4	Extremely Low Vulnerability	ELV

where k_i is repeatedly denoted as hydraulic conductivity, while h_i is represented as the thickness of subsurface materials within the the vadose zone.

Table 1 above illustrates the connecting law between the hydraulic resistance (C) and aquifer vulnerability index (AVI) and serves as aids in evaluating the vulnerability status of any given geologic model. Considering the field 2-D electrical resistivity investigation, the current and potential electrode pairs were increased at 5 m constant spread via the entire measurement until the highest spread is attained. The implication is that the series of measurement were observed in consecutive steps of 5 m, 10 m, 15 m, 20 m, and so on, progressively till the exhausted highest spread length of 200 m was reached. The conversion of the apparent resistivity was done using measured resistance at different intervals through the expression given in equation 5:

$$\rho_a = 2\pi a R_a \tag{5}$$

where the electrode spread is denoted by a and the resulting resistivity values were utilized in the generation of the ERT model utilizing the RES2DINV.EXE software program.

4. Results

4.1 Output of the VES data

The computer iteration of the resistivity soundings displayed in Figure 7 reveals the curves representing the inverse model of the geoelectrical parameters while the observed geoelectrical parameters as derived from the inverse model curves are hereby displayed in Table 1. On a general note, the resistivity sounding curves obtained from the surveyed area was a typical 4 layer (H type), with few 5-layer (KH). The H-type curve with about 85.4% of occurrence and KH-type curve with about 14.6% of occurrence were deduced from the area. Worthington et al. revealed that the curves as obtained from the field often reflect image geoelectrically revealing the condition of the area lithologic units in sequence and as a result this can be can be qualitatively utilized in assessing the groundwater prospects of

the area³¹. The H and KH curves are typical curves often serve as reflections of probable groundwater occurrence are pertinent to the study area³². The geoelectrical parameters of the lithologic units from the interpreted sounding curves were delineated as shown on Table 2 since electrical resistivity methods are basic reflection of the observed changes in earth resistivity^{4 & 33-35}. Considering the consistency of the geoelectrical parameters, the layers delineated in the midst of the sounding curves were specifically shown particularly along deeper sections of relatively uniform model resistivities and thicknesses (Table 2). The establishment of the lithology for the delineated geoelectrical layers was achieved by the integration the available information acquired from the previous drilled-well core samples as obtained from boreholes and hand-dug wells, observed local geology and previous published studies³⁶⁻⁴¹. The geoelectrical layers that were then delineated ranking from top to bottom were typified as top soil, sandy clay/clayey sand, shale/clay, sand lens, lateritic/kaolinitic clay, clayey sand, clay/shale, sandstone, weathered limestone and saturated sandstone. The topsoil is primarily of lateritic soil and partly unconsolidated sandy clay constituents with observed resistivity value that ranged from 26.90 to 842.20 Ωm with a mean value of 177.96 ± 250.28 . Lateral continuity was observed across the study area of resistive layer underlain the top soil; characterized as sandy clay/clay/clayey sand. The large observed variation in the model resistivity of this layer is a resultant effect of the differences in the extent of compaction of the unit alongside the lateral variations in constituent minerals. The second geoelectrical layer is underlain by sandy clay or shale/clay unit that is laterally discontinuous and characterized by a low resistivity while the lithological units were karstic limestone, saturated sandstone and sand. The delineated aquiferous layers were overlain by these top layers. Compaction and lithification were the possible attributes that accounted for the high resistivity values as observed in these layers. Large variations were observed in confined differentiation status of aquifer types. The borehole locations associated with VESEWE7 and VESEWE8 alongside with VESEWE14, VESEWE15, VESEWE21, VESEWE24 and VESEWE25 boreholes are unconfined while the rest locations displayed confined aquiferous conditions (Table 2).

4.2 Groundwater vulnerability in terms of aquifer protective capacity

In hydrogeological field studies, aquifer transmissivity is expressed to be resultant multiplication of its hydraulic conductivity for the thickness of the layer while the resultant multiplication of the resistivity for its thickness is defined and consequently represented as being the transverse unit resistance (T_r), on a pure theoretical basis. Therefore, the transmissivity of any aquiferous unit gave a direct proportionate increase to its transverse unit resistance directly and vice-versa⁴². Low resistivities and low hydraulic conductivities are typical of clay dominated layers. Hence, the protective capacity of the overburden unit could be regarded as being proportional to the ratio of the thickness to resistivity of the unit. In all the investigated study locations displayed less 1.0 protective capacity values except VESEWE9 and VESEWE17 whose protective capacities are greater than 1.0 Siemens with VESEWE17 being the investigated location with the highest protective capacity. The values range from 7.7002×10^{-3} Siemens to 1169.48×10^{-3} Siemens (Table 1).

Table 2. Computed geoelectrical parameters of Ewekoro

VES Stations	Aquife r Resisti vity $\rho_a(\Omega m)$	Depth to Aquifer (m)	Longit udinal Condu ctance (S)	Probable Aquifer System	Inferred Lithology	Hydraulic Conductivity (m/s)	Transmissivity ($m^2 s$)	Protective Capacity (<i>Siemens</i>)
VESEWE1	26.7	46.9	0.5801	Confined	Limestone/Sandstone	44.39085×10^{-3}	1025.4287×10^{-3}	865.31×10^{-3}
VESEWE2	281	8.04	0.1041	Confined	Limestone/Sandstone	7.114064×10^{-3}	227.65000×10^{-3}	387.935×10^{-3}
VESEWE3	104	37.7	0.2351	Confined	Limestone/Sandstone	25.44385×10^{-3}	694.61675×10^{-3}	659.607×10^{-3}
VESEWE4	175	74.1	0.2653	Confined	Limestone/Sandstone	15.26058×10^{-3}	1066.7150×10^{-3}	833.333×10^{-3}
VESEWE5	7.55	32.6	0.5290	Confined	Limestone	50.95356×10^{-3}	1650.8934×10^{-3}	529.049×10^{-3}
VESEWE6	419	39	0.0824	Confined	Limestone	2.633922×10^{-3}	81.651544×10^{-3}	721.293×10^{-3}
VESEWE7	74.06	65.76	0.3538	Unconfined	Limestone	31.56477×10^{-3}	1952.2807×10^{-3}	701.158×10^{-3}
VESEWE8	96.3	70	0.3195	Unconfined	Limestone	26.89435×10^{-3}	1758.8856×10^{-3}	682.934×10^{-3}
VESEWE9	88.2	83	0.5131	Confined	Limestone/Sandstone	28.50939×10^{-3}	481.80866×10^{-3}	1128.33×10^{-3}
VESEWE10	70.3	57.9	0.3901	Confined	Limestone/Sandstone	32.43096×10^{-3}	716.72424×10^{-3}	740.079×10^{-3}
VESEWE11	166	9.83	0.0377	unconfined	Limestone	16.28222×10^{-3}	491.72292×10^{-3}	100.807×10^{-3}
VESEWE12	366	11.9	0.0247	unconfined	Limestone	3.857709×10^{-3}	108.40162×10^{-3}	100.671×10^{-3}
VESEWE13	615	13.35	0.0136	unconfined	Limestone	0.642283×10^{-3}	3.5967838×10^{-3}	143.962×10^{-3}
VESEWE14	4765	11.8	0.0082	Unconfined	Limestone	6.776527×10^{-3}	1910.9807×10^{-3}	323.312×10^{-3}
VESEWE15	126	15.13	0.0498	Unconfined	Limestone	21.71652×10^{-3}	275.79986×10^{-3}	94.9367×10^{-3}
VESEWE16	99.2	61.2	0.3629	Confined	Limestone/Sandstone	26.33855×10^{-3}	758.55612×10^{-3}	885.341×10^{-3}
VESEWE17	1.03	61.2	1.1468	Confined	Limestone/Sandstone	53.40249×10^{-3}	1537.9919×10^{-3}	1169.48×10^{-3}
VESEWE18	175	96.6	0.3453	Confined	Limestone+Sand	15.26059×10^{-3}	1429.9170×10^{-3}	1122.81×10^{-3}
VESEWE19	123	56.1	0.2879	Confined	Limestone	22.19070×10^{-3}	532.57690×10^{-3}	782.779×10^{-3}
VESEWE20	106	62.5	0.3427	Confined	Limestone	25.08007×10^{-3}	438.90121×10^{-3}	809.561×10^{-3}
VESEWE21	163	71	0.0012	unconfined	Limestone+Sand	16.63774×10^{-3}	953.34237×10^{-3}	9.88459×10^{-3}
VESEWE22	407.2	54	0.0026	Confined	Limestone+Sand	2.867480×10^{-3}	139.64626×10^{-3}	61.6017×10^{-3}
VESEWE23	438.5	60.3	0.0007	Confined	Limestone+Sand	2.288905×10^{-3}	108.49409×10^{-3}	24.4968×10^{-3}
VESEWE24	139.4	37.4	0.0021	Unconfined	Limestone	197.1921×10^{-3}	5639.6951×10^{-3}	7.70015×10^{-3}
VESEWE25	80.8	74	0.0296	Unconfined	Limestone	37.86069×10^{-3}	1847.6019×10^{-3}	36.2018×10^{-3}

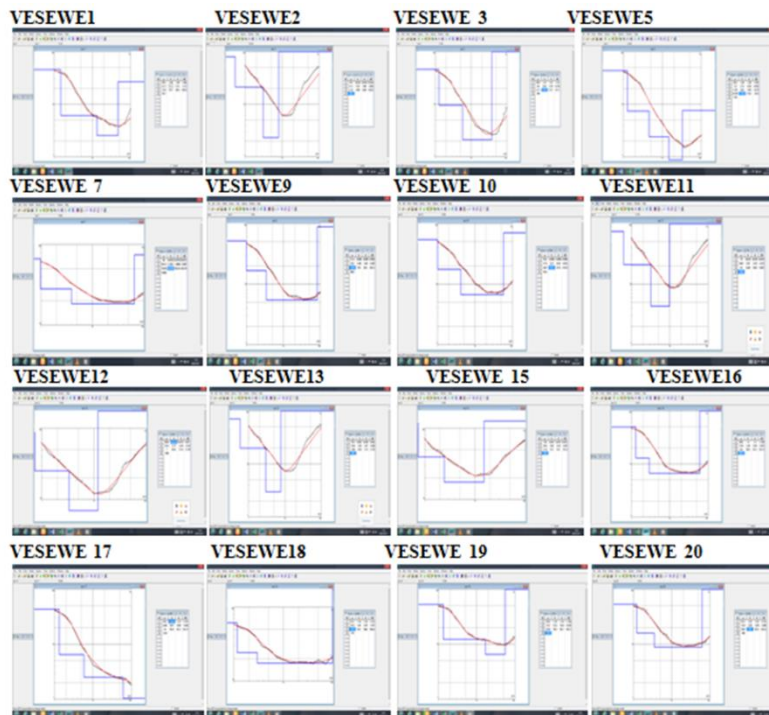


Figure 5. Typical VES curves representing investigated sounding points in Ewekoro²¹

In the entire study locations where the longitudinal conductance (S) and hence, the protective capacity (P_c) values in the study areas are less than 1.0 Siemens ($P_c < 1.0$ Siemens); they are classified as low and are characteristics of depositional successions of overburden layers with no impermeable clay/shale appreciably overlying rock. Such subsurface model is suggestive of high rates of infiltration from precipitation as well as surface contaminants into the aquifer system. However, the investigated locations where the protective capacity values are greater than 1.0; $P_c < 1.0$ Siemens (VESEWE9 and VESEWE17); imply that these locations have considerable layers of Clay separating the subsurface aquiferous zones (Table 1). In addition to high transmissivity and low protective capacity values in most of the investigated sites in the study area, the aquifers were very close or relatively close to the surface (<100m) and thus prone or susceptible to contamination over large areas once the aquifer receives a load of contaminant dose from surface to near surface. Nevertheless, groundwater potential in this study area is high due to high transverse unit resistance (R) with good suitability for the development of potable water supply boreholes²¹.

4.3 Aquifer vulnerability potentials using 2D electrical resistivity imaging

The inversion of the observed apparent resistivity pseudosection and inverse model resistivity section gives the 2D model resistivity of the subsurface. The figures were generated through the use of robust software called RES2DINV. Consequent to the resultant output of the subsurface geological situations of the investigated area being typically sedimentary, the resistivity values show the structure of the study areas in layers. A trend of the general geoelectrical-lithology of the subsurface somewhat related to result observed in resistivity as typically revealed in the inverse models of the 2D resistivity. Existence of reasonable correlation is observed between the 2D inverse models and the delineated geoelectrical layered parameters derived from the sounding curves. Also, the lateral continuities of geoelectrical layer (geoelectrical-lithology) and near-surface heterogeneity observed in the resistivity soundings were depicted conspicuously in the inverted 2D resistivity images. It is worthy of note that the delineated topsoil observed in the resistivity soundings (VES) was not distinct in the 2D images (2D-ERT); this is as a result of its very small thickness values that ranged from 0.4m to 1.7m averaging 1.11m in relation to the minimum electrode spread of 10.0m adopted for the 2D survey in the study area (Figures 6 through 10).

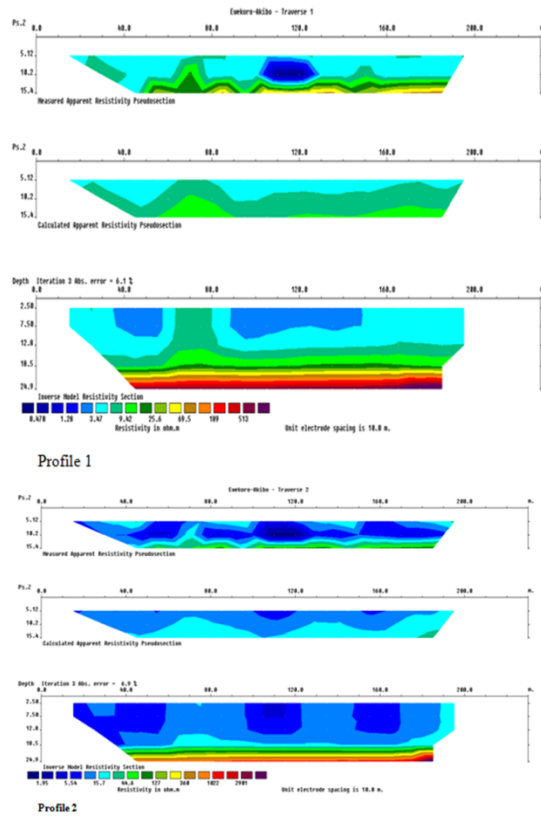


Figure 6. 2D-ERT inverse model along Ewekoro tranverse 1 (Profiles 1 and 2)

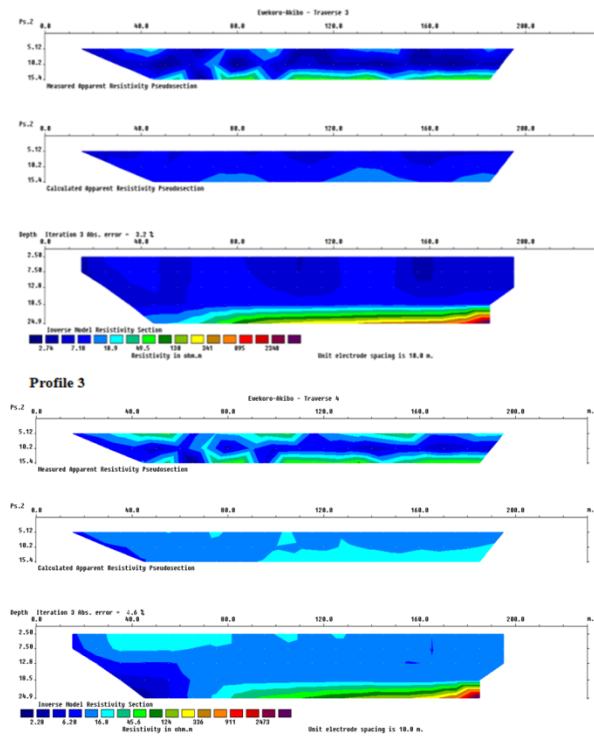


Figure 7. 2D ERT inverse model along Ewekoro tranverse 2 (Profiles 3 and 4)

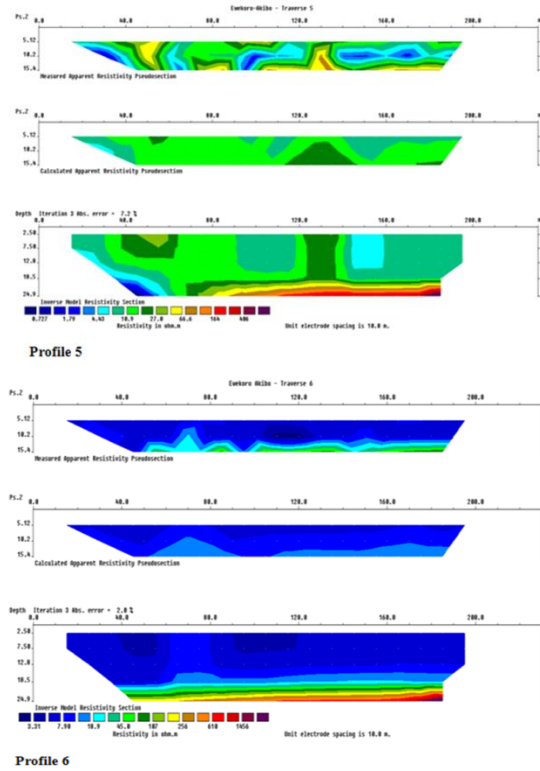


Figure 8. 2D ERT inverse model along Ewekoro tranverse 2 (Profiles 5 and 6)

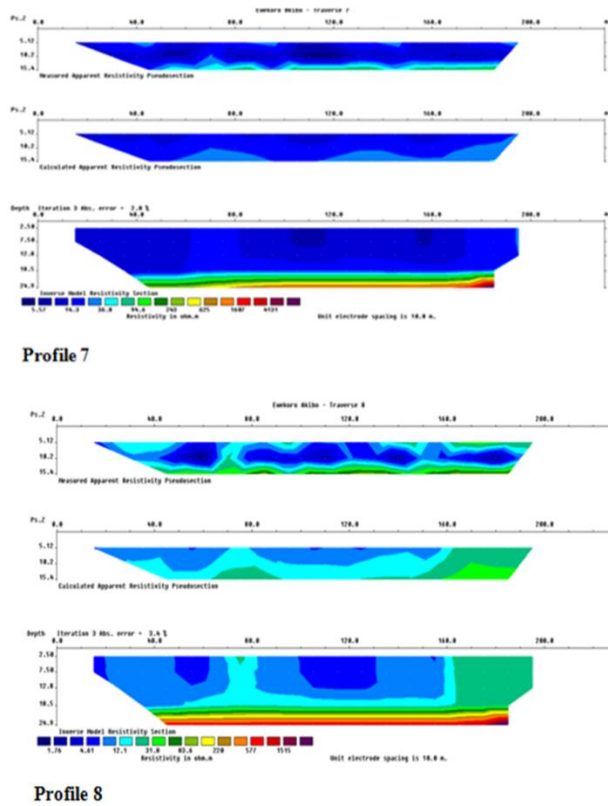


Figure 9. 2D ERT inverse model along Ewekoro tranverse 2 (Profiles 7 and 8)

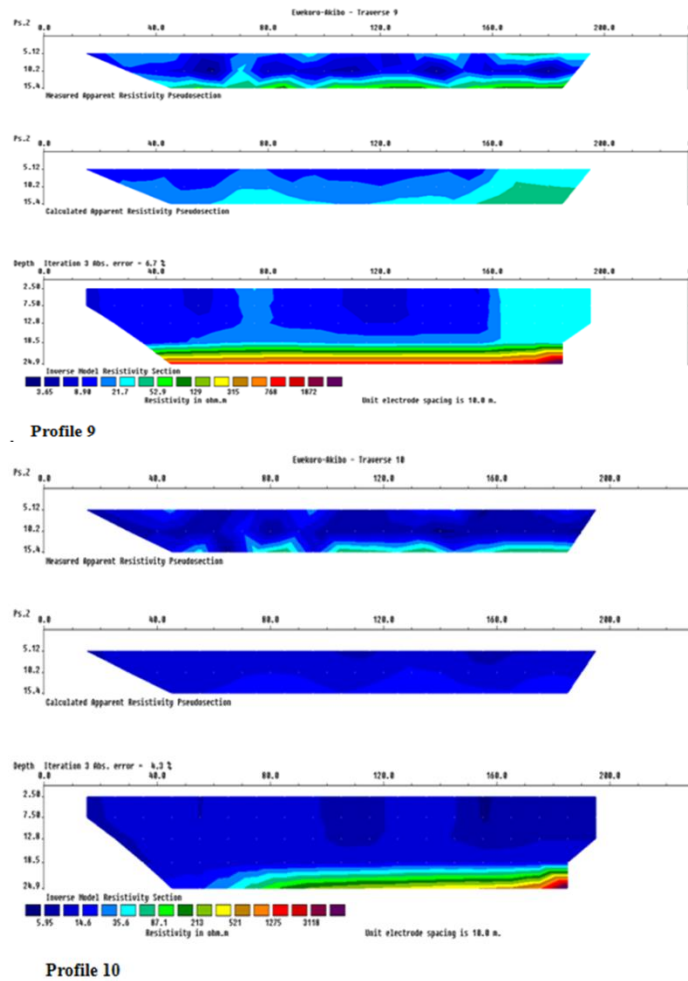


Figure 10. 2D ERT inverse model along Ewekoro tranverse 2 (Profiles 9 and 10)

5. Discussion

5.1 Geoelectric interpretation of subsurface lithology in Ewekoro

5.1.1 Tranverse 1 (Profiles 1 and 2)

Profile 1 inverse resistivity model (Figure 6) revealed very low resistivity anomalies below $3.47\Omega\text{m}$ at lateral positions between 35m to 58m and 90m to 150m from the surface of the section to depths of about 10m. Highly conductive zones were noticed from the surface to depths of about 17m at lateral distances of approximately 15m to 65m and 80m to 200m. The conductive zone is inferred to be typically Clay underlain by Clayey sand with different degree of saturation. Bedrocks with higher resistivity values above $513\Omega\text{m}$ constitute the base of the section.

Profile 2 inverse resistivity model equally revealed very low resistivity anomaly at horizontal distances between 15m to 59m, 96m to 123m and 148m to 170m as three principal condensed regions of very high conductivity with resistivity values below $1.95\Omega\text{m}$ from the surface of the section to depths of 20m, 15m and 15m respectively. These

areas indicate possible leachate accumulations in the Clayey sand bed which displayed a wide and continuous spread of low resistivity zones which laterally extends from 15m to 200m. The relatively high resistivity values encountered can be attributed to different degrees of mineralogical composition of the solid rock at the base of the section underlying the Clay layers (Figure 6).

5.1.2 Tranverse 2 (Profiles 3 and 4)

Profile 3 inverse resistivity model (Figure 7) showed three conductive zones with very low electrical resistivity signature below $2.74 \Omega\text{m}$ at approximated lateral distances of about 15m to 25m, 48m to 51m 83m to 122m and 146m to 200m at depth not greater than 20m. This region dominates the leachate accumulation and migration. This region was suggested to be Clay soil with varying degree of saturation and possible migration of contaminant seepages to the underlying rock materials.

Profile 3 inverse resistivity model possess resistivity values that ranged from $2.28\Omega\text{m}$ to $2473 \Omega\text{m}$. The possible contaminant plumes could only be found at the NW edge of which migrated laterally and vertically downwards from the surface continuously until it merges with the depth of 24.9m as it stretches gradually from the lateral position of 15m to 64m. This suggested that the massive contaminant plume migration into the subsurface might have possibly reached the water table thereby polluting the regional groundwater system (Figure 7).

5.1.3 Tranverse 3 (Profiles 5 and 6)

Profile 5 inverse resistivity model (Figure 8) revealed resistivity values that ranged from $0.73 \Omega\text{m}$ to $406 \Omega\text{m}$. The confined blue portion shows the possible leachate conductive zones with resistivity values below $0.73 \Omega\text{m}$ which accumulated at the bottom of the section at lateral position of 38m to 54m; this suggested that the contaminant plumes must have percolated slowly down to the subsurface due to the predominance of Clayey sand and presence of rocks that have been fractured/weathered found dominating the model with resistivity values ranging from $10.9 \Omega\text{m}$ - $27.0 \Omega\text{m}$ while the bedrock displayed resistivity values of about $406 \Omega\text{m}$.

Profile 6 inverse resistivity model showed two regions of possible contaminant accumulations with resistivity values below $3.31\Omega\text{m}$ from the surface of the model to a depth of about 10m at lateral positions of about 39m to 55m and 90m to 120m. Enclosing the conductive regions were materials suspected to be Shale/Clay materials mixed with decomposing wastes which covers about 80% of the entire section with considerable and relatively consistent thickness. The migrations of contaminant seepages from the surface to the condensed region were well observed from the surface of the section to depths of about 20m. This was due to the fairly steep topography of the site. Clayey sand probably mixed with water and weathered rock materials were observed laterally beneath the conductive zones at lateral distance of about 35m to 200m with the observed resistivity that ranged in values from $18.9 \Omega\text{m}$ to $107 \Omega\text{m}$ (Figure 8).

5.1.4 Tranverse 4 (Profiles 7 and 8)

Profile 7 inverse resistivity model (Figure 9) showed three possible regions of high conductivity with resistivity value below $5.57 \Omega\text{m}$ from the surface of the section to depths of about 13m to 20m at lateral profile length of about 15m to 162m and 81m to 173m respectively. These regions cover about 80% of the entire section with considerable thickness of lateral and vertical migrations across the entire section. The massive and extensive nature of these regions across the section inferred to be Sandy clay suggested possible leachate accumulations and migration which could have impeded the subsurface with consequent lethal impacts on the local and regional groundwater system of the area. Underlying these regions is Clayey sand which is in turn laterally underlain by weathered rock materials and bedrocks of much higher resistivity values that range from $243 \Omega\text{m}$ - $4131 \Omega\text{m}$ observed only at the base of the section.

Profile 8 inverse resistivity model showed very low resistivity anomalies below $1.76 \Omega\text{m}$ of lateral extension of approximate distance of 15m to 20m, 38m to 43m and 98m to 131m from the surface of the section to a consistent depth of about 10m depicting regions of condensed zone of very high conductivity. Generally, conductive zones were observed from the surface to depths of about 20m at lateral distances of about 15m to 162m enclosing the condensed region of possible accumulations and migrations of contaminant seepages. Sandy clay enclosed these conductive zones and in turn underlain by Clayey sand while a uniform, continuous and lateral distribution of weathered rock materials and bedrocks of much higher resistivity values ranging from $31.8\Omega\text{m}$ to $1515 \Omega\text{m}$ were found at the lower section (Figure 9).

5.1.5 Tranverse 5 (Profiles 9 and 10)

Profile 9 inverse resistivity model (Figure 10) showed near surface low resistivity values below $3.63 \Omega\text{m}$ from the surface of the section to depths of about 20m and 19m at lateral extension of about 15m to 70m and 82m to 159m respectively. These low resistivity zones which indicated the presence of Sandy clay mixed with decomposing wastes cover the middle of the model and were more condensed at the NW and centralized area of the section compared to the extremes of the SE. Underlying the conductive zone are Clayey sand formation and weathered rock materials probably containing Clay sand were noticed beneath this zone extending uniformly and continuously at considerable lateral distance of 38m to 200m.

Profile 10 inverse resistivity model revealed a similar near surface low resistivity values below $5.95 \Omega\text{m}$ from the surface of the section to depths of about 3m. Three condensed region of very high conductive zones were delineated and enclosed by a Sandy clay formation which spreads widely, uniformly and continuously at a lateral extension of 15m to 200m. It is thicker in the NW than in the middle and SE section of the model. These enclosed conductive zones are underlain by Clayey sand materials which are underlain in turn by Limestone and the basal Sandstone formation of varying higher resistivity values ranging from $521\Omega\text{m}$ - $3118 \Omega\text{m}$ (Figure 10).

5.2 Vadose zone characterization of geohydraulic parameters in Ewekoro

The two geohydraulic parameters specifically termed as hydraulic conductivity and hydraulic resistance were computed utilizing the integration of the principal geoelectrical



parameters namely the resistivity and depth of the layers above the aquiferous zone by adopting earlier stated equations; equation 3 and equation 4 respectively (Table 3). The observed hydraulic conductivity (k) ranged from 0.0082 cm/s in VESEWE24 to 5.149cm/s in VESEWE1 while the corresponding hydraulic resistance (C) which evaluates groundwater vulnerability extent ranged from 0.0075 day⁻¹ in VESEWE21 to 15,445.98 day⁻¹ in VESEWE25. The observed variation of these parameters is an indication of the argillaceous materials presence in the subsurface sediments and this typically characterizes the dynamic behavior of an aquifer to allowing groundwater flow through their protective layers. Very low to moderate and very high resistivity values from 1.0 Ωm to 4765 Ωm were identified. VESEWE1, VESEWE5, VESEWE8 VESEWE9, VESEWE10, VESEWE16 VESEWE17 and VESEWE25 possessing relatively much higher groundwater potentials values judging by the observed layer resistivity falling below 100 Ωm⁴.

Table 3. Vadose zone estimation of geohydraulic parameters in Ewekoro

Lithology	Latitude (°E)	Longitude (°N)	Thickness (m)	Aquifer Resistivity ρ_a (Ωm)	K(cm/s)	C(day)	Log C	Vulnerability Implication
VESEWE1	3.202968	6.901082	46.9	26.7	5.1484534	1.0462	0.0196	EHV
VESEWE2	3.202409	6.900684	8.04	281	4.6217266	0.1911	-	EHV
VESEWE3	3.201068	6.900384	37.7	104	5.020695	0.8390	-	EHV
VESEWE4	3.200722	6.901373	74.1	175	4.4872873	1.7922	0.2534	EHV
VESEWE5	3.203448	6.899762	32.6	7.55	5.1004887	0.7500	-	EHV
VESEWE6	3.203242	6.899873	39	419	5.09535	0.8619	-	EHV
VESEWE7	3.201905	6.899289	65.76	74.06	4.3936151	1.6296	0.2121	EHV
VESEWE8	3.201783	6.897345	70	96.3	4.29138	1.7602	0.2456	EHV
VESEWE9	3.202085	6.900732	83	88.2	4.7876915	1.8734	0.2726	EHV
VESEWE10	3.203467	6.884735	57.9	70.3	4.7430878	1.3395	0.1269	EHV
VESEWE11	3.200053	6.894753	9.83	166	4.6283867	0.4542	-	EHV
VESEWE12	3.199405	6.893631	11.9	366	4.4840577	0.2893	-	EHV
VESEWE13	3.198532	6.885386	13.35	615	4.6651891	0.1846	-	EHV
VESEWE14	3.198926	6.892652	11.8	4765	4.6685492	0.2789	-	EHV
VESEWE15	3.200106	6.885736	15.13	126	4.0482649	0.3888	-	EHV
VESEWE16	3.191532	6.890598	61.2	99.2	4.9063406	1.3937	0.1442	EHV
VESEWE17	3.201839	6.893456	61.2	1.03	0.5135496	2.2704	0.3561	EHV
VESEWE18	3.196568	6.894773	96.6	175	4.5164594	2.3716	0.3751	EHV
VESEWE19	3.193248	6.942893	56.1	123	4.9275818	0.1348	-	EHV
VESEWE20	3.199006	6.943245	62.5	106	4.7980441	1.4339	0.1565	EHV
VESEWE21	3.197998	6.942646	71	163	1.545965	0.0075	-	EHV
VESEWE22	3.199175	6.891007	54	407.2	1.3319025	4.1530	0.6184	EHV
VESEWE23	3.199152	6.893687	60.3	438.5	0.1433435	60.6241	1.7827	HV
VESEWE24	3.194219	6.892001	37.4	139.4	0.00814565	61.6705	1.7901	HV
VESEWE25	3.197942	6.903056	74	80.8	1.7409803	15445.98	4.1888	ELV

5.3 Variation of hydraulic parameters of Ewekoro aquifer and its vulnerability implication

The variation of the aquifer parameters at different locations in the study area are displayed in Figures 11, 12 and 13 respectively contoured for aquifer resistivity map, overburden thickness map and hydraulic conductivity map. This variation is evidently seen in the fairly steeply dipping slopes in the larger portion of the map. In the 3D map representation (Figure 13) there is only one visible and prominent peak which correspond to the area with the highest resistivity value (VESEWE14) in 2D.

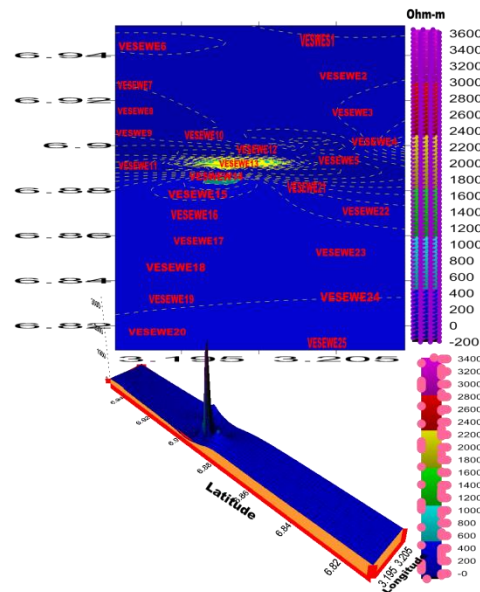


Figure 11. 2D/3D -view of the aquifer resistivity map of Ewekoro

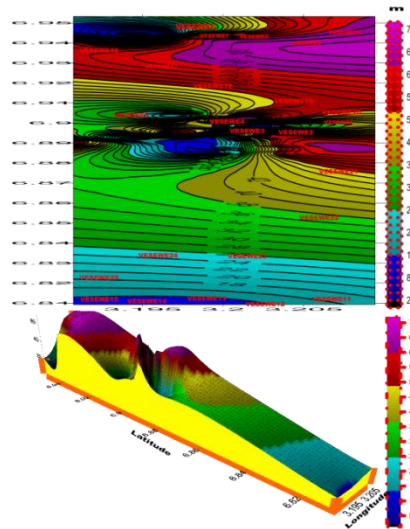


Figure 12. 2D/3D -view of the overburden thickness map of Ewekoro

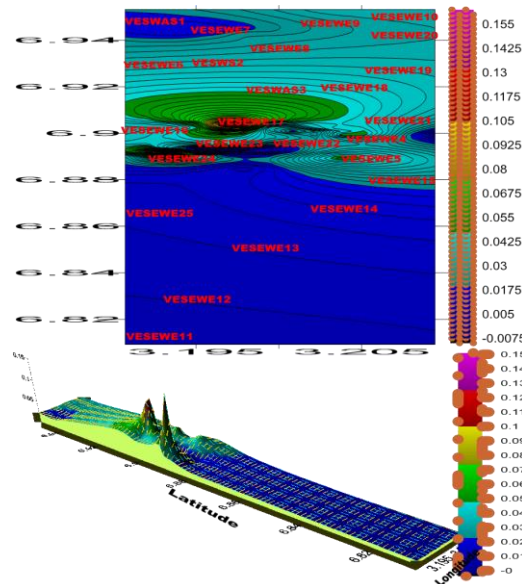


Figure 13. 2D/3D – view of the hydraulic conductivity map of Ewekoro

The resistivity values appearing most frequently ranged between 41 ohm-m and 58 ohm-m suggestive of materials of slight clayey and/or saturated with water⁴³; typically made of saturated clay but poorly permeable to the interstitial formation for the abstraction of groundwater⁴⁴. The depth to overburden is greatest at VESEWE9 with a very high overburden thickness value of 83m found at the North-East section of the map with a conspicuous rise. VESEWE4 (74.1m), VESEWE10 (57.9m), VESEWE16 (61.2m), VESEWE17 (61.2m), VESEWE19 (56.1m), VESEWE20 (62.5m), and VESEWE22 (53.9m) depicted considerably very high overburden thickness values. High overburden thickness is equally observed in some other VES locations the study area; these are VESEWE1, VESEWE3, VESEWE5 and VESEWE6, while the area possessing the thinnest overburden is found in VESEWE18 (2.97m) seen at the Southwest section of the map 2D (Figure 12). Areas with VES stations whose overburden thickness values were higher than 26.0m were consequently regarded to be of better groundwater potentials compared to other locations possessing lower overburden thickness values. In this area, larger portion of the locations in the North-East section of the map have their overburden thickness greater than 26m while some sizeable portions of the locations in the South-West of the map have their overburden thickness less than 26m; these are VESEWE2, VESEWE7, VESEWE8, VESEWE11, VESEWE12, VESEWE13, VESEWE14, VESEWE15, VESEWE18, VESEWE21, VESEWE23 and VESEWE24 while locations with overburden thickness values between 1m and 10m above are hereby considered as low/thin overburden thickness. The overburden thickness values of limestone aquifer contoured in this section (Figure 12) clearly depicted the varying depths of the encountered limestone in all the investigated profiles. As the overburden thickness consisting all materials overlying the basal limestone strata, it reveals aquifers occurring at various depths across the investigated locations⁴⁵⁻⁴⁶. The generated contour-map reveals a section of thick overburden/depression, displayed by the observed dense contour closures across different sections of the investigated locations. Regions of varying thin overburden/depression are however also observed along other parts. The areas with high overburden thickness when compared with the resistivity values showed very low aquifer resistivity values which discloses the existence of saturation zones

beneath the limestone strata while the the overburden serve as a protective coverage shielding the targeted groundwater reservoir from possible pollution migrating from the surface. Furthermore, variation in hydraulic conductivity is also observed in most investigated sites in the study area except VESEWE24 with the highest hydraulic value of 197.1921×10^{-3} m/s with prominent peak having a small area of spread as shown in the 3D map in association with few other locations with fairly high hydraulic conductivity values; VESEWE5, VESEWE17 and VESEWE25 while VESWEWE14 has the lowest hydraulic conductivity value of 6.776527×10^{-17} m/s (Figure 13). Hydraulic resistance serves as an indispensable geoelectrical formation parameter often utilized in estimating the extent of the resistance of an aquifer to fluid flow vertically via the protective overlying layers while the connection between the aquifer vulnerability index (AVI), C and log C displayed in Table 3 reveals that AVI in most of the investigated sites were extremely high (88%) in accordance to the adopted grading of Stempvoort et al.²⁸, as VESEWE23 and VESEWE24 (8%) exhibited high vulnerability status and only VESEWE25 depicted low vulnerability status (4%). The ERT profiles (Figures 6-10) reveal the vertical and lateral changes in resistivity along the subsurface in area. Generally, we can infer from the resistivity changes that the percolation of contaminant seepages (leachates) is not only surficial in some investigated but has invaded aquifers in other locations judging by the depth to the aquifer as seen in Table 2, indicating that the aquiferous zones of the study area are generally vulnerable or prone to contaminant seepages. The location around VESWAS25 with extremely low vulnerability may consequently be the resultant effect of the compact nature of the investigated locations (Table 3).

6. Conclusions

The VES and ERT outputs were utilized in evaluating the aquifer vulnerability status of the investigated area. The application of the resistivity techniques of geophysical prospecting enabled the extrapolation of geoelectrical and consequent hydraulic parameters. The changes in the recorded geoelectrical parameters depicted low to relatively high resistivity values across the investigated area. The (ERT) is in agreement with the observed VES sounding results where high resistivity values were observed at the aquifer layer. The basic properties comprising of resistivity and thickness of the protective strata were utilized in the estimation of hydraulic conductivity cum hydraulic resistance required for the evaluation of the aquifer vulnerability index (AVI) for the later classification of the vadose zone vulnerability implications. The ERT profiles revealed the vertical and lateral heterogeneities of the subsurface, and the output of the profiles were reflections of low to relatively high resistivities across the subsurface both at lateral and vertical extents. The computed geohydraulic parameters provided the necessary geoelectrical details considering the aquifer protective strata which enhanced the identification and consequent description of the vulnerability status of the delineated aquifer layers. The observed notable changes of the computed aquifer parameters as revealed in the generated contour maps both in 2D and 3D representations are reflections of consequent changes in the subsurface hydrogeological formations that are relatively inhomogeneous. The integration of AVI and ERT alongside VES investigations in this investigation gave a comprehensive outcome of the groundwater protection status of the investigated area revealing the extent of protection in the entire



locations within the study area in relation to their susceptibility to contaminant seepages. These parameters hereby provided the required information necessary for groundwater resource management studies and equally serve as control measures to assessing the vulnerability conditions of saturation zones in consequent to the subsurface geology of the study area.

7. References

1. Hinsby, K; Purtschert R & Edmunds, M. 2006. Groundwater age and water quality vulnerability. In: Quevauviller P (Ed) Groundwater Science and Policy. *Chemical Society Reviews, CSR* (In Prep): 6-10.
2. George JN; Ibuot JC & Obiora DN. 2015a. Geoelectrohydraulic of Shallow sandy in Itu, Akwa-Ibom State (Nigeria) using geoelectrical and hydrogeological measurements. *Journal of African Earth Sciences*, 110 (2): 52–63.
3. Obiora DN; Ajala AE & Ibuot JC. 2015. Evaluation of aquifer protective capacity of overburden units and soil corrosivity in Makurdi, Benue State, Nigeria using electrical resistivity method. *Journal of Earth System and Science*, 124 (1): 125–135.
4. Ishola, SA; Makinde, V; Aina, JO; Ayedun, H; Akinboro, FG; Okeyode, IC; Coker JO & Alatishe, OO. 2016. Aquifer protection studies and groundwater vulnerability assessment in Abeokuta South Local Government Area, South-West Nigeria, *Journal of Nigerian Association of Mathematical Physics*, 33 (1): 347-362.
5. Ishola, SA. 2024a. Groundwater protection assessment using frequency domain electromagnetic method and direct current electrical resistivity method in Papalanto South-West Nigeria. *Nigerian Journal of Theoretical and Environmental Physics*, 2 (1): 1-27. <https://doi.org/10.62292/njtep.v2i1.2024.1>.
6. Ishola SA. 2024b. Aquifer characteristics and groundwater reservoir protective capacity rating in Obafemi-Owode Local Government Area, Ogun State South-West Nigeria. *Federal University Wukari (FUW) Trends in Science and Technology Journal*, 9 (1): 392-398. www.ftstjournal.com.
7. Bjerg, PL; Hinsby K; Christensen, TH & Gravesen, P. 1992. Spatial variability of hydraulic conductivity of an unconfined sandy aquifer determined by a mini slug test. *Journal of Hydrology*, 136 (1-4): 107–122.
8. Hossain ML; Das SR & Hossain, MK. 2014. Impact of landfill leachate on surface and groundwater quality. *Journal of Environ Science and Technology*, 7 (1): 337-346.
9. Ibuot, JC; Obiora, DN; Ekpa, MM & Okoroh, DO. 2017. Geoelectrohydraulic Investigation of the surficial aquifer units and corrosivity in parts of Uyo L. G. A., Akwa-Ibom, Southern Nigeria. *Journal of Applied Water Sciences*, 7 (1): 4705-4713.
10. Ugwuanyi, MC; Ibuot, JC & Obiora, DN. 2015. Hydrogeophysical study of aquifer characteristics in some parts of Nsukka and Igbo Eze South Local Government Areas of Enugu State, Nigeria. *International Journal of Physical Sciences*. 10 (15): 425-435.
11. Hölting, B; Härtlé, T; Hohberger, KH; Nachtigall, KH; Villinger, E; Weinzierl, W; Wrobel, JP 1995. Konzept zur Ermittlung der Schutz- funktion der Grundwasserüber- deckung. *Geol Jb*, 63 (1): 5-24.
12. Weatherington-Rice, J; Christy, SD; Angle, MP; Gehring, R & Aller L. 2006. Drastic hydrogeologic settings modified for fractured tills: Part 1 Theory and Part 2 Field Observations. *Ohio Journal of Science*, 106 (2): 45-63.
13. Stempvoort, D; Ewert, L & Wassenaar, L. 1992. AVI: A method for groundwater protection mapping in the prairie Provinces of Canada. *Prairie Provinces Water Board Report*, 1 (14): 13-14.
14. Samsudin, AR; Rahim, B; Yaacob, WZW & Hamzah U. 2009. Mapping of Contamination Plumes at Municipal Solid Waste Disposal Site Using Geotechnical Imaging Technique, A Case Study in Malaysia. *Journal of Spatial Hydrology*, 6 (2): 13-22.



15. George, NJ; Emah, JB & Ekong, UN. 2015b. Geohydrodynamic Properties of Hydrogeological Units in Parts of Niger Delta, Southern Nigeria. *Journal of African Earth Sciences*, 105 (2): 55–63.
16. Obiora, DN; Ibuot, JC & George, NJ. 2016. Evaluation of aquifer potential, geoelectrical and hydraulic parameters in Ezza North, Southeastern Nigeria, using geoelectrical sounding. *International Journal of Environmental Science Technology*, 13 (2): 435-444.
17. Lashkaripour, GR & Nakhaei, M. 2005. Geoelectrical investigation for the assessment of groundwater conditions; a Case Study. *Ann Geophys*, 48 (6): 937-944.
18. Ibuot, JC; Akpabio, GT & George, J. 2013. A survey of the repositories of groundwater potential and distribution using geoelectrical resistivity method in Itu Local Government Area (LGA), AkwaIbom State, Southern Nigeria. *Cent Eur J Geosci*, 5 (4): 538-547.
19. Aleke, CG; Ibuo, JC & Obiora, DN. 2018. Application of electrical resistivity method in estimating geohydraulic properties of a sandy hydrolithofacies: a case study of Ajali Sandstone in Ninth Mile, Enugu State, Nigeria. *Arabian Journal of Geosciences*, 11 (1): 322. DOI: <https://doi.org/10.1007/s12517-018-3638-8>.
20. Putranto, TT; Santi, N; Dian, A; Widiarso, D.A & Dimas, PD. 2018. Application of aquifer vulnerability index (AVI) method to assess groundwater vulnerability to contamination in Semarang Urban Area. In: *MATEC Web of Conferences Series*, 159: 1-36.
21. Ishola, SA. 2019. Characterization of groundwater resource potentials using integrated techniques in selected communities within Ewekoro Local Government Area South-West Nigeria. *Department of Physics, FUNAAB Ph.D. Thesis*.
22. Loke MH. 2009. Electrical imaging surveys for environmental and engineering studies, a guide to 2D and 3D surveys. Workshop Held in USM: 22-23.
23. Ishola SA; Makinde V; Gbadebo AM; Mustapha AO & Orebiyi EA. 2021. Quality assessment of groundwater system in Itori community of Ewekoro Local Government Area, South-West Nigeria. *Science and Technology (SCI & TECH) Multidisciplinary Engineering Science Studies*, 5 (12): 2-7. <http://scitechpub.org/index.php/vol-5-issue-12-December-2021>.
24. Bashir, IY; Izham, MY; & Main R. 2014. Vertical Electrical sounding investigation of aquifer composition and its potential to yield groundwater in some selected towns in Bida Basin of North Central Nigeria. *Journal of Geography and Geology*, 6(1): 60–69.
25. Obaje NG. 2009. *Geology and Mineral Resources of Nigeria*. 120. Springer, Berlin.
26. Ushie, F; Harry, T; & Affiah, U. 2014. Reserve estimation from geoelectrical sounding of the ewekoro limestone at Ppalanto, Ogun State, Nigeria. *Journal of Energy Technologies and Policy*, 4(5): 28.
27. Billman, HG. 1992. Offshore stratigraphy and paleontology of the dahomey (benin) embayment. West Africa, *Ist. NAPE Bull*, 7 (2): 121-130.
28. Stempvoort, DV; Ewert, L & Wassenaar, L. 1993. Aquifer Vulnerability Index: A GIS-compatible method for groundwater vulnerability mapping, *Canada Water Resources Journal*, 18 (1): 25-37.
29. Gemail, KS; El-Shishtawy, AM; El-Alfy, M; Ghoneim, MF, & Abdel-bary, MH. 2011. Assessment of aquifer vulnerability to industrial waste water using resistivity measurements, a case study, along El-Gharbyia main drain, Nile Delta, Egypt. *Journal of Applied Geophysics*, 75 (1): 140-150.
30. Heigold, PC; Gilkeson, RH; Cartwright K & Reed, PC. 1979. Aquifer transmissivity from surficial electrical methods. *Groundwater*, 17 (4): 338-345.
31. Worthington, RH; Smart, C & Ruland, W. 2002. Assessment of groundwater velocities to the municipal wells at Walkerton. In: Stolle D, Piggott AR, Crowder J.J (eds) *Ground and Water: Theory to Practice*. Proceedings of the 55th Canadian Geotechnical and 3rd Joint IAH-CNC and CGS Groundwater Specialty Conferences, Niagara Falls, Ontario, October 20-23, 2002.
32. Omosuyi, GO. 2010. Geoelectric assessment of groundwater prospect and vulnerability of overburden aquifers at Idanre, Southwestern Nigeria. *Ocean Journal of Applied Sciences*, 3 (1): 9-28.



33. Oyedele, KF & Adeyemo, AO. 2001. Surface electrical resistivity measurement in the characterization of groundwater potentials of the typical basement terrain, Northern Nigeria. *African Journal of Environmental Studies*, 2 (1): 52-54.
34. Aizebeokhai, AP, Olayinka, AI & Singh, VS. 2010b. Application of 2D and 3D geoelectrical resistivity imaging for engineering site investigation in a crystalline basement terrain, southwestern Nigeria. *Environ Earth Sci*, 61 (7): 1481-1492.
35. Olabode, SO & Muhammed, MZ. 2016. Depositional facies and sequence stratigraphic study in parts of Benin (Dahomey) Basin, SW Nigeria. Implications on the Re-Interpretation of Tertiary Sedimentary Successions. *International Journal of Geosciences*, 7 (1): 210-228. <https://www.scirp.org>. Retrieved on June 2nd, 2025.
36. Badmus, BS & Olatinsu OB. 2009. Geoelectric mapping and characterization of limestone deposits of Ewekoro formation, Southwestern Nigeria, *Journal of Geology and Mining Research*. 1 (1): 8-18. <http://www.academicjournals.org/jgmr>.
37. Akinyemi, LP; Odunaike, RK & Adeyeloja A. 2015. Physicochemical characterization of limestone deposits at Ewekoro, Ogun State, South-West of Nigeria and the *Environment Impact*. *Journal of Environment and Earth Science*, 5 (1): 18-36. www.iiste.org.
38. Oladosu, YC & Ogundipe OY. 2017. Micropaleontological studies of Ewekoro Sediments Southwestern Nigeria. *Journal of Geology and Geophysics*, 6 (1): 280. <https://doi.org.10.4172/2381-8719.1000280>.
39. Majolagbe, AO; Yusuf, KA & Duru, AE. 2013. Characterisation n Environmental Media: A Case Study of Cement Production Area, Ewekoro, Southwest, Nigeria. *European Scientific Journal*, 3 (1): 1857-7431.
40. Aizebeokhai, AP & Oyebanjo, OA. 2013. Application of vertical electrical soundings to characterize aquifer potential in Ota, Southwestern Nigeria. *International Journal of Physical Sciences*, 8 (46): 2077-2085.
41. Aizebeokhai, AP & Oyeyemi, KD. 2014. The use of multiple-gradient array for geo-electrical resistivity and induced polarization imaging. *Journal of Applied Geophysics*, 12 (1): 10-12. <http://10.1016/J.Jappgeo.2014.10.023> .
42. Ward, SH & Hohmann, GW. 1987. Electromagnetic theory for geophysical applications. In: Nabighian MN (Ed.), *Electromagnetic methods in applied geophysics*, Investigations in Geophysical Series. *Society of Exploration Geophysics*, 1 (1): 131-312.
43. Ajayi, CO. & Hassan. 1990. The delineation of aquifer overlying the basement complex in the western Part of the Kubarni Basin of Zaria, Nigeria. *Journal of Mining and Geology*, 26 (1): 117-124.
44. Abiola, O; Enikanselu, PA & Oladapo, MI. 2009. Groundwater potential and aquifer protective capacity of overburden units in Ado-Ekiti, Southwestern Nigeria. *International Journal of Physical Sciences*, 4 (3): 120-132.
45. Aizebeokhai AP, Alile OM, Kayode JS, & Okonkwo FC. 2010a. Geophysical investigation of some flood prone areas in Ota, south- western Nigeria. *American-Eurasian Journal of Science Research*. 5 (4): 216-229.
46. Omosuyi, GO; Adegoke, AO & Adelusi, AO. 2008. Interpretation of electromagnetic and geoelectrical sounding data for groundwater resources around Obanla-Obakekere, near Akure, Southwestern Nigeria. *The Pacific Journal of Science and Technology*, 9 (2): 508-525.



Data availability

The data that support the findings of this study are available from the authors upon reasonable request.

Declaration of competing interest

The authors declare that they have no competing financial interests or personal relationships that could have appeared to influence the work reported in this paper.

Use of AI tools declaration

The authors declare that they have not used Artificial Intelligence (AI) tools in the creation of this article.





Original Article

Proof of the true motion of the North Celestial Pole

Xiaoqiang Guo ¹

Abstract

Based on an overview of the understanding of the movement of the North Celestial Pole by astronomical circles throughout history, both in China and abroad, the paper uses a comparative study method involving astronomy, geology, and geography to verify the true movement trajectory of the North Celestial Pole and explore its guiding significance in the theory of Earth evolution and its practical application value in modern global satellite positioning and navigation. In addition, the paper redefines or explains related concepts such as the ecliptic pole, precession, and nutation.

Key words: The ecliptic pole; the north celestial pole; obliquity of the ecliptic; right ascension 14h; vernal equinox; precession of the equinoxes

Affiliation Info: ¹ Engineer, the Leshan Electric Power Co., Ltd., Sichuan Province, P.R. China.

Corresponding Author : Guo, XQ, Engineer; Email: 2837532525@qq.com.

Citation: Guo, XQ. 2025. Proof of the true motion of the North Celestial Pole. *Naturalis Scientias*, 2 (2): 574-585. DOI: <https://doi.org/10.62252/NSS.2025.1034>. www.naturalisscientias.com.

Copyright © 2025 by the author. Published by *Naturalis Scientias*. This is an open access article under the Creative Commons Attribution-NonCommercial 4.0 International (CC BY-NC 4.0) License. (<https://creativecommons.org/licenses/by-nc/4.0/>).

About the author: Xiaoqing Guo, he/him, an engineer of Leshan Electric Power Co., Ltd., Sichuan Province, China; independent researcher, research direction: Earth sciences and related disciplines; award-winning author of the "Spark of Scientific Wisdom" column of the Chinese Academy of Sciences, contracted author of "Baidu Reading", and certified writer of the "Toutiao" platform; mailing address: No. 81, North Section, Yongjiang Road, Wutongqiao District, Leshan City, Sichuan Province, China.

郭晓强，男，中国四川省乐山电力股份有限公司工程师；独立研究者，研究方向：地球科学及相关学科；中科院《科学智慧火花》栏目获奖作者，《百度阅读》签约作者，《今日头条》平台认证作家；通讯地址：中国四川省乐山市五通桥区涌江路北段 81 号。



北天极真实运动方式的证明

郭晓强

(乐山电力股份有限公司, 乐山 611130)

摘要

论文在概述古今中外天文学界对北天极运动认识过程的基础上, 采用天文学、地质学和地理学等学科相互对比研究的方法, 求证了北天极的真实运动轨迹, 探索了其在地球演变理论方面的指导意义、及其在现代全球卫星定位导航方面的实际应用价值。此外, 论文还重新定义或解释了黄极、岁差和章动等相关概念。

关键词: 黄极; 北天极; 黄赤交角; 赤经 14H; 春分点; 岁差

1. 引言

人类自进入有文字时代以来, 就开始对星空进行观察记录, 并不断积累以提高自身对星空的认识水平。从最古老的两河文明到古希腊文明, 人们建立了基于黄道坐标系的托勒密的“地心说”天文学体系。中国人则依据原始赤道坐标系, 先后提出了“浑天说”和“盖天说”等天文学理论架构。

公元前 2 世纪, 古希腊天文学家喜帕恰斯 (Hipparchus, 约公元前 190~前 125) 发现了春分点在黄道上西移的现象。中国晋代天文学家虞喜在公元 4 世纪发现了冬至点在 28 宿中的“退行”现象, 并将其定为“岁差”¹。

应该指出的是, 这是两种具有内在逻辑联系、但并不相同的天文现象。后来, 中国天文学界将上述两种天文学现象统一命名为岁差。

第一个将岁差与地球自转联系起来的, 是伟大的波兰天文学家哥白尼。他在《天体运行论》一书中专门用一节分析讨论这一问题, 并描绘了地球自转轴延长线 (北天极) 围绕其平衡位置 I 做“扭曲小王冠式”运动, 揭示出岁差叠加章动现象的原因是地球自转轴的移动造成的²。此后, 牛顿根据力学原理与其他天文学家合作提出了著名的“陀螺”假说, 即地球自转轴以 23.46 度的固定角度围绕北黄极作圆锥运动的理论假说, 进一步解释了产生岁差现象的原因³。



天文学界关注岁差问题的最初始原因，是它关系到历法的正确与否。牛顿提出的“陀螺”假说较好地解决了由于春分点移动而产生的回归年长度问题，并因此得到国际天文学界的一致认可。但随着天文学观测手段的现代化、天体测量学专业的兴起与发展，对岁差章动现象本质的研究已远远超出历法范畴。与此同时，牛顿假说的瑕疵也逐渐显露出来。这个假说推定的北天极围绕黄极旋转的移动方式和速度，与实际天文观测数据存在很大差异。依据这个假说建立起来的 IAU 岁差章动模型，由于其计算所得与实际观测数值之间存在极大误差而不断修改⁴。

正是在上述背景下，本文作者认为有必要采用系统论的方法，对北天极运动轨迹进行重新论证。

2. 论证及讨论

经多年研究思考，本文作者提出了一个全新的北天极运动方式，即北天极以类正弦曲线的运动方式沿赤经 14H 移动。下面将从天文学、地理学、地质学、气候学和候学等四个方面逐一进行论证。

2.1 天文学史料

先来看一下北极星变迁的历史记录。

右枢 (α Dar) 是国际天文学公认的距今约 5000 年前的北极星，勾陈一 (α UMi) 是现代北极星。中国古代天文学采用原始赤道坐标系，关注的重点是北天区，因此留下了北极星变迁的可靠记录和观测资料。英国科学家李约瑟依据牛顿假说描述过中国古代北极星变迁问题⁵。中国现代天文学家陈久金教授在研究过北极星的轨迹变迁问题后得出，“中国天文学的发展历史，最能清楚地表明天文学由萌芽到形成的过程。从公元前 3000 年以来，就有右枢、天乙、太乙、天帝、纽星等一系列曾经使用过而随时间推移逐渐被放弃了极星，由此可见中国天文学的古老程度。”⁶

天乙是与右枢角距很小的邻星，帝星 (β UMi) 也称天帝、北极 (4 UMi)。在华夏古典星图中，纽星被称为天枢。也因此，中国历史上北极星的候选名单应该依次为：右枢、帝星、北极和纽星。若将右枢和勾陈一作一直线相连，则该直线正好为赤经 14H。帝星、北极和纽星均分布在该直线两侧。

除右枢外，中国历史上的北极星没有一颗位于牛顿“陀螺”假说设定的北天极移动轨迹附近。需要说明的是，帝星充当北极星的古代记录不够确凿。而“北极” (4 UMi) 充当北极星的记录则包括但不限于如下内容：“中宫天极星，其一明者，泰一之常居也。”这里提到的“中宫天极星”就是“北极”。这一史料或可证明，“北极”应该是先秦至汉朝的北极星⁷。纽星 (北极 5) 亦称天枢，曾是古代北极星的历史记录：“北极纽星，天之极也。以纽为不动处，梁祖景烁以仪测之……”⁸。



图 1. 北天极真实移动方向示意图

Figure 1. Schematic diagram of the true movement direction of the North Celestial Pole

2.2 天文学观测

笔者根据国家天文台发布的《天文学年历》（1955-2015）“北极星视位置”资料⁹，并结合有关历史记录，分析整理得出，北天极为一沿赤经 14H 方向摆动前进的移动轨迹（图 1 和 2）。

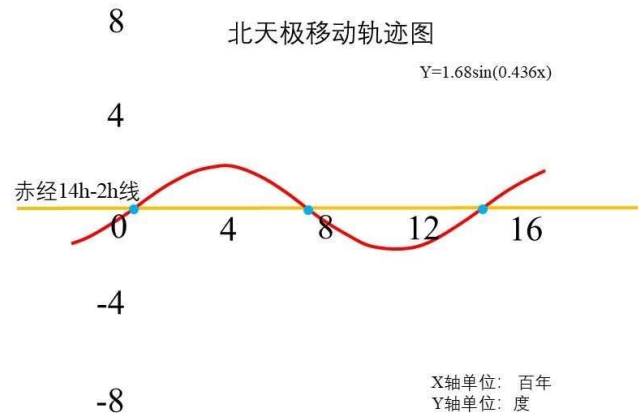


图 2. 北天极真实运动轨迹示意图

(为突出该曲线的波动特征，本文作者将 X 轴长度压缩为 1/100，即 X 轴长度单位为 100 年)

Figure 2. Schematic diagram of the actual motion trajectory of the North Celestial Pole

需要说明的是，上述北天极移动曲线及表达式是依据《中国天文年历》所载北极星 60 年（1955~2015）视位置表计算结果而得。北天极经度变化值为：2.85-1.85=1h，年平均变化值为 0.0167h。纬度变化值为 89.33-89.05=0.28，年平均变化值为 0.28/60=0.0047 度/年（16.80 角秒/年）。

若将北天极移动轨迹假设为一条类正弦曲线，则该曲线以赤经 2h-14h 经圈为横轴。这类正弦曲线可以表示为： $Y=A\sin(\omega x+\Phi)+k$ 。假设周期 T 为 120 年，则可以计算出其最大绝对值（T/4）为 $30*0.25=7.5$ 度=0.5h，即北天极经度变化范围应该为 13.5h~14.5h（ Φ, k 均为 0）。

曲线表达式为： $Y=0.5*\sin(0.052*X)$ 。

示意图中 X 轴为赤经 14H-2H 方向，单位是年；Y 轴为 X 轴垂直方向，单位是 h。

上述曲线及表达式表明，北天极运动轨迹是一条沿赤经 2h~14h 方向波动前进且垂直于黄道平面的类正弦曲线。

2.3 黄极位置及春分点移动方式与速度

黄极是天文学上一个重要的基础概念，但缺乏准确定义。笔者认为，教科书中黄极辞条描述的黄极空间位置是错误的。

经多年研究，本文作者提出黄极的新定义如下：黄极是经过地球质心且位于赤经 14H-2H 平面、与天极间夹角等于黄赤交角的直线在天球上的两个端点。其北端（北黄极）坐标为赤经 14H 00M 赤纬 66.54°、南端（南黄极）坐标赤经 2H 00M 赤纬 -66.54°。

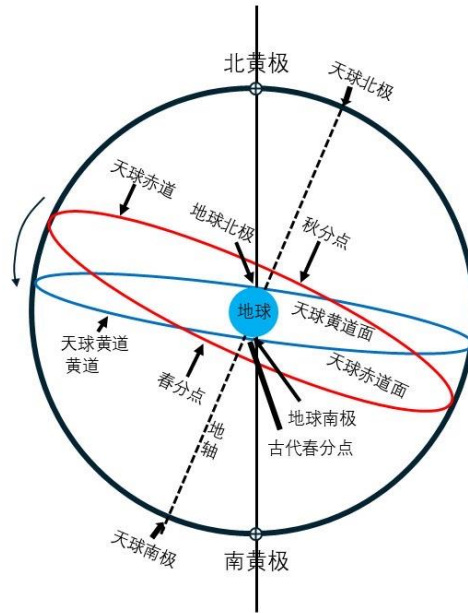


图 3. 春分点位置变化示意图

Figure 3. Schematic diagram of the change in the position of the vernal equinox

关于春分点位置变化示意图即上图 3 上的内容，证明如下： $23.46 \times 3600 / 16.8 = 5027$ 年。这一数据和右枢充当北极星的历史记录高度吻合。古希腊天文学家喜帕恰斯时期发现春分点移动时代距今约 2250 年，当时的春分点在白羊座。按照实测的北天极平均纬向移动速度计算，北天极从古希腊时代至今已移动 $2250 \times 16.8 / 3600 = 10.5^\circ$ 。故古希腊时代的黄赤交角应该为： $23.46 - 10.5 = 12.96^\circ$ 。只有按照这个角度逆时针旋转现代天赤道，才能满足喜帕恰斯时代春分点在白羊座的历史记载。

中国历史上不同时期北极星的坐标见表 1。

表 1. 中国历史上不同时代北极星坐标

Table 1. The coordinates of the North Star in different periods of Chinese history

星名	赤经	赤纬	黄赤交角	距今年代
右枢 α Dra	14 04	64.2833	-2.2567	5510
帝国 β UMi	14 50	74.0833	7.5433	3410
北极 4 Umi	14 08	77.6333	11.0933	2650
纽星北极 5	14 00	83.4766	16.9366	1398
勾陈一	02 50	89.3178	24.1422	-142

资料源于本文所附参考文献 10 和 11

纽星无依氏星名 HP，编号 62572。为方便年代计算，各星的赤纬采用 10 进制。

从表 1 中数字和历史资料可以得出以下判断：帝星应该是中国商周时期的北极星，北极是中国春秋战国至秦汉时期的北极星，纽星是中国隋唐时代的北极星。表格中的计算结果，和史料记载年代高度一致。北天极从北极（4UMi）沿赤 14H 移动到勾陈一（小熊座 α 星），地球的黄赤交角也随之发生变化。黄赤交角从右枢充当北极星时代的 -2.17° ，变成现代的 23.46° 。

前已提及，北天极的真实移动方式是以类正弦曲线轨迹沿赤经 14H-2H 经圈移动。地球这类（第三种）运动方式，必然会引起黄赤交角变化及春分点移动。根据地理学公式，春分点太阳高度角 $=90-X$ ，式中 X 为测量的纬度。上式表明，春分点太阳高度角只和测量的纬度相关，而与经度无关。但黄赤交角却会因春分点测量点黄道经度变化而随之变化。所谓的“春分点移动”，实质上是春分点测量地的黄道经度随黄赤交角增加而向西移动。

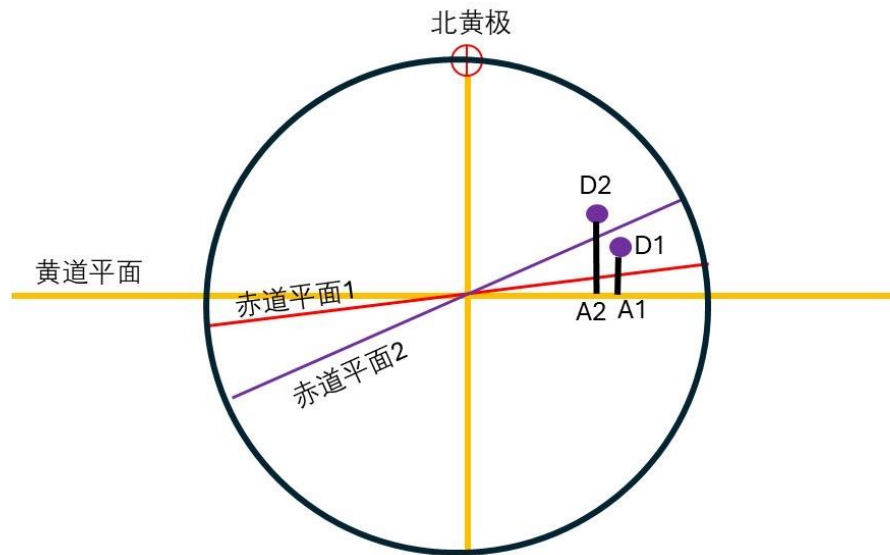


图 4. 黄赤交角引起春分点移动示意图

(D1 和 D2 分别为不同黄赤交角条件下同一经纬度的两个测量点)

Figure 4. Diagram of the movement of the vernal equinox caused by the obliquity of the ecliptic

图 4 中 D1 和 D2 两点为不同黄赤交角下地球表面同经纬度的春分点测量地（假设为格林威治天文台），A1 和 A2 则为它们在黄道上的投影点。从示意图中可以明显看

出，赤道平面 2 春分点在黄道上的投影，比赤道平面 1 的春分点在黄道上的投影西移了一定距离。这就是古希腊天文学家喜恰帕斯认为春分点进动的真实原因。

对赤道坐标系而言，春分点并没有移动。回归年是地球围绕太阳公转 360 度的时间，恒星年则是春分点测量的黄经值变化 360 度的时间。岁差=恒星年-回归年。表达的只是春分点测量地的黄道经度差异值。这就是恒星年和回归年长度不同的真实原因。

国际天文学界将历史上春分点测量的黄道经度变化，解释为春分点向西移动，这是以黄道坐标系为基准得出的判断。牛顿正是依据这一推断，提出了北天极移动的“陀螺”假说（图 5）。

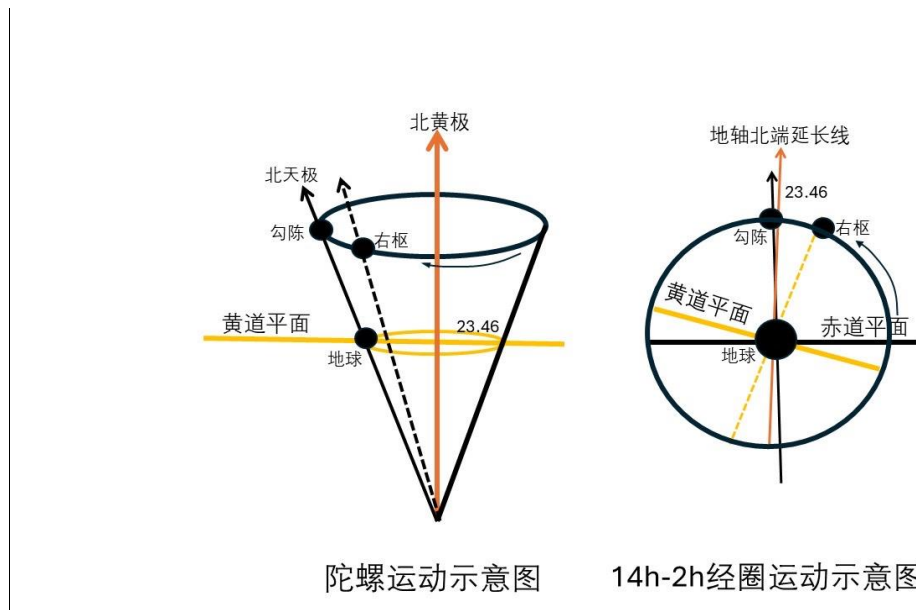


图 5. 北天极两种不同移动方式对比

Figure 5. Comparison of two different ways of moving the North Celestial Pole

从图 5 可以发现，牛顿提出的北天极陀螺运动轨迹是平行于黄道平面的。而本文作者提出的北天极运动轨迹，则是垂直切割黄道平面的。

采用原始赤道坐标系的中国古代天文学家，是以冬至点而不是春分点确定回归年的。公元 330 年，中国晋朝天文学家虞喜发现冬至点在 28 宿中移动，并将此现象定名为“岁差”。它反映了赤道坐标系中北天极的真实移动方式。喜恰帕斯发现的 axial precession 和虞喜发现“岁差”，虽然都是因北天极的移动而产生的天文现象，但准确含义并不相同，是不能简单将二者画等号。

从图 5 还可以看出，北天极从北极（4UMi）沿赤 14H-2H 经圈移动到勾陈一即小熊座 α 星，地球的黄赤交角和春分点也在随之变化。黄赤交角从右枢充当北极星时代的 -2.17° 变化到现代的 23.46° 。春分点测量的黄道经度也沿黄道平面顺时针移动了



一段距离。为此笔者认为，地球的自转轴运动实质是沿赤经 14H 方向切割黄道平面的缓慢旋转运动。这种运动必然会引起黄道平面与天赤道平面升交点（春分点）的移动。春分点的移动速度在古希腊时代是 36 角秒/年，现代天文学测定的速度是 50.27 角秒/年。这一事实证明，春分点移动速度不是一个常数而是一个变数。它应该是北天极纬向平均移动速度与对应三角函数的乘积。但这个函数的具体表达式，尚有待更多天文测量观测数据的整理和研究。

2.4 地理学证明

天文和地理密切相关，这既是中国传统观念，也是客观的自然规律。中国古代积累了丰富的地理实践。《周礼·地官·大司徒》曾这样描述古阳城（今登封）夏至之时太阳投影情况：“……日至之景，尺有五寸，谓之地中……”¹²。引文中关于登封是大地中心的结论肯定是不科学的，但通过其测量数值记录，可以求得当时的黄赤交角数据。

根据上面的“日至之景，尺有五寸”的记录，可以运用三角学公式进行计算。设登封当时夏至日的高度角为 $\arctan A=2.0$ ，查三角函数表 $A=63.43$ 度。已知登封的纬度为 34.6 度。根据北半球各地夏至日太阳高度计算公式：太阳高度角 $A=90-$ （当地北纬度数-黄赤交角度数）。应该有 $90-(34.6-\text{黄赤交角})=A$ 。已知登封的纬度值为 34.6 度， $A=63.43$ 度，经分析整理后得到当时黄赤交角为 8.03 度。这里需要确定《周礼》的成书年代。多数历史学家认为其成书于西周晚期。一般来说，《周礼》记载的史实特别是地理学记录资料，应该早于成书年代。因此笔者认为，《周礼·地官·司徒》记载的“立杆见影”资料应属商周时期，即公元前 1500 年左右，对应帝星充当北极星的年代。由此可以得出： $(2015+1500) * 16.8/3600+8.03=24.43^\circ$ 。这是一个和现代黄赤交角 23.46° 非常接近的数值。

需要指出的是， 8.03° 和前面天文学计算的 7.54° 存在 0.49° 的差异，换算成年代有 100 年左右之别。但笔者认为这个误差是可以接受的。

2.5 地质及气候证据

米氏理论与反映海平面变化和地层沉积的地质勘探资料较为吻合，并因此自上世纪 80 年代以来逐步得到国际地质学界的认同。米氏旋回提出了影响地球气候的 3 个要素和 3 个周期，即岁差周期、黄赤交角变化周期和轨道偏心率变化周期⁶。本文作者认为，这些都可以统一包含在赤北极沿赤经 14H 的移动周期内。据本文作者提出的假说，北天极沿赤经 14H 方向旋转 360° ，需要 $360 * 60 * 60 / 16.8 = 77143$ 年；北天极旋转 180° ，需要 $77143/2=38572$ 年，接近黄赤交角变化 4 万年的周期；北天极旋转 90° ，需要 $77143/4=19286$ 年，非常接近 2 万年的岁差周期。5 个岁差周期，正好等于轨道偏心率周期。

基于北天极的平均移动角速度，现在距离北天极与黄道平面平行、即下一个冰河时代的来临，还有 $(47-23.46) * 3600/16.8$ 年 = 5044 年。而我们人类距离上一个冰河时代，已经有 15099 年了，即 $(47+23.46) * 3600/16.8$ 。

上述两个冰河时代间隔约 2 万年，这也是一个间冰期的时间。地球自转轴旋转一周会经历两次冰期和两次间冰期。而地球的地理南北极颠倒现象，38572 年就会发生一次。

通过上面的叙述可以看出，地球自轴旋转假说完满地吧“米氏旋回”的三个周期统一起来了。

业已证明，“米氏旋回”与地球的海平面高度变化周期及海相地层沉积周期基本一致。而地球海洋平面高度的变化，直接与冰河现象密切相关。当地球自转轴与赤道平面垂直时，两极冰盖基本融化，地表没有四季区别，海洋平面达到最高值；而当地球自转轴与赤道平面平行时，冰河时代来临，海洋平面降到最低值。当地球自转轴与黄道平面垂直或平行之间时，海平面在最低和最高之间变化。而我们人类，当前正处于海平面逐渐降低的过程中。

综上所述，米氏理论的相关研究成果，是支持本文作者所提出的理论假说的。

2.6 物候学依据

中国古气候研究方面的权威竺可桢教授在其专著《物候学》中发表的反映中国古今温度和挪威雪线高度变化的研究成果即图 6，得到全世界气候学界的高度认同⁵。该图表明，距今 5000 年前左右是地球平均温度最高时期。这一时期也正是北天极与北黄极重合、黄赤交角为 0 度的时期。此间地球处于温暖湿润期，海平面达到最高，两级冰盖基本融化。从这一时期开始，两极雪线逐渐下移，地球气温也随之下降。这样的变化趋势与地球黄赤交角从 0°向 23.46°逐渐增加是同步的。显然，图中古代温度是根据文字记述和物候记录推断出来的，而近现代则是采用更直接的温度测量仪器得出的。换言之，图 6 中的曲线形状及其对应时间不是很精准。但从地球气候变化的总趋势看，这一资料也是支持本文所提出的假说的。

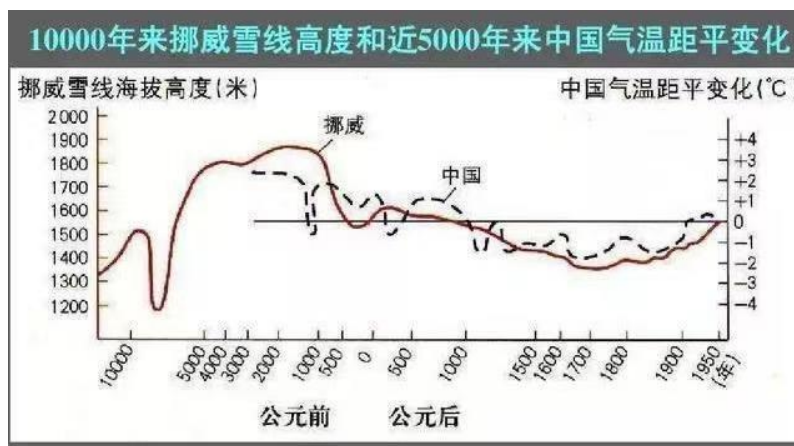


图 6. 一万年来挪威雪线高度（实线）与五千年来中国温度（虚线）变迁图（引自竺可桢）⁵

Figure 6. The height of the Norwegian snowline (solid line) over the past 10,000 years and the temperature in China (dashed line) over the past 5,000 years



3. 结论

通过以上诸多方面的论证可以得出，本文作者提出的北天极沿赤经 14H 移动假说，反映了北天极的真实移动轨迹。这一理论假说，或许在以下几个方面具有重大的划时代意义。

为地球科学研究提供了一把金钥匙。通过北天极的真实运动方式，导出了黄赤交角的循环变化规律，并因此全面合理地解释了周期性冰河时代的成因、地球气候冷暖的变化趋势、地球磁场倒转，以及“沧海桑田”的成因。此外，为历史上关于大洪水的传说、人类发源于非洲及其迁徙原因等自然之谜，提供了可能的答案。也为全面预测未来地球环境的演变趋势，提供了科学依据。

重新定义了“黄极”概念，并将岁差和章动现象统一起来，为建立一套崭新的 IAU 岁差章动模型奠定了科学基础。

需要说明的是，因研究条件和专业限制，笔者给出的只是北天极年近似运动轨迹表达式。至于北天极年的精确运动轨迹，特别是其周日和月运动轨迹等，尚需要天体测量专业方面的补充和完善。

参考文献

1. 艾萨克·牛顿著, 郑太朴译. 2006. *自然哲学之数学原理*. 1-3 卷. 北京: 商务印书馆.
2. 李约瑟. 1975. *中国科学技术史*. 北京: 科学出版社.
3. 陈久金. 1985. *天文学简史*. 北京: 科学出版社.
4. 哥白尼. 2006. *天体运行论*. 北京: 北京大学出版社.
5. 竺可桢. 1980. *物候学*. 北京: 科学出版社.
6. 杜昇云, 苗永宽等. 2013. *中国古代天文学的转轨与近代天文学*. 北京: 中国科学技术出版社.
7. 苗永宽. 1983. *球面天文学*. 北京: 科学出版社.
8. 丁仲礼. 2006. 米兰科维奇冰期旋回理论: 挑战与机遇. *第四纪研究/QUATERNARY SCIENCES*, 26 (5): 710-717.
9. 王明明等. 2009. IAU1976, 1980 及 2000A 岁差章动模型比较. *中国空间技术*, 第五期.
10. 郭晓强. 2021. 黄极准确空间位置及定义. *探索科学*, 第 15 期.
11. 北天区星图: <http://yw.eywedu.com/24/26/mydoc032.htm>.
12. 班固. 公元 54 年. *汉书*. 卷二十六 天文志. 第六.
<https://baike.baidu.com/item/%E5%A4%A9%E6%96%87%E5%BF%97/3050682?fr=aladdin>.



13. 明史. 志第七. 历. <http://www.my285.com/shishu/mingshi/031.htm>.
14. 周礼. 地官. 大司徒. <https://wenku.baidu.com/view/ccdf5cd950e2524de5187ec0.html>.
15. 梦溪笔谈. 卷七. 象数一. <http://baike.so.com/doc/5370527-5606449.html>.
16. 虞喜. 百度. 百科.
17. 中国科学院紫金山天文台. 2014. 2014 年中国天文年历. 北京. 科学出版社.
18. 中国科学院紫金山天文台. 1955-2015. 中国天文年历. 北京. 科学出版社.

Author contributions

Xiaoqiang Guo contributed to the data collection, compilation and interpretation and wrote the paper.

Data availability

The data that support the findings of this study are available from the author upon reasonable request.

Declaration of competing interest

The author declares that he has no known competing financial interests or personal relationships that could have appeared to influence the work reported in this paper.

Use of AI tools declaration

The author declares that he has not used Artificial Intelligence (AI) tools in the creation of this article.





Original Article

Estimation of hydraulic diffusivity and associated hydraulic parameters using pumping test and lithological data in Wasinmi residential community, south-west Nigeria

S. A. Ishola¹

Abstract

Pumping tests were conducted on existing 50 wells (twenty five each) with constant rate pumping test for boreholes and recovery method test for hand-dug wells within district to evaluate aquifer hydraulic parameters and estimate hydraulic Diffusivity within Wasinmi district, South-West Nigeria adopting standard methods of Cooper and Jacob straight line solution to time-drawdown data collected from observation wells. The depth range of 4.3m to 2.4m with a mean depth of 8.3m; mean static water level (SWL) of 1.59m and mean drawdown (DD) of 0.85m while the boreholes tapped fresh water from weathered sandstone aquifer with a depth range of 35m to 75m with a mean depth of 51m, SWL of 17.8m and DD of 8.17m. Borehole discharge varied from 1.0×10^{-2} l/s to 11.0×10^{-2} l/s with a mean of 4.0×10^{-2} l/s with exhibited transmissibility that varied from 1.0×10^{-2} m²/s to 9.20×10^{-2} m²/s with an mean of 4.5×10^{-1} m²/s (40,500 m²/day) while discharge from hand-dug wells ranged from 1.0×10^{-4} to 6.0×10^{-2} l/s with a mean of 2.3×10^{-2} l/s with exhibited transmissibility that varied from 1.0×10^{-1} (8.64 m²/day) to 5.10×10^{-1} m²/s (44,064 m²/day) with a mean of 1.42×10^{-1} m²/s (12,269 m²/day). The hydraulic conductivity varied from 87.96m²/day to 4397.76 m²/day in the boreholes and 594.432 m²/day to 7762.18 m²/day in the hand-dug wells. The mean recovery period of 2254 and 9446 seconds were reported for Wasinmi boreholes and hand-dug wells respectively. Output from the two water sources revealed that the auriferous zones were classified as very high in potentials in the designation of transmissivity magnitudes of 38,880 and 12,269 m²/day for the boreholes and hand-dug wells respectively; based on standard aquifer potentiality classification. This correlates well with the lithological description of the study area displaying fractured shale/clay-shale/clayey sand and weathered sandstone as groundwater bearing unit releasing water into the well with good correlation coefficient between transmissibility and specific capacity ($R^2 = -0.74$ and $R^2 = 0.715$) respectively reported for Wasinmi boreholes and hand-dug well Hydraulic diffusivity varied from 11.816 m²/s to 13,022.87 m²/s in Wasinmi Boreholes and 4.06 m²/s to 6467.26 m²/s in Wasinmi hand-dug wells with the regions of higher hydraulic diffusivity values were comparatively favourable for groundwater development.

Key words: Specific capacity; cone of depression; residual drawdown; hydraulic diffusivity; fractured-shale

Affiliation Info: ¹ Department of Earth Sciences, Olabisi Onabanjo University Ago-Iwoye, P.M.B 2002, Ago-Iwoye, Ogun State, Nigeria.

Corresponding Author : Ishola, S. A. PhD, Exploration Geophysics and Geomathematics; Email: ishola.sakirudeen@oouagoiwoye.edu.ng.

Citation: Ishola, S.A. 2025. Estimation of hydraulic diffusivity and associated hydraulic parameters using pumping test and lithological data in Wasinmi residential community, south-west Nigeria. *Naturalis Scientias*, 2 (2): 586-622. DOI: <https://doi.org/10.62252/NSS.2025.1035>. www.naturalisscientias.com.

Copyright © 2025 by the author. Published by *Naturalis Scientias*. This is an open access article under the Creative Commons Attribution-NonCommercial 4.0 International (CC BY-NC 4.0) License. (<https://creativecommons.org/licenses/by-nc/4.0/>).



1. Introduction

There have been decades of great challenges in groundwater environment since the values of specific yield estimated from pumping test data in an unconfined aquifer is lower than expected; delayed field experience in yield above the declining water table has been attributed as the primary cause of reported uncertainties in specific yield. Specific yield is a significant hydraulic parameter for the assessment of groundwater storage in a specified unconfined aquifer. The principal drainable source of groundwater is abstracted from the declining hydraulic head¹⁻³. Hydraulic diffusivity is relevant to well yield as it dictates how quickly water can move through the pumping. A higher diffusivity means faster water movement and a quicker response to well pumping potentially leading to a higher well yield. Diffusivity is primarily influenced by hydraulic conductivity and specific storage. Understanding hydraulic diffusivity is crucial for well design. A well in an area with high diffusivity might be able to support a higher pumping rate without causing excessive drawdown whereas a well in an area with low diffusivity might have a limited yield and require more careful management. Hydraulic diffusivity is a fundamental parameter in transient groundwater flow simulations which are essential for predicting how well yield might change over time under different pumping scenarios⁴. The volume of the specific yield has great influence on well yields, solute transport and rates of water level declination⁵⁻⁶. Specific yield is also a critical hydraulic parameter in the estimation of evapotranspiration from diurnal water-level fluctuation readings⁷⁻⁸. Challenges observed in quantifying changes in three-dimensional regional aquifer storage are often caused by the sparseness and low reliability of availability specific yield values⁹. Depletion in stream flow induced by groundwater pumping has been reported to be the potential cause of potential water recourse management issue in the High Plains Region of the United States and has functioned as sensitive parameters in the computations of depletion in stream caused by a constructed pumped well in a thin aquifer⁸⁻¹¹. The most commonly utilized techniques for the estimation of specific yields are measurement of the drainage of aquifer materials and pumping tests. Though Johnson summarized quite a number of laboratory methods for the determination of specific yield¹², one of the earliest researches on determination of specific yield of alluvial aquifers from pumping test analyses from published literature was the work of Wenzel et al.¹³; this test was undertaken on eighty-three (83) observation wells at a nearby site within Platte river valley, Nebraska. Also, the published work of Nwankwor et al.¹⁴ reinvigorated more curious interest in groundwater hydrological techniques in the estimation of specific yield from the pumping test data because the specific yield determined from pumping test data remarkably differed from the specific yield obtainable from other techniques. In the course of pumping tests, observed decline in hydraulic head in permeable alluvial aquifers is often far smaller than expected. According to the reported pumping test output in the Platte river valley of Nebraska¹³⁻¹⁶, the recorded drawdown from observation wells between 8m to 20m from the pumping well were found to vary between 1.22 to 0.8m irrespective of the adopted large pumping rate of 2m³/min that lasted for significant time greater than 48 hours. In the course of the pumping operations, drainage occurrence was only observed on the aquifer constituents found above the declining hydraulic head^{8 & 17-18}. Therefore, pumping tests conducted for a limited duration (several number of days for instance) are the ones that often proffer the estimation of the specific yield for limited thickness of the aquifer materials only near the water table.

Therefore, the estimation of the specific yield for the aquifer constituents in a large thickness is highly profitable for water resources evaluation.

Precise documentation of variation in specific yield is scarce although 19. Nwankwor et al.¹⁹ reported that specific yield possess variable values that are significantly high for a given test site; this is principally due to the fact that the expensive state for the construction of observation wells as well as the few available number of observation wells for a pumping test thereby preventing a spatial output for characterization of aquifer specific yield. Hence, a less-exorbitant approach for the determination of the spatial variation of specific yield in an unconfined aquifer is highly necessary. Nwankwor et al.²⁰ in consonance to this concluded that short-term pumping tests are not too reliable approaches for specific yield determination while small-scale laboratory tests may result to values of specific yield that are otherwise reasonable. The specific yield determined from laboratory drainage by Nwankwor et al.¹⁴ has been utilized as a bench mark for the Borden aquifer whose values were determined from repacked aquifer materials; in the course of sampling and repacking of subsurface materials; the original sedimentary structures and particle framework were destroyed⁸. If the specific yield can alternate very largely in its magnitude for an unconfined aquifer, the hydraulic conductivity will also be heterogeneous. Though, the documentation of spatial variation of horizontal hydraulic conductivity is commonly available, the analysis of spatial variation of the vertical hydraulic conductivity is scarce (Butler et al., 2002). Pumping testing operations undertaken at Borden site^{2 & 14-22} to the work of Cape-Cod site in the USA¹¹ were often used to illustrating the procedures for determination of specific yield or for demonstrating the drainage processes in the course of water table decline during pumping. The unconfined aquifer is largely composed of medium-grained sand of glacio-deltaic or glacio-fluvial deposits at the Borden site while highly permeable sand and gravel of glacial outwash were primary constituents of the Cape-Cod^{2 & 11}. The hydraulic Estimation for Hydraulic Diffusivity and Associated Hydraulic Parameters using Pumping Test and Lithological Data in Wasinmi community of Ewekoro Local Government Area of Ogun state was necessitated as a result of daily increase in water demand potentially straining the available water resources and leading to water scarcity and water quality issues. If water resources cannot keep up with the growing demand, water scarcity can occur which has led to conflicts and challenges for communities while over-extraction of groundwater to meet the needs of the growing population can lead to the depletion of aquifers making it harder to access water in the future. The increase in population with resultant pressure on water resources can lead to increase in pollution from human activities including industrial waste and improper sanitation can contaminate water sources making them unsafe for consumption. The presence of different cement manufacturing companies like Lafarge WAPCO, Dangote cement, and other associated industries in Ewekoro where larger members of staff reside in Wasinmi community due to its proximity to the industries has increased the daily demand on the limited resources²³. Also, the output of the public surface water system and the few existing domestic wells and boreholes are quite insufficient to meet the needs of the growing population leading to the reliance on groundwater sources, which can be unsustainable. Therefore, the field experience of uncertainty is a revelation that the hydrodynamics of Wasinmi groundwater system are not quite understood which makes this research tasks and efforts necessary. In this work, constant rate, single well pumping tests were undertaken by the authors in boreholes and hand-dug wells located in Wasinmi autonomous residential communities within Ewekoro Local Government Area of Ogun State, South-West, Nigeria. The



acquired field data from these tests were consequently harnessed in computing the necessary hydraulic parameters namely transmissibility, hydraulic conductivity and specific discharge, among others; this would also go a long way in the selection of appropriate pump size needed for ultimate sustainability of groundwater abstraction from the boreholes extracting water from the aquifer thereby forestalling future borehole failure and meeting the needs of the ever increasing population of the dwellers since the advent of cement manufacturing companies that have increased the number of residents in Wasinmi.

2. Study area

2.1 Physiographic and geological settings

Wasimi is located in parts of Dahomey basin in Ewekoro Local Government Area of Ogun State at an elevation of 79 metres above sea level with coordinates of 6°58'0" N and 3°28'60" E in DMS (Degrees Minutes Seconds) or 6.96667 and 3.48333 (in decimal degree) and its population amounts to 536,068. The history of the people reveals that culture and tradition play a central role in their indigenous beliefs system. The neighbourhood include Ogun state sport academy, an under construction industrial factory site, the proposed Ogun State Cargo, international airport in Wasinmi and so on²⁴. Over fifty percent of the land area of southwestern Nigeria lies within the coastal plain where the relief is generally low with average elevation of about 200 m – 400 m above sea level²⁵. Three major landform units, namely the hills, plains and river valleys, dominate the study area. The hills are the most striking feature, although they constitute less than 30 % of the total surface area. The plains are the most striking landform system in the investigated areas (with an average elevation of 64m above sea level) which ranges between 46 m and 107 m in Wasinmi. The river valleys are the narrowest landform in the area. The rivers in the study area display are in form of sluggish perennial streams in dry season but are turbulent during the wet season. This relief can be described as undulating and the drainage is dendritic²⁴⁻²⁶.

Ewekoro formation is the local geology in the study area which is generally consistent with the regional geology of eastern part of the Dahomey Basin; predominantly comprises of the non-crystalline and highly non-fossiliferous limestone and thinly laminated fissile and probably non-fossiliferous shale²⁵⁻²⁷. Ewekoro formation consists of intercalations of argillaceous sediment. The rock is soft and friable but in some places cement by ferruginous and siliceous materials. The lithological units in Ewekoro formation are clayey sand, clay, shale, marl, limestone and sandstone. The lithology of Ise and Afowo formations as defined by Omatsola and Adegoke²⁷ showed a high degree of similarity. Both are essentially sands and sandstones, but the latter contains thick interbeds of shales. This difference is not sufficient to warrant the establishment of separate lithostratigraphic units²⁵. The two formations were considered synonymous by Okosun²⁶. In that study, it was observed that the Ise, Afowo and Abeokuta formations have similar lithologic and electric log characters. The uppermost beds of Abeokuta formation which crop out in Ijebu Ode area and in the shallow boreholes at Itori, Wasimi and Ishaga onshore consist mainly of fine to coarse grained sand and interbeds of shale, mudstone, limestone and silt. These lithofacies correlate well with the upper portion of the neostratotype in Ojo-1 borehole²⁵⁻²⁶.

The Abeokuta formation was found to consist of grits, loose sands, sandstones, kaolinitic clay and shale and was further characterized as usually having a basal conglomerate or basal ferruginized sandstone. The Abeokuta formation on surface outcrops comprises mainly sand with sandstone, siltstone, silt, clay, mudstone and shale interbeds²⁵. It usually has a basal conglomerate which may measure about 1m in thickness and usually consists of poorly rounded quartz pebbles with silicified and ferruginized sandstone matrix or a softly gritty white clay matrix. In outcrops where there is no conglomerate, a coarse, poorly sorted pebbly sandstone with abundant white clay constitutes the basal bed²⁵. The overlying sands are coarse grained clayey, micaceous and poorly sorted and indicative of short distances of transportation or short duration of weathering and possible derivation from the granitic rocks located to the north. Figure 1 shows the Geology map showing the study area in South-West Nigerian part of Dahomey Embayment, Figure 2 is the data acquisition map which shows the investigated locations in Wasinmi study area within Ewekoro Local Government area (LGA) of Ogun state, South-West, Nigeria, Figure 3 is the inset map showing the study areas in within Nigeria continental domain while Figure 4 is the data acquisition map showing each investigated locations in Wasinmi study area within Ewekoro LGA, Southwest Nigeria.

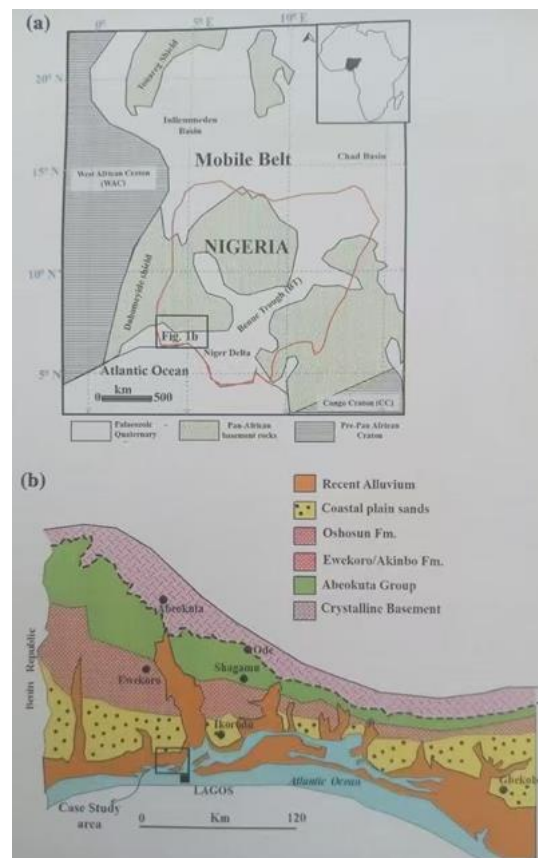


Figure 1. Geological map showing the study area within the South-West Nigerian part of Dahomey embayment^{24 & 28}

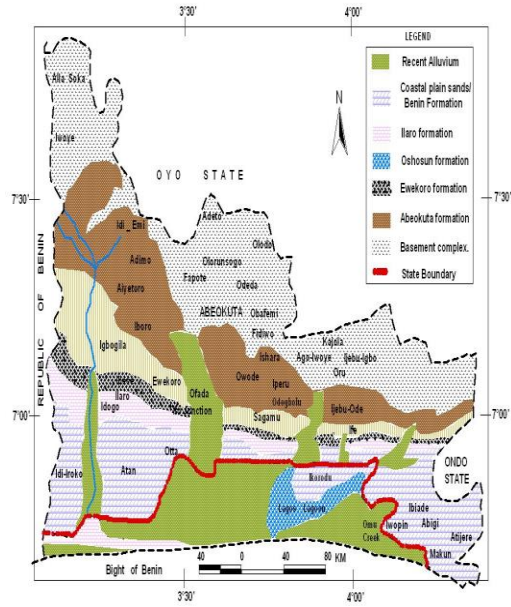


Figure 2. A map of Ogun State showing the geology of the study areas (after Kehinde-Phillips and Obiora & Onwunka)^{30 & 39}

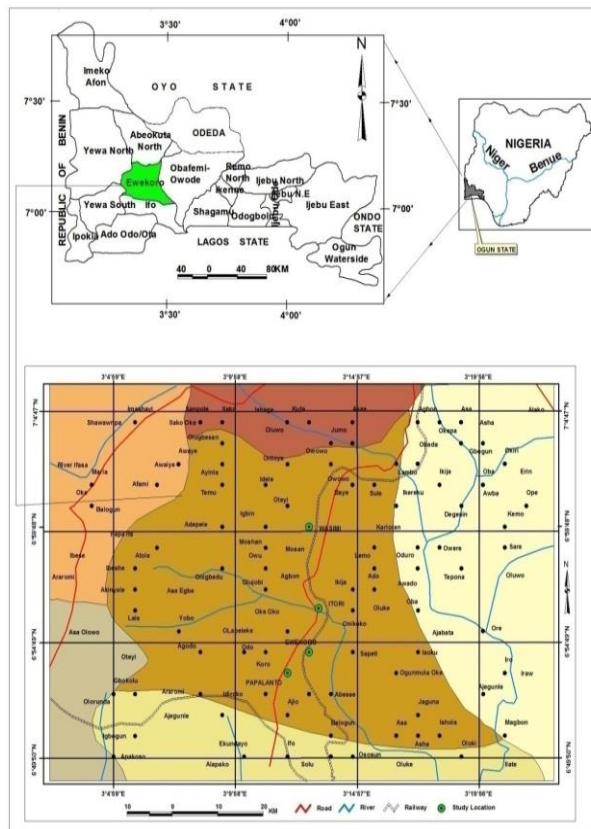


Figure 3. Inset map showing the study areas in Ogun State within Nigeria continental domain using Esri - data/nigeria political information in Arcview GIS 3.2A environment²⁴

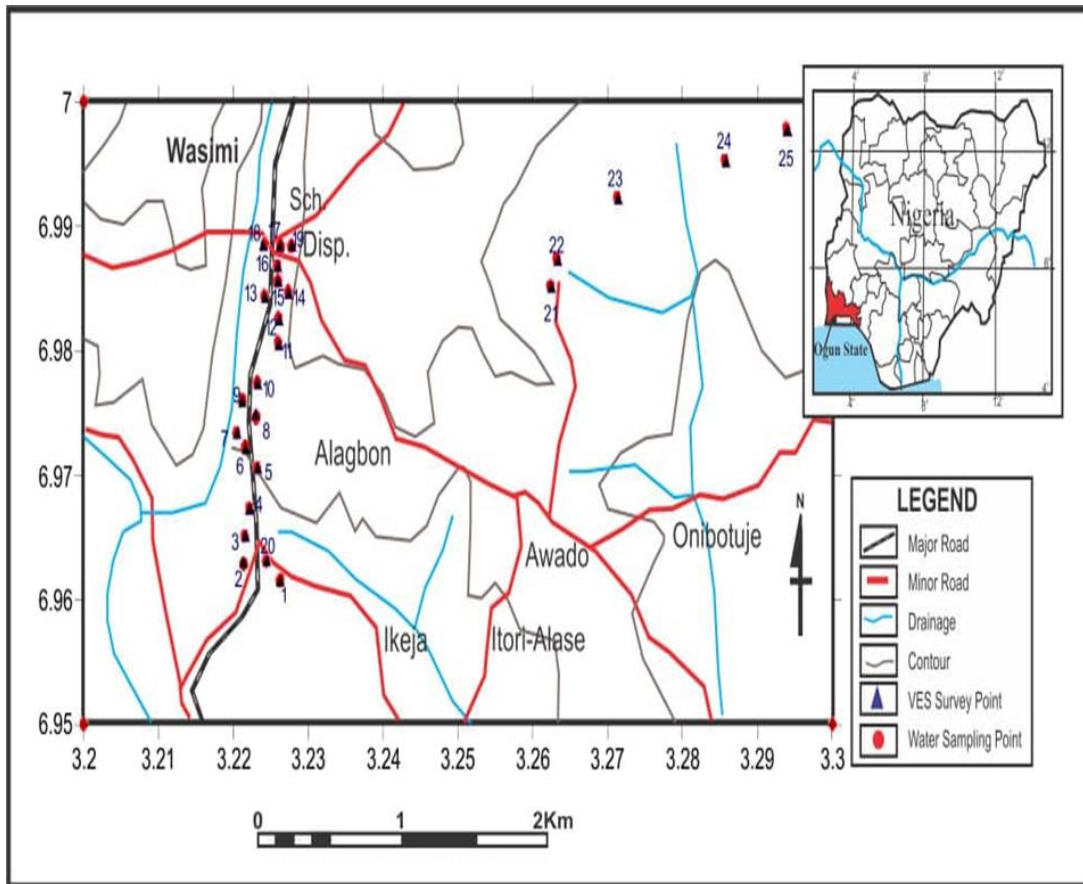


Figure 4. Data acquisition map showing the investigated locations in the Wasinmi study area within Ewekoro LGA, Southwest Nigeria²⁴

3. Materials and methods

3.1 Theoretical background

Specific yield is a measure of the volume of water in which an aquifer takes into or releases from a given storage per unit area of the aquifer per unit change in the water table depth³¹⁻³⁴.

$$S_Y = \frac{V_w}{(A \cdot \Delta H)} \quad 1$$

Where S_Y stands for specific yield of aquifer, V_w represents the volume of the water extracted from the groundwater, A represents the aquifer coverage area, and ΔH represents the alteration in water table. More specific expression is given by Dos-Santos and Youngs³⁵ who stated that the specific yield is the ratio of water flux per unit area via the water table due to the resultant effect of water taken up or released by the unsaturated soil to the rate of the rise or fall of the water table. One of the commonly utilized definitions of specific yield is the ratio of the volume of water that saturated rock or soil yields by gravity to the total volume of the rock or soil^{18 & 36-38} where

$$S_Y = P_s - S_r$$

2

Equation 2 depicts that specific yield stands as the difference between porosity (P_s) and specific retention (S_r) where porosity is the capability of the rock to contain void spaces while specific retention is the actual volume of the retained water by the soil or rock³⁹ which could also be represented by either field capacity⁴⁰⁻⁴¹ or the residual moisture content⁴²⁻⁴³. Duke⁴⁴ reported that the utilization of the field capacity and the residual moisture content serves as veritable attempt for the description of the lower limit of water content at which the water is significantly mobile.

3.2 Variability of aquifer specific yields

The introduction of the capillarity as well as the subsurface water distribution for the detailed understanding of variability of specific yield cannot be overemphasized. These idealized variables are symbolized as ΔH , P_s , P_r and S_r . There is an existence of a small zone above the water that is completely saturated under negative pressure. It is observed that in this zone, the closer the water table, the closer the pressure head tends to zero and the pressure head of the water table is zero; this pressure head is technically called matric potentials¹⁶. The occurrence of this saturated zone is a resultant effect of the impact of surface tension exhibited on the water as well as the attractive forces of the sediments a with capacity to wicking up water from the water table and holding it in place in the pore spaces. This zone is therefore referred to as tension saturated zone. In consonance with the concept of capillary fringe, two definitions are recognized; tension-saturated zone exemplified by Duke, Abdul & Gillham, Sophocleous, and Shah & Ross⁴⁴⁻⁴⁷ and space ranging from water table to the maximum capillary rise height as exemplified in the work of Mccarthy & Johnson⁴⁸. The significant contribution of the impact of the capillary fringe in water table and storage change computations have been reported in previous published literature namely Li et al., Nielsen & Perrochet, and Cartwright et al.⁴⁹⁻⁵¹ among others while numerous studies have equally revealed the variation of specific yield with water table and time^{35-44 & 52-59}. It is only when the water table is deep enough and the time interval is close enough for the attainment of the complete drainage process by gravity or attaining the state of static equilibrium condition that the ultimate specific yield which serves as constant value is regarded as being valid⁴³⁻⁵⁷ while Fahle & Dietrich⁶⁰ stated that restriction should be placed on specific yield to function under a specified time window at specified field situations.

3.3 Expressions of specific yield as a function of water table depth

When equilibrium is attained with enough time, the specific yield is found to be equal to the difference in water content between the initial and final equilibrium soil moisture horizon integrated in vertical manner ranging from land surface to the final water table depth divided by the encountered in water table depth with the assumption that no water sources or sinks are resident in the vadoze zone⁵²⁻⁶¹. The water content as observed between

two equilibrium moisture horizons changes with water table depth. 62. Childs⁶² utilized a hypothetical moisture profile for the description of the variation in specific yield with depth of the water table. Under a deep declining water table where the static equilibrium soil moisture horizon is above the initial water table denoted as IWT while the re-attained equilibrium is defined as observed horizon after IWT declined by ΔH to the final water table denoted as FWT. The static equilibrium horizon can be represented by a water-retention curve like Van-Genuchten curve model or the Brooks-Corey curve model⁶³⁻⁶⁴. The volume of the water released per unit area by mathematical deduction is equal to $(P_s - S_r) \cdot \Delta H$ while that of the specific yield value per unit area is equal to $(P_s - S_r) \cdot \Delta H$ unlike in the declining deep water table situation because the closer the water table is to the ground surface, the smaller the specific yield is⁶⁴. As the capillary fringe zone possesses little or no storage capacity making the specific yield to be tending to zero or almost equal to zero once the water table is found to be sufficiently close to the ground surface; implying that a small amount of downpour can have significant causing a rapid and great change in water table response⁵⁴. In view of the above discourse on water table depth dependence, we have ultimate specific yield (deep water-table case) and the apparent specific yield (shallow water table case) or depth dependence or depth-compensated specific yield⁵⁶⁻⁶⁵. It is worthy of note that some researchers have utilized the ultimate specific yield concept for both deep and shallow water table situations⁵⁶⁻⁵⁹.

When the water table depth is deep enough, the effect of capillary fringe can be ignored and thus apparent specific yields consequently equals the ultimate specific yields. The depth needed to attain the ultimate specific yield is related to the soil texture. The ultimate specific yield can be attained when the water level is deeper than 1m for coarse-textured sediment such as sand⁵⁸; loamy soil⁴³; peat sediment⁵⁷ and a mixture of sand, silt, clay and lateritic⁶⁶ while a given depth exceeding 10m is required for fine-textured sediments to attain ultimate specific yield status⁶⁷. The necessity of expressing the empirical formulae for the computation of apparent specific yield in this work cannot be underestimated. Equation 3 depicts a function of water table depth for the apparent specific yields as proposed by Abdul & Gillham⁴⁴ and Neuman¹⁶ with three assumptions stated; presence of a static equilibrium soil moisture profile above the IWT, possible instantaneous re-attainment of the static equilibrium profile after a change is observed in the water table and the porous medium must be uniform⁴².

$$S_Y = (P_s - S_r) \cdot \left[1 - \left(\frac{h_a}{H} \right)^\lambda \right] \quad 3$$

Where H represents the depth to water-table h_a represents the air-entry pressure head (bubbling pressure) and λ represents the index of pore-size distribution. Furthermore, an improved formular was introduced by Nachabe⁴⁰ to enhance the computation of the apparent specific yield for the primary purpose of addressing the earlier set limitation that Nachabe expression is only valid when the FWT is small in comparison with the IWT depth⁴⁰. Nachabe formula is valid regardless of the water table fluctuation⁴⁰.

$$S_Y = \frac{(P_s - S_r)}{\Delta H} \cdot \left[\Delta H + \frac{h_a}{1 - \lambda} \left\{ \left(\frac{h_a}{H_i} \right)^{\lambda - 1} - \left(\frac{h_a}{H_f} \right)^{\lambda - 1} \right\} \right] \quad 4$$

Where H_i and H_f are the corresponding parameters for the initial water table depth (IWT) and final water table depth (FWT) respectively. It is worthy of note that Abdul & Gillham⁴⁴ and Nachabe⁴⁰ functions are jointly centred on Brooks-Corey water retention curve. The Van-Genuchten has equally been harnessed in the analytical expression of apparent specific yield. Crosbie et al.⁴² went further to explaining that Duke⁴⁴ functions cannot be applied in a layered soil. Therefore, a more generally acceptable solution was proposed in equation 4 centred on a static equilibrium profile featured by the Van-Genuchten curve while a similar expression to equation 5 was equally achieved using the Van-Genuchten water retention curve by Duke⁴⁴ and Cheng⁵⁹.

$$S_Y = (P_s - S_r) - \frac{(P_s - S_r)}{\left[1 + \left\{\alpha \left(\frac{H_i + H_f}{2}\right)\right\}^n\right]^m} \quad 5$$

Where α is related to the air-entering value of the Van-Genuchten curve in reverse order and n is a dimensionless parameter in the Van-Genuchten curve that is restricted generally to values greater than 1, and m is consequently expressed as

$$m = 1 - \frac{1}{n} \quad 6$$

3.4 Expressions of specific yield as a function of time

Since the water in the soil medium is not instantaneously mobile, the shorter the accumulated time, the smaller the value of the specific yield¹⁶. After the commencement of the water table change, the soil medium near the water would attain the static equilibrium first due to the capability of the capillary fringe in making the medium close to the water table in order to possess appreciable water supply^{40 & 68}. However, it takes a very long time, potentially several months or years to extract completely the entire vadoze zone⁸⁻¹⁴. For instance, Prill⁶⁹ and Meizhao et al.¹⁶ discovered that it would take over a year for a 1.71m long column of medium grained sand to attain static equilibrium while 0.6m at the bottom of the column attained the static equilibrium barely 5hrs interval after the commencement of drainage. This is an absolute indication that the specific yield is time-dependent most specifically when the water table is shallow and the soil is fine-textured with high air-entry pressure⁷⁰; if the introduced time-step model is longer than the required time to attaining static equilibrium, the apparent specific yield can be justifiably adopted⁴⁰. However, the time-step in land surface model is usually short (less than an hour) and the static equilibrium condition seldom occurs in such a short time step. Contrary to the apparent specific yield, the transient specific yield is time-dependent. The transient specific yield should therefore be obtained from the initial and time-varying moisture profiles. The theoretical formula for the transient yield was proposed by Martinez-Santos et al.⁷¹ and expressed in equation 7.

$$S_Y = \frac{\Delta W^I}{\Delta t} \bigg/ \frac{\Delta H}{\Delta t} + \alpha(H,t) \quad 7$$

where $\frac{\Delta W^I}{\Delta t}$ accounts for the change encountered in the shape of the moisture profile above the water table over time, $\frac{\Delta H}{\Delta t}$ is the change rate of the water table and $\alpha(H,t)$ is the air constant at the surface at any given time which can be obtained from the measured moisture profile curves. For the static equilibrium condition ($\frac{\Delta W^I}{dt} = 0$), the equation is in line with Duke formula⁴⁴.

Based on the Brooks-Covey curve, the transient specific yield in Nachabe⁴⁰ was computed in equation 8 where

$$S_Y = \frac{K_{sat}}{\Delta H} (\theta_b^n - \theta_{surf}^n)t + (P_s - S_r)(1 - \theta_b) \quad 8$$

where K_{sat} is the saturated hydraulic conductivity; n is an exponent that can be projected to set at $(2 + 3\lambda)/\lambda$; a normalized water content θ is defined as

$$\frac{(P - S_r)}{(P_s - S_r)} \quad 9$$

θ_b is accordingly the temporal evolution of water content profile and θ_{surf} is the water content occurring at the surface and empirically equal to

$$\left(\frac{2h_a}{H_i + H_f}\right) \times \lambda \quad 10$$

Where equation 10 is a typical case description of an instantaneous drop in the encountered water table⁴⁰⁻⁴³. In addition, this expression has several limitations; the initial moisture profile is assumed to be in the static equilibrium condition⁴⁰. The alteration in water table should be recognized and there should be no downward or upward flux in the unsaturated¹⁶. As observed in the above expression, the static equilibrium status is quite uncommon especially in the category of short time-step models. A significant formula was proposed by Pozdniakov et al.⁷⁰ for the purpose of predicting the dynamic specific yield under periodic water table oscillations either via seasonal or diurnal responses. For a vertical column of porous medium with L_0 with the assumption that the lower boundary of the column is saturated fully and the impenetrable upper boundary, the water-head H at time t can be expressed further as

$$H(t)|_{z=L_0} = m_0 + \Delta H_{max} \sin \frac{2\pi t}{T} \quad 11$$

Where m_0 represents the attained height of the column with full water saturation above the column bottom, ΔH_{max} represents the amplitude of the oscillation where $2 \cdot \Delta H_{max} < m$ and T is the period of oscillation. The mean value for half of the period value of the specific yield can be computed by equation 12.

$$S_Y(T) = \frac{\Delta V}{\Delta Z_{gw}} \quad 12$$

$$\Delta Z_{gw} = Z_{gw} \left(t_{mins} + \frac{T}{2}\right) - Z_{gw}(t_{mins}) \quad 13$$

$$\Delta V = \int_{t_{mins}}^{t_{mins} + \frac{T}{2}} K \frac{\partial H}{\partial z} |_{z=L_0} \partial t \quad 14$$

Where Z_{gw} represents the water table level, t_{mins} is the time marker at which the point is in the lower position and K is the hydraulic conductivity determinable with respect to the outcome of Van-Genuchten curve. It should be pointed out that the initial soil moisture profile should be in hydrostatic distribution and that the values of the period of oscillation and the corresponding amplitude are obtained.

3.5 Varying techniques of field utilization for specific yield evaluations

The principal challenge often encountered in evaluating the specific yield is to quantify the amount of water that is gained or otherwise lost⁷². A number of varying field techniques has been proposed for the evaluation of specific yield. Among the conventional techniques include the laboratory drainage technique, pumping testing, the numerical technique, the texture based techniques, water table fluctuation technique and slug-test. Aside from these aforementioned field techniques, newer techniques were proposed in the latter years namely geoelectrical technique, magnetic resonance sounding, and rainfall-water table response techniques. Nevertheless, estimation of specific yield is circumscribed with uncertainty⁷³⁻⁷⁴. Therefore, the determination of an appropriate specific yield value in the field still remains a huge task⁷⁵⁻⁷⁶. There is no widely accepted available technique for the estimation of specific yield due to the fact that the various methods often produce values that are somewhat inconsistent in relation to sediment types thereby defining their respective area of application^{11,39,42,58 & 77}. In this study aquifer pumping testing technique was utilized which necessitated the instalment of pumping as well as observation wells.

3.6 Field data acquisition

Pumping tests were conducted on 25 selected boreholes and 25 hand-dug wells cut across Wasinmi area, with the view to assessing and ascertaining the hydraulic performance in terms of yield-drawdown characteristics of the wells. The results of this study will go a long way to enhancing the water resource management planning. Two principal data sources were utilized in this study. These are primary and secondary data sources. The primary data source comprised of visual inspection and reconnaissance survey where personal visits to locations of existing boreholes and hand-dug wells in the study area; identifying sampling points and collecting well inventories. Borehole drilling contractors and site engineers were equally consulted in Wasinmi on core samples information regarding drilled holes and hand-dug wells in the study area. Existing drilled boreholes and hand-dug wells were identified across the study areas and where there were no boreholes the existing hand-dug wells were used. The depth of the boreholes and the overburden thickness were measured using dip-meter while GPS was used to acquire the coordinates used in producing the data acquisition map of the study area displayed above in Figure 4. Two different methods were used in conducting pumping tests on the selected boreholes

and hand dug wells. These methods are constant rate pumping test and recovery method test.

3.6.1 Constant rate pumping test

Constant rate pumping tests were conducted on the selected boreholes. The materials used for these tests included; 60-litre gallons as a standard measure, generating set to power the pump, stop watch to record time intervals and rubber hose connected to the pipe from the borehole to discharge the water into the gallons. In conducting this test, the initial or static level of the water in the boreholes was measured using a dip-meter. The generating set was thereafter switched on to start the pumping. The pumping was allowed to run continuously for a long period of two hours before the rate of pumping was adjusted for the boreholes to maintain constant discharge. At this point, the water level response in terms of dynamic drawdown was measured to know the drawdown and a calibrated 60-litre gallon was then filled from the constant discharge from the boreholes while a stopwatch was simultaneously set to record the time taken, in seconds, to fill the gallons. This process was repeated for four hours for each of the selected boreholes. It was therefore observed that the water level and the drawdown in the boreholes were constant throughout the four hours pumping. With the constant discharge from the boreholes, a state of equilibrium was maintained between the rate of discharge and the rate of recharge from the aquifer. In this condition of equilibrium, the rate of pumping or discharge is directly proportional to the yield of the borehole or well at the constant drawdown. In other words, the discharge per unit time in litre per second gives the yield of each of the selected boreholes at the constant drawdown⁷⁸. This test was adopted because of the relatively easier field operations, economic advantage, overall logistics and technical ease of rapid computation of aquifer parameters including K and T of auriferous zone of interest at every investigated location. Estimation of aquifer parameters was accomplished by adapting to Cooper et al.⁷⁹ straight-line solution to time-Drawdown data acquired in the observation well which serves as adjustment to Remson and Lang⁸⁰ non-equilibrium well equation as stated below

$$T = \frac{2.3S_Y}{4\pi\Delta S} \quad 19.0$$

$$C_s = \frac{S_Y}{s_m} \quad 20.0$$

$$K = \frac{T_r}{A_{thic}} \quad 21.0$$

Where S_Y = Specific yield (m^3/day), C_s = Specific capacity, T_r = Transmissivity (m^2/day)

s_m = mean drawdown, ΔS = change in draw-down over one log cycle, A_{thic} = saturated thickness of the aquifer. Pumping test of wells serves as the most reliable method for the estimation of hydraulic conductivity^{64-65 & 81-84}.

$$K = \frac{S_Y}{2\pi A_{thic}(h_1 - h_2)} \quad 22.0$$

$$D_H = \frac{T}{s} = \frac{KB}{s} = \frac{K}{S_s} \quad 23.0$$

Equation 21.0 and 22.0 are respectively representing hydraulic conductivities for borehole and hand-dug wells where h_1 is the initial water level before pumping, h_2 is the final water level after pumping also known as drawdown and π is the mathematical constant approximately equal to 3.14159 while equation 23.0 represents hydraulic diffusivity denoted with D_H . The analyses of drawdown and recovery data are utilized to determine the aquifer storage coefficient (S). The storage coefficient can be calculated by using the formula expressed in equation 24.0 while specific storage (S_s) is then calculated through equation 25.0.

$$S = S_s \times A_{thic} \quad 24.0$$

$$S_s = \frac{S}{A_{thic}} \quad 25.0$$

Hydraulic Diffusivity (D_H) is a fundamental parameter in studying groundwater flow being an analytical solution for groundwater flow within a finite length of one-dimensional aquifer. It is a key parameter in groundwater development, determination of how quickly disturbances like starting a well or change in recharge, pumping or changes in boundary conditions propagate through an aquifer with great impact on groundwater management and resource engineering. It is computed as the ratio of transmissibility (T) to storability (S). Hydraulic diffusivity is highly relevant in groundwater studies due to its contributions and applications in Transient groundwater flow system, aquifer disturbance propagation, groundwater management, environmental management, and resource engineering practices. It is highly utilized in pumping tests, numerical modelling and tidal response analysis.

3.6.2 Recovery method Test

Recovery method test was carried out on the identified hand-dug wells by monitoring the recovery status of water levels on the cessation of pumping; dip-meter, generating set and stop watch among others were the materials used for this test. Dip-meter was first released and dipped into the well for the purpose of determining the overall depth of the well and the water level by measurement before outset of pumping. The pump was therefore powered by the generating set and the water in the well was pumped out until it gradually reached the bottom of the well. The stop watch was simultaneously set to record the time taken for the pumping as the reduction in water level was observed at different depth interval. As soon as the bottom level of the pumped well was attained, the well was left undisturbed creating space for recharge while the stop watch equally recorded the time taken for the water replenishment back to previous level before pumping started. The volume of the pumped water pumped was computed by utilizing the diameter and the overall depth measurement of the well. The ratio of the volume of water abstracted to the time taken in the course of abstraction gave the pumping rate in litre per second while the volume per day (m^3/day) resulted to the yield of the well. In the course of the field measurement, three wells comprising of WASWW23 to WASWW25 were found to be completely dried. So, field pump testing could not be performed on them; they were denoted as Not Available for Measurement in Table 2.

Cone of depression are created in aquifer when groundwater is pumped from a well⁸⁴. This represents an actual depression of the observed water levels in an unconfined aquifer while but represents a reduction in the pressure head in the neighbourhood of the pumped well. The land area scaling above the cone of depression is referred to as the area of influence while the distance covered from the centre of the well to the edge of the observed cone of depression is referred to as the radius of influence. In the exploratory well site investigation, the radius of influence grants an insight about the well spacing to be adopted⁸⁵⁻⁸⁷. In this study, proposed equation from Bear⁸⁸ and applied by Shahinuzzaman et al.⁸⁴ was utilized in the determination of the radius of influence as presented in equation 26.0

$$R = 1.5 \sqrt{\frac{T}{S}} \quad 26.0$$

Where R is the radius of influence for both confined and unconfined aquifer, T and S are stated as transmissivity and storage coefficient in a respective order. Drawdown (DD) is the recorded difference between the initial static water level (SWL) and the pumping water level (PWL) at any specified period of time during pumping operation.

$$DD = SWL - PWL \quad 27.0$$

The specific capacity (Cs) represents the pumping flow-rate (Q) per unit drawdown produced in the well.

$$Cs = \frac{Q}{DD} \quad 28.0$$

The specific drawdown (SDD) as a parameter is defined in well hydraulics as the inverse of specific capacity (Cs) as denoted in equation 29.0 and is of paramount significance in the study of aquifer properties.

$$SDD = \frac{1}{Cs} \quad 29.0$$

4. Results

The results of the basic well inventories and hydraulic properties of the aquifers in the study area presented as summary in Tables 1 and 2 for boreholes and hand-dug wells respectively. In the evaluation of the aquifer characteristics in the study area, groundwater supply to boreholes were abstracted from fractured sandstone whose depth ranged from 35m to 75m with a mean depth of 51m, the static water level ranged from 8.45m to 37.4m with a mean value of 17.8m while the drawdown observed varied between 3.67m to 11.4m with mean drawdown of 8.17m. Fractured shales released groundwater into the hand-dug wells whose depth varied between 4.3m to 21.4m with the mean depth of 8.28m while the static water level ranged from 0.24m to 5.42m with the mean static water level of 1.59m.



Table 1. Hydraulic parameters of studied aquifer systems of Wasinmi boreholes

Locations	BASIC HYDRAULIC PARAMETERS						ESTIMATED HYDRAULIC PARAMETERS				
	Well Head (m)	Borehole Depth BHD (m)	Borehole diameter BHD (mm)	Static Water Level SWL (m)	Residual Draw - Down DD (m)	Time (s)	Specific Discharge Q (l/s)	Specific Capacity Cs (m ² /s)	Well Loss WLC (s ² /m ⁵)	Transmissibility Tr (m ² /s)	Optimum Operating Capacity OOC
WASBH1	0.28	40	125	11.9	5.83	850	10.6×10 ⁻²	1.817×10 ⁻²	5.189×10 ⁴	2.180×10 ⁻²	1.926×10 ⁻³
WASBH2	0.25	35	125	8.75	3.67	102	0.772×10 ⁻²	2.390×10 ⁻²	4.771×10 ⁴	2.868×10 ⁻²	2.097×10 ⁻³
WASBH3	0.42	50	125	17.8	6.48	117	7.692×10 ⁻²	1.187×10 ⁻²	10.951×10 ⁴	1.425×10 ⁻²	9.132×10 ⁻⁴
WASBH4	0.42	50	125	17.1	4.28	263	3.415×10 ⁻²	7.980×10 ⁻³	36.693×10 ⁴	9.576×10 ⁻²	2.726×10 ⁻⁴
WASBH5	0.25	55	110	8.45	8.45	298	3.019×10 ⁻²	3.573×10 ⁻³	19.983×10 ⁴	42.88×10 ⁻²	1.079×10 ⁻⁴
WASBH6	0.28	42	110	8.82	8.15	299	3.008×10 ⁻²	3.691×10 ⁻³	90.051×10 ⁴	44.23×10 ⁻²	1.111×10 ⁻⁴
WASBH7	0.15	45	110	10.45	9.22	288	3.121×10 ⁻²	3.385×10 ⁻³	94.649×10 ⁴	40.63×10 ⁻²	1.057×10 ⁻⁴
WASBH8	0.61	55	25	22.59	10.53	306	2.934×10 ⁻²	2.787×10 ⁻³	122.298×10 ⁴	33.44×10 ⁻²	8.177×10 ⁻⁵
WASBH9	0.28	55	125	26.12	6.48	340	2.640×10 ⁻²	4.074×10 ⁻³	92.982×10 ⁴	48.89×10 ⁻²	1.076×10 ⁻⁴
WASBH10	0.36	46	110	13.12	8.32	249	3.613×10 ⁻²	4.342×10 ⁻³	63.747×10 ⁴	52.11×10 ⁻²	1.569×10 ⁻⁴
WASBH11	0.30	42	25	11.4	10.16	259	3.467×10 ⁻²	3.413×10 ⁻³	84.506×10 ⁴	40.95×10 ⁻²	1.183×10 ⁻⁴
WASBH12	0.30	36	110	10	8.57	263	3.415×10 ⁻²	3.985×10 ⁻³	73.472×10 ⁴	47.82×10 ⁻²	1.361×10 ⁻⁴
WASBH13	0.45	42	25	10.75	11.15	135	6.667×10 ⁻²	5.979×10 ⁻³	25.087×10 ⁴	71.75×10 ⁻²	3.986×10 ⁻⁴
WASBH14	0.30	43	25	12.9	10.89	141	6.361×10 ⁻²	5.841×10 ⁻³	26.911×10 ⁴	70.10×10 ⁻²	3.716×10 ⁻⁴
WASBH15	0.25	50	125	22.95	4.25	298	3.016×10 ⁻²	7.096×10 ⁻³	46.732×10 ⁴	85.15×10 ⁻²	2.140×10 ⁻⁴
WASBH16	0.04	60	25	24.06	10.32	243	3.704×10 ⁻²	3.589×10 ⁻³	75.233×10 ⁴	43.07×10 ⁻²	1.329×10 ⁻⁴
WASBH17	0.45	70	25	29.95	11.15	139	6.460×10 ⁻²	5.794×10 ⁻³	26.719×10 ⁴	69.52×10 ⁻²	3.743×10 ⁻⁴
WASBH18	0.43	45	25	9.07	10.25	187	4.789×10 ⁻²	4.673×10 ⁻³	44.693×10 ⁴	56.07×10 ⁻²	2.238×10 ⁻⁴
WASBH19	0.28	70	25	32.9	11.35	343	2.040×10 ⁻²	1.798×10 ⁻³	272.651×10 ⁴	21.57×10 ⁻²	3.668×10 ⁻⁵
WASBH20	0.28	40	25	8.92	11.26	267	3.365×10 ⁻²	2.988×10 ⁻³	99.459×10 ⁴	35.86×10 ⁻²	1.005×10 ⁻⁴
WASBH21	0.45	40	125	21.75	6.45	312	2.877×10 ⁻²	4.460×10 ⁻³	77.931×10 ⁴	53.52×10 ⁻²	1.283×10 ⁻⁴
WASBH22	0.42	52	110	18.08	7.85	154	5.841×10 ⁻²	7.441×10 ⁻³	23.081×10 ⁴	74.41×10 ⁻²	4.346×10 ⁻⁴
WASBH23	0.36	55	110	22.04	8.82	160	5.605×10 ⁻²	6.355×10 ⁻³	28.071×10 ⁴	76.26×10 ⁻²	3.562×10 ⁻⁴
WASBH24	0.28	75	125	37.42	4.15	284	3.169×10 ⁻²	7.635×10 ⁻³	41.335×10 ⁴	91.62×10 ⁻²	2.419×10 ⁻⁴
WASBH25	0.32	74	125	26.48	6.25	947	9.506×10 ⁻²	1.521×10 ⁻³	6.917×10 ⁴	18.26×10 ⁻²	1.446×10 ⁻⁴
MEAN	0.33	51	84.80	17.8	8.17	2254	4.0×10 ⁻²	6.3×10 ⁻³	5.98×10 ⁴	4.5×10 ⁻¹	02.52×10 ⁻⁴
MAX	0.61	.00	125.00	37.4	11.4	3431	11.0×10 ⁻²	2.0×10 ⁻²	2.73×10 ⁶	9.2×10 ⁻¹	2.20×10 ⁻³
MIN	0.04	35.00	25.00	8.45	3.67	850	1.0×10 ⁻²	1.0×10 ⁻⁴	4.77×10 ⁴	1.00×10 ⁻²	1.00×10 ⁻⁶
S.D	0.11	11.58	46.18	8.47	2.49	838	2.0×10 ⁻²	5.0×10 ⁻²	5.60×10 ⁴	2.6×10 ⁻¹	1.00×10 ⁻⁴
CV (%)	33	23	55	48	31	37	50	79	94	58	40



Table 2. Hydraulic parameters of studied aquifer systems of Wasimi hand-dug wells

Locations	BASIC HYDRAULIC PARAMETERS			ESTIMATED HYDRAULIC PARAMETERS							
	Well Head (m)	Well Depth WD (m)	Well diameter MWD (m)	Static Water Level SWL (m)	Residual Draw-Down DD (m)	Time (s)	Specific Discharge Q (l/s)	Specific Capacity Cs (m^2/s)	Well Loss WLC (s^2/m^5)	Transmissibility T (m^2/s)	Optimum Operating Capacity OOC
WASWW1	0.62	5.5	1.00	1.68	0.29	3312	27.17×10 ⁻³	9.37×10 ⁻²	0.0394×10 ⁴	11.244×10 ⁻²	3.381×10 ⁻⁶
WASWW2	0.48	7.6	1.86	1.32	0.13	1620	55.66×10 ⁻³	42.70×10 ⁻²	0.0042×10 ⁴	51.288×10 ⁻²	4.026×10 ⁻⁷
WASWW3	0.83	4.4	0.65	0.32	0.86	9814	9.171×10 ⁻³	10.66×10 ⁻³	1.0225×10 ⁴	1.28×10 ⁻²	4.034×10 ⁻⁶
WASWW4	0.72	7.3	0.79	3.22	0.32	1728	52.08×10 ⁻³	10.85×10 ⁻²	1.1797×10 ⁴	13.02×10 ⁻²	1.456×10 ⁻⁵
WASWW5	1.43	12.6	0.86	2.82	1.72	3708	24.27×10 ⁻³	1.41×10 ⁻²	0.2920×10 ⁴	1.69×10 ⁻²	3.245×10 ⁻⁶
WASWW6	1.48	4.3	0.74	0.66	0.13	1699	52.97×10 ⁻³	40.75×10 ⁻²	0.0046×10 ⁴	48.90×10 ⁻²	1.101×10 ⁻⁶
WASWW7	1.62	4.5	0.91	0.58	0.17	2250	40.00×10 ⁻³	23.53×10 ⁻²	0.0106×10 ⁴	28.24×10 ⁻²	1.155×10 ⁻⁶
WASWW8	0.72	8.7	0.83	1.71	0.19	2268	39.68×10 ⁻³	20.89×10 ⁻²	0.0121×10 ⁴	28.24×10 ⁻²	1.145×10 ⁻⁶
WASWW9	0.43	9.3	1.67	2.39	0.69	15172	5.92×10 ⁻³	8.59×10 ⁻³	1.9662×10 ⁴	1.03×10 ⁻²	7.856×10 ⁻⁷
WASWW10	0.46	7.5	0.38	0.82	1.65	17532	5.13×10 ⁻³	3.11×10 ⁻³	6.2612×10 ⁴	3.73×10 ⁻³	7.889×10 ⁻⁷
WASWW11	0.28	6.8	0.46	1.07	1.99	15775	5.71×10 ⁻³	2.87×10 ⁻³	6.1142×10 ⁴	3.44×10 ⁻³	1.298×10 ⁻⁶
WASWW12	1.85	6.2	0.78	0.78	0.14	1717	52.42×10 ⁻³	37.44×10 ⁻²	0.0051×10 ⁴	44.92×10 ⁻²	1.167×10 ⁻⁶
WASWW13	1.80	6.8	0.82	0.54	0.25	3132	28.74×10 ⁻³	11.49×10 ⁻²	0.0303×10 ⁴	13.79×10 ⁻²	6.862×10 ⁻⁶
WASWW14	1.28	8.8	0.78	0.57	0.14	1541	58.40×10 ⁻³	41.72×10 ⁻²	0.0073×10 ⁴	50.06×10 ⁻²	7.122×10 ⁻⁶
WASWW15	0.90	8.5	0.78	1.12	0.17	9151	9.84×10 ⁻³	5.79×10 ⁻²	0.1757×10 ⁴	6.942×10 ⁻²	2.186×10 ⁻⁵
WASWW16	0.92	6.5	0.69	0.35	0.79	9302	9.68×10 ⁻³	1.23×10 ⁻²	0.8439×10 ⁴	1.469×10 ⁻²	2.657×10 ⁻⁶
WASWW17	1.22	5.5	0.69	0.52	1.04	11988	7.51×10 ⁻³	7.25×10 ⁻³	1.8363×10 ⁴	8.704×10 ⁻³	7.093×10 ⁻⁶
WASWW18	1.50	6.8	0.65	0.24	1.88	20275	4.43×10 ⁻³	2.36×10 ⁻³	5.2526×10 ⁴	2.833×10 ⁻³	3.016×10 ⁻⁶
WASWW19	0.95	16.2	0.62	4.27	1.26	24610	3.66×10 ⁻³	2.90×10 ⁻³	9.4213×10 ⁴	3.483×10 ⁻³	3.428×10 ⁻⁶
WASWW20	0.93	21.4	0.58	5.42	1.65	18389	4.89×10 ⁻³	2.97×10 ⁻³	6.8889×10 ⁴	3.559×10 ⁻³	3.320×10 ⁻⁶
WASWW21	0.82	9.7	0.63	3.03	1.59	19721	4.56×10 ⁻³	2.87×10 ⁻³	7.6343×10 ⁴	3.444×10 ⁻³	3.629×10 ⁻⁶
WASWW22	0.65	7.2	0.66	1.48	1.19	13115	6.86×10 ⁻³	5.77×10 ⁻³	2.5270×10 ⁴	5.767×10 ⁻³	5.877×10 ⁻⁶
WASWW23	0.95	3.6	1.02	NAFM	NAFM	NAFM	NAFM	NAFM	NAFM	NAFM	NAFM
WASWW24	0.90	3.4	0.86	NAFM	NAFM	NAFM	NAFM	NAFM	NAFM	NAFM	NAFM
WASWW25	0.75	3.2	0.78	NAFM	NAFM	NAFM	NAFM	NAFM	NAFM	NAFM	NAFM
MEAN	0.995	8.277	0.8105	1.59	0.83	9446	2.3×10 ⁻²	1.4×10 ⁻¹	2.342×10 ⁴	1.42×10 ⁻¹	3.20×10 ⁻³
MAX	1.85	21.40	1.86	5.42	1.99	24610	6.0×10 ⁻²	5.8×10 ⁻¹	9.421×10 ⁴	5.10×10 ⁻¹	3.48×10 ⁻²
MIN	0.28	4.30	0.38	0.24	0.13	1541	1.0×10 ⁻⁴	1.0×10 ⁻⁴	0.004×10 ⁴	1.00×10 ⁻¹	1.00×10 ⁻⁸
S.D	0.461	3.994	0.3402	1.39	0.68	7584	2.1×10 ⁻²	1.8×10 ⁻¹	3.046×10 ⁴	1.86×10 ⁻¹	3.78×10 ⁻³
CV (%)	46	48	42	87	82	80	89	133	100	131	118

NAFM: Not available for measurement (completely dried wells)

5. Discussion

In Wasinmi Boreholes, the sedimentary aquifer released up to 11.0×10^{-2} l/s with depths to aquifer found to vary between 35m to 75m with the mean of 51m (Table 1). Ewekoro, the closest community to the study area exhibited a yield of 6.0×10^{-2} l/s and the accompanied depth to water found to vary between 35m and 100m with a mean depth of 60.32²³; Ilorin

basement had 17m to 60m with a mean of 32.9m in borehole depth⁸⁹⁻⁹⁰; Ado-Ekiti basement had 40m to 120m and Malawi basement had 24m to 75m with a mean value of 24m⁹¹⁻⁹³. The influence of depth on the observed yield was not totally dependent but other parameters like porosity and permeability played significant roles. The specific yields particularly for an unconfined aquifer varied in standard of 0.01 to 0.3⁹⁴. The observed high value is a reflection of the aquifer potential for a high storage in relation to the water holding capacity of the rock. This is due to the abundance of clayey materials; possessing a high capacity for water storage but low capacity for water transmission. The auriferous zone in the study area is as a result of the effect of weathering of the saturated sandstone and partly cavernous karst limestone in the area⁹⁵⁻⁹⁶. Borehole discharge varied from 1.0×10^{-2} l/s to 11.0×10^{-2} l/s with a mean of 4.0×10^{-2} l/s (Table 1) as compared with Ewekoro aquifer that ranged from 3.0×10^{-2} to 6.0×10^{-2} l/s with an average of 4.0×10^{-2} l/s; Ilorin basement complex ranged from 2.4×10^{-1} l/s to 25.0×10^{-1} l/s with an average of 8.9×10^{-1} l/s; Ado-Ekiti basement ranged from 2.6×10^{-1} l/s to 0.26×10^{-1} l/s and Malawi basement ranged from 2.5×10^{-3} l/s to 5.0×10^{-1} l/s with a mean of 0.078×10^{-1} l/s. The study area exhibited transmissibility that varied from 1.0×10^{-2} m²/s to 9.20×10^{-2} m²/s with a mean value of 4.5×10^{-1} m²/s (38,880 m²/day) as compared to the closest community (Ewekoro aquifer) whose transmissibility varied between 8.04 to 6912 m²/day with a mean of 776.6 m²/day; Ilorin basement complex had 2.0 to 35 m²/day while upper gravelly coastal plain sandy aquifer of Akpabuyo, South-South Nigeria possessed transmissibility value range of 3.61 to 11.4m²/day⁹⁷. The residual drawdown in the investigated location ranged from 3.67m to 11.4m with a mean of 8.17 (Table 1) while the mean static water level was 17.8m with an interval of 8.45m to 37.4m. Average specific capacity (Cs) and Well loss were respectively found to be 6.3×10^{-3} m²/s and 5.98×10^4 s²/m⁵. The longest recovery period was 3431 seconds (WASBH19) and shortest recovery was 850 seconds (WASBH1) with a mean recovery period of 2254 seconds (37.57 minutes). Among the investigated hydraulic parameters in the study area, Borehole Depth is the least variable identified parameters having the coefficient of variation (CV) of 23% (Table 1). This was accompanied by Residual Drawdown (RDD) and Well Head possessing a CV of 31% and 33% respectively (Table 1). In Wasinmi hand-dug wells, the sedimentary auriferous zones produced up to 6.0×10^{-2} l/s with a mean of 2.3×10^{-2} l/s while depths to the well varied from 4.30 to 21.40m with the mean depth of 8.3m. Water discharge from the well ranged from 1.0×10^{-4} to 6.0×10^{-2} l/s with an average of 2.3×10^{-2} l/s. The transmissibility varied from 1.0×10^{-1} (8.64 m²/day) to 5.10×10^{-1} m²/s (44,064 m²/day) with a mean of 1.42×10^{-1} m²/s (12,269 m²/day). The RDD varied between 0.13m to 1.99m with a mean of 0.83m, the mean SWL was found to be 1.59m within a range of 0.24m to 5.42m while the mean Cs and WLC were respectively reported as 1.4×10^{-1} m²/s and 2.34×10^{-4} s²/m⁵. The shortest recovery period was 1541 seconds (WASWA14) while the longest recovery period was 24,610 seconds (WASWA19) with the average of recovery period of 9446 seconds (157.43 minutes). Among all the hydraulic parameters investigated in Papalanto hand-dug wells, measured well diameter is the least variable parameter with value of 42% followed by Well head alongside well depth possessing CV of 46% and 48% in respective order (Table 2). Transmissibility is a very significant hydraulic property of an aquifer which serves as the ratio of dominating density and drained density via a unit width of an aquifer subjected to a unit hydraulic head. It is a function of liquid properties, porous media and the accompanied thickness of the porous media⁹⁸. The plots of specific capacity (Cs) against Transmissibility

(T) on Semilog Scale are in Figure 5a and 5b for Wasinmi Borehole and hand-dug well sites.

High transmissibility values are suggestive of high potentiality which in turn determines the production capacity. Groundwater in the study area exhibited very high transmissibility in both water sources; $4.5 \times 10^{-1} \text{ m}^2/\text{s}$ (38,880 m^2/day) in Boreholes and $1.42 \times 10^{-1} \text{ m}^2/\text{s}$ (12,269 m^2/day) According to potentiality classification, transmissibility values greater than 500 m^2/day are considered high potentials⁹⁹⁻¹⁰². According to transmissibility classification scheme of Krasny¹⁰³ adopted by Jika & Tse¹⁰⁴; the auriferous zone in the study area are classified as high in potentials in the designation of transmissivity magnitude for boreholes and hand-dug wells jointly presented in Table 3.

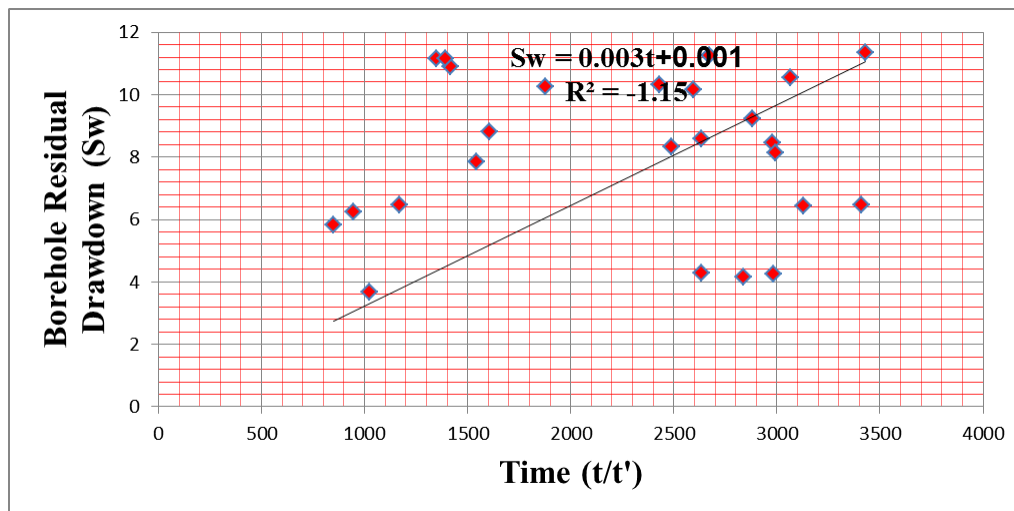


Figure 5a. Plot of residual drawdown (Sw) and time (T) on Semilog scale for Wasinmi borehole sites

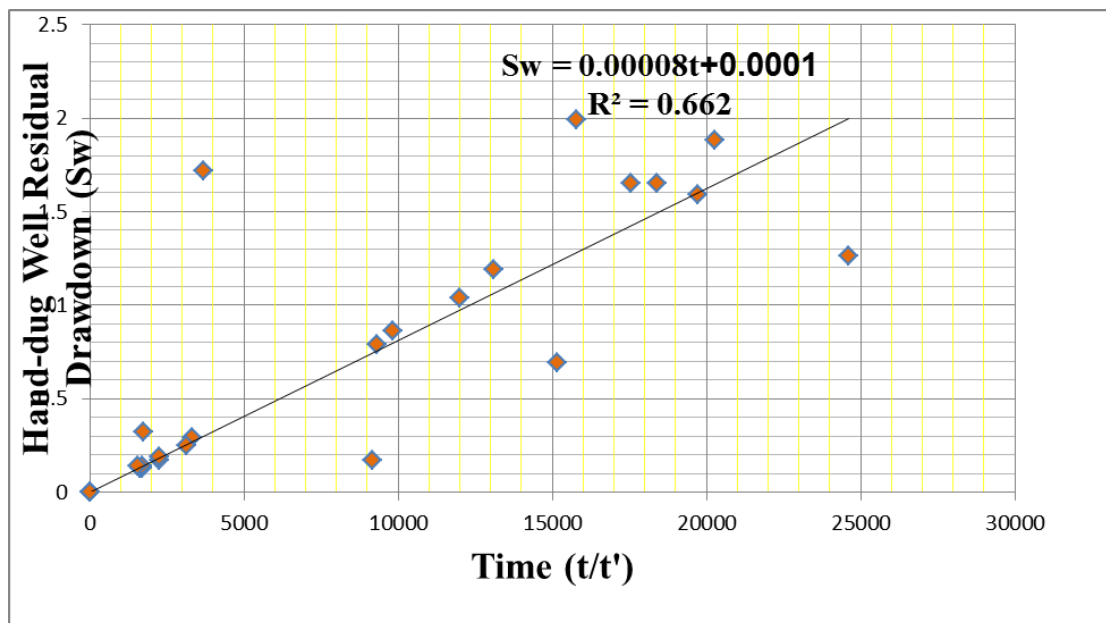


Figure 5b. Plot of residual drawdown (Sw) and time (T) on Semilog scale for Wasinmi Hand- dug well Site

Table 3. Transmissibility potentials of the aquifer system^{99 & 103-107}

Coefficient of Transmissibility (T) Range (m ² /day)	Classification magnitude	Magnitude designation	Coefficient of Transmissibility (T) Range (m ² /day)	Classification magnitude	Magnitude designation
> 500	I	High Potentials	> 1000	I	Very High
100–500	II	Good Potentials	100 – 1000	II	High
50–100	III	Moderately Potentials	10 – 100	III	Intermediate
5–50	IV	Low Potentials	1 – 10	IV	Low
0.5–5	V	Very Low Potentials	0.1 – 1.0	V	Very Low
<0.5	VI	Negligible Potentials	0 – 0.1	VI	Imperceptible

As obtained from the drilling outputs and lithological description of the boreholes drilled in the study area, the saturated thickness of the aquifer were 14m (26m-40m) and 17m (8m-25m); 17m (13m-30m) and 9m (3-12); 25m (5m-30m) and 22m (2m-24m); 50m (12m-62m) and 22m (2.0m-24m); and 63m (7.0-70m) and (2m and 22m) respectively recorded for boreholes and hand-dug wells in location 1 to 4; 5 to 8; 9 to 12; 13 to 16; 17 to 20 and 21 to 25 as displayed in Figure 6a to 6f in respective order. The aquifer thickness as well as the static water level are both veritable information to be considered by drillers and borehole contractors on the selected numbers of casing/screens to be utilized while the depth would equally enhanced the driller preparation towards the preparation of cost estimates for drilling operations being dependent on the length of metre drilled¹⁰⁸. Other associated parameters are also of great significance in terms of drilling operation and water management scheme to be adopted and installed be it manpower (manual) on motorized well pumping system²³. The plots of specific capacity and transmissibility are displayed in Figures 5a and 5b; respectively for Wasinmi Borehole and hand-dug wells. Good correlations are conspicuously observed between transmissibility and specific capacity with correlation coefficient ($R^2 = -0.33$ and $R^2 = 1.00$) respectively reported for Wasinmi boreholes and hand-dug wells (Figure 5a and 5b). This output is a revelation that the higher value of specific capacity of an aquifer and its transmissibility, the greater the prolificacy or production capacity of the well. Hydraulic conductivity values in the study area were found between $1.018 \times 10^{-3} \text{ m}^2/\text{s}$ (87.96 m^2/day) and $50.90 \times 10^{-3} \text{ m}^2/\text{s}$ (4397.76 m^2/day) in Wasinmi boreholes and between $0.688 \times 10^{-3} \text{ m}^2/\text{s}$ (594.432 m^2/day) and $89.84 \times 10^{-3} \text{ m}^2/\text{s}$ (7762.18 m^2/day) in Wasinmi hand-dug wells; this is rated as being very high when compared with the work of Jika & Tse¹⁰⁴ who reported range of values between 6.1×10^{-2} and $6.45 \times 10^{-1} \text{ m}^2/\text{s}$ in Konshisha, North Central Nigeria. The hydraulic properties of the aquifers in the study area are strongly influenced by weathered sandstone which serve as the aquifer materials for the borehole and the presence of shale/clay shale/clayey sand for the hand-dug wells; groundwater from the shallow hand-dug wells are abstracted from the fractured shales/clay-shale/clayey sand because the required depth for fresh water were not reached at the time of the termination of drilling depth. Shale is a sedimentary rock hydraulically known for its fissility; though highly porous its water transmission capability is very poor. Shale does not transmit water in any way except it is fractured¹⁰⁴. These are evident in boreholes and well locations of high transmissibility (WASBH24) and

(WASWW14) exhibiting transmissibility values of $9.2 \times 10^{-1} \text{ m}^2/\text{s}$ (79488 m^2/day) and $50.06 \times 10^{-2} \text{ m}^2/\text{s}$ (43,251.84 m^2/day) respectively around northeast of Onibotuje and northwest of Alagbon. The potentiality of aquifer in the study area is hydraulically high; according to Daniel¹⁰⁹ and Jika & Tse¹⁰⁴, an aquifer with a transmissibility value of less than $12.4 \text{ m}^2/\text{day}$ ($0.5 \text{ m}^2/\text{hr.}$ or $1.44 \times 10^{-4} \text{ m}^2/\text{s}$) can supply sufficient water to meet domestic needs of households but with higher values can altogether serve domestic, industrial and irrigation purposes. The exhibited high aquifer yield in the study area is an implication that the productive capacities from both water sources can be enhanced and sustained, better when high horse power pumps are preferably installed. Hydraulic conductivity in the range of 40.8 to $49.0 \text{ m}^2/\text{day}$ has been reported to be of favourable sites for groundwater development in eastern part of Kushtia district of Bangladesh⁸⁴ while the Hydraulic conductivity values that ranged from 6.1×10^{-2} to 6.45×10^{-1} have also been reported in Konshisha area in the middle Benue trough of North Central Nigeria¹⁰⁴ and the value range of 9.7 to $27.9 \text{ m}/\text{day}$ has been reported for upper gravelly aquifer of coastal plain sandy aquifer of Akpabuyor, south-south Nigeria⁹⁷. Hydraulic conductivity is a significant parameter in hydrogeological studies and has been immensely useful for effective groundwater management, protection and prediction for contaminant transportation.

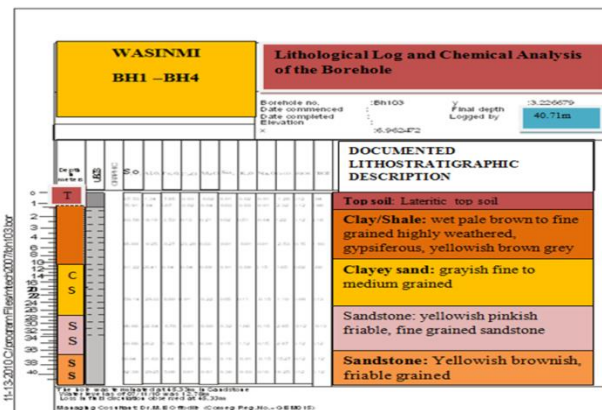


Figure 6a. Lithological description of Wasinmi subsurface around Locations WASBH1 to WASBH4

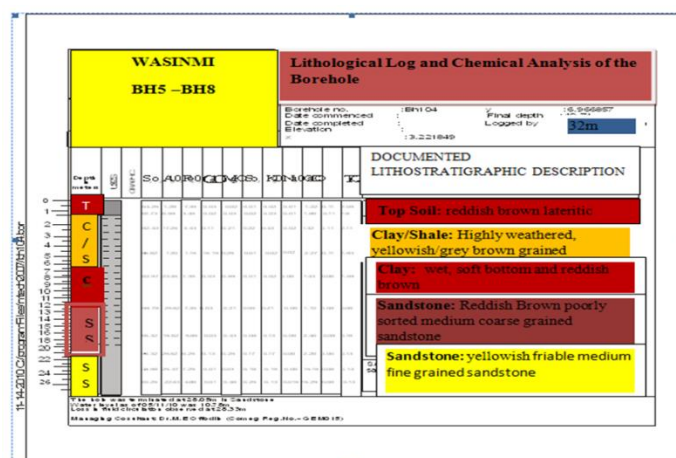


Figure 6b. Lithological Description of Wasinmi Subsurface around Locations WASBH5 to WASBH8

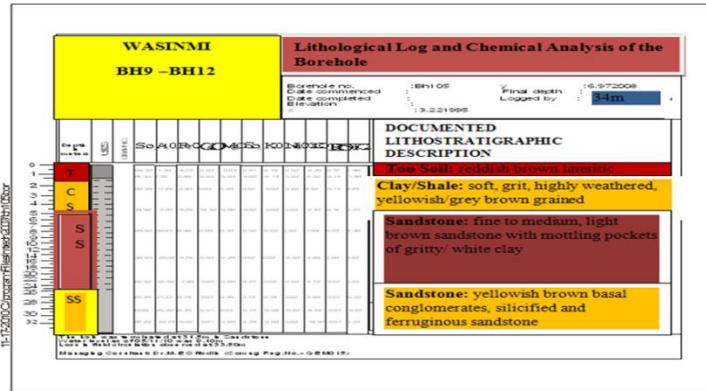


Figure 6c. Lithological description of Wasinmi subsurface around Locations WASBH9 to WASBH12

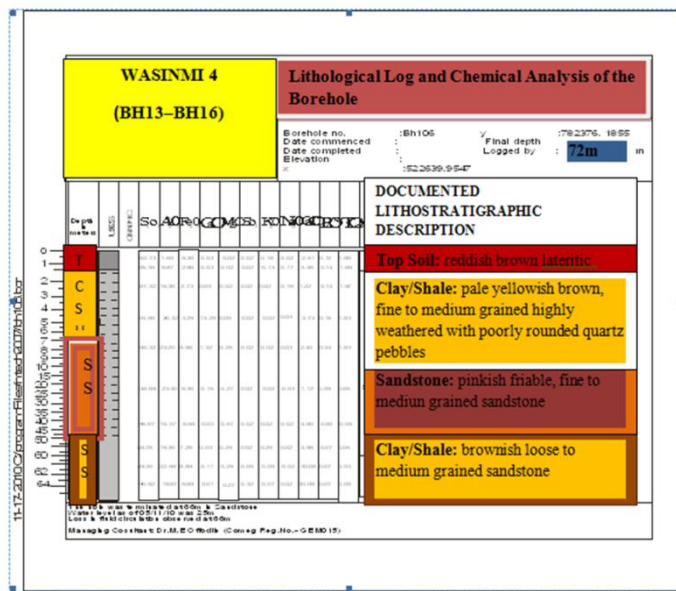


Figure 6d. Lithological description of Wasinmi subsurface around Locations WASH13 to WASBH16

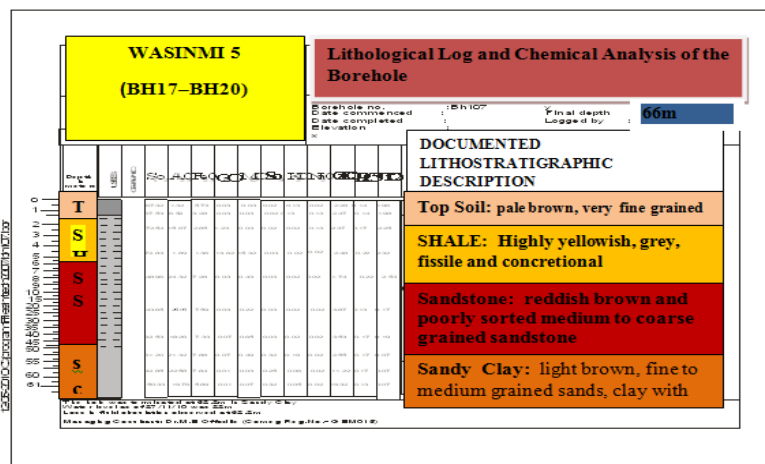


Figure 6e. Lithological description of Wasinmi subsurface around Locations WASBH17 to WASBH20

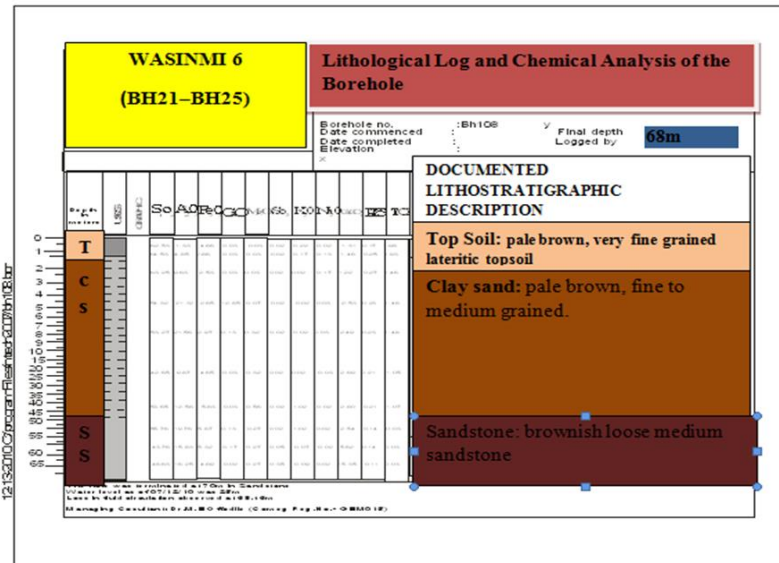


Figure 6f. Lithological description of Wasinmi subsurface around Locations PABH21 to PABH25

It determines the ease at which the fluids flow via the soil matrix system under a unit hydraulic gradient per unit time²³. The hydraulic conductivity status of the study area is dependent on the size of the soil grains, the structure of the soil matrix, class of soil fluid as well as the degree of saturation of soil matrix. Hydraulic conductivity varies with particles size for unconsolidated porous media; clayey and partly shaly materials are responsible for the area that exhibited low values of hydraulic conductivity whereas sandy and gravelly aquifers displayed higher values of hydraulic conductivity. Hydraulic diffusivity varied from 11.816 m²/s (1,020,902.4 m²/day) to 13,022.87 m²/s (1,125,175,968 m²/day) in Wasinmi Boreholes and varied from 4.06 m²/s (350,784 m²/day) to 6467.26 m²/s (558,771, 264 m²/day) in Wasinmi hand-dug wells. The regions of higher hydraulic diffusivity values are comparatively favourable for groundwater development because of the accompanied higher degrees of flow as well as transport connectivity⁸⁴. The output and consequent understanding of hydraulic diffusivity in the study area would go a long way in assisting well-site contractors and engineers to make predictions on the influence of new and prospective wells on the water levels in the neighbourhood of existing wells; it would reveal how quickly water moves through the aquifer thereby equipping farmers on how irrigation practices can be optimized to ensure efficient utilization of groundwater resources; and it would also serve as essential tool for designing an effective correction measures and remediation strategies for the sanitization of possible contaminated groundwater system. Figures 7a and 7b revealed that the output of hydraulic diffusivity in the study area is a reflection of transmissibility output due to their direct connectivity while Figures 8a and 8b showed the distribution of hydraulic conductivity versus hydraulic diffusivity in 3D line/wireframe contour representations in both water contour sources. Therefore, distribution of hydraulic diffusivity is highly significant in aquifer potential assessment of the study area.

The radius of influence in the study area ranged from 4.89m to 64.80m in Wasinmi boreholes and 3.18m to 49.13m in Wasinmi hand-dug Wells (Table 4). Higher values of radius of influence that ranged from 638m to 760m have been reported in eastern part of Kushtia district of Bangladesh⁸⁴. The size of radius of influence in groundwater studies and

well testing practices is primarily a tripartite function namely hydrogeological features like aquifer heterogeneities, presence of faults and recharge rates; aquifer properties like aquifer thickness, porosity and specific yield, and aquifer type (either confined or unconfined); pumping conditions like drawdown, pumping duration among others.

The specific drawdown varied from 0.116m (WABH2) to 2m (WASBH25) in Wasinmi Boreholes and 0.017m (WASWW2) to 0.833m (WASWW11) in Wasinmi hand-dug wells (Table 4). Since drawdown exhibit inverse relationship with specific capacity where low drawdown reflects a high specific capacity and a high drawdown is an indication of low specific capacity. Therefore, wells with similar rate of discharge will abstract less quantity of water from the wells emplaced in the vicinities of high specific drawdown than that of wells occupied in the region of low-valued specific capacity. Higher Specific drawdown of 57m to 126m was reported for Kushtia aquifer⁸⁴.

Table 4. Yield determinant parameters of the Wasinmi groundwater systems

Wasinmi Boreholes						Wasinmi Hand-Dug Wells					
Locations	K (m ² /s)	Ss (l/s)	D _H (m ² /s)	R (m)	SDD (m)	Locations	K (m ² /s)	Ss (l/s)	D _H (m ² /s)	R (m)	SDD (m)
PAPBH1	1.557×10 ⁻³	1.319×10 ⁻⁴	11.816	5.156	0.578	PAPWW1	5.918×10 ⁻³	9.711×10 ⁻⁵	60.94	7.553	0.056
PAPBH2	1.914×10 ⁻³	9.571×10 ⁻⁶	200.00	21.95	0.116	PAPWW2	26.99×10 ⁻³	2.505×10 ⁻⁵	106.49	49.134	0.017
PAPBH3	1.018×10 ⁻³	9.564×10 ⁻⁵	18.716	4.893	0.739	PAPWW3	6.74×10 ⁻⁴	1.226×10 ⁻⁶	549.76	35.157	0.284
PAPBH4	6.843×10 ⁻³	4.252×10 ⁻⁵	160.94	19.03	0.732	PAPWW4	6.853×10 ⁻³	5.695×10 ⁻⁵	120.33	16.454	0.066
PAPBH5	21.45×10 ⁻³	2.125×10 ⁻⁵	1008.9	47.65	1.538	PAPWW5	2.113×10 ⁻³	1.333×10 ⁻⁴	15.85	5.973	0.349
PAPBH6	22.12×10 ⁻³	2.123×10 ⁻⁵	1043.2	48.45	1.486	PAPWW6	61.13×10 ⁻³	3.401×10 ⁻⁴	179.73	20.109	0.018
PAPBH7	20.32×10 ⁻³	2.95×10 ⁻⁵	925.51	45.63	0.179	PAPWW7	35.30×10 ⁻³	2.068×10 ⁻⁴	170.63	19.594	0.027
PAPBH8	16.72×10 ⁻³	9.28×10 ⁻⁶	1801.7	20.13	1.944	PAPWW8	35.30×10 ⁻³	2.261×10 ⁻⁴	156.20	18.747	0.030
PAPBH9	19.56×10 ⁻³	1.048×10 ⁻⁵	1866.0	64.80	1.261	PAPWW9	2.06×10 ⁻³	3.868×10 ⁻⁴	53.26	3.462	0.283
PAPBH10	20.84×10 ⁻³	1.436×10 ⁻⁵	1451.5	57.15	1.384	PAPWW10	7.46×10 ⁻³	1.656×10 ⁻⁴	45.05	3.184	0.728
PAPBH11	16.38×10 ⁻³	6.848×10 ⁻⁶	2391.9	23.20	1.725	PAPWW11	0.688×10 ⁻³	1.511×10 ⁻⁴	4.56	3.202	0.833
PAPBH12	19.13×10 ⁻³	1.469×10 ⁻⁶	13,023	17.12	1.466	PAPWW12	89.84×10 ⁻³	7.936×10 ⁻⁴	113.21	15.960	0.019
PAPBH13	13.54×10 ⁻³	3.015×10 ⁻⁵	450.40	10.05	1.366	PAPWW13	11.49×10 ⁻³	1.332×10 ⁻⁴	86.28	18.578	0.047
PAPBH14	13.23×10 ⁻³	2.876×10 ⁻⁵	459.91	32.17	1.366	PAPWW14	41.72×10 ⁻³	1.603×10 ⁻⁴	260.24	24.200	0.018
PAPBH15	16.07×10 ⁻³	2.698×10 ⁻⁵	5954.8	36.60	0.774	PAPWW15	5.785×10 ⁻³	2.701×10 ⁻⁵	214.18	21.953	0.054
PAPBH16	8.126×10 ⁻³	1.653×10 ⁻⁵	491.62	10.52	0.170	PAPWW16	1.224×10 ⁻³	3.014×10 ⁻⁴	4.06	9.559	0.253
PAPBH17	14.48×10 ⁻³	3.560×10 ⁻⁵	406.78	30.25	1.387	PAPWW17	1.741×10 ⁻³	1.296×10 ⁻⁴	13.43	5.498	1.036
PAPBH18	11.68×10 ⁻³	2.640×10 ⁻⁵	442.47	31.56	1.481	PAPWW18	5.666×10 ⁻³	8.140×10 ⁻⁵	69.61	3.958	0.892
PAPBH19	4.494×10 ⁻³	1.125×10 ⁻⁵	399.47	29.98	2.512	PAPWW19	6.972×10 ⁻⁴	7.076×10 ⁻⁵	61.96	3.930	0.660
PAPBH20	7.471×10 ⁻³	2.013×10 ⁻⁵	371.14	28.90	1.941	PAPWW20	7.122×10 ⁻⁴	1.015×10 ⁻⁴	70.15	3.973	0.745
PAPBH21	29.73×10 ⁻³	2.183×10 ⁻⁵	1362.0	55.36	1.203	PAPWW21	8.00×10 ⁻⁵	1.237×10 ⁻⁶	6467.26	12.071	0.744
PAPBH22	41.34×10 ⁻³	5.061×10 ⁻⁵	816.82	42.87	1.027	PAPWW22	1.340×10 ⁻³	1.775×10 ⁻⁶	75.49	13.037	0.454
PAPBH23	42.37×10 ⁻³	1.856×10 ⁻⁵	2282.7	71.68	1.178	PAPWW23	NAFM	NAFM	NAFM	NAFM	NAFM
PAPBH24	50.90×10 ⁻³	9.222×10 ⁻⁶	5519.4	35.24	0.737	PAPWW24	NAFM	NAFM	NAFM	NAFM	NAFM
PAPBH25	10.14×10 ⁻³	2.767×10 ⁻⁵	366.61	28.72	6.410	PAPWW25	NAFM	NAFM	NAFM	NAFM	NAFM

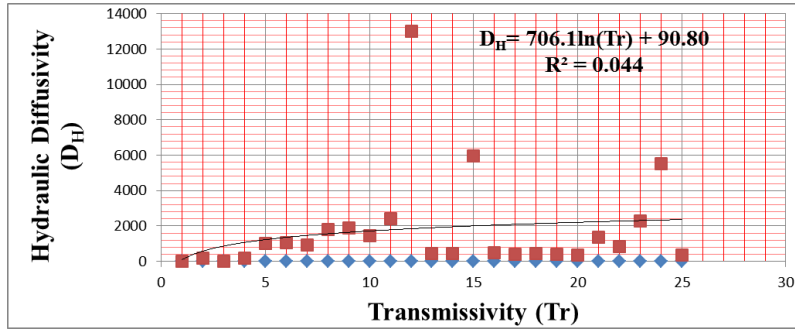


Figure 7a. Plot showing the trends and connectivity between hydraulic diffusivity and Transmissivity on Semilog scale for Wasinmi borehole sites

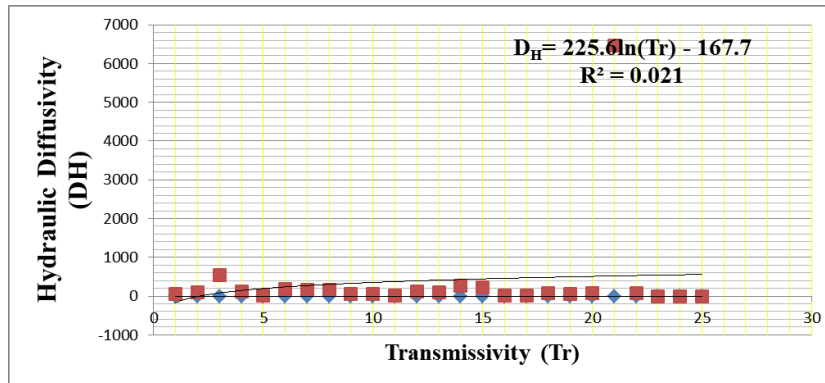


Figure 7b. Plot showing the trends and connectivity between hydraulic diffusivity and Transmissivity on Semilog scale for Wasinmi hand-dug well sites

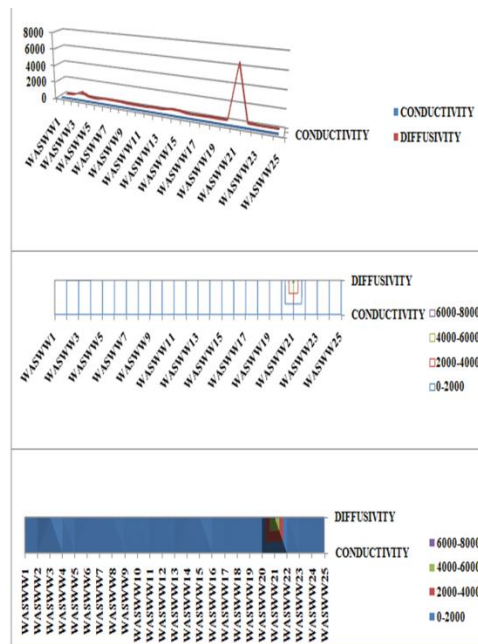


Figure 8a. Plot showing the distribution of hydraulic conductivity versus hydraulic diffusivity in 3D line/wireframe contour representations in Wasinmi borehole sites

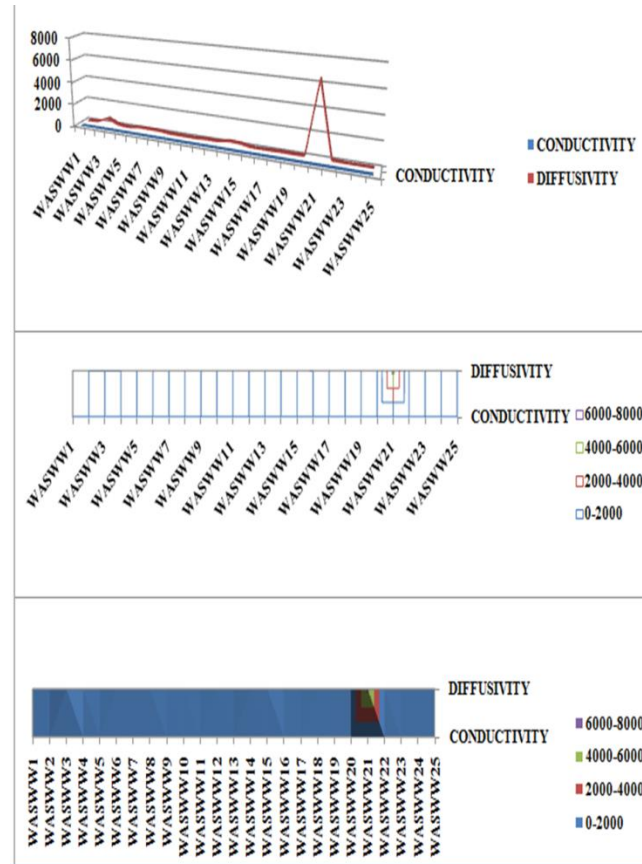


Figure 8b. Plot showing the distribution of hydraulic conductivity versus hydraulic diffusivity in 3D line/wireframe contour representations in Wasinmi hand-dug well Sites.

In Papalanto boreholes, the lowest specific yield of 0.772×10^{-2} l/s at WASBH2 and highest specific yield of 10.62×10^{-2} l/s at WASBH1 recorded around northwest of Ikeja (Figure 4). The lowest specific storage of 9.57×10^{-6} l/s was recorded at WASBH2 and the highest specific storage of 1.319×10^{-4} l/s at WASBH1; this is complemented with the observed variation in yields sites as displayed in Figure 4. It can be inferred from the observed values of specific yield and specific storage that groundwater can be abstracted at varying proportions over all the investigated sites while the variation in the observed specific capacity is significant because it measures the productive capacity of boreholes and helps in the appropriate selection of pump for groundwater abstraction^{23-25 & 89}.

The specific yield for Wasinmi hand-dug wells ranged between 3.66×10^{-3} l/s at WASWW19 and 58.40×10^{-3} l/s at WASWW14 (Figure 4) while the lowest specific storage of 1.23×10^{-6} l/s at WASWW2 and the highest specific storage of 7.94×10^{-4} l/s at WASWW12 (Table 4 and figure 4). Just like the borehole sites, it can be inferred that fresh groundwater can be tapped at varying quantity in Wasinmi hand-dug well sites especially when higher drilled depths are undertaken. The specific storage was found to be generally much smaller than the specific yield in both Wasinmi water sources where specific yield is the volume of water released from storage by a unit volume of an unconfined aquifer under a unit change (Figure 9a and 9b); because the subsurface hydrogeological conditions of the study area are reflections of the elastic compression of the aquifer and constituting water

while the specific yield is a representation of the water released due to gravity drainage in an unconfined aquifer which is much larger volume. The observed values of specific storage are in general representative of the amount of time for drainage.

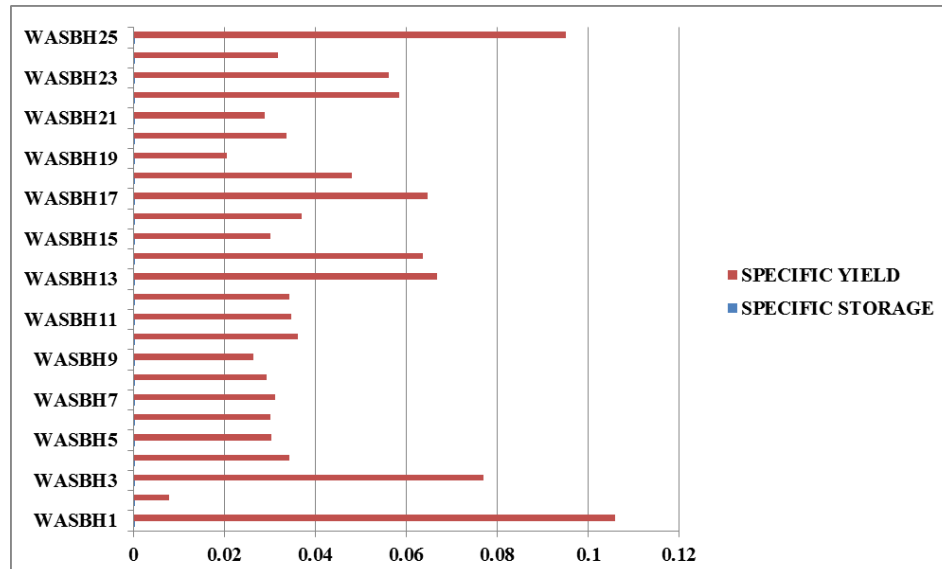


Figure 9a. Variation of specific yield versus specific storage in Papalanto Borehole well-sites

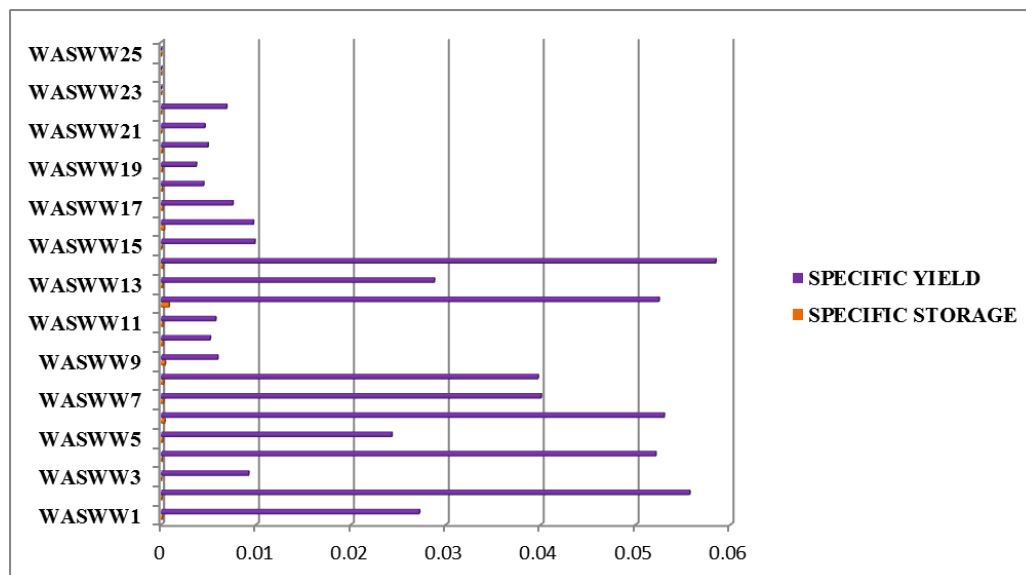


Figure 9b. Variation of specific yield versus specific storage in Papalanto hand-dug well sites

Therefore, as the water content decreases from saturation, the large pores which are most effective in conducting water are the first to drain out. Similarly, the tortuosity of the flow paths may increase while the average properties principally density and viscosity of the soil solution may change. These factors are strong contribution to a rapid decrease of in hydraulic conductivity relative to hydraulic diffusivity with decreasing yield as respectively observed in WASBH12 alongside WASBH13, WASBH16 alongside WASBH25 (Figure 8a) and WASWW21 alongside WASWW22 (Figure 8b) in Wasinmi borehole and



Wasinmi hand-dug wells. Another plausible reason attributable to the sudden decrease or change in the observed hydraulic conductivity relative to hydraulic diffusivity is the type of cationic species in the sediment solution and consequent changes in the hydraulic conductivity of the sediments containing significant quantity of clay most notably, swelling clay¹⁰⁹⁻¹¹².

6. Conclusions

Groundwater has been of immense contribution to the residents of Wasinmi communities despite its varying supply challenges. Pumping test has proving not only as effective but reliable estimation technique for the characterization of aquifer properties. Groundwater system in the study area has been characterized geohydraulically with parameters displaying varying outputs from two water sources namely boreholes and hand-dug wells and their varying contributions to groundwater yields. The weathered sandstone constituted the aquifers from which water are abstracted for boreholes while fractured shale/clayey sand/shale-clay and partly clay are typically responsible for water supply via hand-dug wells due to the fact that the required depth from fresh water aquifers were not reached. The outputs of the estimated hydraulic parameters are highly significant for groundwater productivity and sustainability most specifically high hydraulic conductivity, transmissibility and high specific yields among others. Borehole discharge ranged from 1.0×10^{-2} l/s (864 L/day) to 11.0×10^{-2} l/s (9504 L/day) with a mean of 4.0×10^{-2} l/s (3456 L/day) with exhibited transmissibility that varied from 1.0×10^{-2} m²/s (864 m²/day) to 9.20×10^{-2} m²/s (7949 m²/day) while discharge from hand-dug wells ranged from 1.0×10^{-1} l/s (8640 L/day) to 6.0×10^{-2} l/s (5184 L/day) with an average of 2.3×10^{-2} l/s (1987.2 m²/day) with transmissibility ranging from 1.0×10^{-1} l/s (8640 m²/day) to 5.10×10^{-1} l/s (44064 m²/day). The hydraulic conductivity of the study area ranged from 87.96 m²/day to 4397.76 m²/day in Wasinmi boreholes and ranged from 1541 m²/day to 24,610 m²/day in Wasinmi hand-dug wells. The recorded mean recovery period of 2254 seconds and 9446 seconds were attained by Wasinmi boreholes and hand-dug wells respectively. The two water sources revealed that the auriferous zones are classified as very high in potentials in the designation of mean transmissibility magnitude for boreholes (38,880 m²/day) and hand-dug wells (12,269 m²/day) based on the comparison of their results with standard aquifer potentiality classification. The status of the hydraulic diffusivity is an indication that the zones possessing greater values are comparably favourable for groundwater abstraction and development because of the greater degree of flow they exhibited. In Wasinmi boreholes, the lowest specific yield of 0.772×10^{-2} l/s at WASBH2 and highest specific yield of 10.62×10^{-2} l/s at WASBH1 around northwest of Ikeja and Awado while the lowest specific storage of 9.57×10^{-6} l/s and the highest specific storage of 1.319×10^{-4} l/s at respectively at the same location; revealing that groundwater can be abstracted at varying proportions over the investigated sites. The variation in the observed specific capacity is significant because it measures the productive capacity of boreholes and is of immense assistance for appropriate pump selection. The hydraulic parameters in the area revealed that the auriferous zones for hand-dug well are constituent of fractured shale /clay-shale/clayey sand materials of lower yields than boreholes because the required depths were not reached but the large diameter hand-dug well enhanced the transmission of fluids into the well. The generally observed high yields in the borehole revealed that the aquifer



materials are sufficiently fractured; typical weathered sandstone. In view of this, the observed high yields from both water sources due to high transmissibility necessitates the recommendation of high horse power pumps of about 7.0 to 13.0 h.p. preferably for installation in order to ensure sustainable groundwater withdrawal, effective water management and control in the study area. The results of the specific yield gives an inference that fresh groundwater can be sourced at varying amount in Wasinmi hand-dug well sites especially when higher required depths are undertaken; it is a general reflection of the optimum period of time for drainage. Specific storage of an aquifer is often influenced by the compressibility of the aquifer matrix and compressibility of the water. The specific storage was found to be generally much smaller than the specific yield in both water sources. Well spacing has been proposed for the study area based on the outputs of the estimated radius of influence utilizing an empirical formula under unconfined condition since the aquifer in the area is largely unconfined; observed minimum and maximum radius of influence of the area were 5m to 65m and 3m to 49m for hand-dug wells and boreholes respectively. The overall variation of the estimated hydraulic properties in Wasinmi groundwater system is an indication that the study area is hydrogeologically favourable for groundwater development provided other requirements and boundary conditions are met. Therefore, based on the geohydraulic investigation of the study area, results of this study should be utilized as a comprehensive guide for effective groundwater planning and development in the study area coupled with other pre-drilling and post drilling hydrogeological techniques.

7. References

1. McKay, SE; Kluitenberg, GJ; Butler, JJ Jr; Zhan, X; Aufman, MS & Brauchler, R. 2004. In-situ determination of specific yield using soil moisture and water level changes in the riparian zone of the Arkansas River, Kansas. *EOS Transactions AGU*, 85 (47): 11. [https://citeseerx.ist.psu.edu/viewdoc/download?doi=10.1.1.714.3039\\$rep=rep1](https://citeseerx.ist.psu.edu/viewdoc/download?doi=10.1.1.714.3039$rep=rep1).
2. Bevan, MJ; Endreas, AI; Rudolph, DI & Parkin, G. 2025. A field scale study of pumping-induced drainage and recovery in an unconfined aquifer. *Journal of Hydrology*, 315 (1): 52-70. <https://doi.org/10.1016/J.Jhydrol.2005.04.06>.
3. Tartakovsky, GD & Neuman, SP. 2007. Three-dimensional saturated-unsaturated flow with axial symmetry to a partially penetrating well in a compressible unconfined aquifer. W01410. *Water Resources Research*, 43 (1): 22. <https://doi.org/10.1029/2006WR005153>.
4. Al-Thani, AA; Beaven, RP & White, JK. 2004. Modelling flow to leachate wells in landfills. landfill process modelling workshop. *Waste Management*, 24 (3): 271-276. <https://doi.org/10.1016/j.wasman.2003.11.010>.
5. Walton, WC. 1970. *Groundwater Resource Evaluation*. McGraw-Hill, New York: 664.
6. Said, A; Nachebe, M; Ross, M & Vomacka, J. 2005. Methodology for estimating specific yield in shallow water environment using continuous soil moisture data. *Journal of Irrigation and Drainage Engineering*, 131 (6): 533-538.
7. Montgomery, EI. 1971. Determination of Coefficient of Storage by Use of Gravity Measurements. Tucson, AZ: The University of Arizona: 23-27.
8. Cheng, X; Song, I and Wang, W. 2010. Spatial variability of specific yield and vertical hydraulic conductivity in a highly permeable alluvial aquifer. *Journal of hydrology*, 388 (1): 379-388. <https://doi.org/10.1016/j.jhydrol.2010.05.017>.



9. Gehman, CL; Harry, DL; Sanford, WE; Stednick, JD & Beckham, NA. 2009. Estimating specific yield and storage change in an unconfined aquifer using temporary gravity surveys. W00D21. *Water Resources Research*, 45 (1): 13-14. <https://doi.org/10.1029/2007WR006096>.
10. Neuman, SP. 1972. Theory of flow in unconfined aquifers considering delayed response of the water table. *Water Resources Research*, 8 (4): 1031-1045. <https://doi.org/10.1029/WR008i004p01031>.
11. Moench, AF. 1994. Specific yield as determined by type-curve analysis of aquifer-test data. *Groundwater*, 32 (6): 949-957. <https://doi.org/10.1111/j.1745-6584.1994.tb00934.x>
12. Johnson, AI. 1967. Specific yield-compatibility-compilation of specific yields for various materials. United States Government Printing Office, Washington, DC. *United States Geological Survey Water Supply Paper*. 1662.
13. Wenzel, LK; Cady, RC, & Waite, HA. 1946. Geology and groundwater resources of Scotts Bluff County, Nebraska. United States Government Printing Office, Washington, DC. *US Geological Survey Water Supply Paper*, 659 (1): 41.
14. Nwankwor, G; Cherry, J & Gillham, R. 1984. A comparative study of specific yield determinations for a shallow sand aquifer. *Groundwater*, 22 (6): 764-772. <https://doi.org/10.1111/j.1745-6584.1984.tb01445.x>
15. Neuman, SP. 1974. Effect of partial penetration on flow in unconfined aquifers considering delayed gravity response. *Water Resources Research*, 10 (2): 303-312. <https://doi.org/10.1029/WR010i002p00303>.
16. Meizhao, Lv; Xu ZF; Liang, YZ; Hui, L & Meixia, L. 2021. A comprehensive review of specific yield in land surface and groundwater studies. *Journal of Advances in Modelling Earth Systems*, 13 (1): 13-24. <https://doi.org/10.1029/2020ms002270>.
17. Neuman, SP. 1975. Analysis of pumping test data from anisotropic unconfined aquifers considering delayed gravity response. *Water Resources Research*, 11 (2): 329-342. <https://doi.org/10.1029/WR011i002p00329>.
18. Youngs, E & Smiles, D. 1963. The pumping of water from wells in unconfined aquifers: a note on the applicability of Theis Formula. *Journal of Geophysical Research*. 68 (20): 5905-5907. <https://doi.org/10.1029/JZ068i020p05905>.
19. Kollet, SJ & Zlotnik, VA. 2005. Influence of Aquifer Heterogeneity and Return Flow on Pumping Test Data Interpretation. *Journal of Hydrology*, 300 (4): 267-285. <https://doi.org/10.1016/j.jhydrol.2004.06.011>.
20. Nwankwor, G; Gillham, R; Vander-Kamp, G & Akindunni, F. 1992. Unsaturated and saturated flow in response to pumping of an unsaturated confined aquifer, field evidence of delayed drainage. *Groundwater*, 30 (5): 690-700. <https://doi.org/10.1111/j.1745-6584.1984.tb01445.x>.
21. Akindunni, FF & Gillham, R. 1992. Unsaturated and saturated flow in response to pumping of an unconfined aquifer, numerical investigation of delayed drainage. *Groundwater*, 30 (6): 873-884. <https://doi.org/10.1111/j.1745-6584.1992.ib01570.x>.
22. Nelson, R & Quevauviller, P. 2016. *Groundwater Law in the Book: Integrated Groundwater Management*, 72. <https://doi.org/10.1007/978-3-319-23576-97>.
23. Ishola, SA. 2024. Groundwater resource potentials using frequency domain electromagnetic method and associated water quality techniques in Ewekoro communities, South-West Nigeria. *Federal University Wukari (FUW) Trends In Science and Technology Journal*, 9 (1): 193-200. www.ftstjournal.com.
24. Ishola SA. 2019. *Characterization of Groundwater Resource Potentials Using Integrated Techniques in Selected Communities Within Ewekoro Local Government Area South-West Nigeria*. Department of Physics, FUNAAB Ph.D Thesis.



25. Ishola, SA & Gbadebo AM. 2024. Evaluations of the phreatic shallow aquifers using hydraulic and hydraulic and hydrogeochemical techniques in a typical sedimentary part of Ogun State South-West Nigeria. *Journal of Earth Science and Atmospheric Research*, 7 (1): 54–71.
26. Okosun, EA. 1998. Review of the early tertiary stratigraphy of Southwestern Nigeria. *Journal of Mining and Geology*, 34 (1): 27-35.
27. Omatsola, ME & Adegoke, OS. 1981. Tectonic evaluation and cretaceous stratigraphy of the Dahomey Basin, *J. Min. Geol*, 5 (2): 78-83.
28. Billman, HG. 1992. Offshore stratigraphy and palaeontology of the Dahomey (Benin) Embayment, West Africa, 1st. *NAPE Bulletin*, 7 (2): 121-130.
29. Kehinde-Phillips, T. 1992. Ogun state maps, In: Onakomaya, S; Oyesiku, O & Jegede, K. *Ogun State in Maps*. Rex Charles Publishers, Ibadan: 187.
30. Obiora, DN. & Onwuka, OS 2005. Groundwater exploration in Ikorodu, Lagos- Nigeria: a surface geophysical survey contribution, *Pacific Journal of Science and Technology*, 6 (1): 86-93.
31. Freeze, R & Cherry, J. 1979. *Groundwater*. Englewood Cliffs, NJ. Prentice Hall: 604.
32. Yin, L; Hu, G; Huang, J; Wen, D; Dong, J; Wang, X & Li, H. 2011. Ground waters recharge estimation in the Ordos Plateau, China: comparison methods. *Hydrogeology Journal*, 19 (8): 1563-1575. <https://doi.org/10.1007/s10040-011-0777-3>.
33. Yang, ZL; Cai, X; Zhang, G; Tavakoly, AA; Jin, Q; Meyer, LH & Guan, X. 2011. *The Community Noah Land Surface Model with Multiparameterization Options (Noah-MP): Technical Description*. Austin, TX: Centre for Integrated Earth System Science. Department of Geological Sciences, the University of Texas at Austin.
34. Yin, L; Zhou, Y; Ge, S; Wen, D; Zhang, E & Dong, J. 2013. Comparison and modification of methods for estimating evapo-transpiration using diurnal groundwater level fluctuations in arid and semi-arid regions. *Journal of Hydrology*. 496 (1): 9-16. <https://doi.org/10.1016/j.jhydrol.2013.05.016>.
35. Dos-Santos, A. Jr & Youngs, E. 1969. A study of specific yield in land drainage situations. *Journal of Hydrology*, 8 (1): 59-81. [https://doi.org/10.1016/002-1694\(69\)90031-6](https://doi.org/10.1016/002-1694(69)90031-6).
36. Fetters, C. 1994. *Applied Hydrogeology*. Upper Saddle River, NJ: Prentice Hall.
37. Schwartz, FW & Zhang, H. 2003. *Fundamentals of Groundwater*. John Wiley and Sons Publications, New York: 574.
38. Zhang, J; Van-Heyden, J; Bendel, D & Barthel, R. 2011. Combination of soil-water balance models and water-table fluctuation methods for evaluation and improvement of groundwater recharge calculations. *Hydrogeology Journal*, 19 (8): 1487-1502. <https://doi.org/10.1007/s10040-011-0772-8>.
39. Healy, RW & Cook, PG. 2002. Using groundwater levels to estimate recharge. *Hydrogeology Journal*, 10 (1): 91-109. <https://doi.org/10.1007/s10040-001-0178-0>.
40. Nachabe, MH. 2002. Analytical expressions for transient specific yield and shallow water table drainage. *Water Resources Research*, 38 (10): 111-117. <https://doi.org/10.1029/2001WR001071>.
41. Nachabe, MH; Ahuja, IR & Rokicki, R. 2003. Field capacity of soil-water, concept, measurement and approximation. In BA Stewart and T Howell (Eds). *Encyclopaedia of Water Science*. New-York: Dekker.



42. Crosbie, RS; Doble, RC; Turnadge, C & Taylor, AR. 2019. Constraining the magnitude and uncertainty of specific yield for use in the water table fluctuation method of estimating recharge. *Water Resources Research*, 55 (1): 7343-7361. <https://doi.org/10.1029/2019WR025285>.
43. Loheide II, SP; Butler Jr JJ & Gorelick, SM. 2005. Estimation of groundwater consumption by phreatophytes using diurnal water table fluctuations, a saturated-unsaturated flow assessment. W07030. *Water Resources Research*, 41 (1): 22. <https://doi.org/10.1029/2005WR003942>.
44. Duke, HR. 1972. Capillary properties of soils-influence upon specific yield. *Transactions of ASAE*, 15 (1): 688-691.
45. Abdul, A & Gillham, R. 1984. Laboratory studies of the effects of the capillary fringe on stream-flow generation. *Water Resources Research*, 20 (6): 691-698. <https://doi.org/10.1029/WR0201006p00691>.
46. Sophocleous, MA. 1985. The Role of Specific Yield in Groundwater Recharge Estimations: Numerical Study. *Groundwater*, 23(1), 52-58. <https://doi.org/10.1111/j.1745-6584.1985.tb02779.x>.
47. Shah, PH & Ross, M. 2009. Variability in specific yield under shallow water table conditions. *Journal of Hydrologic Engineering*, 14 (12): 1290-1298. <https://doi.org/10.1061/ASCEHE.1943-5584.0000121>.
48. Mccarthy, KA & Johnson, L. 1993. Transport of volatile organic compounds across the capillary fringe. *Water Resources Research*, 29 (6): 1675-1683. <https://doi.org/10.1029/93WR00098>.
49. Li, L; Barry, D; Parlange, JY & Pattiaratchi, C. 1997. Beach water-table fluctuations due to wave run-up: capillary effects. *Water Resources Research*, 33 (5): 935-945. <https://doi.org/10.1029/96WR03946>.
50. Nielsen, P & Perrochet, P. 2000. Water-table dynamics under capillary fringes experiments and modelling. *Advances in Water Resources*, 23 (1): 503-515. [https://doi.org/10.1016/s0309-1708\(99\)0038-x](https://doi.org/10.1016/s0309-1708(99)0038-x).
51. Cartwright, N; Nielson, P & Perrochet, P. 2005. Influence of capillarity on a simple harmonic oscillating water-table, sand columns experiments and modelling. *Water Resources Research*, 41 (1): 17. <https://doi.org/10.1029/2005WR004023>.
52. Bear, J. 1972. *Dynamics of Fluids in Porous Media*. New York, American Elsevier. 764.
53. Jayatilaka, C & Gillham, R. 1996. A deterministic-empirical model of the effect of the capillary fringe on near-stream area runoff, description of the model. *Journal of Hydrology*, 184 (3): 299-315. [https://doi.org/10.1016/0022-1694\(95\)02985-0](https://doi.org/10.1016/0022-1694(95)02985-0).
54. Cloke, H; Anderson, M; McDonald, J & Renaud, JP. 2006. Using numerical modelling to evaluate the capillary fringe groundwater ridging hypothesis of stream flow generation. *Journal of Hydrology*, 316 (1): 141-162. <https://doi.org/10.1016/J.Jhydrol.2005.04.017>.
55. Butler, Jr JJ; Kluitenberg, GJ; Whitmore, DO; Loheide, SP; Jin, W; Billinger, MA & Zhan, X. 2007. A Field Investigation of phreatophytes-induced fluctuations in the water-table. *Water Resources Research*, 43 (1): 20. <https://doi.org/10.1029/2005WR004627>.
56. Loheide, SP II. 2008. A method for estimating sub daily evapotranspiration of shallow groundwater using diurnal water-table fluctuations. *Ecohydrology*, 1 (1): 59-66. <https://doi.org/10.1002/eco.7>.



57. Mould, D; Frahm, E; Salzmann, T; Miegel, K., & Acreman, M. 2010. Evaluating the use of diurnal groundwater fluctuations for estimating evapotranspiration in wetland environments: case studies in Southeast England and Northeast Germany. *Ecohydrology*, 3 (3): 294-305. <https://doi.org/10.1002/eco.108>.
58. Fan, J; Ostergaard, KT; Guyot, A & Lockington, DA. 2014. Estimating groundwater recharge and evapotranspiration from water-table fluctuation under three vegetation covers in a coastal sandy aquifer of Subtropical Australia. *Journal of Hydrology*, 519 (1): 1120-1129. <https://dx.doi.org/10.1016/j.jhyrol.2014.08.039>.
59. Cheng, DH; Wang, YH; Duan, JB; Chen, X & Yang, SK. 2015. A new analytical expression for ultimate specific yield and shallow groundwater drainage. *Hydrological Processes*, 29 (1): 1905-1911. <https://doi.org/10.1002/hyp.10306>.
60. Fahle, M & Dietrich, O. 2014. Estimation of evapotranspiration using diurnal groundwater level fluctuations: comparison of different approaches with groundwater lysimeter data. *Water Resources Research*, 50 (1): 273-286. <https://doi.org/10.1002/2013WR014472>.
61. Gribovszki, Z; Szilagy, J & Kalicz, P. 2010. Diurnal fluctuations in shallow groundwater levels and stream-flow rates and their interpretations- a review. *Journal of hydrology*, 385 (4): 371-383. <https://doi.org/10.1016/j.jhydrol.2010.02.001>.
62. Childs, EC. 1960. The non-steady state of the water table in drained land. *Journal of Geophysical Research*, 65 (2), 780-782. <https://doi.org/10.1029/jz0605i002p00780>.
63. Brooks, R & Corey, T. 1964. *Hydraulic Properties of Porous Media (Hydrology Papers No 3)*. Fort Collins, Co. Colorado State, University.
64. Van-Genuchten, MT. 1980. A closed-form equation for predicting the hydraulic conductivity of unsaturated soils. *Soil Science Society of America Journal*, 44 (5): 892-898. <https://doi.org/10.2136/sssaj1980.0365995004400050002x>.
65. Sophocleous, MA. 1991. Combining the soil water balance and water-level fluctuation methods to estimate natural groundwater recharge: Practical aspects. *Journal of Hydrology*, 124 (3-4): 229-241. [https://doi.org/10.1016/0022-1694\(91\)90016-B](https://doi.org/10.1016/0022-1694(91)90016-B).
66. Yeh, PJ & Eltahir, EA. 2005. Representation of water-table dynamics in a land surface scheme. Part I: Model Development. *Journal of Climate*, 18 (12): 1861-1880. <https://doi.org/10.1175/JCLI3330.1>.
67. Rossenberry, DO & Winter, TC. 1997. Dynamics of water table fluctuations in an upland between two prairie-pothole wetlands in North Dakota. *Journal of Hydrology*, 191 (1): 266-289. [https://doi.org/10.1016/S0022-1694\(96\)03050-8](https://doi.org/10.1016/S0022-1694(96)03050-8).
68. Sullivan, PL; Price, RM; Miralles-Wiillhelm, F; Ross, M; Scinto, LJ & Dreschel, TW. 2014. The role of recharge and evapo-transpiration as hydraulic drivers of ion concentrations in shallow groundwater on Everglades Tree Islands. Florida, USA. *Hydrological Processes*, 28 (2): 293-304. <https://doi.org/10.1002/hyp.9575>.
69. Prill, RC; Johnson, AI & Morris, DA. 1965. Specific yield-Laboratory experiments showing the effect of time on column drainage. *United States Geological Survey Water Supply Paper*, 1662 (B): 55. <https://pubs.er.usgs.gov/publication/wsp1662B>.
70. Pozdniakov, S.P; Wang, P & Lekhov, VA. 2019. An approximate model for producing the specific yield under periodic water-table oscillations. *Water Resources Research*, 55 (1): 6185-6197. <https://doi.org/10.1029/2019WR025053>.



71. Martinez-Santos, P; Diaz-Alcaide, S; De-la Hera-Porttillo, A & Gomez-Escalonilla, V. 2021. Mapping groundwater-dependent ecosystems by means of multi-layer supervised classification. *Journal of Hydrology*, 603 (1): 128. <https://doi.org/10.1016/j.jhydrol.2021.126873>.
72. Logsdon, S; Schilling, K; Hernandez-Ramirez, G; Prueger, J; Hatfield, J & Sauer, T. 2010. Field estimation of specific yield in a central IOWA crop field. *Hydrological Processes International Journal*, 24 (1): 1369-1377. <https://doi.org/10.1002/hyp.7600>.
73. Haque, MN; Keramat, M & Shalid, S. 2014. Groundwater resource evaluation in the western part of Kushtia District of Bangladesh using vertical electrical sounding technique. *ISH. Journal of Hydraulic Engineering*, 21 (1): 97-110. <https://doi.org/10.1080/09715010.2014.981679>.
74. Onu, N. 2003. Estimates of the relative specific yield of aquifers from geoelectrical sounding data of the Coastal Plains of Southeastern Nigeria. *Journal of Technology and Education in Nigeria*, 81 (1): 69-83. <https://dx.doi.org/10.4314/joten.v8i1.35641>.
75. Papadopulos, SS; Bredehoeft, JD & Cooper, HH, Jr. 1973. On the analysis of slug test data. *Water Resources Research*, 9 (4): 1087-1089. <https://doi.org/10.1029/WR009i004p0187>.
76. Gehman, CL; Harry, DL; Sanford, WE; Stednick, JD & Beckman, NA. 2009. Estimating specific yield and storage change in an unconfined aquifer using temporal gravity surveys. *Water Resources Research*, W0021, 45 (1): 70-72. <https://doi.org/10.1029/2007WR006096>.
77. Wang, P; Grinevsky, SO; Pozdniakov, SP; Yu, J; Dautova, DS & Min, L. 2014. Application of the water fluctuation method for estimating evapotranspiration at two phreatophytes-dominated sites under hyper-arid environments. *Journal of Hydrology*, 519 (1): 2289-2300. <https://doi.org/10.1016/j.jhydrol.2014.09.087>.
78. Pool, DR, & Schmidt, W. 1995. Measurement of groundwater storage change and specific yield using the temporal gravity method near Rillio Creek. 97 (1): 4125. Tucson, Az: *United States Geological Survey Water Resources Investigations Report*.
79. Cooper, HH Jr & Jacob, CE. 1946. A generalized graphic method for evaluating formation constants and summarizing well-field history, *Transactions, American Geophysical Union*, 27 (4): 526-354.
80. Theis, CV. 1935. The relationship between the lowering of the piezometric surface and the rate and duration of discharge of well using groundwater storage. *Transactions American Geophysical Union*, 16 (2): 519.
81. Remson, L & Lang, S. 1955. A pumping-test method for the determination of specific yield. *Transactions-American Geophysical Union*, 36 (2): 321-325. <https://doi.org/10.1029/TR036i002p00321>.
82. Pool, DR & Eychaner, JH. 1995. Measurements of aquifer-storage change and specific yield using gravity surveys. *Groundwater*, 33 (3): 425-432. <https://doi.org/10.1111/j.17445-6584.1995.tb00299.x>.
83. Tizro, AY; Voudouris, K & Basami, Y. 2012. Estimation of porosity and specific yield by the application of geoelectrical method-A Case Study in Western Iran. *Journal of Hydrology*, 454 (1): 160-172. <https://doi.org/10.1016/j.jhydrol.2012.06.009>.
84. Shahinuzzaman, MD; Haque, MN; Uddin, KMN; Alibuddin, M. 2020. Identification of aquifer properties in the eastern part of Kushtia District, Bangladesh. *Journal of Geosciences and Environmental Protection*, 8 (11): 3-7. <https://doi.org/10.4236/Gep.2020.811015.1>.



85. Niu, GY; Yang, ZL; Dickinson, RE; Gulden, LE & Su, H. 2007. Development of a simple groundwater model for use in climate models and evaluation with gravity recovery and climate experiment data. DO7103. *Journal of Geophysical Research*, 112. <https://doi.org/10.1029/2006JD007522>.
86. Niu, GY; Yang, ZL; Mitchell, KE; Chen, F; Ek, MB & Barlage, M. 2011. The community Noah-land surface model with multiparameterization options (Noah-MP): model description and evaluation with local-scale measurements. D12109. *Journal of Geophysical Research*, 116. <https://doi.org/10.1029/2006JD007522>.
87. Fletcher, FW. 1998. Basic Hydrogeological Methods. *Technicom Publication*: 324.
88. Bear, J. 1979. *Hydraulics of Groundwater*. New York. McGraw-Hill. 567.
89. Sule, BF; Balogun, OS & Muraina, LB. 2013. Determination of hydraulic characteristics of groundwater aquifer in Ilorin, North-Central Nigeria. *Academic Journals*, <http://www.Academicjournals.org/SRE11.645>.
90. Muraina, LB. 2009. *Characteristics of Aquifer within Ilorin West Local Government Area, Kwara State Nigeria*. M. Engineering Project Report, Department of Civil Engineering, University of Ilorin, Nigeria: 5-7.
91. Ale, PO; Aribisala, JO & Awopetu, MS. 2015. *Evaluation of Yield of Wells in Ado-Ekiti, Nigeria. Nigeria Civil and Environmental Research*. Department of Civil Engineering, Faculty of Engineering, Ekiti State University, Ado-Ekiti, Ekiti State, Nigeria. www.iiste.org.
92. Chilton, PJ & Smith-Carington, AK. 1984. Characteristics of the Weathered Basement Aquifer in Malawi in Relation to Rural Water Supplies, Challenges in African Hydrology and Water Resources. *Proceedings of the Harare Symposium*, 1984. IAHS Pull. 144.
93. Ohenhen, L; Mayle, M; Kolawole, F; Ismail, A & Estella, AA. 2023. Exploring for groundwater in subsaharanafrica: insights from integrated basement aquifer system, Central Malawi. *Journal of Hydrology Regional Studies*, 47 (4): 4-5.
94. Watson, I & Burnet, AD. 1995. *Hydrology-An Environmental Approach*, CRC Press, 702.
95. Rasmussen, TC & Mote, TL. 2007. Monitoring surface and subsurface water storage using confined aquifer water levels of the Savannah River site, USA. *Vadose Zone Journal*, 6 (2): 327-335. <https://doi.org/10.1029/2001WR000701>.
96. Rasmussen, TC & Crawford LA. 1997. Identifying and removing barometric pressure effects on confined and unconfined aquifers. *Groundwater*, 35 (3): 504-505. <https://doi.org/10.1111/j.1745-6584.1997.tb00111.x>.
97. Amah, EA & Anam, GS. 2016. Determination of aquifer hydraulic parameters from pumping test data analysis: a case study of Akpabuyo Coastal plain sand aquifers, Cross-Rivers State. *IOSR Journal of Applied Geology and Geophysics (IOSR-JAGG)*, 4 (1): 1-8. www.iosrjournals.org.
98. Pollacco, JA; Galves, JF; Web, T; Vickers, S; Robertson. Mcneill SJE; Liburne, L, Rajannayaka, C & Chau, H. 2024. Derivation of physically based soil hydraulic properties in New Zealand by combining soil physics and hydrogeology. CCBY-NC-ND. *European Journal of Soil Science*, 75 (3): 2-4. <https://doi:10.1111/Ejss.13502>.
99. Sen-Zekai, S. 2015. *Practical and Applied Hydrogeology*, Chapter 5, 11-32. www.Sciencedirect.com.



100. Akpan, PJ; Akankpo, AO; Atat, JG; Ibout, JC & Umoren, EB. 2024. Geohydraulic investigation of aquifer parameters in Abak, Southern Nigeria. *Journal of Geosciences and Environment Protection*, 12 (5): 289-301. DOI: 10.4236/Gep.2024.125016.12.
101. Ali, MH; Zaman, MH; Boswas, P; Islam, MA & Karim, NN. 2022. Estimating hydraulic conductivity, transmissibility and specific yield of aquifer in Barind Area, Bangladesh using pump test. *European Journal of Environment and Earth Sciences*, 3 (4): 4.-7.
102. Beven, KJ. 2024. A brief history of information and disinformation in hydrological data and the impact on the evaluation of hydrological models. *Hydrological Sciences Journals*, 69 (5): 519-527. <https://doi.org/10.1080/02626667.2024.2332616>.
103. Krasny, J. 1970. Elaboration and areal expression of some hydrogeological elements in Maps. *Sbor.5 Hydrogeology Conference*. 57-69.
104. Jika, HT & Tse, AC. 2014. Determination of hydraulic characteristics of an aquifer capacity from pumping test: a case study of Konshisha Area, Central Nigeria. *Scientia Africana*, 13 (2): 136-145.
105. Weist, D. 1965. *Transmissivity and Hydraulic Conductivity in Aquifer Potentiality Classification*. 265-272.
106. Gheorghe, A. 1978. *Processing and Synthesis of Hydrological Data*. Abacus Press, Tumbridge Wells, Kant. 222.
107. Rag, D. 1972. *The Design of Sample Surveys*. Mc- Graw Hill, L.T.D., New Delhi, India. 165.
108. Ishola, SA; Makinde, V; Gbadebo, AM; Mustapha, AO & Orebiyi EA. 2021. *Quality Assessment of Groundwater System in Itori Community of Ewekoro Local Government Area, South-West Nigeria*. Nepal Engineering College Science and Technology Publishing. <http://scitechpub.org/index.php/vol-5-Issue-12-December-2021/>.
109. Daniel, DE. 1982. Measurement of hydraulic conductivity of unsaturated soils with thermocouple psychometers. *Soil Science Society of American Journal*, 46 (1): 993-100.
110. Thorbjatnarson, KW; Huntley, D & Mccarty, JJ. 1998. Absolute hydraulic conductivity estimates from aquifer pumping and tracer tests in a stratified aquifer. *Groundwater*, 36 (1): 87-97.
111. Klute, A & Dirksen, C. 1986. *Hydraulic Conductivity and Diffusivity: Laboratory Methods*. 88-90.
112. Mualem, DR & Klute, A. 1984. A predictor-corrector method for measurement of hydraulic conductivity and membrane conductance. *Soil Science Society of American Journal*, 48 (1): 1125-1129.

Acknowledgement

The author is grateful to the Ogun-Oshun River Basin Development Authority (OORBDA) and Federal Ministry of Water Resources for their permission to use the lithological data/core sample description and field logistics. Also, the traditional ruler of Wasinmi; His Royal Majesty, Oba Emmanuel Babatunde Osuntogun Fasoyin, Oniwasinmi of Wasinmi, Owu Kingdom, Abeokuta and the entire autonomous communities within Wasinmi district of Ewekoro Local Government Area for their permission and assistance.



Data availability

The data that support the findings of this study are available from the author upon reasonable request.

Declaration of competing interest

The author declares that he has no competing financial interests or personal relationships that could have appeared to influence the work reported in this paper.

Use of AI tools declaration

The author declares that he has not used Artificial Intelligence (AI) tools in the creation of this article.





Original Article

Preliminary investigation and extent of hydrogeochemical concentration for groundwater exploration using electromagnetic method of terrain conductivity variation and analytical technique in Papalanto, South-West Nigeria

S. A. Ishola¹

Abstract

Ground conductivity measurements were undertaken with Geonics EM 34-3 along 5 traverses with profile lengths varying between 160 and 200m while 50 water samples (25 each from boreholes and hand-dug wells) were collected and analyzed from existing water sources using standard techniques in Papalanto District within Dahomey basin South-West Nigeria. Comprehensive geophysical fieldworks were done adopting Frequency Domain Electromagnetic Method (FDEM) to ascertain both the vertical and lateral variations of subsurface conductivity probing depths of 20 m, 40 m and 60 m seeking different investigated depth. The EM data were acquired at 500 m intervals along 10 profiles. The Vertical Dipole Moment (VDM) in the first layer exhibited the highest and lowest true conductivity of 134.31 and 78.9 mmho/m for EMPAP1 and EMPAP6 respectively and the corresponding Horizontal Dipole Moment (HDM) exhibited the highest and lowest true conductivity values of 1141.92 and 118.0 mmho/m for EMPAP5 (2nd layer) with depth of 9m in HDM and 14m in VDM and EMPAP1 (1st layer) respectively. Lowest true conductivity values of 84.55 and 122.0 mmho/m were recorded in the second layer for VDM and HDM respectively. The highest recorded true conductivity values in the first layer were 133.33 mmho/m (EMPAP1) and 167.48 mmho/m in EMPAP7 (depth 7.8m in HDM and 9.2m in VDM) respectively. The highest depth of penetration respectively recorded for HDM and VDM in the first layer were 33m in EMPAP10 and 14m in EMPAP1 and EMPAP2 while the lowest depth of penetration respectively recorded for HDM and VDM in the first layer were 2m in EMPAP3 alongside EMPAP6 and 6.5m in EMPAP8 as the depths of penetration remained indeterminate in the second layer due to current termination. The output of water quality analyses revealed that Cl⁻ concentrations were found to be generally much more prominent in both water sources Cu²⁺, Pb²⁺, Mn²⁺ and Al³⁺ sometimes Ni concentrations were prominent as potential Toxic Elements and were found to be higher in hand-dug wells than in Boreholes. The observed high concentration Pb²⁺ and Cu²⁺ in the groundwater sources could be attributed to the activities in the study area. The qualitative interpretation of EM results identified areas of hydrogeological importance and forms a predictive and suggestive basis for Vertical Electrical Sounding (VES) investigation; points of positive EM anomalies were considered as priority area for prospective groundwater development necessitating more advanced groundwater exploration techniques and water quality treatment like nanofiltration and reverse osmosis to be undertaken in the study area.

Keywords: Terrain; dipole moment; probing depth; fissures; frequency domain

Affiliation Info: ¹ Department of Earth Sciences, Olabisi Onabanjo University Ago-Iwoye, P.M.B 2002, Ago-Iwoye, Ogun State, Nigeria.

Corresponding Author : Ishola, S. A. PhD, Exploration Geophysics and Geomathematics; Email: ishola.sakirudeen@oouagoiwoye.edu.ng.

Citation: Ishola, S.A. 2025. Preliminary investigation and extent of hydrogeochemical concentration for groundwater exploration using electromagnetic method of terrain conductivity variation and analytical technique in Papalanto, South-West Nigeria. *Naturalis Scientias*, 2 (2): 623-661. DOI: <https://doi.org/10.62252/NSS.2025.1036>. www.naturalisscientias.com.

Copyright © 2025 by the author. Published by *Naturalis Scientias*. This is an open access article under the Creative Commons Attribution-NonCommercial 4.0 International (CC BY-NC 4.0) License. (<https://creativecommons.org/licenses/by-nc/4.0/>).



1. Introduction

The acquisition and interpretations of Electromagnetic method (EM) seem difficult because of the varying subtlety and inherent inhomogeneity of the subsurface coupled with the abrupt changes in lithology, variable thicknesses, and electrical properties of weathered layer and bedrock materials. Pathway to the nature and conditions of the earth crusts is basically one of the most difficult challenge ever encountered by earth scientists because it is principally based on what can be observed per time and how better observers can perceive, predict and interpret his observation¹⁻². Groundwater has been a mysterious nature's hidden and endowed resources that must explored for effective utilization and maximization by the society². Daily exploitation of groundwater has continued to maintain a significant concern at every point in time due to its unavoidable demands by all and sundry; streams, rivers ponds, lakes among other sources, none naturally possesses a high level of sanitary integrity as groundwater because groundwater served and has been serving as excellent natural resource free of microbial loads and generally possess chemical quality of its domain qualifying it for most domestic and industrial utilization³. Terrain conductivity variations are crucial in preliminary groundwater exploration because they can indicate areas with higher groundwater potential. Conductivity surveys like the electromagnetic method help to identify zones with fractured or fissured rock formations and interconnected joints which often favour groundwater accumulation y providing broad overview of subsurface conditions, guiding more detailed study. These areas can then be further investigated with methods like vertical electric sounding (VES) to pinpoint optimal well locations⁴⁻⁷. Terrain conductivity meters are cost effective and can provide a large amount of data quickly making them ideal starting point for groundwater exploration⁸.

One of the significant assistant that exploration activities have offered earth scientists most notably the applied geophysicists is the detailed understanding of the earth interiors in terms of nature, properties, resources and their individual responses to measurable quantities in the field. The primary aim and objectives of applied geophysical investigations are detection, investigation, and drawing line of inferences on the existence, location and extent of underground water, ore minerals, solid minerals, hydrocarbons, geothermal reservoirs, radioactive deposits among others and subsurface geological structures that are connected with them using surface techniques for the measurement of the physical parameters of the earth alongside with the encountered anomalies in these measured parameters. EM method of geophysical prospecting provides a relatively fast approach to detecting and delineating fractures and where this delineated fractured zone possesses high conductivity; it could be inferred as mineralization zones or auriferous zones^{2 & 9-10}. Therefore, a detailed geophysical investigation and hydrogeological understanding of the subsurface conditions in terms of aquifer types and their spatial location are not only necessary but they are basic requirement for efficient characterization of auriferous zone and ultimate unravelling the hidden and seemingly mysterious nature of this endowed resources called groundwater².

Electrical conductivity (EC) in the subsurface water is a useful indicator of water quality as it correlates with the concentration of dissolved ions including those from toxic elements. Increased EC can signal the presence of pollutant, though it does not pinpoint the specific contaminants. Analysing EC alongside other parameters and geological sources can help



assess water quality and identify risks associated with toxic elements¹¹. It implies that increased conductivity generally suggests a higher concentration of dissolved ions which can include potentially harmful metals while not a direct measure of toxicity, good conductivity provides a quick assessment of water's ionic content and highlight areas where further investigation into specific contaminant is warranted. Potential toxic elements (PTEs) like Arsenic (As), Cadmium (Cd), Lead (Pb), and Mercury (Hg) can significantly increase conductivity. Industrial effluent may contain various metals and salts that when dissolved contribute to elevated conductivity levels. Natural geological formations can contribute to high conductivity due to the presence of naturally occurring minerals while conductivity is not a direct measure of toxicity, it serves as a useful screening tool for identifying water sources that may contain elevated levels of toxic elements and require more in-depth analysis. A study in Mokosh Beel, Gazipur found a strong correlation between EC and the concentrations of dissolved metals with values exceeding WHO guidelines¹¹. Conductivity alone does not identify the specific contaminant present, further analysis is needed. Other factors can influence conductivity such as temperature and the presence of non-toxic dissolved solids. Conductivity measurements can be affected by seasonal variations and the type of geological formations¹²⁻¹⁵. Another study near dumpsites found that the total dissolved solids were generally high with elevated conductivity near the site indicating potential contamination. Therefore, good conductivity is a valuable tool for water quality assessment particularly in identifying areas with potential contaminants from dissolved elements. However, it is essential to integrate conductivity data alongside water quality parameters and conduct more specific analysis to identify and qualify the contaminant present¹⁵⁻¹⁸.

The study area is located within the sedimentary part of Southwestern Nigeria and transits largely into the sediments of the Dahomey basin. The subsurface geophysical investigation adopting (EM) conductivity measurement was carried out in the study area for groundwater prospecting. Electromagnetic profiling is a widely used geophysical technique effective in the delineation of overburden rock formation and clay regolith as well as in the detection of fissured media and zones of deep connection to subsurface weathering of the consolidated sedimentary terrains¹⁹⁻²². In numerous geophysical episodes, reconnaissance EM surveys have been utilized in the detection and exploitation of auriferous zones and their accompanied features namely faults, fractures, and joints Ishola *et al.*, 2023². Geophysical methods perform unending notable tasks in sourcing for suitable and productive groundwater reservoirs²³. Electrical resistivity method has been routinely utilized in field exploration for groundwater. However, several other geophysical methods have been successfully applied either as a single technique or in composite approach for field prospecting for groundwater resources in varying geologic environment²⁴⁻²⁸. The electromagnetic method has proven not only as a very useful technique but also its suitability groundwater investigation in both sedimentary and basement terrains, most especially as a reconnaissance tools in the hands of exploration field professionals to understanding the nature and groundwater development feasibility studies of any encountered auriferous zone^{23 & 29-33}. The principal advantage of the EM- methods that has withstood the test of time is that direct contact with the earth surface is not in any way required when compared to Direct Electrical methods². Therefore, the field performance of EM- measurement can be rapidly and simply done than when the DC measurement is utilized for the same task rendering it a high and very relevant technique for rapid



assessment studies in line with other presumably fast and accurate techniques. EM does not register any individual outcome from field reading the difference from adjacent readings are significant and subsurface picture is equally built based on all the acquired readings along the survey line and adjacent lines of investigation². Also, Electromagnetic method can be utilized alone or in integrated form with other exploration geophysical techniques such as gravity, electrical resistivity, seismic refraction, reflection seismology, induced potential methods in the course of sourcing for groundwater which is a function of the scope of prospecting whether it is on local scale or a regional coverage. This study is basically centred on groundwater using by the interpretation of the observed conductivity variation where subsurface site information on the hydrogeological framework of the encountered aquifer units, and delineation of fractured/weathered zones for subsequent drilling and installation water wells in the study area.

2. Study area

The study area is discussed under Existence, Location and Accessibility, Climate, Vegetation, Drainage and Geology in this section.

2.1 Location and accessibility

The entity called Ewekoro Local Government Area (LGA) where the study area belongs first came into existence on 22nd of May, 1981. It lies within Ogun State, South-West Nigeria; which is bounded in the West by Benin Republic, in the south by Lagos State, in the north by Oyo and Osun States, and in the east by Ondo State. In 1984 when the military took over, the region was considered for restructuring. So, it was merged with Ifo Local Government in 1989³³. However, on December 16, 1996 Ewekoro Local Government was restored as an autonomous Local Government by the then Federal Military Government alongside five others in the state, thus increasing the number of Local Government in Ogun State from fifteen to twenty. Papalanto area is bounded by longitude 3^o13¹E and latitude 6^o54¹N; it harbours one of the largest outcrops of Ewekoro limestone that easily attracts attention. It extends from Ibesse, 4km east of Papalanto along Papalanto-Shagamu road to Ogun River, 5km east to Iro community (Ishola, 2019). It occupies a total area of 16,400 km² with a population of 255,156 at 2006 population Census and a postal code area of 112 with an average elevation of 64m above sea level. The area is mildly densely populated with 297 people per km² with the nearest town larger than 50,000 inhabitants takes about 0:15 hour by local transportation. The indigenous dwellers of Ewekoro Local Government area are mainly the Egbas, particular the Egba Owus. The people engage primarily in farming and trading activities. The area is essentially in rural settlement³³. The climate is not different from that of these towns and villages earlier mentioned and adjoining towns such as Ifo, Sagamu and others. However, the advent of West African Portland Cement Company (WAPCO) changed the economic sphere of this once sleepy and serene town³³. The Ewekoro cement production facility of the WAPCO established in 1959 is the oldest cement factory in Nigeria. Although quality limestone has been discovered in this settlement since the colonial period, mining and quarrying did not commence until early 70s when attempt were made to mine and export. However as a follow up to the first and

second National development plans, the company was established with Larfage of France being the major technical partner. The company has since being privatized. The annual cement production from the factory using wet and semi-wet clinker production technology varied between 254,000 and 479,000 metric tonnes (WAPCO, 2000). Figure 1 shows the geological map of the Study Area within the Nigerian Part of Dahomey Embayment. Figure 2 Displays the Google Earth imagery of the selected Investigated study area within in Ewekoro Local Government Area (LGA), the map of Ogun State showing the geology of the study areas is presented in Figure 3, the inset map showing political divisions of the study area within Nigerian continental environment is shown in Figure 4, the map showing the selected investigated locations in the study area is shown in Figure 5 while Figure 6 the accessibility of the study areas amidst the investigated points in Ewekoro LGA. The entire study area is generally accessible by major roads and several footpaths, although the road from Abeokuta town to the investigated area is tarred. In addition to Ewekoro-Papalanto road, the survey locations can equally be accessed through a major road from Lagos State through Sango-Ifo express road³⁴⁻³⁵.

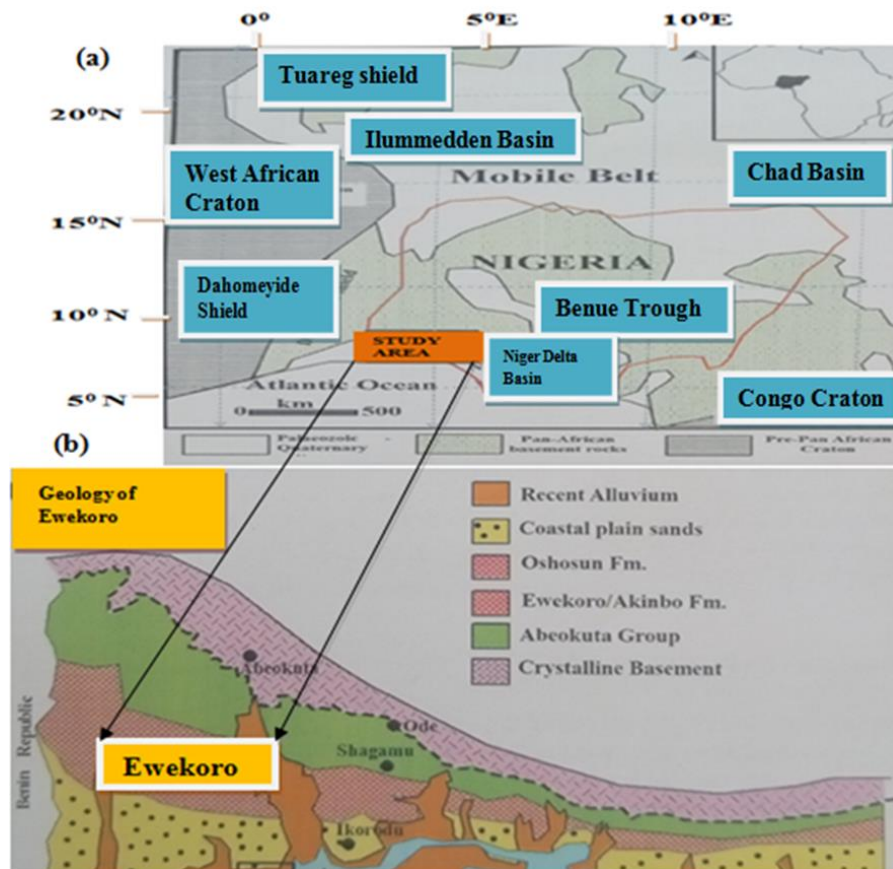


Figure 1. Geological map showing the selected locations of the study area within the Nigerian part of Dahomey Embayment^{33 & 36}



Figure 2. Display of Google earth imagery of the selected investigated study area within in Ewekoro LGA, south-west Nigeria³⁷

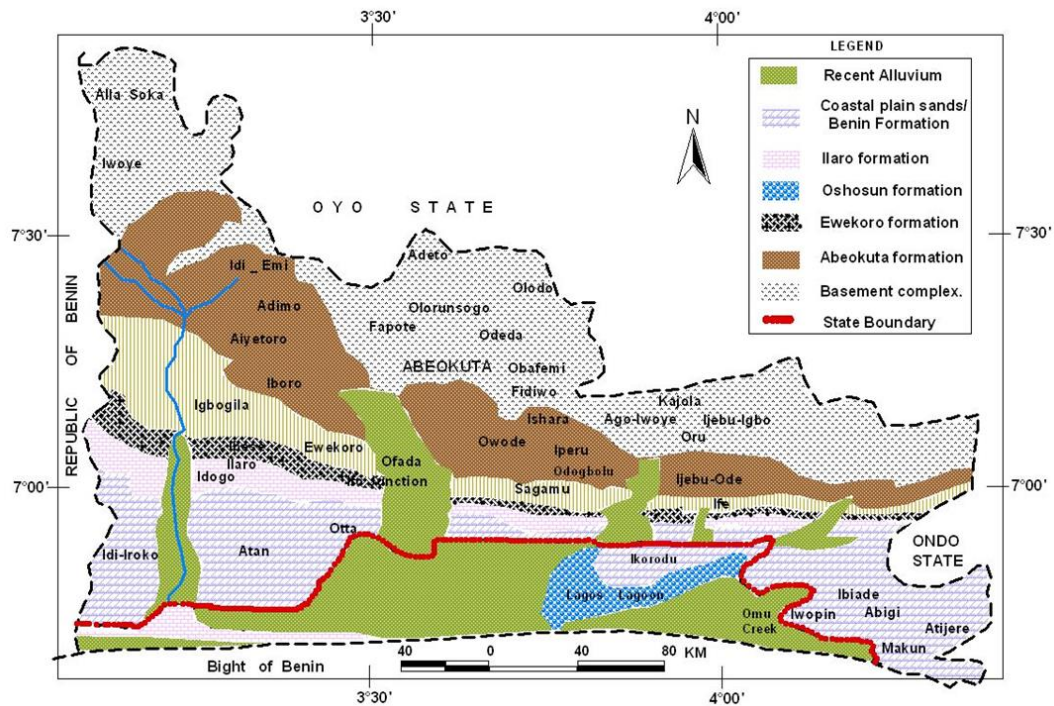


Figure 3. A map of Ogun State showing the geology of the study area^{34 & 38}

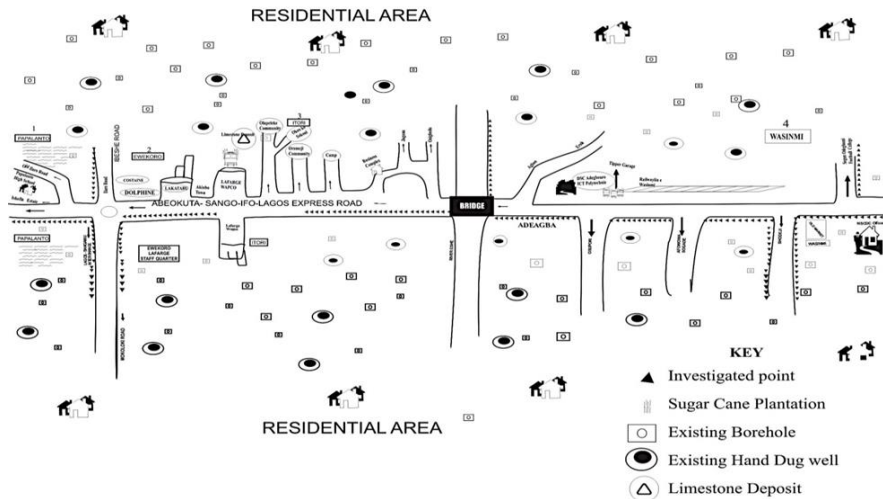


Figure 6. Location and accessibility of the investigated points in Ewekoro LGA³⁷

2.2 Weather and climate

The study areas is generally a low lying to gentle undulating terrain that falls within the humid tropical climate characterized by two distinct seasons predominant in the tropics in the southern part of Nigeria namely, the wet and dry seasons. The wet season usually occur from March to October, the climate is dominated by the tropical maritime air mass or moisture laden Southwest winds from the Atlantic Ocean that produces heavy rainfall; most of the rainfall comes in torrential showers resulting in high run-off while the dry season occurs from November to late February or early March under the influence of the dry continental air mass or North-Easterly winds from Sahara desert. The little dry season in the mid-west season of July/August months is dominant in the area³⁹⁻⁴⁰. The Harmattan season, a season of dusty high winds, unusual cold and extremely dry conditions, lasts from November to February. It is caused by the tropical continental air from the Sahara Desert which displaces the tropical Maritime air from the Gulf Guinea⁴¹. Ewekoro has no distinct temperature seasons; the temperature is relatively constant during the year. The wet season ensures adequate supply of water and continuous presence of moisture in the air. Hence, the study area experiences high diurnal and annual temperature, lack of cold season, high precipitation, low pressure, high evapotranspiration and high relative humidity⁴⁰⁻⁴². The temperatures at night are cooler than during the daytime. November is an average, the month with most sunshine. February is the warmest with an average monthly temperature of 33.5⁰C at noon. August is coldest with an average temperature of 21.9⁰C. Rainfall and other precipitation peaks around June. The time around January is the driest.

The study area has a mean annual temperature of 27⁰C in July and 32⁰C in February, and the average monthly temperature of 25.7⁰C. It has relative high humidity of 71.09 % and long wet season that ensures adequate supply of water and continuous presence of moisture in the air. The annual rainfall is estimated to be 1194.33mm⁴⁰⁻⁴³. Cold and hazy conditions are usually prevailing especially towards the end of the year while hot and dusty conditions are experienced during dry season. Hence, the study area is characterized by high diurnal and annual temperature, high precipitation, low pressure, high evapo-transpiration and high relative humidity. The major water bodies in the region are Yewa and Ogun rivers which



flow into Lagos lagoon while their tributaries are found in Ewekoro Local Government Area as Alaguntan River, Akinbo River and Eshe River. There are however streams running parallel in the area. Also ponds are not left out. Due to the alternation of wet and dry seasons, the water table fluctuates in response to the seasonality of rainfall. During the wet season, groundwater level rises towards the surface and drops as the dry season sets in. In terms of environmental hazards, the following parameters 20%, 70%, 70%, 0%, 0%, 0% for Earthquake, Flood, Drought, Landslides, Volcano and Cyclone have been estimated and predicted in their respective order in Ewekoro. Ewekoro can have low impact or less earthquakes (on the average of one every 50 years) with occurrences at < 5 Richter. There is a medium to high occurrence of periods with extreme drought. Flooding risk is medium high although, during the wet season, parts of the city become flooded as a result of heavy rainfall, low relief, high tides and poor structural planning of buildings and drainage facilities^{33 & 43-44}.

2.3 Natural vegetation and site description

The natural vegetation of Ogun State which the study areas belong consists of the forest and the savanna which affect the floristic composition of the plant communities. The forest vegetation is of two types, namely, the fresh water swamp forest and the lowland rain forest. The savanna found in the State is mainly of the derived savanna type. The rainforest vegetation is typified by perennial trees which may vary in height forming storey with characteristics thick vegetation due to high rainfall. The vegetation changes with seasons with the incoming of the rains, the green grasses are back to life and the foliage of the trees becomes green and thick. Where the soil is wet due to river drainage denser fringing forest are found. During dry season some of the trees, which develop umbrella shaped canopies shed their leaves in order to minimize loss of water by transpiration^{33 & 45}. Human activities on the natural vegetation have reduced the original forest to secondary forest bush, regrowth and thickets. One very important impact of the quarry is deforestation. This simply means the loss of vegetation cover that is necessitated by the need to move equipment to the site, removal of the topsoil or (overburden) stemming of explosives and removal of blasted limestones. These effects are normally reduced by appropriate mitigating actions such as massive reclamation of the mined areas using new overburden materials and a forestation programme that involve planting of varieties of trees that have ornamental values, that can hold the soil structure well and could cover the exposed land well. Limestone mining in Ewekoro had resulted into the conversion of many farmlands and settlements into quarry sites. The house types on the site are mainly the makeshift type built for use on no permanent basis. The few landowners on the factory site are resident on site to participate in cement business and no longer to farm as it was before now.

2.4 Topography and drainage pattern

Ogun State which the study areas belong is drained by many big perennial rivers that are consequent in nature and numerous obsequent streams. The rivers include Ogun, Oshun, Yewa, Opebi, Yemoji and Ore with Ogun River being the dominant one in the study areas which runs across it from north to south³³. The hydrographical centres of most of these rivers are not within Ogun State but in other states. Most of the perennial rivers often have

braided channels and extensive flood plains and basins in lower parts. Majority of the subsequent and obsequent rivers and streams often dry up completely during the dry season while the consequent rivers often have their water levels and discharges reduced, thereby leaving extensive flood plains at their sides. The river valleys are the narrowest landform in the area. The river is a sluggish perennial stream in dry season but a turbulent one during the wet season. This relief can be described as undulating and the drainage is dendritic³³.

2.5 Physiography and geology of the study area

The physiography of the study area is that of extensive lowland that is generally undulating with a gently sloping dissected escarpment known as southern uplands as reported by Jones and Hockey²³. The area is drained mainly by Ewekoro River which according to²³ is obsequent, endoergic and forms a dense network all over the area with anastomotic pattern along its course. In terms of regional geology, the study area belongs to the eastern part of the Dahomey Basin extending from the Volta Delta (Southwestern Ghana) to the western flank of the Niger Delta in Nigeria⁴⁶. The stratigraphy of the basin has already been studied by various authors²³. However, the general succession of the sedimentary rock units of Ogun State which consists of Abeokuta formation lying directly above the basement complex is that of underlying rock which comprises of Abeokuta Group, followed by Ewekoro, Akinbo, Oshosun and Ilaro formations respectively while on top of Ilaro formation is the coastal plain sands (Benin formation)⁴⁷.

Overlying the Abeokuta Group conformably is the Imo group, which comprises of shale, limestone and marls. The two-lithostratigraphic units under this group are: Ewekoro formation and Akinbo formation. Adegoke⁴⁸ described the formation as consisting of shaly limestone and is divided it into three microfacies. Ogbe⁴⁹ further modified this and propose a fourth unit. The Ewekoro formation also overlies the Araromi formation in the eastern Dahomey basin being an extensive limestone body which is traceable over a distance of about 320Km from Ghana in the West, towards the eastern margin of the Dahomey basin in Nigeria. This type section is the limestone unit exposed in the Ewekoro quarry⁵⁰. The Ewekoro Formation at the type locality Ewekoro is composed of about 11m – 12m of limestone. It is sandy at the base grading downward into Abeokuta formation. The Ewekoro Formation is overlain of Phosphate Glauconitic grey shale²³. The limestone is classified (based on microfacies) into biomicrosparite, shelly biomicrites, algal biosparite and phosphate biomicrites in that stratigraphic order. Elueze and Nton⁴⁷ has reported that the limestone is associated with shallow marine origin due to abundance of coralline, algae, gastropods, pelecypods, echinoid fragments and other skeletal debris. It is Palaeocene in age. Overlying the Ewekoro formation is Akinbo formation and it comprises of shale, glauconitic rock bank, and gritty sand to pure grey and with little clay lenses of limestone sequence from Ewekoro formation grades literally into the Akinbo shale very close to the base⁴⁹. The claystones are concretionary and are predominantly kaolinite. The base is characterized by the presence of a glauconitic band with lenses of limestones⁴⁹⁻⁵¹. This unit is the lateral equivalent if the Imo formation in the southeastern Nigeria. Ogbe demonstrated that the shales on either side of Okitipupa Ridge differ markedly from each other in physical features⁴⁹. He then proposed the name Akinbo formation for the unit in the western side of the ridge, and selected the section exposed in the Ewekoro and Shagamu



quarries as the type locality. The age of the formation is Palaeocene to Eocene. Overlying the Akinbo formation in Imo group is the Oshosun formation. It is a sequence of mostly pale greenish-grey laminated phosphate marls, light grey white-purple clay and shale with interbeds of sandstones. The shale is thickly laminated and glauconitic. It also consists of claystone underlain by argillaceous limestone of phosphate and glauconitic materials in the lower part of the formation. According to Okosun⁵², the basal beds consist of the following facies; sandstones, mudstones, claystones, clay-shale or shale. This formation is phosphate-bearing deposits which are best developed near the Oshosun village by Russ in 1924²³. Eocene age has been assigned to this formation⁵³⁻⁵⁴. The sedimentation of the Oshosun formation was followed by a regression, which deposited the sandstone unit of Ilaro formation³⁵ conformably overlying the Oshosun formation and consists of gritty clay, gritty sand, massive and yellowish brown shale, poorly consolidated and cross-bedded sandstones, fine to coarse grained sand, bluish grained sand, bluish grey mudstones grading into glauconitic shale of the underlying Oshosun formation³⁵. The Benin formation is the youngest sedimentary unit in the eastern Dahomey Basin. This stratigraphic sequence is also known as coastal plain sands²³. It has a recent deposit called the tertiary alluvial deposit on it. It consists of soft, poorly sorted clayey sand and pebbly sands with lenses of clays and lignite. The sands are in parts cross-bedded and show transitional to continental characteristics. The age is from Oligocene to Recent. The thickness of the limestone is between 3m and 40m; the thickest being at Fashola community (38.3m) and the thinnest at Jaguna (1.6m). The range of overburden thickness is between 2m to 16m while the limestone thickness ranges between 1.5m to 38.2m. The reserve estimation was calculated to be 7.75×10^8 cubic meters and adjudged to be of economic value if exploited especially around Fashola town in Papalanto⁵⁵.

3. Materials and methods

3.1 Theoretical background

Electromagnetic method utilized the site response to the propagation of electromagnetic fields². Electromagnetic field comprised of an alternating electric intensity and magnetizing force. The speed at which EM can be made to propagate is much greater than the electrical method justifying the fact that electromagnetic method does not require contact with the ground. Therefore, an electromagnetic field can be developed by generating an alternating current through either a small coil comprising many turns of wire or a large loop of wire⁵⁶. The concept of electromagnetic field is better be defined in terms of four significant vector functions namely E, D, H and B where, E is the electrical field in V/m; D is the dielectric displacement in Coulomb/m²; H is the magnetic field intensity in A/m and B is the magnetic induction in Tesla^{2 & 33}. Maxwell's equations adopting Faraday's law Experimental evidence reveals that all electromagnetic phenomena are subject to the following four Maxwell equations.

$$\nabla E = - \frac{\partial B}{\partial t} \dots\dots\dots(1)^{2 \& 33}$$

Faraday's law shows us how a time varying magnetic field produces an electrical voltage.



• Maxwell's equations using Ampere's law

Ampere's law revealed how an electric current and/or a time varying electric field generate a magnetic field.

∇H = J + ∂D/∂t (2)^{2 & 33}

Maxwell's Equations infer that lines of magnetic induction are continuous and there are no presence not even a single magnetic poles.

div B = 0 (3)⁵⁷⁻⁵⁸

It also infers that electrical fields can begin and end on electrical charges.

div D = q(4)^{2, 33 & 58}

• Subsidiary equations and wave equation

By applying the following subsidiary equations,

D = εE, B = μH, J = σE (5)^{2, 33 & 58}

Where J = electrical current density in A/m²; q = electric charge in Coulomb/m³; ε = electrical permittivity; μ = magnetic permeability; σ = electrical conductivity⁶⁻⁷. From these four Maxwell equations the electromagnetic wave equation can hereby be derived^{2, 33 & 58}.

3.2 Primary and secondary fields

There is no significant difference between the fields propagated above the surface and the ones penetrated through the subsurface (only slight reduction in amplitude is recorded). If a conductive anomalous body is present, alternating currents (Eddy currents) are induced within the conductor by the magnetic component of the incident EM wave as displayed in Figure 7. The eddy currents generate their own secondary EM-field which travels to the receiver and the receiver equally detects the primary field which travels through the air². The resultant of the arrival of the primary and secondary field is authenticated and registered by the responds of the receiver². As a result of this field interaction, the measured response will differ both in phase and amplitude relative to the unmodulated primary field^{2, 33 & 58}. The detection of the presence of the encountered conductor as well as the necessary information on its geometry and electrical properties are revealed by these aforementioned differences between the transmitted and received electromagnetic fields. The depth of penetration of an electromagnetic field is dependent on the frequency as well as electrical conductivity of the medium through which propagation is made². Electromagnetic fields are therefore attenuated during their passage through the ground⁵⁹⁻⁶⁰. The amplitude of EM-radiation serves as a function of depth relative to its original amplitude A₀ is given as

A_d = A₀e⁻¹(6)^{2, 33 & 59}.

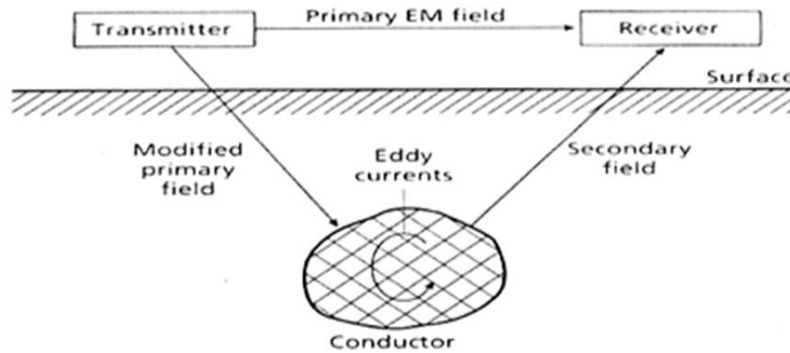


Figure 7. General principle of electromagnetic surveying²

The depth at which the amplitude of the field A_d is decreased by the factor e^{-1} compared with its surface amplitude A_0 is defined as the depth of penetration d given as

$$d = \frac{503.8}{\sqrt{\sigma f}} \dots\dots\dots (7)^{2, 33 \& 59}$$

Where d is in metres, the conductivity s of the ground is in $S m^{-1}$ and the frequency of the field is in Hz.

Just as the frequency of the electromagnetic field and the conductivity of the ground decrease, the depth of penetration thus increases². Therefore, equation (7) represents a theoretical relationship. Whereby the frequency used as a result of the EM survey can be tuned to a desired depth range in any particular medium. Empirically, an effective depth of penetration z_e can be defined as the depth as the maximum depth at which a conductor may lie and still produce a considerable electromagnetic anomaly as shown in equation 8.

$$z_e = \frac{10}{\sqrt{\sigma f}} \dots\dots\dots (8)^{2, 33 \& 59}$$

Penetration is dependent on factors such as the nature and magnitude of the effects of near-surface variations in conductivity, the geometry of the subsurface conductor and instrumental noise making this relationship an approximate one. Constraints are placed on the EM method due to the dependence of the depth of penetration on frequency. Very low frequencies are normally difficult to develop and measure and the maximum penetration attainable in the field is usually of the order of 500m⁵⁸⁻⁶². 10m spacing are $f = 10$ Hz, $d = 503$ m; $f = 100$ Hz, $d = 159$ m and $f = 1000$ Hz, $d = 50.3$ m; are examples of different Depths of penetration and their corresponding frequencies.

3.3 Principle of operation and interpretation technique of EM 34-3

The electromagnetic ground conductivity Survey Method utilized in this work is based on a well-established applied geophysical method. EM 34-3 terrain conductivity meter manufactured by Geonics Limited was obtained from the Department of Geosciences, University of Lagos, South-West Nigeria. A direct reading of the apparent conductivity (σa) of the ground in units of millimhos per metre (SI equivalent units are millisiemens per metre (mS/m) was provided by a change in conductivity of 5.0 mS/cm assumed to be measurable with the instrument. induction number has been defined as the ratio of the



intercoil spacing (s) divided by the skin depth (δ)³³. In FDEM method, a GEONICS EM-34 meter possesses separate coils that were connected by a reference cable which provided the basis of the system in lengths of 10m, 20m and 40 m long. The effective depths of investigations are 7.5 m (HD) and 15 m (VD); for a frequency of 6.4 KHz and separation of 10 m; for a separation of 20 m and frequency of 1.6 Hz, is obtained a depth investigation of 15 m (HD) and 30 m (VD); for the separation of 40 m and frequency of 0.4 Hz, the investigation⁵⁹⁻⁶³.

The instrument operates on the measurements at Low Induction Number providing a direct reading of the quadrature as the apparent conductivity in mS/m. The secondary magnetic field is a complicated function of the inter-coil spacing, (s), the operating frequency (f), and the ground conductivity (σ). However, the technical definition is stated as “operation at low values of induction number” the very simple function of these variables in secondary magnetic field is incorporated in the design of the EM 34-3²⁻³. The product of s and the skin depth d, known as the induction number, is far less than unity. Therefore, the ratio of the intercoil spacing (s) divided by the skin depth is known as the induction number B where the induction number is less than one, then the ratio of the secondary to the primary of magnetic fields at the receiver is directly proportional to apparent conductivity. The ratio of the secondary (H_s) to primary (H_p) magnetic fields at the receiver at low induction numbers ($B \ll 1$) is given by Ishola and Pieter et al.^{33 & 63}.

$$\frac{H_s}{H_p} = \frac{i\omega \mu\beta\sigma S^2}{4} \dots\dots\dots(9)$$

Equation (9) provided the apparent conductivity as recorded by the instrument².

$$\sigma = \frac{i\omega \mu\beta\sigma S^2}{4} \left(\frac{H_s}{H_p}\right) \dots\dots\dots (10)$$

where: H_s is the amplitude of the secondary electromagnetic field at the receiver coil; H_p represents the amplitude of the primary electromagnetic field at the receiver coil; ω is the angular frequency ($\omega = 2\pi f$); f is frequency (Hertz); μB is the magnetic permeability of vacuum or free space ($1.2566 \times 10^{-6} \text{ m kg C}^{-2}$); σ represents the measured ground conductivity (mho/m); s is the inter coil spacing (m) while the presence of $i = \sqrt{-1}$ depicts that the quadrature component is measured^{2 & 33}. Therefore, the ratio of H_s/H_p is proportional to the ground conductivity σ . Since depth d depends on the product of estimation of the maximum probable value of σ allows the selection of f such that the above condition of low induction number is satisfied. The depth of penetration is independent of the conductivity distribution of the subsurface but depends upon σ ⁶⁴. Measurements taken at low induction number thus provide an apparent σ_a given by Ishola and Oyegoke et al.^{33 & 65}.

$$\sigma_n = \frac{1}{\rho_a} = \left(\frac{4}{\omega \mu_0 S^2}\right) \left(\frac{H_s}{H_p}\right) q \dots\dots\dots(11)$$

The above relationship enables the construction of electromagnetic instruments that procures a direct reading of ground conductivity down to predetermined depth. The measuring system is also predesigned so as to ensure that with the selection of frequency f, for a given inter-coil separation (s), a designed response of H_p for a given transmitter, the only unknown H_s which is measured by the instrument with the subscript q denoting the



quadrature phase³³. Therefore, to measure the terrain conductivity in the field the search coil is either held horizontally (measurement in vertical dipole moment) or vertically (horizontal dipole mode). The results obtained from this field operations are generally displayed in the form of conductivity profiles. Today, inductive electromagnetic survey methods are widely harnessed to map near-surface geology by mapping variations in the electrical conductivity of the ground. These variations are generally functions of certain factors like changes in soil structure, clay content, porosity, resistivity of the soil water, and degree of water- saturation in the soil^{33 & 59}.

3.4 Field data acquisition

3.4.1 Electromagnetic ground conductivity survey

In Papalanto study locations, five traverses were created with the station intervals of 500m. The length of each traverse ranged from 150m to 200m. Three traverses were established in the West and the East trending the North-South direction and two traverses to the North and South in the NW-SE direction. On each traverse, the first Profile was created in the W-E direction and second Profile created in the N-S direction with both Profiles having a Profile length of 200m. Electromagnetic profiles were selectively created in autonomous communities within Papalanto District for the primary purpose of outlining shallow conductive hydrogeological structures that could possibly be connected water circulation of the local hydrogeological units of the area^{33 & 66}. The outcome of this investigation would be highly significant in in the future delimitation of a protected zone from contaminant infiltration²³. The investigated area has been a natural environment engaged with industrial operations in cement production, loading and transportation of cements and marketing of cement products; agricultural activities in sugarcane farming and food crops, artisanal works and numerous business activities. The myriads of these activities have led to the increase in human and biological population which in turn increase the demands for more water supplies and has consequently necessitated the need for preliminary investigation to meet the current challenge. The data was acquired along 5 North-South profiles with 2 electromagnetic measurements made along each traverse. The lengths of each traverse varied between 150 m and 200 m to show conductivity changes with distance and depth for each location with an intercoil spacing of 10m, 20m, and 40 m. The distance between the beginnings of each measurement points to the beginning of another measurement point was 500 m. At each site two measurements were made using both horizontal and vertical dipole mode. The main conductivity contrasts, can now be interpreted roughly as the shallow expression of fractures within the sedimentary filling of the hydrogeological structure of the area^{23 & 66-67}.

The procedure of the field operation involves An AC electric current is applied to a transmitter coil, the transmitter Tx is energised with an alternating current at a specific frequency, audio frequencies (100 - 5000 Hz), depth is 30 m (HD) and 60 m (VD)⁵⁹. Usually three frequencies are used seeking for different investigation depths; this generates a primary electromagnetic (EM) field in the coil. The primary time varying magnetic field generated from the transmitter and arising from this effect induces small current in the subsurface which is assumed uniform. These currents generate a secondary magnetic field,



(Hs) which is sensed or detected, together with the primary field, (Hp) by the receiver coil, in the form of total field (HT)²; both magnetic fields are sensed by the receiver coil and a reading of apparent conductivity is given. The value of apparent conductivity depends on many factors. These are porosity, conductivity of pore fluid, pore surface area, degree of saturation of subsurface sediments, temperature, and (when present) clay content; the transmitter and receiver, are located vertically upward with the axis of the coil being horizontal to the subsurface; in the second mode (vertical magnetic dipole mode, VDM) the coils were placed lying flat horizontally with axis of the coil being vertical to the subsurface. Profiles with 10m, 20m and 40m of separation between transmitter and receiver were performed, using 6.4 KHz, 1.6 KHz and 0.4 KHz respectively in order to probe at varying depth and resolution; In either of the modes, the transmitter operator stops at the measurement station, the receiver operator (the researcher) then moves the receiver coil backwards or forwards until the meter indicates correct inter-coil spacing. At this point the receiver operator reads the terrain conductivity from a second meter. The procedure takes about 10 - 20 seconds. The measurement is first carried out in the horizontal coil orientation (vertical dipole mode) and later the corresponding vertical coil orientation (horizontal dipole mode) along the same profile. The vertical coil orientation gives information about the shallow subsurface while the horizontal coil orientation penetrates deeper into the subsurface²; the apparent conductivity readings were taken at each station along the traverses and recorded in mmho/m (milli mho per metre) while other features and artefacts that could alter or affect the reading such as metals, vehicles and so on were noted against the station.

3.4.2 Collection of subsurface water samples

Water samples were collected from existing and functional 25 boreholes and 25 hand-dug wells at different and strategic sampling points within Wasinmi communities. Most of the borehole water samples were obtained from private boreholes which serve as a source of household water supply, and also serve as a good source of livelihood for the families through sales to village buyers; a few others were a public borehole situated at a marketplace in the study area. Physic-chemical analyses were carried out principally to identify and quantify the physical properties and chemical constituents of collected water samples. This includes pH, cations, anions, trace elements and so on. Determination of a water quality status is often realizable by extensive utilization of water chemistry analysis due to the possible interaction it has with its environment, which is predominantly the groundwork of studies of water quality, pollution, hydrology and geothermal waters.

Samples collected were immediately stored in clean air-tight, leak-proof plastic bottles and labelled appropriately while 1 ml concentrated HNO₃ per litre of sample was used for the preservation of the samples for metals. All water samples were consequently stored in an insulated cooler containing ice (maintained at 4 °C) and transported to the laboratory. Physic-chemical properties namely Electrical Conductivity (EC), Total Dissolved Solids (TDS), Temperature, Dissolved Oxygen (DO) and pH were determined in-situ using Hannah Combo TDS/pH/EC/Temperature meter series multi-parameters (model HI991300), whereas Hannah (model HI9147) equipment was used for DO for the purpose of ensuring that they are not subjected to physical alteration such as temperature while JYD-IA DO meter was later used to measure BOD₅ after the expiration of five days

incubation. Other physicochemical parameters, bacteriological evaluation and metals levels were measured in the laboratory using standard procedures⁶⁸⁻⁶⁹.

A very neat container (or that which the water samples to be tested has been rinsed with) was used for collection with the sensor on the meter dipped into it while the metre displayed the values it measured on a digital screen for recording. The same procedures were consecutively repeated for other water samples. These measured parameters were compared with WHO and other standard specifications. The geographical coordinates of sample points were also taken with GPS meter and their locations were indicated on the data acquisition map (Figure 4). Samples specifically meant for anion determination were collected in 500 ml bottles, unfiltered and unpreserved, and later stored below 8 °C prior to analysis while the third sampling bottles were used for the determination of microbial loads. Ion Chromatography (IC) was used for the analysis of anions while Nitrate, Phosphates, Bicarbonate, Chloride and Sulphate were measured after chromatography separation utilizing conductivity detectors. Inductively Coupled Mass Spectrometer (ICP-MS) and Inductively Coupled Optical Emission Spectrometry (ICP-OES) were used Heavy metals and trace metals detection. Water samples were filtered to less than 0.45 µm using a Pall Corporation GN-6 metrical sterilised membrane to improve accuracy and prevent cloudiness of the water while ensuring that the minute particles of clay sizes were removed before analysis. When lower levels of contamination were present, ICP-MS provided lower detection limits for measurement while ICP-OES was useful for higher concentrations, such as cases of high levels of contamination. Furthermore, cell-based ICP-MS serves as a very veritable integration tool for the removal of possible interferences that might prevent the detection of contamination at its emergence. These analyses were ultimately carried out in order to study the concentration levels of each analyzed parameters and variation of geochemical concentrations in water samples have been affected by the activities in the study area. The depth measurements of the investigated boreholes and existing hand-dug wells were determined using Heroin Water level meter. All the laboratory sample analyses were conducted in the Central Laboratory, Institute of Agricultural Research and Training (IART), Obafemi Awolowo University, Moor Plantation Ibadan Campus.

3.5 Data processing and interpretation

3.5.1 Electromagnetic ground conductivity survey data

The acquired data were qualitatively checked by observing if negative apparent conductivity was recorded. Field note was used particularly as a guide to identify if certain anomalously high apparent conductivity values due to artefacts were present. The precautionary measures taken in the field among others using EM-34 transverses were restricted to areas far away from the overhead and underground utility cables and buried iron pipelines⁶⁶⁻⁶⁷. The apparent conductivity reading of the horizontal dipole orientation on each traverse was plotted against station midpoint. This was also carried out separately for the vertical dipole orientation. The crossplots of apparent conductivity on the different spacing enabled a view of how the conductivity varies with depth. Qualitative analysis and interpretation were further carried out on the plotted data.

3.5.2 Analyses of water sample data



Descriptive and Multivariate analyses (Mean, Standard Deviation, and Correlation) were performed on a series of the water quality data acquired from the study area. The adherence to the analytical quality control was ensured through procedural blank measurements, duplicate analyses of water samples and standardization of analytical laboratory devices³³. Box-plot of the Physic-chemical and Elemental concentrations were built using the mean concentrations with 95% confidence interval as the median and the quantil values defined at 25% and 75% of the total values where the variation of the defined intervals by the two methods (mean and median) were analyzed using Sigma plot Software in order to give detailed visual information of the hydrogeochemical parameters as well as their degree of concentrations from Wells and Boreholes whose outcome is likely to help in reducing the negative effects of these parameters in human health.

4. Results

4.1 Electromagnetic profiling survey results of Ewekoro

The electromagnetic profiling data are presented as plots of conductivity (in mmho/m) against station intervals (in m). Typical EM profiles from the study area are shown in Figures 7 through 16 while the characteristics of the true conductivity are displayed in Table 1.

Table 1. The true conductivity in Papalanto

Papalanto EM Profiles	Delineated layers	True Conductivity HDM (mmho/m)	True Conductivity VDM (mmho/m)	Depth of Investigation (HDM) (m)	Depth of Investigation (VDM) (m)
EMPAP1	1 st Layer	118	133.33	9	14
	2 nd Layer	138	134.31	-	-
EMPAP2	1 st Layer	122	116	4.3	14
	2 nd Layer	127	121.88	-	-
EMPAP3	1 st Layer	146	90	2	9.8
	2 nd Layer	151.2	100	-	-
EMPAP4	1 st Layer	150.59	86.29	7.8	11
	2 nd Layer	158.92	91.11	-	-
EMPAP5	1 st Layer	131.15	87.32	8.9	16
	2 nd Layer	1141.92	94.55	-	-
EMPAP6	1 st Layer	138	78.9	2	17
	2 nd Layer	140.4	84.55	-	-
EMPAP7	1 st Layer	167.48	96.78	7.8	9.2
	2 nd Layer	176.34	98.18	-	-
EMPAP8	1 st Layer	143.32	98.6	8.4	6.5
	2 nd Layer	182.22	99.6	-	-
EMPAP9	1 st Layer	121.13	106.92	3.1	10
	2 nd Layer	123.99	121.96	-	-
EMPAP10	1 st Layer	130	115.88	33	10.4
	2 nd Layer	206	122.13	-	-

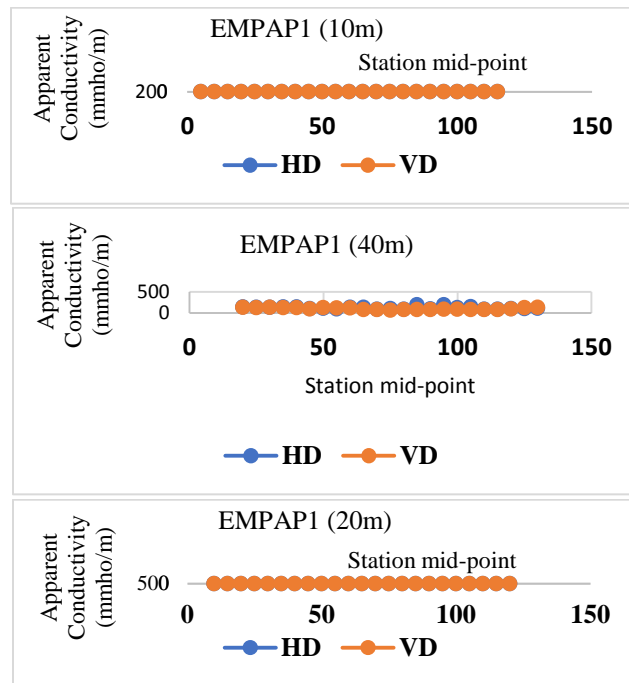


Figure 8. Plot and values of apparent and real conductivity of horizontal dipole orientations along the Papalanto Traverse 1 (Profile 1)

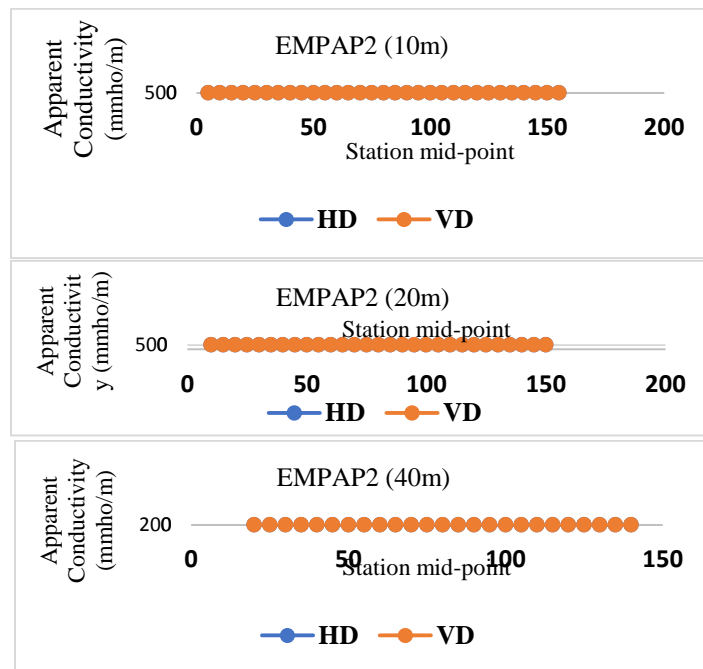


Figure 9. Plot and values of apparent and real conductivity of horizontal dipole orientations along the Papalanto Traverse 1 (Profile 2)

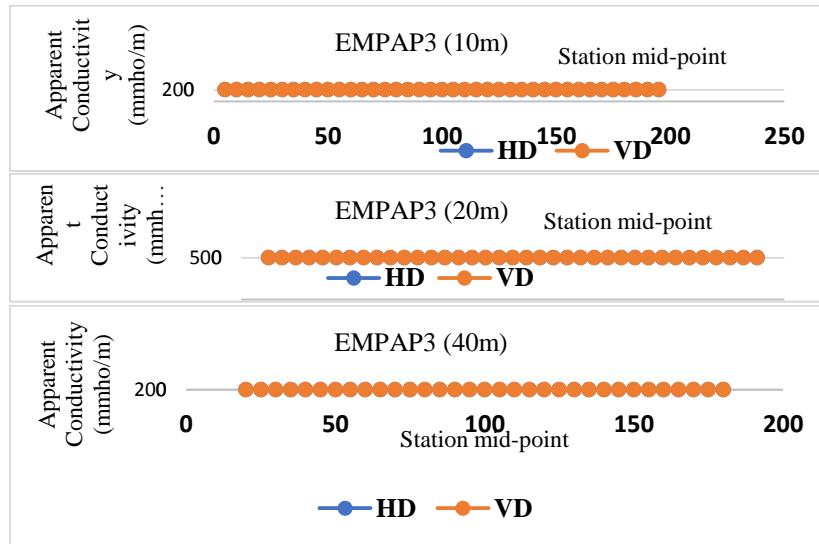


Figure 10. Plot and values of apparent and real conductivity of horizontal dipole orientations along the Papalanto Traverse 2 (Profile 3)

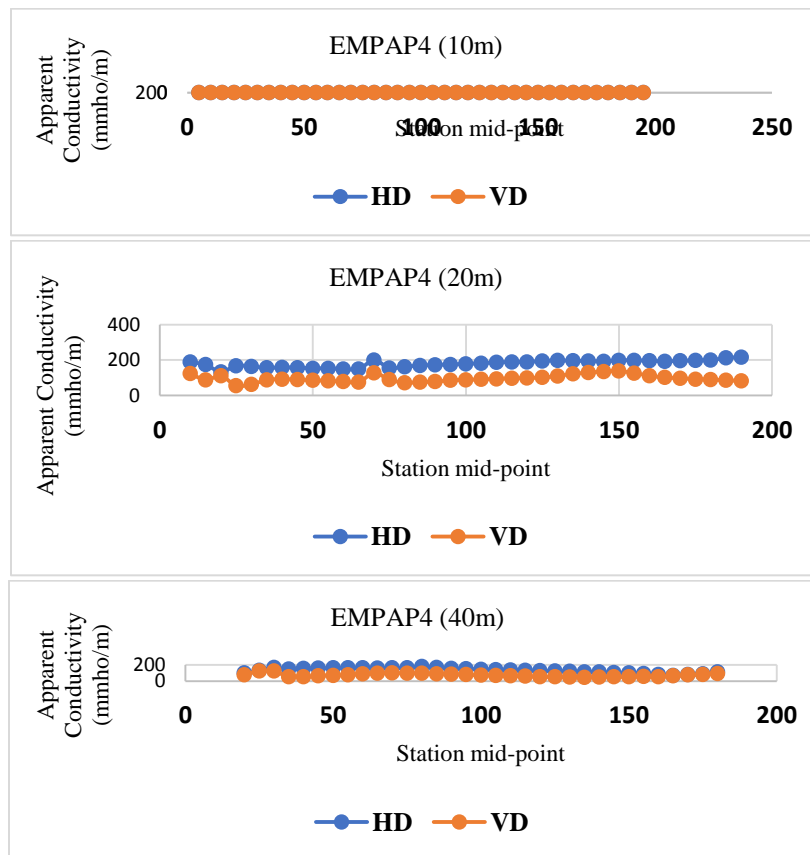


Figure 11. Plot and values of apparent and real conductivity of horizontal dipole orientations along the Papalanto Traverse 2 (Profile 4)

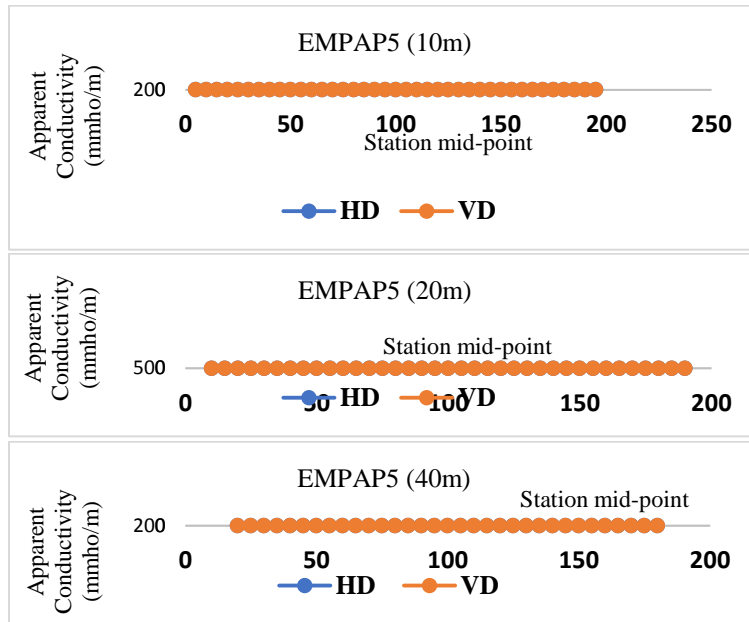


Figure 12. Plot and values of apparent and real conductivity of horizontal dipole orientations along the Papalanto Traverse 3 (Profile 5)

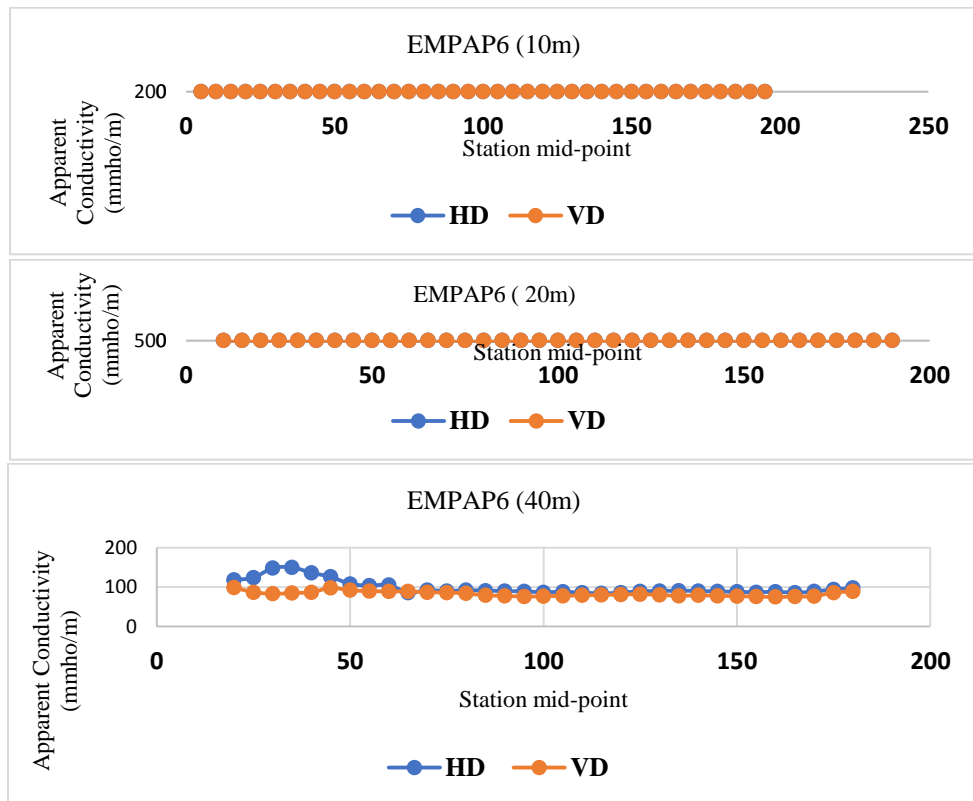


Figure 13. Plot and values of apparent and real conductivity of horizontal dipole orientations along the Papalanto Traverse 3 (Profile 6)

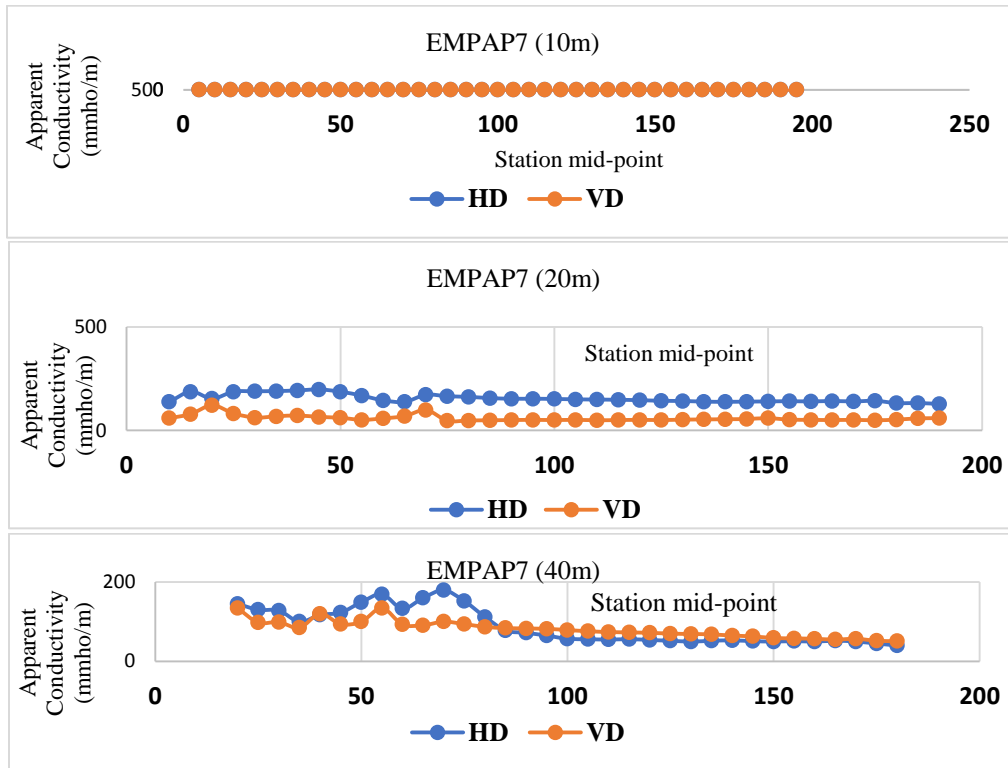


Figure 14. Plot and values of apparent and real conductivity of horizontal dipole orientations along the Papalanto Traverse 4 (Profile 7)

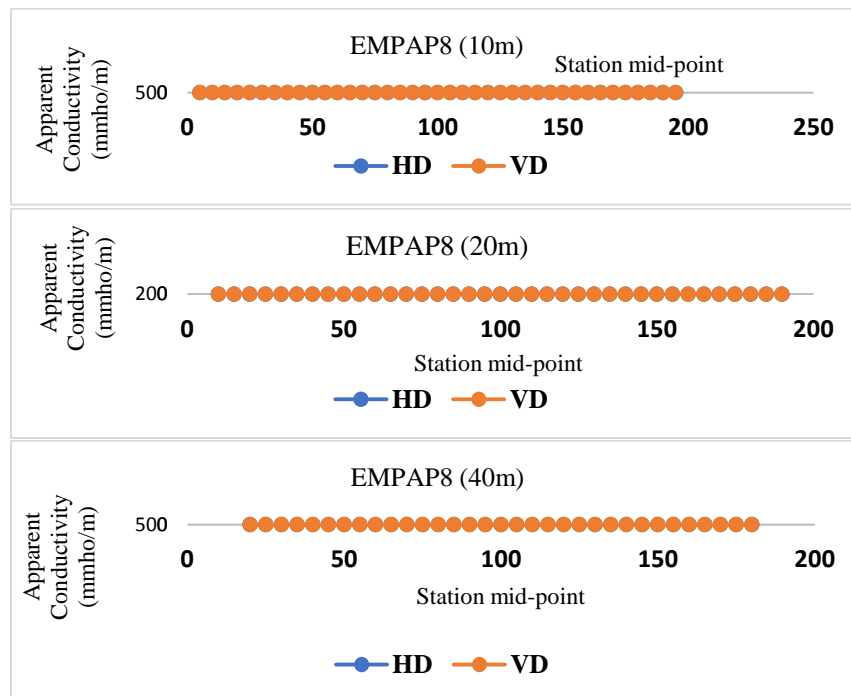


Figure 15. Plot and values of apparent and real conductivity of horizontal dipole orientations along the Papalanto Traverse 4 (Profile 8)

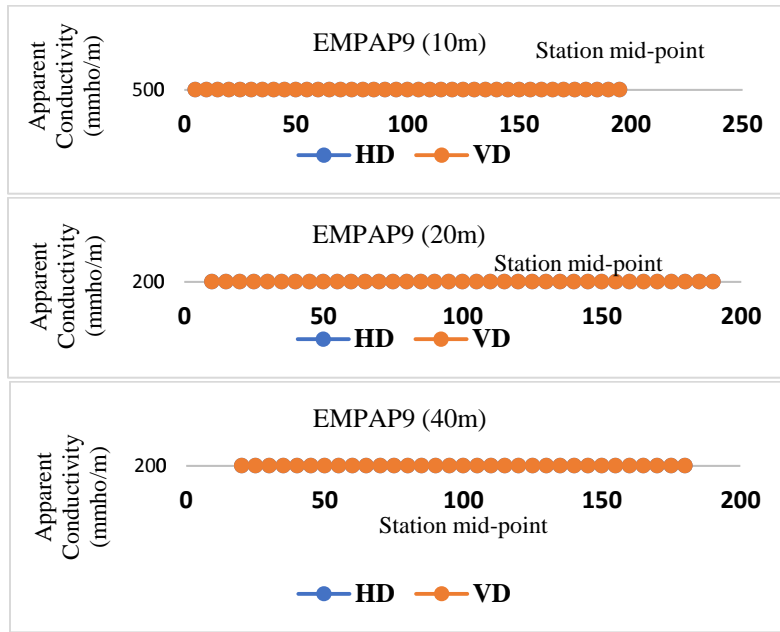


Figure 16. Plot and values of apparent and real conductivity of horizontal dipole orientations along the Papalanto Traverse 5 (Profile 9)

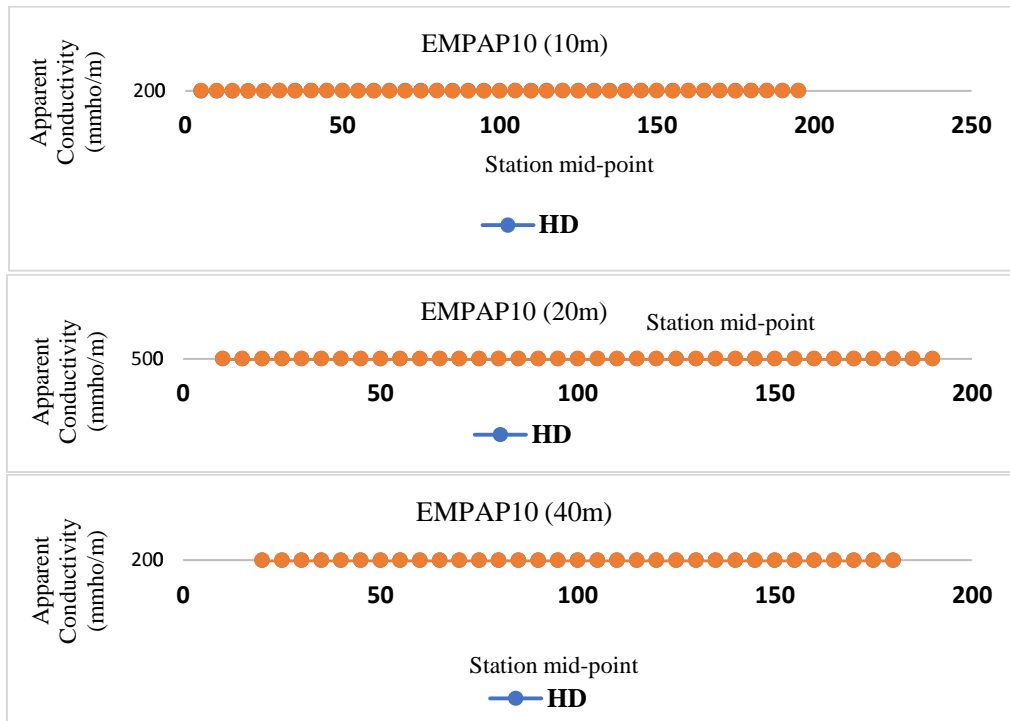


Figure 17. Plot and values of apparent and real conductivity of horizontal dipole orientations along the Papalanto Traverse 5 (Profile 10)

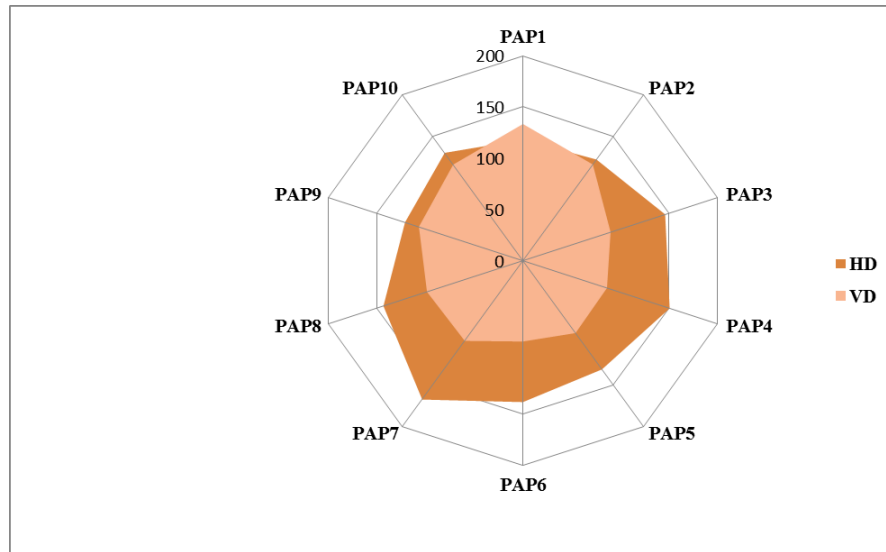


Figure 18. Distribution of Papalanto subsurface conductivity profile for the 1st layer

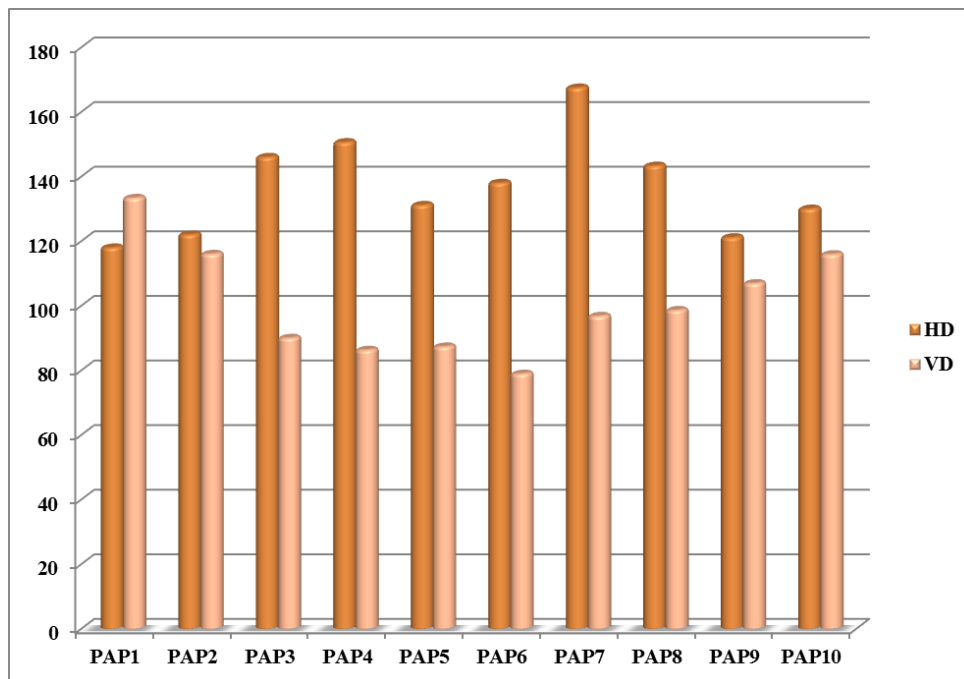


Figure 19. Papalanto subsurface conductivity profile variation for the 1st layer

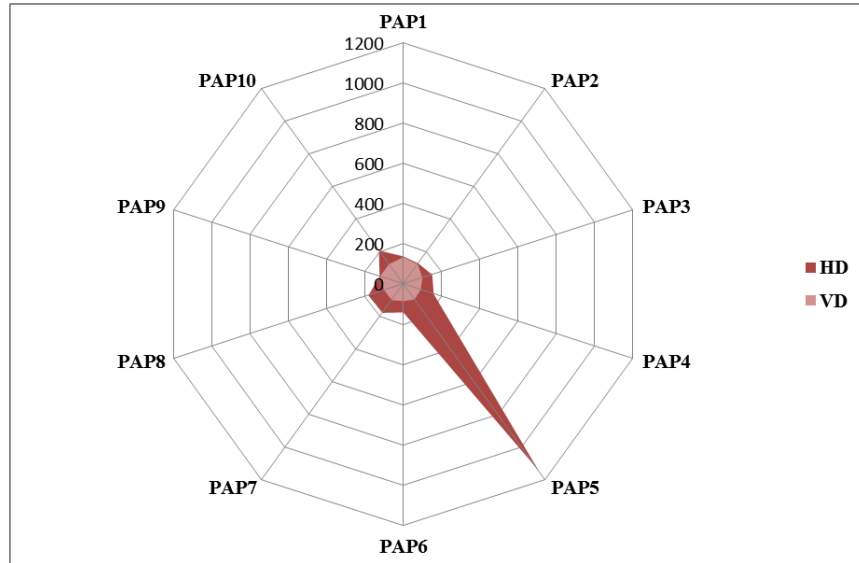


Figure 20. Distribution of Papalanto subsurface conductivity Profile for the 2nd layer

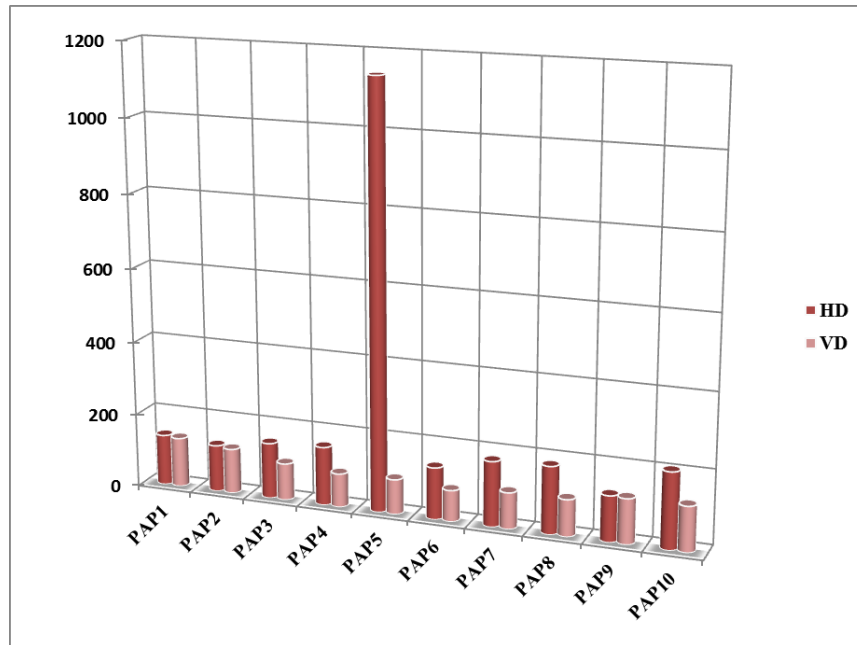


Figure 21. Papalanto subsurface conductivity profile variation for the 2nd layer

4.2 Subsurface water quality results

The results of the analyzed Concentrations of Elemental and Physic-Chemical Parameters observed in wells and boreholes of the study areas using confidence intervals and quantil (box-plots) are displayed in Figures 21 through 24.

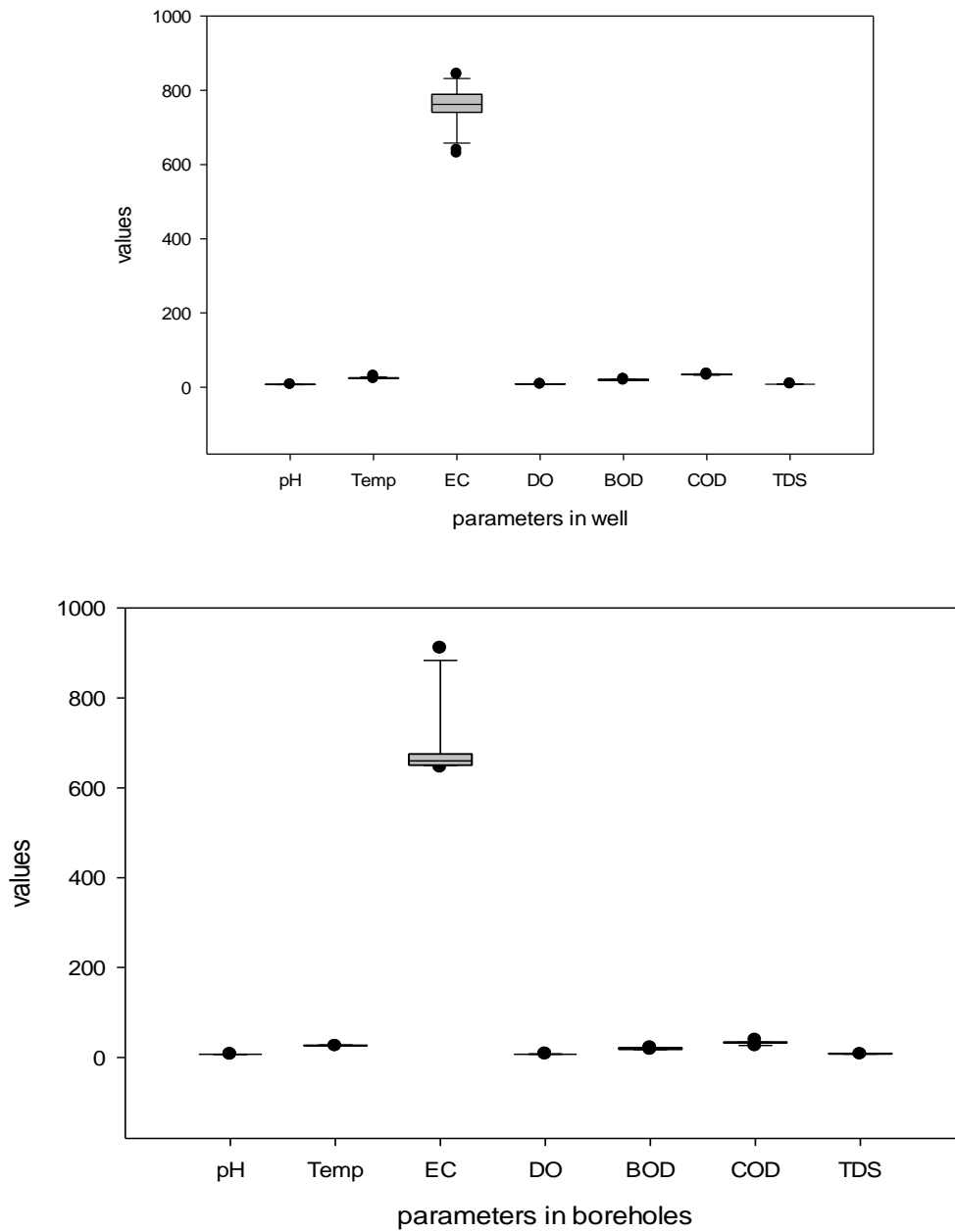


Figure 22. Comparative display of physicochemical parameters in groundwater from the hand-dug wells and boreholes of Papalanto

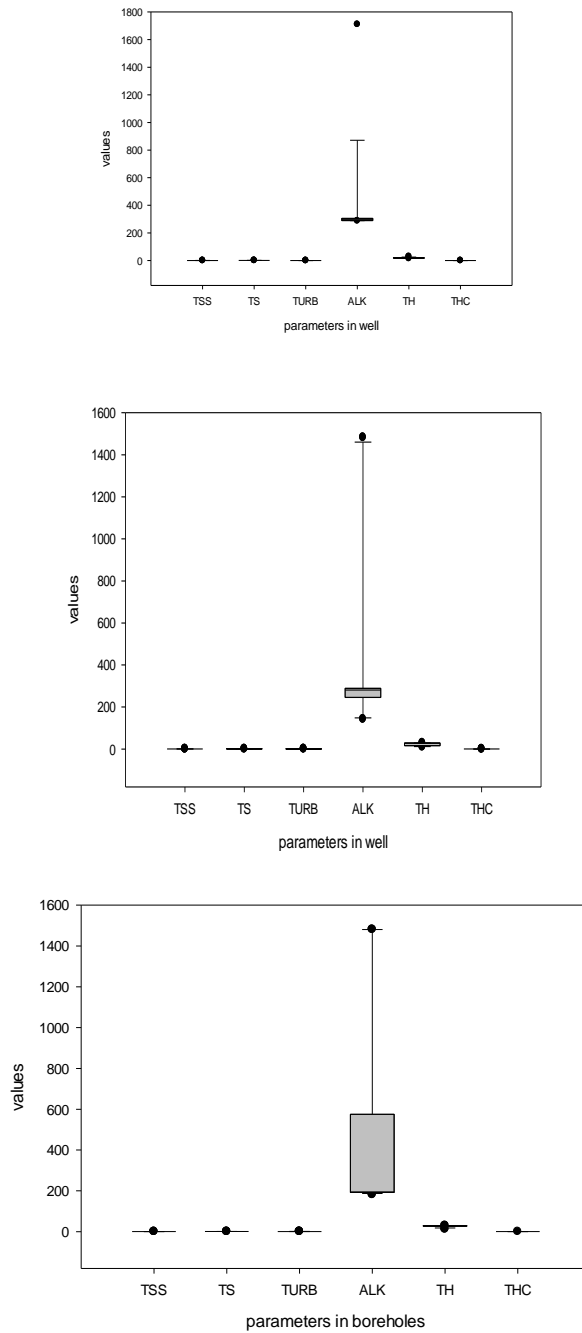


Figure 23. Comparative display of physicochemical parameters in groundwater from the hand-dug wells and boreholes of Papalanto

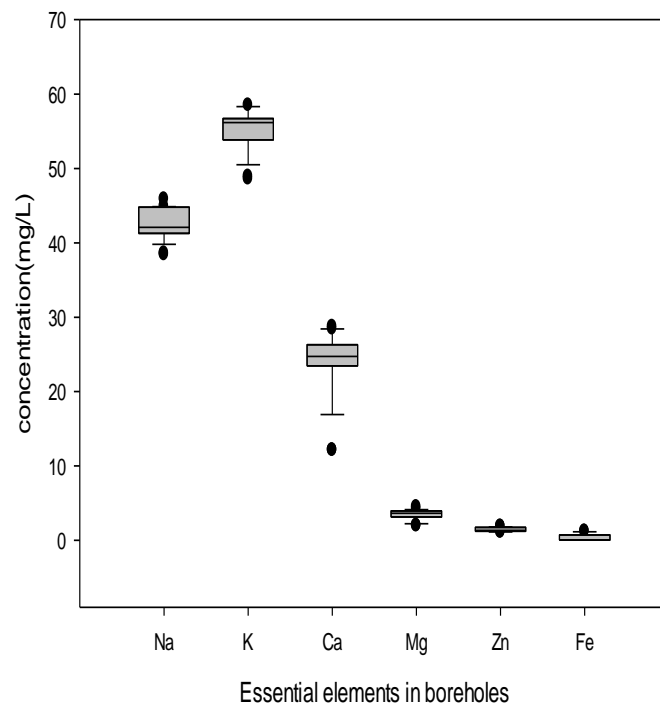
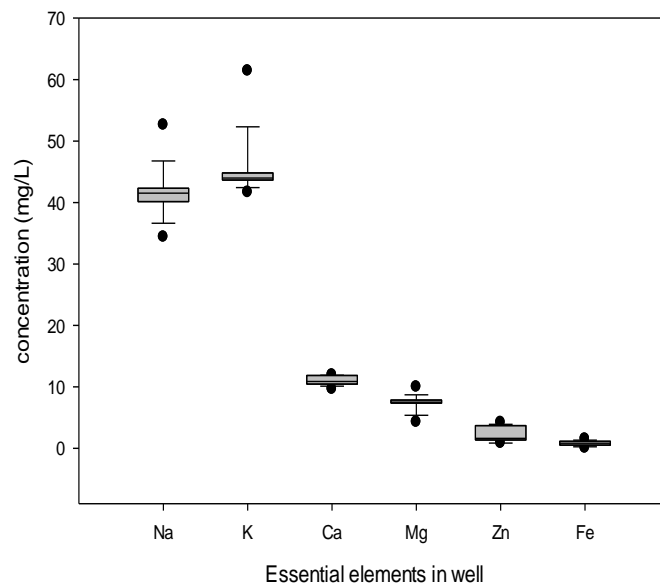


Figure 24. Comparative display of essential elements in groundwater from the wells and boreholes of Papalanto

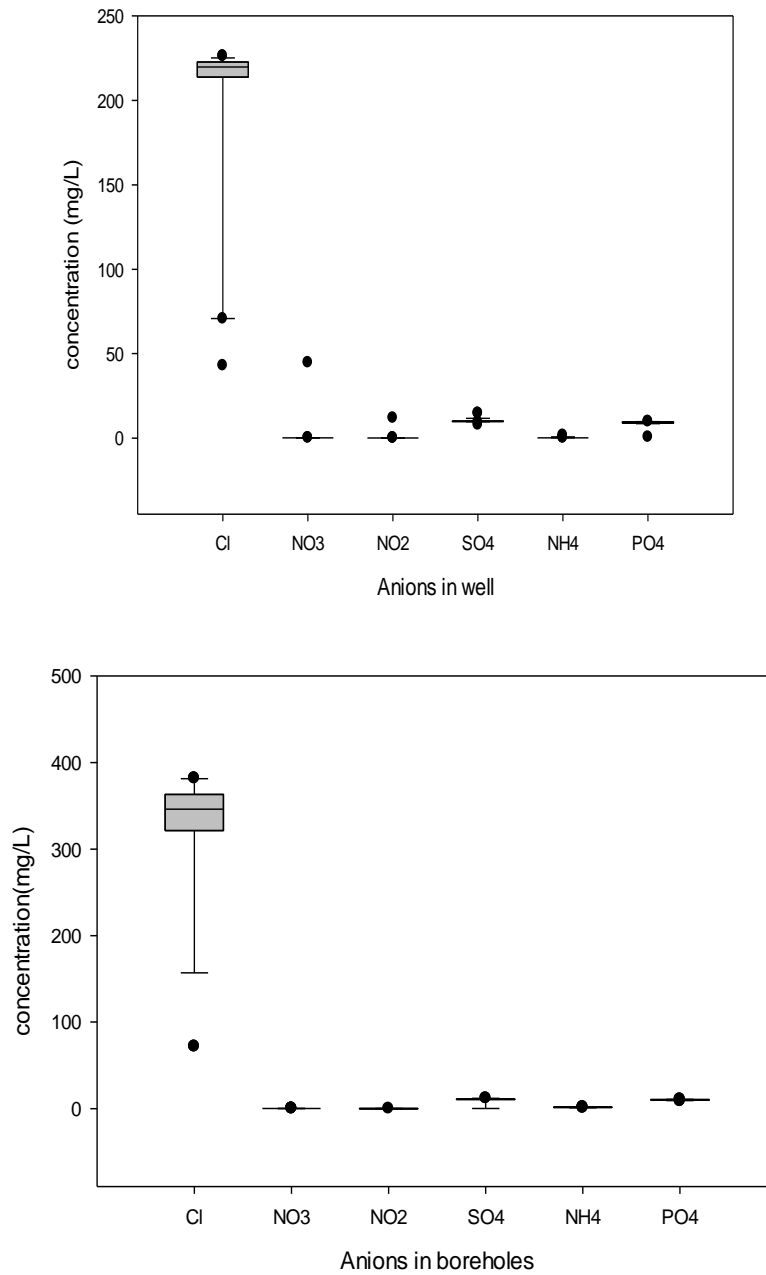


Figure 25: Comparative display concentration of Anions in groundwater from the wells and boreholes of Papalanto

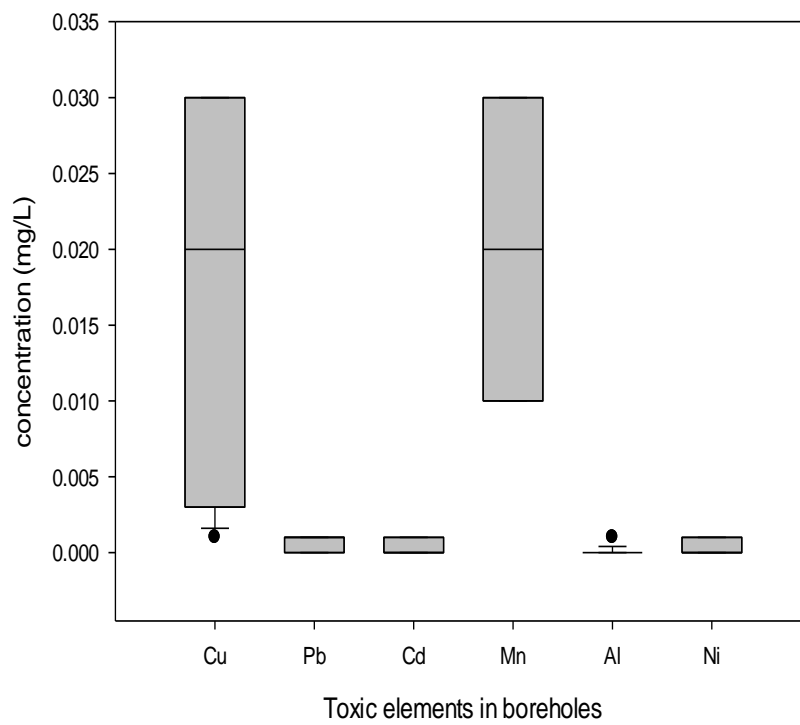
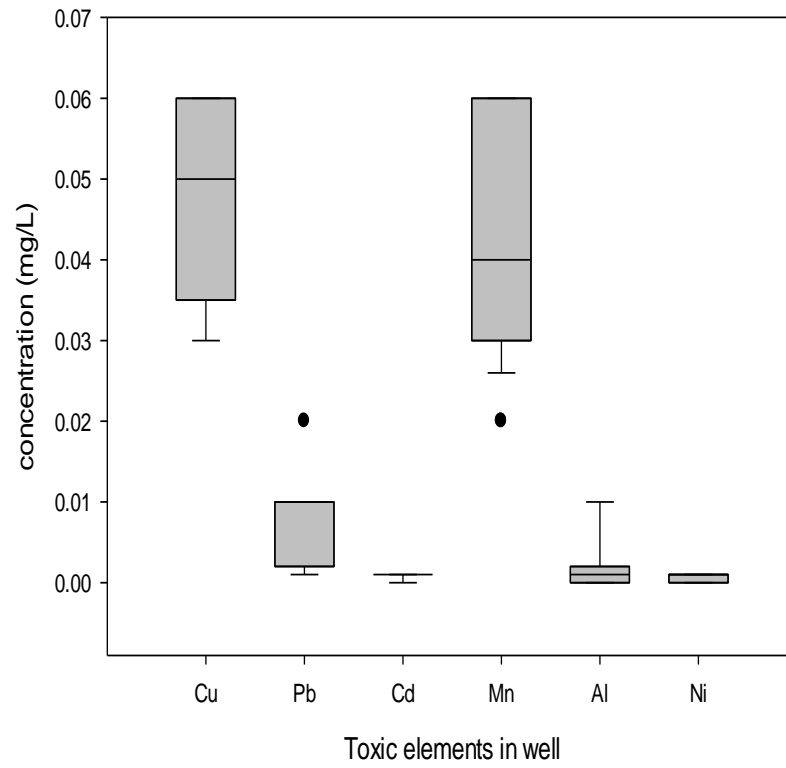


Figure 26. Toxic elements concentration in groundwater from the wells and boreholes of Papalanto showing (Cu^{2+} , Pb^{2+} , Mn^{2+} , Ni and Al^{3+})

5. Discussion

5.1 Electromagnetic ground-conductivity survey

The Apparent Conductivity Profiles (EMPAP1 to EMPAP2) along the traverses conducted in the West and across the NW-SE direction of Papalanto study area at 10m, 20m and 40m are displayed in Figures 7 and 8. The traverse displays appreciable variation in conductivity while locations of few recognizable positive peaks and broad anomalies which could be as a result of weathering of the subsurface geological horizon were delineated. These locations could be inferred as zones of interest for groundwater exploitation and consequently described as weathered to highly weathered/fractured zones and may serve as suitable auriferous regions for water supply needs of the study area⁶⁷. The observed varying degrees of conductivity values were delineated as represented in the plots with the most conductive area and the corresponding least conductive area respectively inferred to be conductive and resistive zones. The calculated true conductivity values for the first and second layer with their corresponding depth values were recorded for both horizontal and vertical dipole orientations in all the traverses. The highest true conductivity value of 1141.92 mS/m was recorded by Horizontal Dipole in the 2nd layer for EMPAP5 while the lowest true conductivity value of 78.9 mS/m was recorded by Vertical Dipole in the 1st layer for EMPAP6 (Figures 11 and 12).

The EM anomalies vary significantly; some are sharp while others are broad⁷⁰. The traverse displays appreciable variation in conductivity while the areas where there are few recognizable positive peaks and broad anomalies were delineated against their conductivity values. Zones with peak positive vertical dipole anomalies are inferred conductive (fractured zones) typical of water-filled fissures⁷¹, or effect of appreciable weathering²; the higher the peak of the signature, the deeper the level of the rock fracture⁷². These zones are considered priority areas for depth sounding. These locations could be inferred as zones of interests in groundwater exploitation and consequently described as weathered to highly weathered/fractured zones which may serve as suitable auriferous regions for water supply needs of the study area⁶⁷. In this traverse, locations of fewer or no observable linear spread and few haphazard variations were observed signifying the inhomogeneity of the study area despite the slight insignificant correlation between the horizontal and vertical dipole orientations. This is typically seen in EMPAP7, EMPAP8 and EMPAP10. The lowest and highest conductivity values of 86.29 and 1141.92 mmho/m were respectively recorded for both the vertical dipole and horizontal dipole moments (Figures 13, 14 and 16). The traverse displays significant variation in conductivity except at a distance of about 10m to 50m and 50m to 100m in Profile EMPAP7 and 10m to 70m and 100m to 200m in Profile EMPAP8 where there are few observable positive peaks and broad anomalies of 205mmho/m, 198mmho/m, 179mmho/m, 199mmho/m, 172mmho/m and 190mmho/m. The observed varying degrees of conductivity values were delineated as represented in the plots with the most conductive area having a conductivity value of 205mmho/m and the least conductivity area having a conductivity value of 40mmho/m respectively inferred to be conductive and resistive zone. Consequently, Vertical Electric Sounding should be conducted in Profile EMPAP7 and EMPAP8. The traverse displays significant variation in conductivity except at a distance of about 10m to 90m in Profile EMPAP9 and 50m to

150m in Profile EMPAP10 where there are few observable positive peaks and broad anomalies of about 198mmho/m, 169mmho/m, 137mmho/m, 189mmho/m, 222mmho/m and 162mmho/m which could be as a result of the weathering of the subsurface geologic structures in the study locations.

The observed varying degrees of conductivity values were delineated as represented in the plots with the most conductive area having a conductivity value of 222mmho/m and the least conductive area having a conductivity value of 45mmho/m respectively inferred as conductive and resistive zones; these are appreciable prospects for groundwater exploration. Consequently, other groundwater investigation techniques like Vertical Electric Sounding should be carried out in Profile EMPAP9 and EMPAP10. Varying high conductivity value range 64mmho/m to 198mmho/m, 45mmho/m to 169mmho/m and 45mmho/m to 137mmho/m were respectively recorded for 10m, 20m and 40m dipole spacing in a respective order obtained from the horizontal and vertical dipole orientations in the Electromagnetic Profiling of EMPAP9 while a conductivity range of values of 68 mmho/m to 189mmho/m, 55mmho/m to 222mmho/m, 52mmho/m to 162mmho/m were equally recorded in increasing order of 10m, 20m and 40m dipole separations observed on the horizontal and vertical dipole orientations on the Electromagnetic Profiling of EMPAP10 in a respective order of varying investigation depth and resolution along the same traverse EMT₅. The high conductivity observed on both Profiles (EMPAP9 and EMPAP10) is indicative of probable invasions of the subsurface by the contaminant plumes; this contaminant plume is related to leachates from the exotic materials and decaying wastes from the surface percolating the subsurface through the porous and permeable layers of overlying rock thereby migrating its ways down to the subsurface. The results of the horizontal and vertical dipole orientations on both Profiles are strongly correlated with few sinusoidal peaks and haphazard variation with high amplitude peak points are suggesting heterogeneity of the subsurface area under investigation. The Profiles are suggestive of the subsurface being polluted to a reasonable level of influence of the contaminant seepages which may possibly degrade the groundwater quality of the investigated locations. The distribution of Papalanto subsurface conductivity Profiles and their corresponding conductivity variation in each profile are displayed in Figures 17 and 18 for the first layer and Figures 19 and 20 for the second layer.

5.2 Water quality

Electrical Conductivity (EC) and Alkalinity (ALK) were generally prominent in all the tested Physic-chemical parameters with EC higher in wells than in boreholes with ALK displayed higher concentrations in Boreholes than in wells (Figures 21a and 21b). In all the tested Essential elements, Na⁺ and K⁺ concentrations were generally much more prominent in both hand-dug wells and Boreholes in all the investigated area slightly lower in hand-dug wells and boreholes in Ewekoro and Papalanto (Figure 22). In all the analyzed radicals notably anions, Cl⁻ concentrations were found to be generally much more prominent in both the Wells and Boreholes of all the investigated areas followed by SO₄²⁻. Cl⁻ and SO₄²⁻ were lower in hand-dug wells than in boreholes in Papalanto except for SO₄²⁻ that exhibited relatively similar concentrations in both Wells and Boreholes (Figure 23). Cu²⁺, Pb²⁺, Mn²⁺ and Al³⁺ sometimes Ni concentrations were prominent in all the tested Potential Toxic Elements. Cu²⁺, Pb²⁺, Mn²⁺, Ni and Al³⁺ were higher in Wells than in Boreholes. Cu²⁺ and

Mn^{2+} concentrations were higher in Wells than in Boreholes. The high concentration Pb^{2+} and Cu^{2+} in the study area could be as a result of the use of leaded petrol in cars, generators because some of the wells are located by the roadside and around the farm settlement and also because of the oil spillage around the welding and mechanic workshop very close to the well notably in Olapeleke in Itori and Shodeji in Wasinmi and Mokoloki road along Papalanto; this hydrocarbon contains lead and copper as additives with greater chances in oil spillage. The lower level of Nickel could be as a result of the absence of igneous rock in the study area (Figure 23).

The higher concentration of both the Physic-chemical and Elemental parameters in boreholes can be attributed to difference in depths as most of them were mobilized from the rocks or nearby river. Seepage of ocean or river water into groundwater has been recognized as an important pathway of some terrestrial chemicals into groundwater. However, the interaction of groundwater and ocean can equally introduce chemicals into the oceans and vice-versa⁷³ while the higher concentrations observed in Wells could be as a result of input from anthropogenic sources rather than weathered rocks. Most of the physico-chemical parameters were higher in wells than in boreholes (Figures 21a and 21b). Boreholes are generally covered while wells are often exposed which makes the water in them susceptible to being polluted easily compared to the borehole water sources. Concentrations of Fe in Ewekoro groundwater could occur as results from the presence of Clay deposits in the area and possible leaching of metallic waste into the groundwater system. Also, the latter may be due to the dissolution of Fe-hydroxides under reducing condition. Fe content in groundwater diminishes under oxidizing conditions via precipitation and subsequent filtration of Fe-hydroxides during ground-water flow⁷⁴. Conversely, Fe contents in groundwater are elevated by decomposition of Fe- hydroxides⁷⁵. The existing hand-dug wells are relatively shallow and susceptible to contaminant loads migrating from the surface. These groundwater sources are invariably unfit for human consumption. Therefore, a need for the existence of a local and national statutory unit charged with responsibility for continuous monitoring of water bodies, sensitization and education of the rural populace in Wasinmi on the adverse health implications of the invasion of toxic materials and other pollutants in their water supply sources.

6. Conclusions

Geophysical survey involving electromagnetic profiling carried out in Papalanto Districts provided preliminary information on subsurface conductivity variation for detection of possible fracture in a typical sedimentary section of South-West Nigeria. Interpretation of the EM profiles identified some conductive zones that serve as priority location for depth for further subsurface investigation and consequent drilling for groundwater sources. The varying calculated true conductivity values were consequently recorded with the corresponding depth values in all the investigated profiles in the study area both for the horizontal and vertical dipole orientations for the first layer and the second layer. 1141.92 mmho/m was recorded as the highest true conductivity value for the Horizontal Dipole in the second layer; this occurred in Profile EMPAP5 while the highest true conductivity value for the Vertical Dipole in the first layer was 134.31 mmho/m which occurred in Profile EMPAP1. The appreciable variation in conductivity with recognizable positive

peaks and broad bowl shaped anomalies observed in the high conductivities in both orientations HDM and VDM orientations is a resultant effects of weathering of the subsurface geological horizon in the study locations and are possible indications of the vulnerability of its subsurface hydrogeological environment to invasion of contaminant seepages and consequent possible pollution of the investigated locations of the study area. Sites with higher electromagnetic anomaly (high positive peaks) can be expected to be aquifers, implying locations suitable for the development of groundwater resource. Analysis of the geophysical survey data revealed that the study area could play a significant role in providing adequate portable water for the rural dwellers. However, air- filled, altered or fissured bedrock, or predominantly clayey regolith may sometimes exhibit such anomalies. The above indicates a probable zone of thick overburden with primary to secondary fractured aquifer system with a great depth extent. In this study, data from the geophysical investigation has provided qualitative information on the hydrogeological framework and subsurface disposition of major aquifer units in the study area. Based on the results obtained from this survey, it can be concluded that integration of electromagnetic profiling is not efficient enough to determine the groundwater potential in the study area as it can only provide qualitative interpretation. It is, however, recommended that more advanced and composite geophysical and other hydrogeological investigation tools such as aerial remote sensing, seismic refraction, electrical resistivity tomography and reflection seismology for groundwater, should be deployed in further hydrogeological studies of the area. The qualitative output of water quality analyses revealed that Cl^- concentrations were generally much more prominent in both the Wells and Boreholes of all the investigated areas followed by SO_4^{2-} . Still, Cl^- and SO_4^{2-} were lower in hand-dug wells than in boreholes in Papalanto except for SO_4^{2-} that exhibited relatively similar concentrations in both Wells and Boreholes. Cu^{2+} , Pb^{2+} , Mn^{2+} and Al^{3+} sometimes Ni concentrations were found to be abundant as potential toxic elements. Cu^{2+} , Pb^{2+} , Mn^{2+} , Ni and Al^{3+} were higher in Wells than in Boreholes. The high concentration Pb^{2+} and Cu^{2+} in the study area were possibly attributed to the activities in the study area.

7. References

1. Alabi, AA; Ganiyu, SA; Idowu, OA; Ogabi, AK & Popoola, OI. 2021. Investigation of groundwater potentials using integrated geophysical methods in Maloko-Asipa, Ogun-State. *Applied Water Sciences*, 11 (70): 21. <https://doi.org/10.1007/s13201-021-01388-3>.
2. Ishola SA; Emumejaye K & Ajetumobi AE. 2023. Biogeochemical assessment and health implications of borehole groundwater system using principal component analysis in Itori community, South-West Nigeria. *Dutse Journal of Pure and Applied Sciences*, 9 (4b): 121-138. <https://dx.doi.org/0.43/4/dujopas.v9i4b.11>.
3. MacDonald, A; Davies, J & Dochartagh, BEO. 2002. Simple methods for assessing groundwater resources in low permeability areas of Africa. *British Geological Survey Commissioned Report*, CR/01/168N: 22-23.
4. Aly, SA; Faraq, KSI; Atya, MA & Badr, MAM. 2018. The use of electromagnetic terrain conductivity and DC-resistivity profiling techniques for bedrock characterization at the 13th of May city extension, Cairo, Egypt. *NRIAG Journal of Astronomy and Geophysics*, 7 (1): 107-122. <https://doi.org/10.46717/igj.56.k.18ms.2023.3.29>.



5. Okpoli, CC & Ozomoge, P. 2019. Groundwater exploration in a typical southwestern basement terrain. *NRIAG Journal of Astronomy and Geophysics*, 9 (1): 289-308. <https://doi.org/10.1080/20909977.2020.1742441>.
6. Tyoh, AA; Ajegana-Idemodia, EA & Lucky-Muhammad, M. 2025. Electromagnetic methods. *Conference of the Institute of Geosciences and Earth Resources*, NSUK. <https://doi.org/10.13140/RG.2.2.34257.85606>.
7. Huang, X.; Tang, J; Xiao, X; Jiang, Q; Yang, Z & Hu, S. 2022. A novel apparent resistivity for land based controlled source electromagnetism. *Journal of Geophysics and Engineering*, 9 (3): 562-577. <https://doi.org/10.1093/jge/gnac137>.
8. Azmy, EM; El-Weir, AK; Helaly, A. & Faraq, KSI. 2023. Joint electromagnetic terrain conductivity and dc-resistivity survey for bedrock and groundwater characterization at New Al-Obour City, Egypt. *Iraqi Geological Journal*, 56 (1): 762-776. <https://doi.org/10.1016/j.nrgjag.2018.03.005>.
9. Benson HJ. 1990. *Microbiological Applications: A Laboratory Manual in General Microbiology*. Brown Publishers, Dubuque: 459.
10. Onwuegbuchulam, CO; Ikoru DO; Nwugha, VN & Okereke, CN. 2016. Application of very low frequency- electromagnetic (vlf-em) method to map fractures/conductive zones in Auchi South western Nigeria. *The International Journal of Engineering and Science*, 5 (5): 7-13. www.theijes.com.
11. Mahmud, M; Rahmann, MS, Dina, SA; Masher, MR, Choudhury, TR; Begum, BA & Samad, A. 2025. Potential toxic elements in surface water of Mokosh Beel, Gazipur, Bangladesh: Ecological and human health risk assessment for recreational users. *Helyon*, 2 (3): 39-45. <https://doi.org/10.1016/j.heliyon.2025.e.42421>.
12. Ngwese, SN; Mouri, H; Akoachere, RA & McKinley, CC. 2025. Assessment of potentially harmful elements in surface and groundwater from the granite-gneissic auriferous formations in Bertona city and Environs, East Region, Cameroon, Central Africa: effects on human health. *Groundwater for Sustainable Development*, 29 (1): 45-76. <https://doi.org/10.1016/j.gsd.2025.101420>.
13. Vetrimurugan, E; Brindha, K & Nwandwe, OM. 2016. Human exposure risk to heavy metals through groundwater used for drilling in an intensively irrigated river. *Applied Water Science*, 7 (1): 3267-3280.
14. Mohammadpour, A; Gharehchahi, E; Gbaraghani, MA; Shahsavani, E; Golaki, M; Berndtsson, R; Khaneghah, AM; Hashemi, H and Abolfathi, S. 2024. Assessment of drinking water quality and identifying pollution sources in a chromite mining region. *Journal of Hazardous Materials*, 480 (1): 322-334. <https://doi.org/10.1016/j.hazmat.2024.136.50>.
15. Mokarram, M; Najafi-Ghiri, M; Negahban, S & Roshan, G. 2016. Relationship between landform and soil salinity in the surface and subsurface soil, a case study: Southeast of Fars Province, Iran. *Modelling Earth System and Environment*, 2 (1): 65-73.
16. Mokarram, M & Sathyamoorthy, D. 2016. Investigation of the relationship between Landform classes and electrical conductivity of water and soil using a fuzzy model in a GIS environment. *Solid Earth*, 7(3), 873–880. <https://doi.org/10.5194/se.7875-216>.
17. Okareh, TO; Soka-Adeaga, AA; Akin-Brandon, T; Soka-Adeaga, MA & Soka-Adeaga, ED. 2023. Assessment of heavy metals contamination in groundwater and its implications for public health education, a case study of an industrial area in South-West Nigeria. Chapter 30 in *Groundwater; New Advances and Challenges*. <https://doi.org/10.5772/intechopen.1095750>.
18. Krishna, AK; Mohan, KR & Dasaram, B. 2019. Assessment of groundwater quality, toxicity and health risk in an industrial area using multivariate statistical methods. *Environmental Systems Research*, 26 (1): 22-37.
19. Beeson, S. & Jones, CRC. 1988. The combined EMT/VES geophysical methods for siting boreholes. *Groundwater*, 26 (1): 54-63.



20. Hazell, JRT; Cratchley, CR & Preston, AM. 1988. The location of aquifers in crystalline rocks and alluvium in Northern Nigeria using combined electromagnetic and resistivity techniques. *Quarterly Journal of Engineering Geology*, 21 (1): 59-175.
21. Olayinka, AI. 1990. *Electromagnetic Profiling and Resistivity Soundings in Groundwater Investigation near EgbedaKabba and Kwara State*.
22. Olayinka, AI; Amidu SA & Oladunjoye, MA. 2004. Use of electromagnetic profiling and sounding for groundwater exploration in the crystalline basement area of Igbeti, Southwestern Nigeria. *Global Journal of Geological Science*, 2 (2): 243-253.
23. Ishola SA; Makinde, V; Mustapha, AO; Gbadebo, AO; Ganiyu, SA; Aluko, TJ & Ayedun, H. 2021. Integrated hydro geophysical and biogeochemical characteristics of groundwater sources in Ewekoro communities, South-West Nigeria. *Science and Technology*, 5 (12): 6-9. www.scientechpub.org.
24. Worthington, PR. 1977. Geophysical investigations of groundwater resources in the Kalahari Basin. *Geophysics*, 42 (4): 838-849.
25. Palacky, GJ; Ritsema, IL & De-Jong, SJ. 1981. Electromagnetic prospecting for groundwater in Precambrian terrains in the republic of Upper-Volter. *Geophysical Prospecting*, 29 (1): 932-955.
26. De-Jong, SJ; Dirks, FJH; Kikietta, A; Palacky GJ & Ritsema, IL. 1981. Experimentations de methods electromagnetiques appliqués a la recherche des eaux, souterraines en terrain de sodocristallin en Haute Volta. *Bulletin comiteinterafrika d' etudes hydrauliques (C.I E.H.) hydrogeology*, 44 (1): 17-26.
27. Amadi, UMP & Nurudeen, SI. 1990. Electromagnetic survey and the search for groundwater in the crystalline basement complex of Nigeria. *Journal of Mining and Geology*, 26 (1): 45-53.
28. Olorunfemi, MO; Ojo, JS; Olayinka, AI & Mohammed, MZ. 2001. Geophysical investigation of suspected springs in Ajegunle-Igoba, near Akure, Southwestern Nigeria. *Global Journal at Pure and Applied Sciences*, 7 (2): 311-320.
29. Egwebe, O; Aigbedion, I & Ifedili, SO. 2004. A geo-electric investigation for groundwater at Ivbiaro Ebesse, Edo State, Nigeria. *Journal of Applied Science*, 22 (1): 146-150.
30. Ariyo, SO; Adeyemi, GO & Oyebamiji, AO. 2009. Electromagnetic VLF survey for groundwater development in a contact terrain: a case study of Ishara-remo, Southwestern Nigeria. *Journal of Applied Sciences Research*, 5 (1): 1239-1246.
31. Okafor, P & Mamah, L. 2012. Integration of geophysical techniques for groundwater potential investigation in Katsina-Ala, Benue State, Nigeria. *Pacific Journal of Science and Technology*, 13 (2): 463-474. <http://www.akamaiuniversity.us/PJST.htm>.
32. Alisa A. 1990. *Telluric Current*, A Dictionary of Earth Sciences Ed. Oxford University Press. 64-66.
33. Ishola SA. 2019. Characterization of Groundwater Resource Potentials Using Integrated Techniques in Selected Communities within Ewekoro Local Government Area South-West Nigeria. Department of Physics, *FUNAAB Ph.D Thesis*.
34. Kehinde-Phillips, T. 1992. State maps, In: Onakomaya, SO; Oyesiku K and Jegede (eds), *Ogun State in Maps*. Rex Charles Publishers, Ibadan. 187.
35. Ishola, SA & Gbadebo, AM. 2024. Evaluations of the phreatic shallow aquifers using hydraulic and hydraulic and hydrogeochemical techniques in a typical sedimentary part of Ogun State South-West Nigeria. *Journal of Earth Science and Atmospheric Research*, 7 (1): 54-71.
36. Billman, HG. 1992. Offshore stratigraphy and palaeontology of the Dahomey (Benin) Embayment, West Africa, 1st. *NAPE Bulletin*, 7 (2): 121-130.
37. Ishola, SA; Olufemi ST & Ogunleye, SO. 2024. Impact of wastes on soil properties of an active dumpsite in Oru-Ijebu, South-West Nigeria. *Federal University Wukari (FUW) Trends in Science and Technology Journal*, 9 (1): 193-200. www.ftstjournal.com.
38. Obiora, DN & Onwuka, OS. 2005. Groundwater exploration in Ikorodu, Lagos- Nigeria: A surface geophysical survey contribution. *Pacific Journal of Science and Technology*, 6 (1): 86-93.



39. Oguntoyinbo, JS; Areola, OO & Filani, M. 1978. *Geography of Nigerian Development*, 2nd Edition, Ibadan. Heinemann Educational Books (Nig) Ltd. 45-70.
40. Gbuyiro SO; Lamin, MT & Ojo O. 2002. Observed characteristics of rainfall over Nigeria. *Journal of Nigeria Meteorological Society*, 3 (1): 1-17.
41. Adetunji, J; Mcgregor, J & Ong, CK. 1979. Harmattan haze. *Weather Journal*, 34 (11): 430-436. <https://doi.org/10.1002/j.1477-8696.1979.tb03389.x>.
42. Omogbai, BE. 2010. Rain days and their predictability in South-Western Region of Nigeria. *Journal of Human Ecology*, 31 (3): 185-195.
43. WAPCO. 2000. *Environmental Audit Report of the West African Portland Cement Plc., Ewekoro and Shagamu Quarries submitted to the Federal Ministry of Environment, Abuja* by the West African Portland Cement Plc., Elephant House, Alausa-Ikeja Lagos, Nigeria, 150-155.
44. WAPCO.2001. *Environmental Impact Assessment of the Proposed Clinker Line of the West African Portland Cement Plc., at Ewekoro submitted to the Federal Ministry of Environment, Abuja*, By the West African Portland Cement Plc., Elephant House, Alausa-Ikeja Lagos, Nigeria, 1-12.
45. Ayedun, H; Arowolo, YA; Gbadebo, AM., & Idowu, OA. 2013. *Groundwater Contamination by Metals, Trace and Rare Elements in Basement and Sedimentary Areas of Ogun and Lagos State*. Unpublished Ph.D Thesis. Federal University of Agriculture Abeokuta, South-West Nigeria. 120-266.
46. Ogbe, FGA. 1972. Stratigraphy of strata exposed in the Ewekoro quarry, Western Nigeria. In: African Geology (eds), *University Press, Nigeria*, 305-322.
47. Nton, ME; Eze, FP & Elueze, AA. 2006. Aspects of source rock evaluation and diagenetic history of Akinbo shales, Eastern Dahomey basin, South-West Nigeria. *AAPG Bulletin*, 9 (1): 35-49.
48. Nton, ME. 2001. *Sedimentological and Geochemical Studies of Rock Units in the Eastern Dahomey Basin, Southwestern Nigeria*, University of Ibadan, 315.
49. Adegoke, OS. 1977. Stratigraphy and palaeontology of the Ewekoro formation (Palaeocene) of Southern Nigeria. *Bulletin of American Palaeontology*, 71 (1): 1-1250.
50. Elueze AA & Nton ME. 2004. Organic geochemical appraisal of limestones and shales in part of Eastern Dahomey basin, South-West Nigeria. *Journal of Mining Geology*, 40 (1): 29-40.
51. Adegoke, OS; Adeleye, DR; Ejeagba, DM; Odebode, MO & Petters, SW. 1980. *Geological Guide to Some Nigerian Cretaceous-recent Localities Shagamu Quarry and Bituminous Sands of Ondo and Ogun States*. Nigerian Mining and Geoscience Society: 1-44.
52. Coker SL & Ejedawe JE. 1983. Hydrocarbon source potential of cretaceous rock of Okitipupa uplift. *Nigeria Journal of Mining and Geology*, 20 (1): 168-169.
53. Okosun, EA. 1998. Review of the early Tertiary stratigraphy of Southwestern Nigeria, *Nig. Journal Mining and Geology*, 34 (1): 27-35.
54. Agagu, OK. 1985. *A Geological Guide to Bituminous Sediments in Southwestern Nigeria*. Department of Geology University of Ibadan, 212.
55. Fidelis U; Thomas H & Uduak A. 2014. Reserve estimation from geoelectrical sounding of the Ewekoro limestone at Papalanto, Ogun State, Nigeria. *Journal of Energy Technologies and Policy*, 4 (5): 28-33.
56. Magawata, UZ; Bonde, DS & Abdullahi, BU. 2017. Seepage investigation on an existing dam using very low frequency electromagnetic (VLF-EM) methods: A case study of Shagari Earth Dam, Sokoto, North-Western Nigeria. *International Journal of Geosciences*, 11 (2): 45-53. <https://doi.org/10.4236/ijg.2020.112003>.
57. Ishola, SA. 2025. The impact of magnetotelluric based natural electric field technique in earth's conductivity assessment of a cassava processing site South-West Nigeria. *Journal of Earth Science and Atmospheric Research*, 8 (1): 15-45.
58. Kearey, P & Brooks, M. 2002. *An Introduction to Geophysical Exploration*, Blackwell: 201.
59. GEONICS. 1990. *EM-34 User's Manual*, GEONICS Ltd., Canada: 3.
60. Vogelsang, D. 1995. *Environmental Geophysics, a Practical Guide*, Springer Verlag, 1995.



61. McNeil, JD. 1980. *Technical Note: TN-6. Electromagnetic terrain conductivity measurements at low induction numbers*. Ontario, Canada: 1-15.
62. Omosuyi, GO; Adeyemo A & Adegoke, AO. 2007. Investigation of groundwater prospect using electromagnetic and geoelectrical sounding at Afunbiowo, near Akure, Southwestern Nigeria. *Pacific Journal of Science and Technology*, 8 (2): 172-182.
63. Pieter, HR; Lahti, J; Hild, CR., Bate, B & Phillips, D. 1992. Case histories of shallow time domain electromagnetic in environmental site assessment. *Journal of Groundwater in Monitoring and Remediation*, 12 (4): 110-117.
64. Oyegoke, SO; Ayeni, OO; Olowe, KO; Adebajo, AS. & Fayomi, OO. 2020. Effectiveness of geophysical assessment of boreholes drilled in basement complex terrain at Afe Babalola University, using electromagnetic method. *Nigerian Journal of Technology*, 39 (1): 36-41.
65. McNeill, JD. 1990. Use of electromagnetic methods for groundwater studies, in geotechnical and environmental geophysics. *Investigations in Geophysics*, 5 (1): 191-218.
66. Venu K. & Linga SJ. 2017. Identification of ground water potential zones using electrical resistivity and VLF-EM methods in Gaarakuntapalem Village, Maadugulapally-Mandal, Nalgonda District, Telangana State. *India Asian Journal of Applied Science and Tech*, 9 (1): 479.
67. MacDonald, A; Davies, J; Calow, R & Chilton, J. 2005. *Developing Groundwater, A Guide for Rural Water Supply*. 1- 358. www.itdgpublishing.org.uk.
68. APHA. 1992. American Public Health Association. Standard method for examination of water and waste water, 12th ed. American Public Health Association Inc., New York. American Water Works Association.
69. APHA. 1998. American Public Health Association. *Standard Method for Examination of Water and Waste Water*, 20th ed. American Public Health Association Inc., New York. American Water Works Association.
70. Omosuyi, GO; Ojo, JS & Olorunfemi, MO. 2008. Geoelectrical sounding to delineate shallow aquifers in the coastal plain sands of Okitipupa Area, Southwestern Nigeria. *Pacific Journal of Science and Technology*, 9 (2): 562-577.
71. Alvin, KB; Kelly, LP & Melissa, AS. 1996. Mapping groundwater contamination using Dc resistivity and VLF geophysical methods. *Geophysics*, 62 (1): 80-86.
72. Ugwu, SA & Nwosu, JI. 2009. Detection of fractures for groundwater development in Oha-ukwu using electromagnetic profiling. *Journal of Applied Science Environment Management*, 13 (4): 59-63.
73. Burnett SL. & Beuchat, LR. 2001. Human pathogens associated with raw produce and unpasteurized juices, and difficulties in contamination. *Journal of Industrial Microbiology and Biotechnology*, 27 (6): 104-110.
74. Sumikawa, K. 1990. On the groundwater of Nishinomiya district, Kinki, Japan with special reference to the characteristics of permeability of the aquifer and chemical composition of the Miyamizu. *J. Sci. Hiroshima Univ. Ser. C*, 9 (1): 361-376.
75. Sumikawa, K. 1994. The Miyamizu: Science of high quality waters. In: Takamurath (ed.), *Japanese Association of Groundwater Hydrologists*. Gidhosiuppenn, Tokyo. 196.

Acknowledgement

The author is grateful to Department of Geosciences, University of Lagos for releasing the Geonics ground-conductivity meter for this research. Also, the traditional ruler of Papalanto; His Royal Majesty, Oba Abdu-Razaq Olayiwola Famuyiwa, Onipapa of Papalanto, Owu Kingdom, Abeokuta and the entire autonomous communities within Papalanto district of Ewekoro Local Government Area for their acceptance, permission and assistance.

Data availability

The data that support the findings of this study are available from the author upon reasonable request.



Declaration of competing interest

The author declares that he has no competing financial interests or personal relationships that could have appeared to influence the work reported in this paper.

Use of AI tools declaration

The author declares that he has not used Artificial Intelligence (AI) tools in the creation of this article.

